Regulation of Inflammation in Cystic Fibrosis

by

Claudine Guilbault

Department of Medicine,
Division of Experimental Medicine

McGill University, Montreal

August 2005

This thesis is presented in partial fulfillment of the requirements for the degree of Ph.D. in Experimental Medicine

Your file Votre référence
ISBN: 978-0-494-25161-4
Our file Notre référence
ISBN: 978-0-494-25161-4

Aux amours de ma vie,

Marko, Mathieu et Olivier

ABSTRACT

Cystic fibrosis (CF) female patients have a worse prognosis compared to their male counterparts. CF patients infected with *Pseudomonas aeruginosa* have also been shown to have dysregulated cytokine profiles. Therefore, we studied the importance of sex and interleukin-10 in the susceptibility of C57BL/6 mice to pulmonary infection with *P. aeruginosa*. The results clearly demonstrate that both wildtype and interleukin-10 knockout (KO) female mice are more susceptible to *P. aeruginosa* infection than males, and that they mount a stronger inflammatory response in the lungs.

Several animal models of CF show most of the CF symptoms; however, only a few of these display the CF lung phenotype. The cystic fibrosis transmembrane conductance regulator (*Cftr)*-KO mice that we developed in collaboration with Drs. Tsui and Kent represent a unique model of spontaneously occurring lung disease. We studied the characteristics of this model and analyzed the differences between the lungs of wildtype and *Cftr*-KO mice by assessing their histopathological status, gene and protein expression and fatty acid profiles.

We recently developed a novel non-invasive method of lung infection. The studies described contain major improvements for lung infection techniques employing *P. aeruginosa* bacteria embedded in agar beads. This novel and less invasive technique is crucially important in studying the host response to bacterial infection using the *Cftr*-KO mouse model.

CF lung disease is also characterized by imbalanced lipid profiles. Interestingly, docosahexanoic acid (DHA) has been shown to have anti-inflammatory properties and to reverse intestinal and pancreatic pathologies in a CF mouse model. We have therefore treated our *Cftr*-KO mice developing spontaneous lung disease with DHA and observed a reduction in lung inflammation in the CF-affected organs compared to the untreated *Cftr*-KO mice.

It has also been demonstrated that ceramide is crucially important for *P. aeruginosa* internalization. Fenretinide is a synthetic retinoid inducing the cellular level of ceramide. Using our *Cftr*-KO mouse model, we tested the effect of fenretinide treatment during the course of lung infection with *P. aeruginosa.* Interestingly, we observed major decrease in the bacterial burden of *Cftr*-KO mice that were treated with fenretinide.

RÉSUMÉ

Les femmes atteintes de la Fibrose Kystique (FK) ont un pronostique comparativement plus pauvres que les hommes. De plus, les gens atteints de la FK qui sont infectés avec la bactérie *Pseudomonas aeruginosa* possèdent un profil de cytokines déséquilibré. Nous avons donc déterminé la susceptibilité des souris C57BL/6 aux infections pulmonaires causées par *P. aeruginosa* en fonction du sexe et de la cytokine anti-inflammatoire interleukine-10. Les résultats obtenus démontrent clairement que les femelles, autant celles normales que celles déficientes en interleukine-10, sont plus susceptibles que les males aux infections causées par *P. aeruginosa* dans les poumons.

Plusieurs des modèles de souris FK démontrent la majorité des symptômes associés à la FK; toutefois, très peu d'entres-eux présentent les phénotypes de la FK associés aux poumons. Les souris *Cftr* knockout (*Cftr*-KO) que nous avons développées représentent un modèle unique de maladie pulmonaire spontanée. Nous avons étudié les caractéristiques de ce modèle animal et nous avons analysé les différences entre les poumons des souris normales par rapport aux poumons de souris FK en analysant le statut histopathologique, l'expression des gènes et des protéines ainsi que le profil d'acides gras.

Nous avons récemment développé une nouvelle méthode d'infection des poumons chez la souris. Ces études démontrent des améliorations majeures par rapport aux méthodes utilisées précédemment. Cette méthode améliorée est importante dans l'étude de la réponse inflammatoire de l'hôte durant l'infection pulmonaire dans le modèle animal de la FK.

La FK est aussi caractérisée par un profil lipidique déséquilibré. Il a été démontré que l'acide docosahexanoique (DHA) possédait des propriétés anti-inflammatoires. Nous avons traité les souris de notre modèle animal de FK avec

du DHA. Ce dernier a provoqué une réduction de l'inflammation des poumons comparativement aux souris *Cftr*-KO non traitées.

De plus, le sphingolipide céramide est nécessaire pour l'internalisation de *P. aeruginosa*. Le fenretinide est un rétinoïde synthétique induisant un niveau cellulaire de céramide. Nous avons testé les effets de l'administration de fenretinide lors de l'infection des poumons avec *P. aeruginosa* dans notre modèle animal. Les résultats démontrent une diminution importante du nombre de bactéries dans les poumons lorsque les souris sont traitées avec du fenretinide.

ACKNOWLEDGEMENTS

I am eternally indebted to my supervisor Dr. Danuta Radzioch, whose scientific knowledge and experience led me where I stand today. Danuta, thank you for your endless patience, understanding, enthusiasm and passion for life. You always had the time to listen to me and offer me advice. I will be forever grateful.

I would also like to thank my Ph.D. committee members, Dr. Patricia Tonin, Dr. Diane Gosselin, Dr. David Eidelman and Dr. Basil Petrof, some of whom became collaborators on this project.

Patricia Martin, collègue de travail et surtout amie, pour ta passion pour ton travail, pour ta présence d'esprit et ton efficacité sans pareil, pour ta joie de vivre continuelle, milles mercis. Sans toi, je n'aurais jamais pu avoir deux beaux enfants pendant mes études doctorales. Merci à Claude Lachance, ami et collègue de travail. Claude, merci pour ton oreille attentive, tes conseils réfléchis et pour toutes les discussions stimulantes de bord et d'autres de notre banc de travail (en réseau). Many thanks to Aurélie Nelson for her efforts, allowing me the opportunity to enjoy in peace of mind my first son's first months. I am also grateful to Sergio DiMarco, Marie-Linda Boghdady, Dominique Marion, and Zienab (Sahar) Saeed for their technical assistance as well as for their patience for the neverending manuscripts corrections.

Un gros merci à Jordan Carrière et sa mère Nicole Côté. Jordan, un membre de ma famille éloignée, a été diagnostiqué de la Fibrose Kystique à l'âge de 10 ans, pendant la troisième année de mon doctorat. Cela a quintuplé ma motivation à poursuivre les recherches que j'avais enterprises, en donnant un sens aux résultats que j'obtenais. Merci Jordan pour ton courage et surtout persévère, le monde de la recherche travaille pour toi.

Most importantly, thanks to all my family, Ginette, Michel and François for their continued support, Emmanuel for his understanding, my sons Mathieu and Olivier which gave a new sense to my life, and my fantastic husband Marko for his unconditional love!

PRÉFACE

The author of this thesis has chosen to present it in the format of "manuscript-based thesis"; the following section indicates the "Contributions of Authors".

The Introduction chapter is in part built on the following review book chapter; "Animal models used for the study of cystic fibrosis" by Aurélie Nelson, Claudine Guilbault and Danuta Radzioch, published in *Recent Development in Cellular Research; 2003 (1): 91-130* by *Research Signpost Editior.* Both AN and CG, first authors, contributed equally to the literature search, writing and correcting processes.

The Chapter II is based on the published peer-reviewed manuscript "Influence of gender and IL-10 deficiency on the inflammatory response during lung infection with *Pseudomonas aeruginosa* in mice" by Claudine Guilbault, Peter Stotland, Claude Lachance, MiFong Tam, Anna Keller, LuAnn Thompson-Snipes, Elizabeth Cowley, Thomas A. Hamilton, David H. Eidelman, Mary M. Stevenson, and Danuta Radzioch, published in the journal *Immunology 2002 Nov; 107(3) :297-305.* PS performed the IL-10 neutralization studies, CL offered technical assistance during the animal harvest, MT from the MMS laboratory was in charge of the infection, LTS provided the initial IL-10 knockout mice breeding pairs, EC from the DHE laboratory participated in the assessment of differential alveolar cell counts, and TAH provided N51/KC analysis. CG was in charge of the planification of the experiments and all other experimental procedures*, data analyses and formatting and writing of manuscript.

The Chapter III is based on the manuscript entitled "Distinct pattern of lung gene expression in the *Cftr*-KO mice developing spontaneous lung disease compared with their littermate controls" by Claudine Guilbault, Jaroslav Novak,

Patricia Martin, Marie-Linda Boghdady, Zienab Saeed, Marie-Christine Guiot, and Danuta Radzioch, published in the *Physiological Genomics* Journal, *13;25(2):179-93, April 2006.* JN performed statistical analysis specific to microarray data, PM provided technical assistance with the animal work, MLB provided technical assistance with histological related-work under the supervision of MCG and ZS provided technical assistance for protein assessment in lung samples. CG was in charge of the planification of the experiments and all other experimental procedures*, data analyses and formatting and writing of manuscript.

The Chapter IV is based on the published peer-reviewed manuscript "Cystic fibrosis lung disease following infection with *Pseudomonas aeruginosa* in the *Cftr* knockout mice using novel non-invasive direct pulmonary infection technique" by Claudine Guilbault, Patricia Martin, Daniel Houle, Marie-Linda Boghdady, Marie-Christine Guiot, Dominique Marion and Danuta Radzioch, published in *Laboratory Animals; 39; 336-352, July 2005.* PM provided technical assistance with the animal work and, DH provided original ideas and technical assistance for the perfection of the infection methodology. MLB provided technical assistance with histological related-work under the supervision of MCG, DM offered technical assistance during the animal harvest. CG was in charge of the planification of the experiments and all other experimental procedures*, data analyses and formatting and writing of manuscript.

The Chapter V is based in part on published manuscript "Protective effect of DHA treatment in non-infected CFTR knockout mice with CF lung disease" by Claudine Guilbault, Aurélie Nelson, Patricia Martin, Peter Stotland, Marie-Christine Guiot, Juan B. DeSanctis, and Danuta Radzioch, published in *Immunology 2004: 79-88, July 2004.* AN offered assistance with DHA diet supplementation experiments, PM provided technical assistance with the animal work, PS took part in the weight analysis data collection, MCG supervised the histological related-work, JBD was in charge of the fatty acids analyses. CG was

in charge of the planification of the experiments and all other experimental procedures*, data analyses and formatting and writing of manuscripts.

The Chapter V also includes the most recent experiments demonstrating the protective effect of fenretinide supplementation on cystic fibrosis lung disease. PM provided technical assistance with the animal work, JBD provided original ideas related to the project and was also in charge of the fatty acids analyses. CG has been in charge of the experimental design* and has also been preparing the manuscript.

The research included in this thesis (the last six years) has been supported by the grants from the Canadian Cystic Fibrosis Foundation. Also, Danuta Radzioch (National Scholarship) and Claudine Guilbault (Master and Ph.D. scholarships) were supported by the Fonds de la Recherche en Santé du Québec.

* Experimental procedures includes: experiment and harvest preparations, diet supplementation, bacteria inoculum preparation, infection procedure, care of mice colony, experiment harvest, DNA - mRNA - proteins analyses, bacterial load determination, organ histopathology evaluation, cell culture and statistical analysis.

Key words:

Arachidonic acid
Affimetrix gene chips
Bronchoalveolar lavage
Ceramide
Cystic fibrosis conductance transmembrane regulator (CFTR)
Cftr-knockout mice
Cystic fibrosis
Docosa-hexanoic acid
Direct pulmonary infection
Fatty acid
Fenretinide
Gender
Gene expression
Interleukin-10
Infection
Lipid
Lung
Mouse model
Protein expression analysis
Pseudomonas aeruginosa
Real-time quantitative Reverse-transcribed polymerase chain reaction
Spontaneous lung disease

TABLE OF CONTENT

Abstract 3
Résumé 5
Acknowledgements 7
Preface 8
Keywords 11
Table of content 12
List of tables 17
List of figures 19
List of appendices 21
List of abbreviations 22

Chapter I. Introduction
1.1 Cystic fibrosis (CF); an overview 24
1.1.1 Incidence of CF in North America 24
1.1.2 CF diagnostic and symptoms 27
1.1.3 Cystic Fibrosis Transmembrane conductance Regulator (CFTR); the gene and the protein 27
1.1.4 CFTR gene mutations 29
1.1.5 Phenotypic effects resulting from CFTR mutation; in brief 30
1.1.6 Multi-systems manifestations of CFTR mutation; in details 31
1.1.6.1 Intestinal disease
1.1.6.2 Pancreatic disease
1.1.6.3 Lung disease and inflammation
1.1.6.4 Nasal and tracheal electrophysiological profiles
1.1.6.5 Other manifestations of the disease
1.1.7 Genotype and phenotype correlation 34
1.1.8 Reasons for disease severity in human 35
1.1.8.1 Nutrition
1.1.8.2 Gender
1.1.8.3 Genetic backgrounds
1.1.8.4 Independently segregating modifier genes
1.1.9 Relationship between CFTR basic defect and lung disease 41
1.1.9.1 Role of CFTR in determining the volume or ionic
1.1.9.2 CFTR: receptor for *P. aeruginosa* LPS?
1.1.9.3 Relationship between infection and inflammation
1.1.10 Remedies and treatments 44
1.1.10.1 Antimicrobial / anti-infective approach
1.1.10.2 Mucus regulation
1.1.10.3 Gene therapy – stem cells based intervention
1.1.10.4 CFTR protein rescue
1.1.10.5 Ion transport restoration
1.1.10.6 Nutrition
1.1.10.7 Anti-inflammatory
1.1.10.8 Early screening – early intervention – prevention
1.1.10.9 Complementary and alternative therapy

1.1.11 Clinical Research 47
1.2 Animal models to study CF 47
1.2.1 CF mouse models 50
1.2.1.1 Genotypes 50
1.2.1.2 Phenotypes 55
1.2.1.2.1 Intestinal disease
1.2.1.2.2 Pancreatic disease
1.2.1.2.3 Lung disease and inflammation
1.2.1.2.4 Nasal and tracheal electrophysiological profiles
1.2.1.2.5 Other manifestations of the disease
1.2.1.3 Reasons for disease severity in mouse 64
1.2.1.4 CFTR mice models and bacterial infections 65
1.2.1.4.1 Infection with *Staphylococcus aureus* and *Burkholderia cepacia*
1.2.1.4.2 Infection with *Pseudomonas aeruginosa*
1.2.2 Other animal models for CF disease studies 69
1.3 Rational 71
1.3.1 Premises 71
1.3.2 Hypothesis 72
1.3.3 Specific objectives 72

Chapter II. Influence of gender and IL-10 deficiency on the inflammatory response during lung infection with *Pseudomonas aeruginosa* in mice

2.1 Abstract 76
2.2 Introduction 77
2.3 Material and Methods 79
2.3.1 Mice
2.3.2 *Pseudomonas aeruginosa*
2.3.3 Inoculum's preparation and infection of mice
2.3.4 Bronchoalveolar lavage
2.3.5 Lung homogenates
2.3.6 Cytokine measurements
2.3.7 Anti-Murine IL-10 mAb and Neutralization Protocol
2.3.8 Statistical analyses
2.4 Results 83
2.4.1 Gender differences in susceptibility to *P. aeruginosa* lung infection in B6 mice 83
2.4.1.1 Survival of mice infected with *P. aeruginosa*
2.4.1.2 Variations in body weight during lung infection
2.4.1.3 Recruitment of alveolar cells to the site of infection
2.4.1.4 Cytokines levels in the lungs of infected B6 mice
2.4.1.5 Bacterial burden in the BALF and lungs
2.4.2 Influence of IL-10 in *P. aeruginosa* lung infection in mice 87
2.4.2.1 Survival of mice infected with *P. aeruginosa*
2.4.2.2 Variations in body weight during lung infection

2.4.2.3 Recruitment of alveolar cells to the site of infection
2.4.2.4 Levels of TNF alpha in the lungs of infected IL-10 KO and WT mice
2.4.2.5 Levels of N51/KC in the lungs of infected IL-10 KO and WT mice
2.4.2.6 Bacterial burden in the BALF and lungs
2.4.3 Effects of anti-IL-10 neutralization on the course of *P. aeruginosa* infection 100
2.5 Discussion 101

Chapter III. Gene expression profilling in the lungs of *Cftr* KO mice developing spontaneous lung disease
3.1 Abstract 109
3.2 Introduction 110
3.3 Material and Methods 112
3.3.1 Mice
3.3.2 Lung histopathology
3.3.3 RNA extraction
3.3.4 Microarray experiment
3.3.5 Microarray data processing
3.3.6 Subsequent gene expression analyses
3.3.7 Real-time polymerase chain reaction
3.3.8 Method of mouse lung infection with *P. aeruginosa* instilled in agarose beads
3.3.9 Immunostaining (IHC)
3.3.10 IgGs measurements
3.3.11 Statistical analyses
3.4 Results 118
3.4.1 Mouse model of CF
3.4.2 Genes differentially expressed between WT and *Cftr*-KO mice – microarray analyses
3.4.3 Other potential candidate genes
3.4.4 Validation of gene expression differences found by microarray data
3.4.5 Gene ontology classification
3.4.6 Protein expression in the lungs
3.5 Discussion 145

Chapter IV. Cystic fibrosis lung disease following infection with *Pseudomonas aeruginosa* in the *Cftr* knockout mice using novel non-invasive direct pulmonary infection technique
4.1 Abstract 156
4.2 Introduction 157
4.3 Material and Methods 160
4.3.1 Mice
4.3.2 *Pseudomonas aeruginosa (P. aeruginosa)*
4.3.3 Inoculum preparation

4.3.4 Description of the method of mouse lung infection with *P. aeruginosa* instilled in agarose beads
4.3.5 Mice evaluation
4.3.6 Bronchoalveolar lavage
4.3.7 Lung homogenates
4.3.8 Lung histopathology
4.3.9 Cytokine measurements
4.3.10 Statistical analyses
4.4 Results 167
4.4.1 Method of infection 167
4.4.2 *P. aeruginosa* dose determination for the establishment of lung infection 167
4.4.2.1 Bacterial burden in the lungs and survival
4.4.2.2 Alveolar cells in BALF samples
4.4.2.3 Weight monitoring during *P. aeruginosa* lung infection
4.4.3 *P. aeruginosa* direct pulmonary infection in KO and WT mice 174
4.4.3.1 Weight monitoring during *P. aeruginosa* lung infection
4.4.3.2 Bacterial burden in the lungs and survival
4.4.3.3 Alveolar inflammatory cells in BALF samples
4.4.3.4 Cytokine expression in the lungs of *P. aeruginosa* infected WT and KO mice
4.5 Discussion 183

Chapter V. Protective effect of the treatment with DHA and fenretinide in *cftr* knockout mice with CF lung disease
5.1 Protective effect of DHA treatment in non-infected *Cftr*-knockout mice with CF lung disease 191
5.1.1 Abstract 191
5.1.2 Introduction 192
5.1.3 Material and Methods 193
5.1.3.1 Mice
5.1.3.2 Fatty acid diet supplementation
5.1.3.3 Fatty acid analysis
5.1.3.4 Lung histopathology
5.1.3.5 Statistical analyses
5.1.4 Results 196
5.1.4.1 Monitoring of weight
5.1.4.2 Free and phospholipid-bound DHA profiles in organs
5.1.4.3 Lung histology analysis
5.1.5 Discussion 204
5.2 Protective effect of fenretinide on lipid metabolism and susceptibility to *P. aeruginosa* in mice with cystic fibrosis lung disease 206
5.2.1 Abstract 206
5.2.2 Introduction 206
5.2.3 Materials and Methods 208

5.2.3.1 Mice
5.2.3.2 Fenretinide diet supplementation
5.2.3.3 *Pseudomonas aeruginosa* inoculum preparation
5.2.3.4 Description of the method of mouse lung infection with *P. aeruginosa* instilled in agarose beads
5.2.3.5 Bronchoalveolar lavage
5.2.3.6 Lung homogenates
5.2.3.7 Fatty acid analysis
5.2.3.8 Ceramide/Sphingolipids analysis
5.2.3.9 Statistical analyses
5.2.4 Results 212
5.2.4.1 Ceramide/sphingolipids levels observed in the lungs
5.2.4.2 Weight monitoring during PA lung infection
5.2.4.3 Alveolar inflammatory cells in BALF samples
5.2.4.4 Bacterial burden in the lungs
5.2.4.5 Lipid profiles
5.2.5 Discussion 232

Chapter VI. General discussion
6.1 Summary of the results 239
6.2 Future directions 248
6.3 Importance of the other fields of research 249

ChapterVII. Claims to originality 252

Appendix I. Supplementary illustrations of the direct non-invasive method of lung infection 254
Appendix II. Over-expressed Genes in *Cftr*-KO compared to WT mice; genes with either unknown function or with a fold difference lower than 1.5 255
Appendix III. Genes differentially expressed between *Cftr*-KO and WT mice 258
Appendix IV. List of other published manuscripts 268
Appendix V. List of abstracts and published Conference Proceedings 269
Appendix VI. Certificates of compliance 272

References 273

LIST OF TABLES

Chapter I

Table 1.1 Cystic fibrosis research progressions since 1989 48

Table 1.2 Cystic fibrosis mouse models 51

Table 1.3 Cystic fibrosis other animal models 70

Chapter II

Table 2.1 Sex differences in B6 mice during *P. aeruginosa* lung infection 86

Table 2.2 Recruitment of inflammatory cells into the lungs of infected mice 96

Table 2.3 Lack of correlation between the numbers of viable *P. aeruginosa* in the lungs of infected mice and weight or age at day 4 post-infection 97

Table 2.4 Effects of IL-10 neutralization on *P. aeruginosa* lung infection in B6 mice 101

Chapter III

Table 3.1 Histopathological evaluation of lungs from non-infected *Cftr*-KO and WT mice 118

Table 3.2 Genes differentially expressed between *Cftr*-KO and WT females 122

Table 3.3 Genes differentially expressed between *Cftr*-KO and WT males 125

Table 3.4 Genes differentially expressed between *Cftr*-KO and WT mice common to females and males 128

Table 3.5 Candidate genes located within previously identified region associated with lung phenotypes* corresponding to "interstitial thickening", "alveoli count", and "fibrosis" 132

Table 3.6 Primer sequences for the validation of selected candidate genes 133

Chapter IV

Table 4.1 Characteristics of mice used in direct pulmonary infection procedures 170

Table 4.2 Cytokine levels in lung homogenates of *P. aeruginosa* infected *Cftr*-KO and WT mice 3 days post-infection 182

Chapter V

Table 5.1 Survival of *Cftr*-KO mice and their WT controls fed with different diets 199

Table 5.2 Mean weight loss of WT and *Cftr*-KO mice during chronic lung infection with *P. aeruginosa* 213

Table 5.3 Effect of fenretinide treatment on the mean weight loss of WT and *Cftr*-KO mice during chronic lung infection with *P. aeruginosa* 216

LIST OF FIGURES

Chapter I

Figure 1.1 Jordan was diagnosed with CF when he was 10 years old 25

Figure 1.2 Relative frequency of complications associated with adult CF 26

Chapter II

Figure 2.1 Survival rate of WT and IL-10 KO mice after intratracheal infection with different doses of *P. aeruginosa* entrapped in agar beads 85

Figure 2.2 Mean weight loss of WT and IL-10 KO mice during *P. aeruginosa* lung infection 90

Figure 2.3 Alveolar inflammatory cells in the lungs of *P. aeruginosa* infected mice 93

Figure 2.4 Recruitment of inflammatory cells in the lungs of *P. aeruginosa* infected mice 95

Figure 2.5 Bacterial burden in the lungs of *P. aeruginosa* infected mice 99

Chapter III

Figure 3.1 Histopathological status of the lungs of uninfected WT and *Cftr*-KO mice 120

Figure 3.2 Dispersion plots of the average values from microarray analysis 124

Figure 3.3 Cluster analysis of microarray experiment in WT and *Cftr*-KO mice 131

Figure 3.4 Validation of the difference in mRNA expression between WT and *Cftr*-KO mice for selected genes 135

Figure 3.5 Gene ontology-based analysis; effect of *Cftr*-deletion on gene expression in the lungs of mice 138

Figure 3.6 Representation of candidate genes potentially involved in the manifestation of the lung disease phenotype observed in the *Cftr*-KO mice developing spontaneous lung disease 141
Figure 3.7 Immunostaining on the lungs of WT and *Cftr*-KO mice 144

Chapter IV

Figure 4.1 Direct pulmonary method of infection 164
Figure 4.2 Site of injection into the lungs 169
Figure 4.3 Determination of the *P. aeruginosa* dose with direct pulmonary infection technique 173
Figure 4.4 Histological examination of the lungs of uninfected WT and *Cftr*-KO mice 176
Figure 4.5 Inflammatory response in WT and *Cftr*-KO mice during lung infection with $1x10^6$ *P. aeruginosa* embedded in agar beads 179
Figure 4.6 Cytokines expression into the lungs of WT and *Cftr*-KO infected mice 181
Figure 4.7 Intratracheal method of infection 185

Chapter V

Figure 5.1 Mean weight gain of WT and *Cftr*-KO female and male mice fed with liquid (Bioserv, Peptamen) or standard solid diet 198
Figure 5.2 DHA incorporated in phospholipids in uninfected WT and *Cftr*-KO mice 201
Figure 5.3 Histological examination of the lungs of *Cftr*-KO mice and their WT controls 203
Figure 5.4 Ceramide levels observed in the lungs and plasma 215
Figure 5.5 Bacterial burden in the lungs 219
Figure 5.6 DHA/AA index ratio observed in the lungs and plasma 222
Figure 5.7 DHA incorporated in phospholipids expressed as percentile of total fatty acids in the lungs and plasma 225

Figure 5.8 Concentration of DHA incorporated in phospholipids in the lungs and plasma 227
Figure 5.9 Free DHA expressed as percentile of total fatty acids in the lungs and plasma 229
Figure 5.10 Concentration of free DHA in the lungs and plasma 231
Figure 5.11 Concentration of AA incorporated in phospholipids 234

LIST OF APPENDICES

Appendix I. Supplementary illustrations of the direct non-invasive method of lung infection

Appendix II. Over-expressed Genes in *Cftr*-KO compared to WT mice; genes with either unknown function or with a fold difference lower than 1.5

Appendix III. Genes differentially expressed between *Cftr*-KO and WT mice

Appendix IV. List of other published manuscripts

Appendix V. List of abstracts and published Conference Proceedings
Conference Proceedings
Abstracts

Appendix VI. Certificate of compliance
Animal use protocol certificate
Radioactivity certificate

LIST OF ABBREVIATIONS

AA	arachidonic acid
ABC	ATP-binding cassette
ABPA	allergic bronchopulmonary aspergillosis
ASL	airway surface liquid
ATP	adenosine tri-phosphate
B6	C57BL/6
BAL(F)	bronchoalveolar lavage (fluid)
BHA	butylated hydroxyanisole
cAMP	cyclic adenosine mono-phosphate
CF	cystic fibrosis
CFTR	cystic fibrosis transmembrane conductance regulator
CFU	colony-forming unit
DHA	docosahexanoic acid
DIOS	distal intestinal obstruction syndrome
ENaC	epithelial sodium channel
FEN	fenretinide
HE	Haematoxylin and eosin
IHC	immunohistochemistry
IL-	interleukin
KO	knockout
LPS	lipopolysaccharide
MMP	matrix metalloproteinase
MT	Masson's Trichrome
ORCC	outwardly rectified chloride channel
PAS	Periodic-Acid Schiff
PCR	polymerase chain reaction
PMN	polymorphonuclear cells
QTL	quantitative trait loci
ROMK	regulator-dependent up-regulation of Kir1.1
RT	reverse transcription
SEM	standard error of the mean
SNP	single nucleotide polymorphism
SPF	specific pathogen free
TNF	tumor necrosis factor
WT	wildtype

CHAPTER I

CHAPTER I.
INTRODUCTION

In part based on published review article

Nelson, A., Guilbault, C., Radzioch, D. Animal models used for the study of cystic fibrosis. Recent Development in Cellular Research. 2003 (1): 91-130. Research Signpost.

1.1 Cystic fibrosis (CF); an overview

1.1.1 Incidence of CF in North America

Cystic fibrosis is the most common autosomal recessive genetic disorder affecting Caucasian populations (55). It affects over 3 400 children and adults in Canada and approximately 30 000 in the United States. It is estimated that one in every 2 500 children born in Canada has CF. The disease is however more prevalent in certain geographical areas, such as in the Saguenay-Lac-Saint-Jean (Quebec, Canada) where the incidence is increased to 1 in 891 births (266;56) (Figure 1.1). Four percent of Canadians carry a defective version of the gene responsible for CF. When Dorothy Andersen described the disorder in 1938, the median survival age was less than one year (158). In the 1960s, most children with CF were not expected to live long enough to attend kindergarden. Cystic fibrosis is no longer only a disease associated with children since the median age of survival of Canadians with CF is now between 35 to 40 years. CF adults, however, may experience additional health challenges including CF-related diabetes and osteoporosis (Figure 1.2). Conversely, the median survival age varies greatly according to gender disparity. Male CF patients from Canada, United States and United Kingdom have a median survival rate of 34.4 years, whereas female CF patients have a median survival rate of 29.1 years (259). The reasons for this is however unclear.

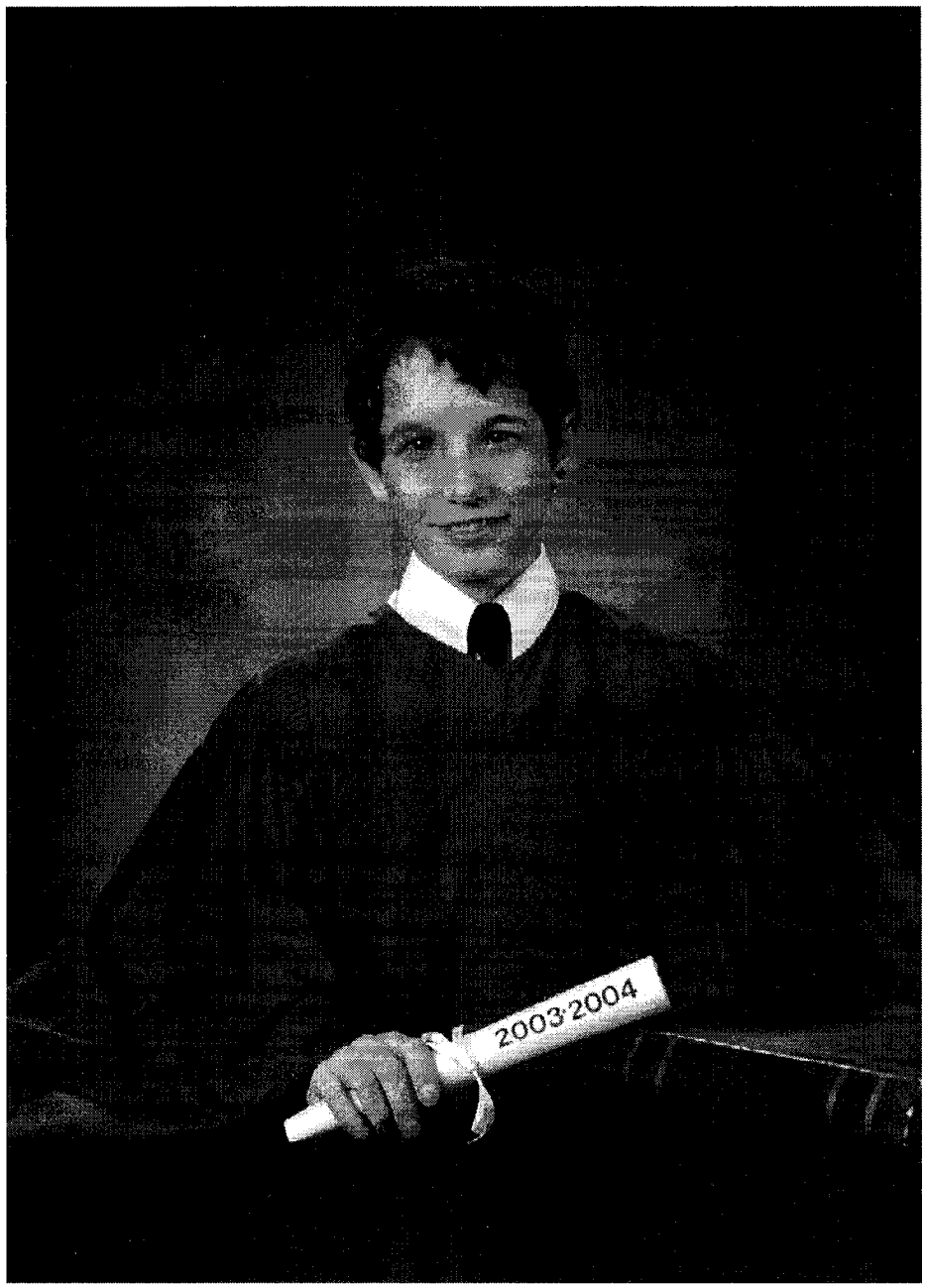

Figure 1.1 Jordan was diagnosed with CF when he was 10 years old (Laval, Quebec).

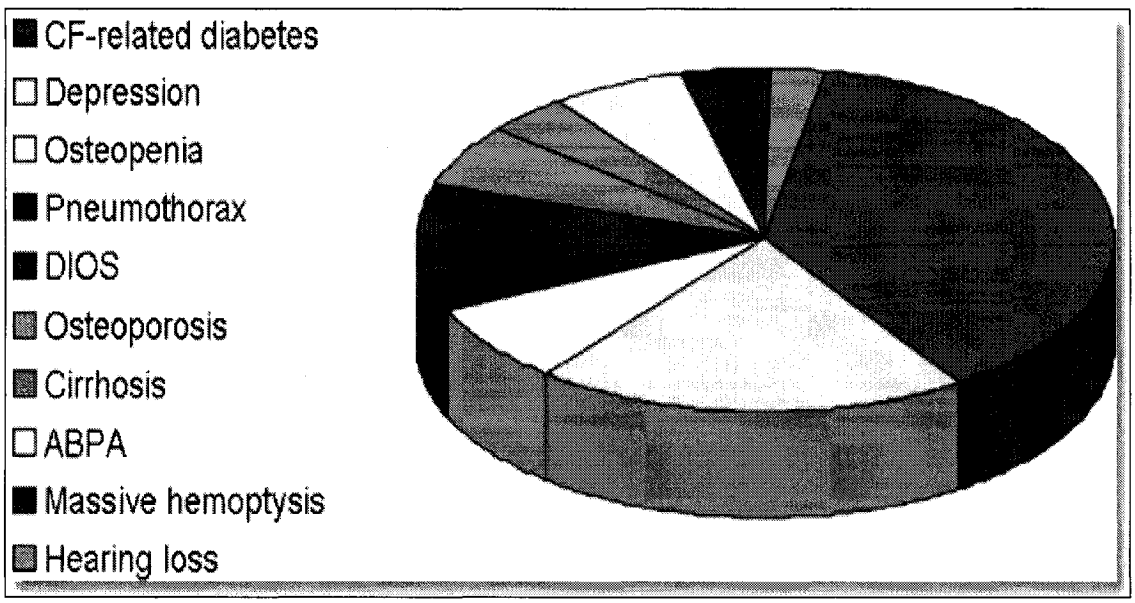

Figure 1.2 Relative frequency of complications associated with adult CF [1].

[1] Taken from http://www.hopkins-genomics.org/cf/cf_epid.html

1.1.2 CF diagnostic and symptoms

CF was first described as a disease in the late 1930s. At that time, it was usually recognized only after a child had died, often as a result of malnutrition or pneumonia. Medical awareness of CF has increased tremendously over the subsequent years. Nevertheless, cystic fibrosis can still be confused with other common diseases such as asthma, chronic bronchitis, pneumonia, and celiac disease. The sweat test is the standard diagnostic test for CF. This simple and painless procedure measures the amount of salt in the sweat; high salt level indicates CF disease. Modern genetic diagnostic tools have also emerged like single nucleotide polymorphism (SNP) analysis, polymerase chain reaction (PCR) analysis, microarray analysis, sequencing analysis and are used to confirm the initial diagnosis obtained from the sweat test and nasal poyential difference.

People with CF have a variety of symptoms that vary from person to person. These include salty-sweat, persistent coughing, wheezing or shortness of breath, excessive appetite but poor weight gain, and greasy, bulky stools.

1.1.3 Cystic Fibrosis Transmembrane conductance Regulator (CFTR); the gene and the protein

In 1989, the cystic fibrosis transmembrane conductance regulator (CFTR) gene was identified by a series of elegant experiments involving saturation mapping and chromosome walking and jumping techniques (106;142;221;227). The CFTR gene is positioned on the long arm of chromosome 7 (7q31.3), comprises 27 exons and is 250 kb long (39;106). Based on the autosomal recessive mode of inheritance, researchers have estimated that the CF gene carrier frequency is about 1 in 25 among the Caucasian population (106;298). The CFTR protein is a transmembrane glycoprotein of 1480 amino acid residues that functions as a cyclic adenosine monophosphate (cAMP) dependent chloride conductance channel (49). The CFTR protein is a member of the adenosine triphosphate (ATP)-binding-cassette (ABC) membrane transporter superfamily. It is made of two homologous halves with each half containing a nucleotide binding domain that binds ATP and a membrane-spanning domain with 6 segments that helps form a channel pore

spanning the cell membrane. The two halves are connected by a regulatory domain (R) that is phosphorylated by a cAMP-dependent protein kinase. CFTR appears to be located primarily in the apical membranes of the epithelial cells (130;123;106;1). Originally recognized as a cAMP-dependent apical chloride conductance channel, it was then identified as a cAMP-dependent negative regulator of Na^+ channels (ENaC) (267). CFTR has also been postulated to have a role as a regulator of a separate chloride channel called the outward rectifying chloride channel (ORCC) (73;90). Furthermore, a role in chloride transport across the membrane of mitochondrial organelles has also been suggested for CFTR, as well as roles in regulation of the Cl^-/ HCO_3^- exchanger and the ROMK K^+ channel (161;246).

The CFTR protein is expressed in all epithelial cells affected in CF, including the lungs, nasal polyps, pancreas, sweat glands, liver, large intestine, colon and the testis (265). How the genetic, protein and epithelial transport defects cause the range of disease expression observed is not well understood. CF is characterized by abnormalities in salt and water transport, resulting in thick mucus secretions by the respiratory tract, pancreas, gastrointestinal tract, sweat glands and other exocrine tissues. An abnormal chloride level in sweat (more than 60 mmol/l) is a hallmark of CF and provides a good diagnostic test (265). Progressive infection and inflammation in the lower airways limits the length and impairs the quality of life for most patients with CF. Other pathological manifestations in humans include pancreatic insufficiency and malabsoprtion of fats and proteins, increased energy expenditure and weight loss, neonatal meconium ileus and intestinal obstruction, male infertility due to obstructive azoospermia and reduced fertility for females (202;236;266). Cirrhosis of the liver and development of a cholecystis and choledocholithiasis can also be consequences of CF (299).

The most serious consequence of CFTR protein dysfunction is a progressive, and ultimately fatal, inflammatory lung disease characterized by repeated acute and chronic bacterial infections. Infections associated with active and damaging host inflammatory responses start early in the life of CF patients. Initially, the lower respiratory tract of CF infants gets colonized with *Staphylococcus aureus* (S.

aureus), *Haemophilius influenzea* (*H. influenzae*), and Respiratory Syncitial viruses (150;174;266). The incidence of these infections decreased due to more efficient treatments against these infectious agents. Infection with *Burkholderia cepacia* (*B. cepacia*) is also frequent and often has a fatal outcome, depending on the *Cftr* genotype of the patient (223). However, chronic infection of the lungs with mucoid strains of *Pseudomonas aeruginosa* (*P. aeruginosa*) tend to persist in most patients and results in an exaggerated neutrophilic inflammatory response. *P. aeruginosa*, an opportunistic gram-negative pathogen, acquires a mucoid phenotype shortly after the initial infection (174;222;293). Microcolonies of *P. aeruginosa* in the lungs become encapsulated in a biofilm made of alginate, an extracellular polysaccharide. The production of alginate as well as the release of toxins and proteases from *P. aeruginosa* may be important in preventing the host from mounting a protective local immune response. The mucoid biofilm not only impedes opsonizing antibodies, polymorphonuclear leukocytes (PMNs) and macrophage phagocytosis, but it also contributes to further activation of the inflammatory cells and the antigen presenting cells. This leads to continuous induction of the inflammatory process with persistent cellular recruitment to the sites of infection. The progression of inflammation during *P. aeruginosa* infection is characterized by a dysregulated production of cytokines manifested by high levels of pro-inflammatory cytokines (interleukin 1 (IL-1), IL-6, IL-8, tumor necrosis factor (TNF), S100A8, S100A9) and low levels of the anti-inflammatory cytokine IL-10 reported in bronchoalveolar lavage (BAL) fluid (121;141;186;266). This excessive inflammation results in progressive destruction of the airway walls and bronchiectasis (49), characterized by an irreversible dilatation and destruction of the bronchial walls (202).

1.1.4 CFTR gene mutations

Over 1300 mutations[2] in CFTR have been detected to date (202). The mutations have been categorized into five classes. Class I mutations are

[2] A complete database composed of the 1388 *Cftr* mutations is available on the web site of the Hospital for Sick Children; http://www.genet.sickkids.on.ca/cftr/

characterized by defective CFTR protein production (no synthesis of the protein) such as; nonsense G542X, frameshift 394delTT and splice junction 1717-1G →A. Class II mutations correspond to defective processing of CFTR (no maturation of the protein), often due to misfolding of the CFTR protein such as; missense, AA deletion ΔF508. Class III mutations are characterized by a protein that is defectively regulated (blocked regulation) such as; missense G551D. Class IV mutations result in a CFTR protein with a defect in Cl^- channel regulation (decreased conductance) such as; missense R117H. Finally, class V mutations are characterized by defective CFTR protein production that leads to a reduced synthesis (decreased abundance of the protein) such as; missense A455E, alternative splicing 3849+10kbC→ T (295). The most common mutation observed in CF patients is ΔF508. ΔF508 is a class II mutation which affects more than 70% of CF patients. It is characterized by the deletion of three base pairs in exon 10, resulting in the deletion of phenylalanine (49). More than 50% of Canadians with CF carry two copies of the most common mutation ΔF508; furthermore, 85% of all individuals with CF in Canada carry at least one copy of ΔF508[3]. However, certain mutations of CFTR are more frequent in specific populations. For example, a high frequency of the mutations "G542Y" and "W1282" has been shown for Ashkenazi Jewish population whereas German populations have a higher frequency of the mutation "2143delT" (236).

1.1.5 Phenotypic effects resulting from CFTR mutation; in brief

A defective *Cftr* gene causes the body to produce abnormally thick, viscous mucus that clogs the lungs and leads to life-threatening lung infections. These thick secretions also obstruct the pancreas, preventing digestive enzymes from reaching the intestines. Therefore, persons with CF must consume artificial enzymes with every meal and snack, to help them absorb adequate nutrition from their food. The mucus also can block the bile duct in the liver, eventually causing permanent liver damage in approximately six percent of CF patients. CF can also cause reproductive problems as more than 95% of men with CF are sterile. But,

[3] Data from the Canadian Cystic Fibrosis Foundation

with emergence of new technologies, some males have been able to reverse these reproductive deficiencies. Although many women with CF are able to conceive, limited lung function and other health factors may make it difficult for them to carry a child to term.

1.1.6 Multi-systems manifestations of CFTR mutation; in details

1.1.6.1 Intestinal disease

In the human patients, CF is manifest in the small intestine by decreased Cl^- and fluid secretion, which may contribute to the meconium ileus encountered in about ten percent of the neonates (74). In older patients, CF is manifest by intestinal obstructions due to maldigestion, accumulation of viscous mucus and disturbed fluid and electrolyte transport in the gastrointestinal tract (216;156).

1.1.6.2 Pancreatic disease

Pancreatic insufficiency causing maldigestion and malabsorption of fats and proteins is a hallmark of the disease, occurring in 90% of the patients by one year of age (202). Certain genotypes impart pancreatic sufficiency. In the pancreas, the acinar epithelia secrete digestive enzymes, and the ductal epithelia, containing CFTR proteins, secrete an HCO_3^- rich liquid that flushes the enzyme into the duodenum. The transport of HCO_3^- plays an important role in the function of the secretory epithelia and in CF. Absence of HCO_3^- transport in patients with CF usually results in pancreatic insufficiency, whereas partially reduced HCO_3^- transport usually results in pancreatic sufficiency. HCO_3^- and pH affect viscosity and bacterial binding proportion of mucin (190). In human CF patients, plugging of the pancreatic ducts with mucins leads to enlarged acini and eventually to fibrosis. The disease was actually named after this pathophysiological process (cystic fibrosis of the pancreas). Pancreatic insufficiency is a prominent manifestation of CFTR dysfunction in humans, but has not been clearly demonstrated in CF mouse models.

1.1.6.3 Lung disease and inflammation

Lung disease represents the primary concern in CF, since about 95% of the morbidity and mortality in CF humans is due to excessive pulmonary inflammation. In the CF patient, a consistent finding in the airways is mucus plugging with bacterial infection (106). As the disease progresses, bronchiolitis and bronchiectasis, goblet cell hyperplasia extending into the bronchioles and submucosal gland hypertropy become classical symptoms of the disease. An animal model mimicking lung disease is likely to be very valuable. However, a surprising lack of pulmonary pathology was noted in most of the CF mice models developed so far, probably because of the distinct anatomy of airways between mouse and human.

Defects in the function or expression of CFTR within the airways lead to early and persistent respiratory infections. Initially, *S. aureus* and *H. influenzae* are usually isolated. *S. aureus*, a gram-positive bacterium, is one of the first colonizing agents of CF lungs in infants. These infections usually wane, and are replaced by *P. aeruginosa* which takes over as the major pathogen. A small number of patients will get infected with other organisms such as *Strenotrophomonas maltophilia, B. cepacia, Aspergillus fumigatus* and non-tuberculous mycobacteria, some of which appear to be increasing in prevalence (25;53).

B. cepacia infects mainly adolescents and adults. Infection with this gram-negative bacterium has very different clinical outcomes, ranging from being an asymptomatic carrier to causing fatal necrotizing pneumonia and septicemia (62;100;274). The reasons of CF patients' predisposition to infection with *B. cepacia* are unclear. Host factors such as underlying lung damage, repeated exposure, and specific bacterial factors, such as presence of cable pili, production of extracellular enzymes and the ability of some strains of *B. cepacia* to replicate intracellularly, might play a role (234). *B. cepacia* strains have been subdivided into genomovars. The most common groups cultured from sputa of CF patients are genomovars II, III, and IV (167). Genomovar II has been renamed *Burkholderia multivorans* and genomovar III, *Burkholderia stabilis* (234). In the *B. cepacia* complex, genomovar III is the most infectious strain in CF patients. Reasons for its

higher virulence include its stronger binding to mucins, to epithelial cells, and to tissue sections from the lungs of CF patients (234;89;28). Since it is the most commonly seen strain of *B. cepacia*, genomovar III was used to mimic *B. cepacia* infections in CF mice models.

The prevalence of *P. aeruginosa* infection is not totally understood. However, it is clear that the initial acute inflammatory response that usually serves as a first line of defense in the normal lung milieu, fails to control *P. aeruginosa* infection in the lungs of CF patients. *P. aeruginosa* acquires a mucoid phenotype between the initial infections or shortly after (309;293). A considerable production of alginate creates a biofilm around the bacteria leading to the encapsulation of microcolonies of *P. aeruginosa* in the lungs (181) protecting the bacteria against the host's defense mechanisms. The development of the mucoid phenotype impedes opsonising antibody, and PMN and macrophage phagocytosis. However, it also contributes to the activation of inflammatory cells and antigen presenting cells. This constant induction of an inflammatory response leads in the long run to a vicious cycle of cellular recruitment to sites of infection (12). In fact, the transfer from an acute to a chronic inflammatory state is shown by continuous PMN infiltration to the lung.

1.1.6.4 Nasal and tracheal electrophysiological profiles

In the CF patients, both the upper (nasal) and lower (trachea, bronchi) airways exhibit hyperabsorption of Na^+ (155) and reduced cAMP-mediated Cl^- secretion (155;296). The hyperabsoption of Na^+ and osmotically linked water absorption of the airway epithelia is thought to play a role in the production of thick, sticky mucus, and possibly in the reduction of the volume of airway surface liquid, thus decreasing mucociliary clearance and predisposing airways to disease. Electrophysiological analyses of nasal and tracheal airway epithelia in mouse models of CF allow the discrimination of mutant mice from wild type mice.

1.1.6.5 Other manifestations of the disease

A relative high number of adult CF patients (20-50%) exhibit some form (mild or severe) of hepatobiliary disease (106). About 2 to 5 % of CF patients die due to complications arising from liver disease (202).

Most male human CF patients are infertile due to obstruction of the vas deferens and distal epididymis (120). In contrast, female CF patients only show a minor reduction of fertility, possibly due to abnormal mucus secretion in the cervix.

In human CF patients, the pathology of the submandibular, sublingual glands, and submucosal glands include dilated ducts, inspissated secretions and atrophy of the acini (106).

Reports describe enamel defects in human CF patients, but the interrelationship between tetracycline discolorations, enamel defects and dental cavities are not obvious (302). However, it appears that some human CF patients have hypomineralized enamel, corresponding to white spots on the teeth (212).

Patients with CF are often of smaller height compared to average and have difficulty regaining weight once it drops. In addition to the malabsorption of fats and proteins, other factors such as increased caloric demands for fighting infection and perhaps breathing may also contribute to this problem (202).

1.1.7 Genotype and phenotype correlation

The genotype/phenotype relationship is not applicable to all the phenotypes observed. Small corrections in the genotype activity can have marked electrophysiological and dramatic pathological consequences (49). Although a strong association between genotype and pancreatic status has been found (ΔF508 homozygous patients show pancreatic insufficiency), no correlation has yet been made between genotype and lung disease. Indeed, CF patients displaying the same CFTR mutation show a remarkable heterogeneity in the severity of their lung disease. The reason for this variation in disease severity is unknown, but it has been proposed to be due to independently segregating modifier genes and/or environmental factors. The study of CF animal models would enable the

verification of this hypothesis. Mice models have proven extremely useful for determining the chromosomal location, physical mapping and cloning of a candidate gene, and subsequent discovery and cloning of the orthologous human gene in other studies (266). Inbred mouse strains have been also useful in the identification of genes other than CFTR that influence the severity of the CF disease, as described in section 1.2.

Soon after the CFTR gene was cloned, a multicenter study done on thousands of CF patients reported that the patients with ΔF508 mutation exhibit pancreatic insufficiency (236). This confirmed the link between the CFTR genotype and pancreatic status. Later on, a series of other mild mutations were associated with pancreatic sufficiency. Mild mutations are usually missense mutations involving exon 5, 7, and 17b of the *Cftr* gene, giving rise to amino acid changes in the first and second transmembrane domains (236). Mild phenotype associated mutations have been shown to have a dominant effect.

Correlations between liver disease, pulmonary disease and CFTR mutations were more difficult to prove. CF patients with ΔF508 mutations exibit different liver phenotypes. Similarly, CF patients with a G542X mutation possess variable liver phenotypes. Therefore, it appears that other factors, such as environmental factors or independently segregating modifier genes influence liver disease in CF patients. Lung disease also seems to depend on factors other than CFTR since ΔF508 patients show heterogenous lung phenotypes and dizygotic twins and siblings genotypically identical exhibit different lung diseases (236).

1.1.8 Reasons for disease severity in humans

1.1.8.1 Nutrition

Early studies of the relationship between malnutrition and survival rate in CF children showed a direct relationship between the two. In the early 80s, a comparative study done between two CF clinics, in Boston and Toronto, showed that patients treated at the Toronto's clinic, due to its high emphasis on nutrition, had higher rate of survival among children (223). As well, pancreatic insufficiency

is linked to maldigestion, malabsorption of nutrients and is associated with intestinal abnormalities. On the other hand, CF is associated with deficiencies in certain fatty acids, independently of the patient's nutritional status. Correcting these deficiencies might have potential beneficial effects for CF patients. Freedman and colleagues have shown that administration of docosahexaenoic acid (DHA) orally to CFTR ^{m1UNC} knockout mice on mixed genetic background reverses the membrane lipid imbalance, increasing phospholipid bound DHA and decreasing phospholipid bound arachidonic acid (AA) (84). Furthermore, this treatment resulted in a reversal of the ileum and pancreatic diseases. The effects of DHA on lung disease remain to be elucidated.

1.1.8.2 Gender

As mentioned earlier, gender plays an important role in the survival rate of CF patients. Female CF patients have a mean survival age about four years shorter than male CF patients (259). The reason for this difference in the survival rate is unknown. However, it has been shown that gender may influence meconium ileus, immune responses and lung disease (115;116;236;315). Studies on the severity of lung disease in girls and boys with CF have shown that girls have a higher mortality rate and a higher rate pulmonary function impairment than boys (54). Bacterial colonization of lungs also seems to be influenced by gender. For some unknown reasons, it appears that girls acquire *P. aeruginosa* earlier than boys, and that they acquire the mucoid form significantly earlier than boys (59). As well, our laboratory has shown that C57BL/6 (B6) female mice are more susceptible to *P. aeruginosa* infection than B6 males (112;59). Females have a higher inflammatory response in terms of the amount of secreted cytokines, which correlated with a higher bacterial load, and a more severe weight loss compared to males. This study confirmed that sex hormones can affect the immune response (46;183), and that females are more prone to bacterial colonization, leading to more severe lung disease in CF. Furthermore, energy expenditure appears to be increased in CF female compared to CF male patients. This represents a good measurable mediator of gender difference in some aspects of CF (259).

Rozmahel and colleagues, showed that the modifer gene influencing the meconium ileus phenotype in CF mice is gender dependent (230). Whether there is a comparable gene for lung disease or a human homologue remains to be determined. Sweezey and collaborators suggested that androgens, estrogens and progestins interact with the upstream regulatory elements of CFTR as well as other proteins important for the regulation of the airway surface liquid composition in rats (270;271;272;273). Progesterone and β-estradiol inhibit cAMP-stimulated chloride conductance in pancreatic cells, and this conductance is also inhibited *in vitro* by transfecting an antisense to CFTR into the cells. Therefore, it seems that progesterone and β-estradiol can reduce the CFTR chloride conductance (271). However, the link between sex hormones and the mutated CFTR genes remains to be established. The same group also showed that female rats have higher levels of the ENaC than male rats. ENaC seems to play an important role in the desiccation of airway secretion in CF rats. Therefore, female rats are at a disadvantage compared to male rats in the secretion of mucus. More studies are needed to verify this hypothesis in other animals, and eventually in humans.

1.1.8.3 Genetic backgrounds

The genetic background seems to play an important role in the regulation of CF disease severity, as illustrated by human polymorphisms resulting in heterogeneity of the CF disease. The impact of the genetic background on infection has been studied in mice. Resistance to *P. aeruginosa* infection was verified in BALB/C, DBA/2, A/J and C57BL/6 mice (187;186;121;98). The BALB/C strain was shown to be resistant to the bacterial infection. It cleared the infection in 3-7 days and strongly recruited inflammatory cells to the bronchoalveolar spaces. The DBA/2 strain was very susceptible to the infection and showed a high bacterial burden, high mortality rate as well as deficient recruitment of the inflammatory cells to the bronchoalveolar spaces. The A/J and B6 strains showed an intermediate degree of susceptibility. Resistant BALB/C mice showed efficient control of the inflammatory response to bacterial invasion, with a pronounced increase in the production of TNF after infection, leading to the recruitment of

PMNs and macrophages to the sites of infection (308;237;186;98;99). These mice also developed chronic inflammation and little tissue damage, a phenotype similar to CF patients who get their airways plugged with *P. aeruginosa* surrounded by PMNs in a cellular exudate. On the other hand, susceptible B6 mice showed acute infection with an exaggerated neutrophilic inflammatory response and extensive tissue damage as well as greater weight loss (275;186;98). This information showed that resistance to *P. aeruginosa* seems to be a dominant trait controlled by more than one gene (121).

Therefore, since B6 mice showed an excessive inflammatory response to *P. aeruginosa* and had a lower mortality rate than DBA/2 mice, they were chosen as a background to mimic lung disease in CF mice models. As mentioned above, B6-CFTR^{tm1UNC} mice is the only mouse model that exhibits spontaneous and progressive lung disease. This confirmed that severity of the lung disease is influenced by the animal's genetic background. A recent study showed that both congenic strains B6-CFTR^{tm1UNC} and BALB/C-CFTR^{tm1UNC} mice demonstrate a neutrophil influx in the lungs (115). However, the difference in lung disease between the two strains seems to lie in neutrophil activation. Neutrophil activation and neutrophil accumulation seem to be regulated by genes mapped outside of the CFTR locus (284). The influence of genetic background was also demonstrated with CFTR^{tm1HSC} mice on a mixed background displaying only 30% survival whereas homozygous CFTR^{tm1HSC} / CFTR^{tm1HSC} mice displayed different rates of survival according to their background (230).

1.1.8.4 Independently segregating modifier genes

The study of the CF disease in CF mouse models with different backgrounds has allowed the mapping of modifier genes, exterior to the CFTR locus. CFTR^{tm1HSC} homozygous mice bred to congenicity on different inbred strain backgrounds led to the mapping of the modifier locus of intestinal disease severity. Genetic linkage analysis indicates the presence of the modifier locus *cfm1* at the proximal region of mouse chromosome 7 (50;147;230). This gene seems to code for an alternative Ca^{2+}-mediated Cl^- secretory pathway in the intestinal tract of

these mice which is able to compensate for CFTR (236;106). This result led to a multitude of studies on modifier loci in humans. The presence of a modifier gene modulating human intestinal disease, designated *CFM1*, was shown by Zielenski and colleagues, in a study conducted on 197 pairs of CF siblings. They showed that *CFM1* was located on human chromosome 19q13 (315). Salvatore *et al.* confirmed the presence of the modifier gene on human chromosome 19 and further stated that this genetic factor could be dominant (236). Another study based on the results from 89 CF humans proposed the hemochromatosis gene as a possible modifier locus for meconium ileus expression (236;226). Studies in both the CF mouse models and in CF patients showed that the loci modulating intestinal disease are not involved in modulating pulmonary expression.

There is preliminary evidence supporting the existence of modifying genes contributing to the heterogeneity of CF lung disease (128;122;93;26;3). For example, it was noticed that monozygotic CF twins show an increased concordance of lung disease severity versus dizygotic CF twins. Since only a few mouse models exhibit signs of lung disease, it took longer to identify the modifier gene locus regulating the pulmonary phenotype than for that regulating meconium ileus. Kent *et al.*, by developing the B6-CFTR^{tm1UNC} mouse model, showed that secondary genetic factors can influence the severity of the lung disease in the CF mice (147). Haston and colleagues used quantitative trait loci (QTL) analysis based on the genome scan of B6 and BALB/C CF mice, to identify a region on mouse chromosome 6 as a putative genetic locus (115). A number of genes mapped to the QTL region in mouse may influence CF lung disease. These genes code for α1-antitrypsin 1-4, phospholipase A2 group VII; lymphocyte antigens 9, 14, 39, and 55; IL-13 receptor α1; tissue inhibitor of metalloproteinase; collagen Xα1; laminin α2; histocompatibility 9, 25, 60; and transforming growth factors β2 and β3. As well, possible candidate genes also include estrogen-related receptorβ, and estrogen receptor which are modifier genes of sex related susceptibility.

A number of studies have also evaluated the candidate genes regulating lung pathology in CF human patients. Due to the high complexity of the pulmonary phenotype, candidate genes have been proposed at different levels: in susceptibility

to infection, inflammatory response, mucociliary clearance, epithelial tissue repair and damage as well as at the molecular level, providing alternative chloride conductance, regulating splicing and also regulating the expression of CFTR. A first group focused on the genes involved in the local innate and adaptive immune responses and in inflammation. They proposed polymorphisms in genes coding for anti-*P. aeruginosa* IgG3, TNF, glutathione transferase M1, M3 and P1, nitric oxide synthase, mannose-binding lectin protein, and/or tumor growth factor β (TGFβ) to modulate lung disease severity (3;93;128;236). A second group focused on the role of α-1-antitrypsin (A1AT) as a modifier gene. Mahadeva *et al.* reported that A1AT deficiency is not associated with a more severe pulmonary disease, whereas other groups reported a higher risk of infection for CF patients carrying the A1AT deficiency. (122;171;170;236). A third group proposed genes involved in the composition of the airway surface liquid (ASL). These genes code for surfactant proteins A1 and A2 (236;93). Finally, genes coding for hBD1 and hBD2, beta defensins, have been proposed as modulators of airway infection. It is clear that the heterogeneity of the lung disease phenotype is controlled by a multitude of factors, including genetic and environmental.

The liver phenotype also seems to be associated by secondary genetic factors. A study done in CF patients showed that mutations of the mannose-binding lectin gene alter the severity of liver disease (88). Another study showed by mutagenesis that the A1AT protease inhibitor, hemachromatosis and TGFβ genes are possible modifier genes (236). They further demonstrated that the A1AT and the mannose-binding lectin genes act as independent risk factors for CF liver disease. They also showed that there is a variant that overexpresses TGFβ and interacts with A1AT gene mutations, thereby increasing the adverse effect of both genes on CF expression. Another distinctive trait of CF is lower body weight. Haston and colleagues used QTL analysis to map the genetic factors influencing the weight of CF knockout mice (114). Body weight is a genetically complex trait, influenced by gender: QTL showed that five loci influencing body weight were detected, with four out of the five acting in a sex-specific manner. Significant linkage was made to chromosome 13 and suggestive loci were also found on chromosomes 1, 6 and 7.

Haston and colleagues hypothesized that regulation of fatty acid processing and lipid storage may influence the body weight of CF mice. A number of genes playing a role in fatty acid processing have been found in the linkage regions. These genes include peroxisome proliferator-activated receptor γ (sex specific), insulin-like growth factor-1, phospholipase A2 group IVA, adrenergic receptor β kinases 1 and 2 and fatty acid coenzyme A ligase. However, further studies need to be done to determine which specific gene plays a role in CF mice, and whether it has homologous function in CF patients.

Genetic backgrounds and independently segregating modifier genes play an important role in the severity of a number of phenotypes associated with CF. Some of these genes have been identified but a number of them remain to be discovered. Identification of all modifier genes will permit a better understanding of the clinical heterogeneity of CF.

1.1.9 Relationship between CFTR basic defect and lung disease

The mechanisms by which CFTR mutations cause lung disease remain uncertain. A number of mechanisms have been proposed to explain the link between CFTR defect and the clinical disease, such as abnormal airway surface liquid composition, defective airway submucosal gland secretion, defective intracellular vesicle function, loss of CFTR regulation of other transporting proteins, defective intrinsic antimicrobial function, hyperabsorption of airway fluid, excessive inflammatory responses and others (278). There is no consensus on which mechanism predominates.

1.1.9.1 Role of CFTR in determining the volume or ionic composition of ASL lining the lung epithelia.

Defective CFTR has been hypothesized to be linked to abnormal ASL composition, low ASL volume and/or low ASL secretion. Abnormal ASL composition can be further subdivided into three hypotheses: the "high-salt hypothesis", the "low-pH hypothesis" and the "low-oxygenation hypothesis". These hypotheses are not mutually exclusive. Welsh and Smith proposed the

"high-salt hypothesis", emphasizing the role of CFTR as an anion channel. They proposed that defective CFTR causes reduced transepithelial Cl^- conductance, resulting in high levels of salt in ASL (299). High salt concentrations were further hypothesized to inhibit the activity of the antimicrobial β-defensins 1 and 2, as well as lysozymes. The "low-pH hypothesis" suggests that the ASL is abnormally acidic, inhibiting mucociliary clearance mechanisms (37). Another hypothesis, the "low-oxygenation hypothesis", suggests that ASL oxygen content is lower in CF patients due to higher oxygen consumption and to slower oxygen diffusion in the ASL. This might be in turn the event which triggers biofilm formation by the non mucoid strain of *P. aeruginosa*, resulting in chronic infection. Boucher and colleagues proposed the "low volume hypothesis", emphasizing CFTR's ability to inhibit the activity of the epithelial Na^+ channel on the apical surface. This hypothesis suggests that a defective CFTR protein results in an increase in Na^+ transport, accompanied by Cl^- and H_2O absorption due to osmosis. This results in a decrease in ASL volume, dehydration and mucociliary dysfunction (286;299). Finkbeiner and colleagues on the other hand proposed that defective CFTR results in reduced fluid secretion by airway submucosal glands, explaining the "low secretion hypothesis".

Testing in mice has proven difficult since the majority of CF mouse models develop little or no lung disease and have important physiological differences in their airways compared to humans due to the fact that the airway epithelium of many strains of mice expresses alternative Cl^- channels and contains almost no submucosal glands (214;286). Furthermore, harvesting the ASL is technically difficult, and different techniques (filter paper and capillary methods, micropipettes, ion-sensitive microelectrodes, radio-tracer dilution method, microdialysis and ion-sensitive fluorescence indicators) have given variable results (286). Using capillary electrophoresis, we showed that B6-$CFTR^{tm1UNC}$ mice exhibit no significant differences with controls in ASL ionic composition. However, when infected with *P. aeruginosa*, control mice showed an increase in the salt concentration of ASL (41). Other studies, using fluorescence measurement and X-ray microanalysis, showed that CFTR mutation does not affect the ASL salt

concentration (310;286;136;137;138). Lower ASL Cl^- concentration in CF mice compared to wild type mice has also been reported (178). Furthermore, no difference in the pH of ASL has been seen between CF mice and their control littermates. Therefore, it seems that the majority of studies report no difference between the ASL ionic composition of uninfected CF mice and that of control mice. However, most of the studies were done in the upper airways of the CF mice, whereas it has been suggested that airway disease begins in the lower airways (286). Studies of the ASL in other animal models have suggested that the ASL depth is abnormal in CF, resulting in impaired mucociliary clearance. A similar abnormality might be present in CF patients.

1.1.9.2 CFTR: receptor for *P. aeruginosa* lipopolysacharide (LPS)?

Pier and colleagues proposed that CFTR is an epithelial receptor for the outer-core oligosaccharide of *P. aeruginosa* (206). They hypothesized that CFTR is like a pattern-recognition ligand that internalizes the bacteria after recognition. Internalization of *P. aeruginosa* by the epithelial cells results in shedding of the cells, which leads to bacterial clearance by mucociliary transport. This mechanism has been proposed to have a protective role in the normal lung and to be defective in CF. This hypothesis was tested in mice models by Schroeder and colleagues, who showed that transgenic CF mice have reduced clearance of *P. aeruginosa* due to decreased cellular internalization of the bacteria. (242). Chronos and colleagues in contrast to Schroeder and colleagues, demonstrated that the transgenic mice and wildtype mice exhibit equal clearance of *P. aeruginosa* (242;33). Chronos and colleagues used a mucoid strain of *P. aeruginosa* which has been suggested to have lost the bacterial ligand for CFTR.

1.1.9.3 Relationship between infection and inflammation

The relationship between inflammation and infection is complex. The interest in the role of inflammation in determining the outcome of *P. aeruginosa* infection was first aroused by the fact that CF patients using high doses of steroids and of non-steroidal anti-inflammatory drugs (such as ibuprofen) showed a

significant slowing in the rate of decline of lung function (149;139). In contrast, studies done in young children have suggested that inflammation occurs independently of infection. High levels of pro-inflammatory cytokines and neutrophils and free elastase activity were reported in the BAL of CF infants in the absence of *Pseudomonas* infection (169;99;84;85). As well, the development of progressive inflammatory lung disease in the congenic strain B6 *Cftr* knockout (KO) mice, without bacterial infection, suggests that inflammation is independent of infection. It was also reported that the severity of pulmonary disease induced by *P. aeruginosa* may vary from one patient to the other, even though they carry the same CFTR mutation (84;50). This heterogeneity in the severity of the lung disease suggests the presence of modifier genes exclusive of the CFTR locus and/or of environmental factors. A recent study done using an *in vivo* model based on the maturation of human fetal CF and non-CF small airways in severe combined immunodeficiency mice has shown that inflammation may occur independently of infection, due to a dysregulation in neutrophil recruitment (278).

1.1.10 Remedies and treatments

The treatment of CF depends upon the stage of the disease and the organs involved. Clearing mucus from the lungs is an important part of the daily CF treatment regimen. Chest physical therapy is a form of airway clearance done by vigorous clapping on the back and chest to dislodge the thick mucus from the lungs[4]. Other types of treatments include tobramycin solution, an aerosolized antibiotic used to treat lung infections; azithromycin, an antibiotic recently proven to be effective in people with CF whose lungs are chronically infected with the common *P. aeruginosa* bacteria [5] and Pulmozyme®, a mucus-thinning drug shown to reduce the number of lung infections and improve lung function. In addition,

---

[4] Airway clearance techniques such as tapping or "clapping" the chest and the back vigorously (percussion) or PEP (positive expiratory pressure) or Mask Therapy to help loosen the mucus which clogs the lungs;

[5] taking antibiotics in pill, intravenous (IV), and or inhaled forms, to ease congestion and protect against and fight lung infection;

approximately 90% of all CF patients take pancreatic enzyme supplements to help them absorb nutrients in digestion[6]. Overall, for persons with CF, life includes a daily routine of therapy as well as day-to-day management of infections and periodic visits to a CF clinic. Otherwise, most individuals with cystic fibrosis lead ordinary lives, for many years, in terms of education, physical activity, and social relationships. Eventually, however, lung disease places increasing limits on daily life and can lead to lung transplantation when possible.

The different possible therapeutics which are currently under study, in clinical trials or already available to patients are mentioned below;

1.1.10.1 Antimicrobial agents

- TOBI; aerosol antibiotic
- AZITHROMYCIN; oral antibiotic
- CP-A1-002 (aztreonam); intravenous antibiotic
- *Pseudomonas* vaccines
- MP-610,205; bacterial efflux pump inhibitor that may increase the effectiveness of antibiotics
- SLIT-amikacin; liposomal formulationof the antibiotic amikacin

1.1.10.2 Mucus regulation

- Pulmozyme
- Hypertonic saline
- Lomucin

1.1.10.3 Gene therapy – stem cells based intervention (Adeno associated virus, compacted DNA)

The basis for the gene therapy strategy for CF is the prevention of disease development by direct replacement of CFTR gene function (50). Gene therapy has

---

[6] taking pancreatic enzymes with all meals, to aid digestion; taking nutritional supplements and vitamins to promote good nutrition;

been focused on lung pathology because it is the most common cause of mortality among CF patients. To date, the gene delivery systems used have included recombinant adenoviruses, recombinant adeno-associate viruses (AAV), lentiviruses, Sendai viruses and cationic lipids (50;52;305). CF mice models have been used to test the efficiency and safety of these different ways of delivery. It has been difficult to address which cells to target in the lungs since the pathogenesis of CF in mice and humans is not totally understood. The airway epithelium and the submucosal glands have been the best candidates, according to the different hypotheses emitted so far on lung disease (ASL composition, low secretion, etc.) as explained before (24;20).

1.1.10.4 CFTR protein rescue

- Gentamicyn
- Curcumin; correct abnormal processing of CFTR in the cell
- PTC124; promotes read-through of premature truncated codons in the CFTR mRNA
- Vertex/UCSF; correctors of the CFTR traffickingdefect or potentiators of CFTR-mediated transport

1.1.10.5 Ion transport restoration

- INS37217; correct the ion transport defect in CF
- SPI-8811; oral agent believed to bypass transport defect of Cl- ions
- Moli 1901; thought to affect the ion transport defect in CF patients
- Parion 552-02; thought to correct the CF ion transport defects by acting primarily on abnormal
- INO 4995; thought to correct the ion transport defect by acting on both the abnormal chloride and sodium transport

1.1.10.6 Nutrition

- theraCLEC; non-porcine pancreatic enzyme replacement
- yasoo; oral antioxidant vitamin formulation for CF patients.

1.1.10.7 Anti-inflammatory

- DHA; infant formula fortified with DHA on pathogenesis of CF in newly diagnosed patients
- Nacystelyn; antioxidant
- HE-2000; oral immune-regulating hormone
- SIMVASTIN; HMG-CoA reductase inhibitor that increases nitric oxide production

1.1.10.8 Early screening – early intervention – prevention

Prior to any symptoms of CF and treatments to obliterate these symptoms, all diagnosed patients should be informed how to follow preventive measures to avoid or at least to delay infection that in most cases is inevitable. They should be made aware of how to avoid getting or spreading microorganisms.

1.1.10.9 Complementary and alternative therapy

Lung transplantation is a difficult and personal decision; however, it is sometimes the only resort left to sustain the life of CF patients whose lungs lost the function to the extent that they can no longer provide support to cardiovascular system.

1.1.11 Clinical Research

Since the discovery of the CFTR gene, research teams around the world have focused on finding a cure for CF. The major advances are listed in Table 1.1.

1.2 Animal models to study CF

Since the description of cystic fibrosis in 1939, our understanding of the molecular and biological basis of CF has become more comprehensive in part due to the study of animal models. It must be noted that animal models often differ in their expression of the disease as compared to humans. For example, some strains of *Cftr*-KO mice models do not display pancreatic insufficiency which is prominent in CF patients, due to the presence of an alternative murine chloride channel that can partially compensate for the mutated CFTR gene. However, animal models represent a good surrogate for the complexities of the human system. The animal models used to study CF include mouse, rat, ferret, rabbit, sheep, pig and cat (241;193). Mice used as an animal model have several advantages; they share 78% homology with humans in the CFTR protein, the cost of their purchase and maintenance although very high is still relatively inexpensive

Table 1.1 Cystic fibrosis research progression since the gene discovery in 1989*

1989	Cystic Fibrosis Foundation-supported scientists discovered the gene that, when defective, causes cystic fibrosis (CF), and the gene's defective protein product - the Cystic Fibrosis Transmembrane conductance Regulator (CFTR).
1990	Researchers made a "normal" copy to the CF gene and used it to correct human CF cells *in vitro*.
1991	New drugs that target the CF cell defect continue to be tested.
1992	Scientists designed and tested various new methods of gene therapy in the laboratory to deliver normal genes to the lungs and nasal passages of people with CF.
1993	1) Landmark human gene therapy studies for CF began, assessing safety and efficacy of the adenovirus as a gene delivery system. 2) In the first published CF gene therapy study, University of Iowa scientists reported that CF cells could be corrected by gene therapy in people with the disease. 3) Pulmozyme®- the first new drug developed to treat CF in 30 years - was approved by the Food and Drug Administration (FDA) only five years after it was made in the lab. The CF Foundation played an integral role in the research by assisting in the recruitment of clinical trial participants.
1994	The first repeat doses of gene therapy were given to individuals with CF (treating nasal passages).
1995	1) Results from a four-year CF Foundation-sponsored clinical trial showed that - under controlled conditions - high does of ibuprofen reduced the rate of lung inflammation in people with CF. 2) The first aerosolized adeno-associated virus (AAV) CF gene therapy protocol began. 3) The first non-viral CF gene-delivery system, using liposomes (fat capsules), began.
1996	University of Iowa researchers reported that antimicrobial peptides found in the lungs - which are partly responsible for warding off infections - may be compromised by high concentrations of sodium (salt), possibly explaining the frequency of bacterial infections in the lungs of people with CF.
1997	1) In partnership with the University of Washington and the PathoGenesis Corporation (now Chiron), CF Foundation-supported scientists began to map the genetic structure (genome) of the bacterium, *Pseudomonas aeruginosa*, the most common source of CF lung infections. 2) The FDA approved the drug, TOBI® (tobramycin solution for inhalation) as a treatment for CF lung infections. Clinical trial results showed that this reformulated version of the common antibiotic improved lung function in people with CF and reduced the number of hospital days. TOBI® is delivered in a more concentrated dose directly to the site of the CF lung infections and is preservative-free.
1998	1) The CF Foundation created the Therapeutics Development Program to provide matching research awards to biotechnology companies to stimulate the development of new CF therapies. Through a new Therapeutics Development Network (TDN) of seven specialized CF centers, this program provides the resources and infrastructure needed to conduct CF clinical trials in the early phases. 2) INS365 (now INS37217) became the first drug to begin clinical trials through the TDN. The drug appears to enhance lung secretions by improving chloride movement in CF cells. 3) A 10-year CF Foundation investment facilitated high-throughput screening for CF by scientists at the University of California at San Francisco. This technology enables researchers to test more potential CF drug compounds in one day, than once possible in a year.

1999	1) The TDN's Coordinating Center at the University of Washington was endorsed by the National Institutes of Health and received a $3.4 million grant. 2) The CF Foundation established its own Data Safety Monitoring Board to monitor patient safety parameters of both CF Foundation-supported and TDN-facilitated clinical trials.
2000	1) Cystic Fibrosis Foundation Therapeutics, Inc. (CFFT) was established as the nonprofit drug discovery and development affiliate of the CF Foundation. 2) A milestone-driven research award of up to $46.9 million was made by CFFT to what is now Vertex Pharmaceuticals to bring high-throughput screening to the CF drug discovery effort.
2001	1) A microchip containing the entire genetic map of *Pseudomonas aeruginosa* was made available to CF researchers to accelerate the study of the organism's genes. A collaborative Internet-based system - supported by CFFT - was established at the University of North Carolina at Chapel Hill. 2) CFFT made a multi-million dollar investment to develop a more efficient and patient-friendly pancreatic enzyme supplement called TheraCLECTM Total that has the potential to benefit nearly all CF patients.
2002	1) Results from the CFFT-supported Phase III clinical trial on azithromycin showed that patients with CF who took the antibiotic experienced an almost 50 percent reduction in hospitalizations, a significant improvement in lung function, and weight gain. 2) Targeted Genetics announced encouraging results from a Phase II CF gene therapy clinical trial using the AAV. Safety and tolerability of the therapy was demonstrated as well as the first-ever evidence of lung function improvement after gene transfer. 3) CFFT awarded funding to six teams of scientists from around the world to search for new molecular targets in CF cells using cutting-edge proteomics (the study of proteins). 4) The TDN expands to 14 centers to accommodate the growing number of CF clinical trials and to provide greater geographic opportunities for individuals with CF to participate in clinical trials.
2003	1) The TDN expanded again from 14 to 18 clinical research centers. 2) CFFT-supported scientists determined the three-dimensional structure of an integral part of the CFTR protein, opening the door to the design of drugs to correct defective CFTR. 3) A new form of CF gene therapy showed promise in Phase I clinical trials; it uses compacted DNA rather than a virus to get healthy genes into CF cells. 4) Targeted Genetics launched a Phase IIb clinical trial using the AAV; this trial represented the largest, most advanced gene therapy trial to date in CF.
2004	1) Researchers at Beth Israel Deaconess Medical Center in Boston reported a strong link between the CFTR protein and fatty acid imbalances in the cells of people with CF, suggesting a strong therapeutic direction. 2) In a Yale University study, curcumin (a component of the spice turmeric) appeared to correct CFTR function in mice that had the DeltaF508 mutation; a clinical trial of curcumin in humans is planned. 3) Encouraging results were obtained in a Phase II clinical trial of INS37217, demonstrating both safety and improvements in lung function. 4) With the CF Foundation's encouragement and assistance, the FDA announced that it is now requiring manufacturers of pancreatic enzyme supplements to obtain FDA approval for their products; an FDA review found that inconsistencies in the formulation, dosage and manufacturing processes could significantly compromise the safety and effectiveness of the drugs in patients.

* These data where taken from Cystic Fibrosis Foundation website (www.cff.org)

compared to other larger animal models. Moreover, they reproduce faster than most other animal models and they can be easily genetically modified into transgenic, knockout or well-defined inbred strains. Furthermore, they offer a significant advantage over other animal models in terms of the availability of experimental tools (specific antibodies, SNPs, microsatellites). Monoclonal antibodies against important mouse inflammatory and immunological molecules, recombinant cytokines, and other tools are readily available because mice have been extensively used as animal models for a number of other infectious and inflammatory diseases. Therefore, the following section will focus mostly on the different CF mouse models generated to date and their applications and will then summarize briefly the other animal models that have been used to study CF.

1.2.1 CF mouse models

1.2.1.1 Genotypes

Only three years after the CFTR gene was identified and cloned, the generation of the first CF mouse model was reported (256). Several other models were created shortly after. To date, eleven CF mouse models have been characterized (Table 1.2). All of the CF mouse models have been generated by the same general technique, using gene targeting in embryonic stem cells to disrupt the endogenous CFTR genotype. Two types of gene targeting have been done: the first one used a replacement strategy to disrupt the CF gene, creating in most cases absolute nulls, with no normal CFTR protein production. This strategy led to the production of six mouse models. The second type of gene targeting used insertion into the target gene without loss of any genomic sequence, resulting in mutants expressing low levels of WT *Cftr* mRNA. Five mouse models were developed using that approach. These models allowed establishing animal models for the two most common human mutations: ΔF508 and G551D.

Table 1.2 Cystic fibrosis mouse models

	Mutation	Usefulness
$CFTR^{tm1UNC}$	Exon 10 replacement	Survival rates, using a liquid-nutrient diet and colyte
	No CFTR mRNA detectable	Transgenic mice containing FABP-hCFTR gene to correct intestinal disease Susceptibility to *S. aureus, B. cepacia, P. aeruginosa* Resistance to *V. cholerae* Congenic strain B6 (lung disease) and BALB/C
$CFTR^{tm1HGU}$	Exon 10 insertional	Susceptibility to *S. aureus, B. cepacia, P.aeruginosa*
	10% of wt CFTR mRNA	
$CFTR^{tm1CAM}$	Exon 10 replacement	Transgenic mice containing hCFTR gene to correct
	No CFTR mRNA detectable	intestinal pathology Resistance to *V. cholerae*
$CFTR^{tm1BAY}$	Exon 3 insertional duplication <2% wt CFTR mRNA	
$CFTR^{tm3BAY}$	Exon 2 replacement No CFTR mRNA detectable	
$CFTR^{tm1HSC}$	Exon 1 replacement No CFTR mRNA detectable	Modifying genes for meconium ileus
$CFTR^{tm1EUR}$	ΔF508 exon 10 insertional	
	'hit and run' Mutant CFTR mRNA normal levels	
$CFTR^{tm2CAM}$	ΔF508 exon 10 replacement Mutant CFTR mRNA 30% of wt levels	Resistance to *S. typhi*
$CFTR^{tm1KTH}$	ΔF508 exon 10 replacement Mutant CFTR mRNA Low in intestine	Susceptibility to *P. aeruginosa*
$CFTR^{tm1G551D}$	G551D exon 11 replacement Mutant CFTR mRNA 53% of wt levels	Susceptibility to *P. aeruginosa*
$CFTR^{tm2HGU}$	G480C exon 10 insertional 'hit and run' Mutant CFTR mRNA normal levels	

Snouwaert and colleagues and Clarke and collaborators generated the first CF mouse model of CF at the University of North Carolina in 1992 (256;34). The endogenous CFTR gene in murine embryonic stem-cell lines was targeted so that the resulting disrupted CFTR gene contained a stop codon in the coding sequence of exon 10. The targeted cell lines were introduced into early C57BL/6/129 mouse embryos and transferred to B6D2/129 pseudopregnant foster mothers. The resulting offsprings were mated to B6D2/129, C57BL/6/129 or BALB/C/129 mice to generate heterozygotes, which were crossed to produce homozygous offspring, named $CFTR^{tm1UNC}$ knockout mice. The $CFTR^{tm1UNC}$ knockout mice possessed two copies of the defective gene resulting in an absence of the protein CFTR. The survival rate of these mice was very low; less than 5% survived to maturity. The original strain of $CFTR^{tm1UNC}$ knockout mice had a mixed genetic background.

Later, studies showed the importance of the genetic background. Kent and colleagues hypothesized that the mixed genetic background of the $CFTR^{tm1UNC}$ original strain may influence the development of lung pathology (147). Therefore, $CFTR^{tm1UNC}$ mice heterozygous at the *Cftr* locus were backcrossed onto the B6 background for eighteen generations to ensure 100% homozygosity for B6 strain alleles, as determined by microsatellite typing. The novel congenic strain was designated B6-$CFTR^{tm1UNC}$/$CFTR^{tm1UNC}$ knockout mouse (147). This mouse model was recently further characterized in relation to the CF multiorgan phenotypes (71) as well as in terms of inflammatory response using a less invasive infection technique (110).

At about the same time as $CFTR^{tm1UNC}$ knockout mice were produced, Dorin and colleagues generated another strain of knockout mice on an MF1/129 genetic background, designated $CFTR^{tm1HGU}$, by insertional mutagenesis targeted to exon 10 of the *Cftr* gene (66;65). However, in the $CFTR^{tm1HGU}$ CF mouse, because of the targeting strategy used (insertional rather than replacement gene targeting), exon skipping and aberrant splicing produced about 10% normal *Cftr* mRNA, resulting in a much milder disease phenotype. About 95% of the mice survived to maturity.

Ratcliff and colleagues created another strain of *Cftr* mutant mice, on a mixed genetic background of MF1/129 and C57BL/6/129, using a strategy similar to the North Carolina group, by replacement mutation of exon 10, resulting in a null mutation (220). The phenotype of these mice, designated $CFTR^{tm1CAM}$, is very similar to that of the $CFTR^{tm1UNC}$ knockout mice except that it further exhibits lacrimal gland pathology.

Researchers in Texas and Iowa have generated a C57BL/6/129 CF mouse, designated $CFTR^{tm1BAY}$ by duplication of exon 3 in the mouse *Cftr* gene. These mice produce less than 2% of normal levels of wild type mRNA, but exhibit a severe phenotype with a high mortality rate. Forty percent of the *Cftr*-KO mice survived past day 7 (198). Two years later, Hasty and colleagues, by replacement of exon 2, created another null mutation mouse model, designated $CFTR^{tm3BAY}$. The $CFTR^{tm3BAY}$ knockout mice showed 40% survival rate at one month of age.

Rozmahel and colleagues generated another strain of *Cftr*-deficient mice, designated $CFTR^{tm1HSC}$ knockout mice, by disruption of exon 1 of the *Cftr* gene. Initially, these mice were generated on a mixed genetic background and displayed a severe phenotype with only 30% survival (230). In subsequent studies, the original founder mouse was crossed with different inbred strains to generate F1 mice of different genetic backgrounds, and the heterozygous F1 mice were intercrossed to produce homozygous $CFTR^{tm1HSC}$ / $CFTR^{tm1HSC}$ knockout mice. According to their genetic background, these knockout mice expressed different disease severity and survival rates.

In general, most CFTR mutations in humans result in loss of function due to abnormal processing of CFTR and failure to insert CFTR into the plasma membrane. The *Cftr* gene knockout mice mimic these forms of CF. However, the importance of creating a ΔF508 CF mouse model stems from the fact that this mutation is the most commonly encountered among CF patients. The study of this particular mutation in animal models might give insight into novel therapies for CF patients. Models for the CF ΔF508 mutation have been generated by introducing this mutation into the endogenous mouse *Cftr* gene.

Van Doorninck *et al.* have generated a ΔF508 mice model by inserting the mutation into exon 10 using a double homologous recombination ("hit and run") technique. The mice generated on a FVB/129 background, designated $CFTR^{tm1EUR}$, are viable. They do not show severe disease, possibly explained by the presence of the mutant CFTR protein at normal levels, which could provide enough residual function. Several studies have shown that the ΔF508 CFTR protein exhibits partial function as a Cl^- channel, with a similar conductance and a decrease in open channel probability (47). Colledge and colleagues also generated ΔF508 knockout mice by replacement of exon 10 on a C57BL/6/129 background. In contrast to the null mutants $CFTR^{tm1CAM}$ that experienced only 20% survival, these ΔF508 mutants, designated $CFTR^{tm2CAM}$, exhibited approximately 65% survival. This higher rate of survival was most likely due to the fact that $CFTR^{tm2CAM}$ express about 30% of the normal level of mutant *Cftr* mRNA (220). Zeiher and collaborators generated ΔF508 knockout mice by replacement of exon 10 on a C57BL/6/129 background, using the same method as Colledge and colleagues. However, the knockout mice, designated $CFTR^{tm1KTH}$, had a survival rate of 40% only, and expressed nearly no mutant mRNA levels in the intestinal tract (312).

A CF mutant mouse carrying the human G551D mutation in the *Cftr* gene has also been generated (58). The G551D mutation is a class III mutation, affecting the regulatory domain of the CFTR protein (236). $CFTR^{tm1G551D}$ was generated by replacement of exon 11 in CD1/129 mice, and showed 27% survival under normal conditions. The mutant *Cftr* mRNA expression resulted in a residual activity of about 4%.

The most recent mouse model was developed to mimic the human mutation G480C (60). Dickinson and colleagues have generated a G480C mouse model by inserting the mutation in exon 10 using a double homologous recombination ("hit and run") technique. The mice, designated $CFTR^{tm2HGU}$, were generated on a C57BL/6/129 background and normally survive to maturity. As for $CFTR^{tm1EUR}$, their high rate of survival could be related to the use of the hit and run strategy, resulting in expression of normal levels of a mutant CFTR protein.

1.2.1.2 Phenotypes

1.2.1.2.1 Intestinal disease

An intestinal phenotype appears to be the hallmark of all CF mouse models. With the exception of $CFTR^{tm1HGU}$, $CFTR^{tm1EUR}$ and $CFTR^{tm2HGU}$, all models show a fairly severe pathology. Most models show abnormal electrophysiological profiles, runting and failure to thrive, goblet cell hyperplasia, mucin accumulation in the crypts of Lieberkuhn, crypt dilatation and intestinal obstruction with resultant perforation, peritonitis and death (58;72;117;198;230;256;281). Intestinal obstructions are physiologically very similar to the meconium ileus observed in CF humans. As well, CF mouse models have similar electrophysiological profiles as CF humans: they both show decrease in the baseline transepithelial potential difference and decrease in the cAMP stimulated Cl^- secretions. Therefore, it seems that CF mice models mimic well the intestinal disease observed in humans with CF.

$CFTR^{tm1UNC}$ mice developed severe bowel disease, which led to intestinal obstruction, perforation, fatal peritonitis and death of all but one mouse before 40 days (256). Other studies using the $CFTR^{tm1UNC}$ mice reported milder pathology in the duodenum (256;72). The ileocecal and large intestinal regions appear to be the most common sites of intestinal blockage and rupture in the most severely affected mouse models. CFTR ^{tm1UNC} models also showed a defect in the production of HCO_3^- in the duodenum and jejunum (105;106). HCO_3^- is important to protect the intestinal mucosa from the acid produced by the stomach. The intestinal phenotype of $CFTR^{tm1CAM}$ knockout mice is similar to that of $CFTR^{tm1UNC}$ knockout mice and they also have similar high mortality and intestinal obstruction. $CFTR^{tm1BAY}$ mice also exhibit a severe phenotype with high mortality and intestinal obstruction. The intestinal pathology is characterized by hyperplasia and eosinophilic concretions in the crypts (198). The ileocecal region appears to be the most common site of intestinal blockage. $CFTR^{tm1HSC}$ mice (even if generated on a mixed background) displayed a severe phenotype with intestinal obstruction and only 30% survival. Homozygous $CFTR^{tm1HSC}$ / $CFTR^{tm1HSC}$ mice demonstrated different severities of

the intestinal disease and survival according to their background, as will be discussed in the subsequent section (230).

$CFTR^{tm1HGU}$ mice showed no apparent intestinal obstruction and therefore 95% of these animals survived. Due to insertional mutagenesis, these mice expressed up to 20% wild type *Cftr* mRNA in the intestine (65). In their jejunum, the cAMP-mediated Cl^- secretory response was only reduced by about 50% compared to normal mice. However, they exhibited abnormalities of the colon. As well, $CFTR^{tm1EUR}$ mice exhibit no reduction in their life span due to intestinal complications, and show a nearly normal Cl^- secretory response to increases in cellular cAMP. This ΔF508 mouse expresses levels of mRNA for the mutant CFTR protein comparable to the levels of wild type CFTR in control animals (86). Furthermore, it was proposed that the high level of ΔF508 CFTR mRNA may allow more of the mutant CFTR to be correctly processed, allowing more functional protein to reach the plasma membrane. $CFTR^{tm1KTH}$ and $CFTR^{tm2CAM}$ exhibit a marked reduction in the CFTR mutant mRNA levels in the intestinal epithelia (38;312) and showed only mild pathology.

The $CFTRt^{m1G551D}$ mouse exhibits a very small cAMP mediated Cl^- secretory response (4-5% of normal) in both the small and large bowel (58). Although this mouse model has a significant mortality due to intestinal complications (67% survival in specific pathogen free (SPF) conditions), the reported rate of survival is much higher than observed in most other CF mouse models. Studies in humans also show less occurrence of meconium ileus in G551D compared to ΔF508 mutants (113).

The high mortality of most CF mouse models due to intestinal obstruction has limited the utility of these mice models. Survival has been shown to be influenced both by diet and housing conditions (148;147;72). Placing the $CFTR^{tm1UNC}$ KO mice on a nutrient-rich liquid diet to minimize intestinal obstructions greatly increased their survival (148). As well, placing $CFTR^{tm1G551D}$ mice under SPF conditions limited their intestinal obstruction and improved their survival rate from 27% in a conventional animal facility to about 60% under SPF conditions (58). Furthermore, it has been shown that substituting drinking water

with an electrolyte solution containing 6% polyethylene glycol (colyte) allows consumption of normal mouse food and also greatly prolongs the life span of the $CFTR^{tm1UNC}$ mouse in a way similar to giving them nutrient-rich liquid diet (105). The colyte is advantageous in that it is much less expensive and requires less demanding conditions than giving peptamen.

Previous studies have shown that the threshold of CFTR activity required to eliminate intestinal pathology is quite low, since as little as 5% of murine CFTR expression can restore normal survival in mice (70;58). Based on this observation, a number of studies have tried to restore normal intestinal function by inserting human CFTR into the intestine of mouse KO. In one study, an hCFTR cDNA was targeted to the KO mouse CFTR locus using a "knock-in" replacement strategy (229;228). The CF mouse showed no improvement in either intestinal disease or survival. A second study used a yeast articifical chromosome to express the hCFTR gene in a $CFTR^{tm1CAM}$ mouse model (173). cAMP-stimulated Cl^- secretion was increased and the survival of these mice was normal. A third study done by Whitsett and colleagues showed also promising results (313). Human CFTR (hCFTR) was expressed in the $CFTR^{tm1UNC}$ mice under the control of the rat intestinal fatty acid-binding protein gene promoter (FABP). The mice survived and showed partial correction of the intestinal pathology, with functional correction of ileal goblet cells, of crypt cell hyperplasia and of cAMP-stimulated Cl^- secretion. hCFTR was most abundant in the ileum, jejunum, and duodenum, with much less expression in the cecum. Unlike wild type CFTR, the hCFTR mRNA was not expressed in the crypts but rather in the villi. Transfer of the hCFTR increased the mouse survival and could be a useful strategy to correct physiological defects in patients with CF (313). Furthermore, FABP-hCFTR mice represent a unique model system because they have corrected intestinal symptoms displayed by CF mice, but they still retain some of the other phenotypes associated with CF mice.

Another method was developed, based on this technique, to correct the intestinal pathology in $CFTR^{tm1CAM}$ transgenic mice (70). Bedwell's group constructed a trangenic mouse with a null mutation in the endogenous CFTR locus ($CFTR^{tm1CAM}$) that also expressed a human CFTR-G452X cDNA under the control

of FABP. In a previous study, Bedwell and colleagues showed that aminoglycoside antibiotics could suppress premature stop mutation in the CFTR gene in a human bronchial epithelial cell line (11). They then investigated whether the daily administration of aminoglycoside antibiotics (gentamicin and tobramycin) could restore the expression of a detectable level of hCFTR protein. The results of the study showed that gentamicin, and to a lesser extent tobramycin, could restore the synthesis of functional hCFTR protein and prolong the survival of CF mice.

Furthermore, a recent study has used FABP-hCFTR to demonstrate that inducible nitric oxide synthase (NOS2) expression is dependent on the expression of CFTR. The $CFTR^{tm1UNC}$ mice lack NOS2 expression in both the ileum and nasal epithelium. On the other hand, FABP-hCFTR mice, which express human CFTR in the intestinal epithelium, show NOS2 expression in the ileum but not in the nasal epithelium (262). The FABP-hCFTR mice represent an exciting model system in which secondary effects and changes in cell signaling resulting from lost CFTR function can be explored systematically. The examination of how a loss of CFTR function alters inflammatory signalling pathways might lead to the development of new therapeutic options for the treatment of CF.

1.2.1.2.2 Pancreatic disease

Snouwaert *et al.* reported a relative lack of pathological changes in the pancreas of $CFTR^{tm1UNC}$ mice. There was an apparent change in the size of the pancreas but it seemed influenced by the amount of fat present in the mesentery (256). Subsequent studies of $CFTR^{tm1UNC}$ / $CFTR^{tm1UNC}$ mice kept on a liquid diet showed abnormalities in pancreatic growth and lower activities of two pancreatic enzymes (amylase and lipase) (106). However, the lower levels of pancreatic enzymes might have been due to malnutrition, since the wild type controls showed similar abnormalities, although less severe (132). Another study of $CFTR^{tm1UNC}$ / $CFTR^{tm1UNC}$ mice reported luminal dilatation and the accumulation of zymogen granules at the apical pole of the ductal epithelial cells (84). The $CFTR^{tm1CAM}$ CF mouse was reported to exhibit blockage of some of the small pancreatic ducts in about 50% of the mice examined, although the lesions were not considered severe

enough to alter pancreatic function (220). $CFTR^{tm1BAY}$ and $CFTR^{tm3BAY}$ exhibited acinar atrophy that appeared to worsen as the mice aged. One CF mouse exhibited severe atrophy of the pancreas with mild dilatation of the ducts.

The $CFTR^{tm1HGU}$ mouse exhibits no pancreatic pathology, probably as a result of expression of a significant amount of wild type CFTR. The CF mouse shows no malabsorption or other gut problems. As well, none of the ΔF508 or the G551D models exhibit any obvious pancreatic pathology (312;281;66;65;58;38).

The milder pancreatic pathology observed in CF mice models compared to CF patients appears to depend on two factors. First of all, as explained before, certain mouse models express enough CFTR residual activity to have a normal Cl^- secretory pathway. Second of all, it has been suggested that the murine pancreas contains an alternative channel to CFTR, a Ca^{2+} mediated Cl^- conductance channel, present in both wild type and CF mice (35;103).

1.2.1.2.3 Lung disease and inflammation

The $CFTR^{tm1UNC}$ KO mice had pathological changes in the upper airways but there were no signs of either inflammation or bacterial infection in the lungs (256). Kent and collaborators hypothesized that the mixed genetic background of the original strain might influence the development of lung pathology. Modifier genes could possibly code for an alternative Cl^- channel (147). Therefore, as explained previously, Kent and colleagues reported the development of a congenic strain designated B6-$CFTR^{tm1UNC}$/$CFTR^{tm1UNC}$. Although no spontaneous[7] infection of the lungs occurred, the B6-$CFTR^{tm1UNC}$/$CFTR^{tm1UNC}$ mouse developed spontaneous and progressive lung disease. The major features of the lung disease included failure of effective mucociliary clearance, postbronchiolar over inflation of alveoli and parenchymal interstitial thickening, with evidence of fibrosis and inflammatory cell recruitment (147). Acinar and alveolar hyperinflation is consistent with obstructive small airway disease, which is a characteristic and early feature of human CF (201;10). As significant macroscopic and microscopic structural

[7] Mice were kept in SPF condition, exposure to own intestinal flora did not result in detectable infection in the lungs

differences exist between normal mouse and human lungs, some differences in pathology of mouse and human CF lung disease must be expected. CF patients and CF laboratory mice are also exposed to very different environments.

The $CFTR^{tm1HGU}$ KO mice showed no gross lung disease at birth, but displayed cytokine abnormalities when maintained in standard animal facilities (48). Their response to exposure to certain pathogens is discussed in the section 1.2.1.4. However, it is important to note that these mice demonstrated significantly impaired airway clearance to most pathogens. Further studies have demonstrated significantly impaired mucociliary transport of inert particles *in vivo* and altered submucosal glands (311;19).

In the G551D mouse model, about one third of the CF animals exhibit inspissated eosinophilic material in the lumen of the pharyngeal submucosal glands. The $CFTR^{tm1G551D}$ mouse model developed abnormal regulation of inflammation in the lungs of one third of the *Cftr*-KO mice. Furthermore, the G551D strain displays an innate defect in the immunological response to inflammatory stimuli. Thomas and collaborators showed that elevated levels of S100A8 mRNA, a marker for neutrophilic accumulation, were found to be three to four times higher in the lungs of $CFTR^{tm1G551D}$ mice compared to littermate controls after stimulation with LPS. LPS stimulation also resulted in higher than normal numbers of neutrophils in the lungs as well as a hypersensitive macrophage phenotype (277). As well, $CFTR^{tm1G551D}$ mice showed impaired pulmonary clearance and initial hyperresponsiveness to *P. aeruginosa* (179).

Another interesting phenotype observed in CF mice has been a decrease in pulmonary levels of iNOS, which has been implicated in the development of CF lung disease. The expression of iNOS is significantly reduced in the mixed background strain of homozygous $CFTR^{tm1KTH}$ and $CFTR^{tm1UNC}$ KO mice (262;146).

All the other mouse models examined had normal lung histology and absence of mucus plugging, showing no sign of lung pathology. Therefore, apart from the B6-$CFTR^{tm1UNC}$ mice, no other CF mouse models develop spontaneous lung

inflammation and none developed "spontaneous" chronic bacterial infections similar to what is observed in human CF patients.

1.2.1.2.4 Nasal and tracheal electrophysiological profiles

The murine nasal mucosa is made of about 40% olfactory epithelia and 60% respiratory epithelia. The human nasal mucosa is made of more than 95% of respiratory epithelia (106). Nevertheless, the nasal mucosa of CF mouse models accurately replicate the human profile, also showing hyperabsorption of Na^+ and the Cl^- transport defect (106). Na^+ hyperabsorption is detected by a significant more negative baseline nasal PD (potential difference) *in vivo* and a response to amiloride, a drug that blocks the epithelial sodium channel EnaC. In response to amiloride, all the CF mouse models showed an increased PD in comparison to non-CF controls (312;281;254;230;107;58). In human airway tissue, stimulated Cl^- secretion is mediated almost equally by the CFTR channel and an alternative Ca^{2+}-regulated channel in the apical membrane (21). In human CF tissue, although the cAMP-stimulated CFTR pathway is defective, the Ca^{2+} mediated Cl^- secretory pathway is functional, and sometimes upregulated (21;141;155;296). In the normal murine nasal mucosa, CFTR is the dominant Cl^- secretory pathway. In CF nasal mucosa that expresses no CFTR, there is an upregulation of the Ca^{2+}-mediated Cl^- secretory pathway. With the exception of the $CFTR^{tm1HGU}$ and $CFTR^{tm1EUR}$ mice models, all the CF mouse models showed a decrease in cAMP-mediated Cl^- response and an increase in Ca^{2+}-mediated Cl^- secretory response (50).

Interestingly, the trachea electrophysiological profile of CF mice shows important differences with the human profile, in both Na^+ and Cl^- ion transport. The CF murine lower airways (trachea, bronchi) contain more than 50% of Clara cells, whereas the human lower airways are composed primarily of ciliated cells (106). The very different distribution of cell types in the lower airways between mouse and human might account in part for their differences in electrophysiological profiles. In the human CF patient, the lower airways exhibit Na^+ hyperabsorption and reduced cAMP-mediated Cl^- secretion. In murine models of CF, the trachea exhibits no significant hyperabsorption of Na^+. Some studies

even reported hypoabsoprtion of Na^+ in the tracheas of $CFTR^{tm1CAM}$ and $CFTR^{tm1HGU}$ mice (131;254). This is a surprising finding since wild type CFTR downregulates the rate of Na^+ absorption. One possible explanation for this finding could be that there is very little to no CFTR expression in the murine lower airways. Because it has been speculated that hyperabsorption of Na^+ plays a role in the airway pathology of the human CF patients, another possible explanation for the lack of disease in CF murine lower airways could be the lack of Na^+ hyperabsorption in this tissue (154).

Furthermore, measured Cl^- secretory responses in murine CF tracheas in response to forskolin gave unexpected results. Forskolin increases the intracellular cAMP levels and induces Cl^- secretion. In $CFTR^{tm1UNC}$ and $CFTR^{tm1CAM}$ mice, the Cl^- secretory response to forskolin was identical in tracheas from CF and normal mice (108;38). For all other knockout mouse models for which there is data, the presence of a Cl^- secretory response to forskolin in the CF mouse tracheas was noted, but the response was less pronounced than the one exhibited by normal mice. Therefore, there is significant Cl^- secretion in the CF murine tracheas in response to an increase in cAMP levels. Since the two null CFTR mutation models $CFTR^{tm1UNC}$ and $CFTR^{tm1CAM}$ show Cl^- secretion, it indicates that there must be an alternative cAMP-dependent Cl^- channel to CFTR in the murine lower airways. As well, most studies report no differences in the rate of Ca^{2+}-mediated Cl^- secretionsbetween normal and CF mouse tracheas. Only $CFTR^{tm2CAM}$ and $CFTR^{tm1G551D}$ show an upregulation of the Ca^{2+}-mediated Cl^- secretory pathway in the CF tracheal epithelium (58;38). Furthermore, trachea electrophysiological profiles have varied considerably among different inbred mouse strains, indicating that the ion transport properties in the murine airways are probably regulated by independently segregating modifier genes.

1.2.1.2.5 Other manifestations of the disease

In most of the CF mouse models for which there are data, there appears to be no obvious liver pathology. However, most of the mice studied were young and might have developed hepatic disease if they had grown older, as is the case for humans. In the $CFTR^{tm1G551D}$ mouse, 20% of the mice are reported to exhibit hyperplasia of the bile duct epithelium (266).

The CF mouse gallbladder seems to exhibit more abnormalities than seen in the liver. However, the pathology is quite variable. Some CF mouse models ($CFTR^{tm1G551D}$, $CFTR^{tm1UNC}$ and $CFTR^{tm1Bay}$) have distended gallbladders. $CFTR^{tm1UNC}$ and $CFTR^{tm1G551D}$ mice have their gallbladder filled with black bile (58;256) and the gallbladder wall infiltrated with PMN, suggesting an ongoing inflammatory response. Understanding the gallbladder pathology seen in CF mice might help to find a treatment for the frequent formation of gallstones and gallbladder malformations observed in the human CF patients.

Several studies using various CF mouse models have reported normal fertility in males, and no pathology of the male reproductive tracts. It was speculated that the fertility in the CF male is due to the presence of a Ca^{2+}-mediated Cl^- secretory pathway in the epididymes and seminal vesicles (162). Interestingly, B6-$CFTR^{tm1UNC}$ mice do not express alternative Cl^- channel resulting in 90% of the males to be infertile (unpublished results). CF mouse females also appeared to have no pathology in the reproductive tract. However, $CFTR^{tm1UNC}$ female mice necessitated more time than normal littermates to become pregnant, indicating a possible reduction in fertility (117), and CF knockout females in B6-$CFTR^{tm1UNC}$ were almost completely infertile (unpublished observations).

In the human CF patients, the pathology of the submandibular, sublingual glands, and submucosal glands include dilated ducts, inspissated secretions and atrophy of the acini (106). In the $CFTR^{tm1UNC}$ mouse model, the submaxillary glands show no dilatation of ducts or presence of inspissated material in ducts (256). $CFTR^{tm1Bay}$ mice showed severe dilation of the acini of the minor sublingual gland in young mice. Older animals showed parotid gland atrophy (198).

$CFTR^{tm1G551D}$ mice showed hypercellular salivary gland. No pathology was noted in the $CFTR^{tm1HGU}$ mouse and in the ΔF508 CF mouse models.

$CFTR^{tm1UNC}$, $CFTR^{tm1CAM}$, $CFTR^{tm1EUR}$ and $CFTR^{tm1Bay}$ mice have soft, chalky white, easily fractured incisor enamel, whereas the enamel of normal mice is hard and yellow-brown in color after three weeks of age. The lack of tooth pigmentation is the result of abnormal enamel development. Light microscopy studies revealed that the ameloblasts, the cells responsible for enamel formation, appear to undergo premature degeneration in CF mice (302). White incisor teeth allow fast recognition of homozygous CF progeny, as early as three weeks of age.

As mentioned earlier, patients with CF are often of smaller height compared to average and have difficulty regaining weight once it drops. In addition to the malabsorption of fats and proteins, other factors such as increased caloric demands for fighting infection and breathing may also contribute to this weight loss. As well, all CF mouse models except $CFTR^{tm1HGU}$ and $CFTR^{tm2HGU}$ show a lower body weight than their wild type littermates. Clinically, the ideal body weight percentage is a prognostic for CF survival. The lower body weight of CF mice is thought to be due to intestinal disease, since CF mice in which the defect has been corrected by tissue-specific CFTR transgenesis are of the same weight as non-CF littermate controls (308;114). The decreased weight of CF mice, as will be discussed later, is also linked to the production of pro-inflammatory cytokines, such as TNF.

1.2.1.3 Reasons for disease severity in mouse

The different CF mouse models have very different rates of survival, often related to the severity of their intestinal pathology. For example, $CFTR^{tm1UNC}$ mice have a survival rate <5%, whereas $CFTR^{tm2HGU}$ mice have the same survival rate as their control littermates. These differences in rate of survival reflect mutation-specific effects, independently segregating modifier genes and environmental factors.

This high survival rate of $CFTR^{tm1HGU}$ mice seems to be linked to a low-level production of about 10% of functional CFTR (65). Because of the targeting

strategy used (insertional rather than replacement gene targeting), exon skipping and aberrant splicing produces about 10% normal CFTR mRNA, up to 20% of normal CFTR was expressed in the intestine. These characteristics result in absence of intestinal disease and high survival rate. Low levels of CFTR expression have proven to be sufficient to have normal Cl^-secretion. $CFTR^{tm1EUR}$ and $CFTR^{tm1HGU}$ mice also show normal rates of survival (65;281). The 'hit and run' strategy used to create these mutant mice resulted in normal expression of the mutant CFTR protein, which could provide enough residual function to alter the phenotype of the CF mice. Therefore, specific mutation of CFTR can alter the intestinal disease. However, no specific mutations of CFTR have been found to determine meconium ileus in CF patients. A family with a meconium ileus recurrence rate of 29% suggests that genetic factors influence the intestinal disease.

1.2.1.4 CFTR mice models and bacterial infections

Mimicking different bacterial infections in the CF mice models has unraveled some information on the relationship between infection and inflammation.

Because of the similarities between human and mice gastrointestinal pathophysiology, CF mice models have shown that human CF carriers are more resistant to certain bacteria, namely *Vibrio cholerae (V. cholerae)* and *Salmonella typhi (S. typhi)* (267;106;38). This increased resistance to infectious diseases might maintain mutant CFTR alleles at high levels in selected populations, giving them a "heterozygote advantage". The C57BL/6-$CFTR^{tm1UNC}$ mice were exposed to the cholera toxin (CT) by oro-gastric feeding. Homozygous knockout mice showed less intestinal fluid secretion than wild type mice. Heterozygous mice for the CFTR mutation also showed a decreased response to CT, indicating that CF carriers have a selective advantage over the wild type population against cholera-induced secretory diarrhea. Resistance to cholera is supported by the fact that CFTR is a cAMP-regulated Cl^- channel, and that cholera mediates its action by an irreversible elevation of cAMP, which triggers sustained Cl^- and fluid secretion (267). However, other reports found variable results. Clarke and colleagues, using

$CFTR^{tm1UNC}$ on a mixed genetic background, found a reduced Cl^- conductance in most heterozygous mutant mice compared to wild type mice (36). On the other hand, Evans and collaborators, using $CFTR^{tm1CAM}$, also on a mixed genetic background, found that wild type and heterozygous CFTR mice produced the same acute secretory response to cholera toxin on a short-term basis (43). The authors hypothesized that prolonged stimulation may reveal a heterozygote advantage. As well, it is important to note that the two latter studies were not realized on congenic strains, as the former one, conferring more variability to the study.

Studies of jejunal sections of homozygous $CFTR^{tm2CAM}$ mice infected with *S. typhii* showed that the mutant CFTR fails to translocate the bacterium into the intestinal submucosa. Heterozygous $CFTR^{tm2CAM}$ mice translocate *S. typhii* 86% less efficiently than wild type mice (209). The same group showed that human epithelial cells expressing wild type CFTR ingested significantly more *S. typhii* than cells expressing ΔF508 CFTR. These findings indicate that CFTR is an epithelial cell receptor used by *S. typhi* (and not used by *Salmonella typhimurium*) to enter the GI submucosa in both mice and humans. Furthermore, it suggests that resistance to typhoid may have selected the ΔF508 allele CFTR to a high frequency (4-5%) in the Caucasian population. Maintenance of this allele is best explained by over-dominance, with resistance to a particular disease conferring an advantage for the heterozygote (209). However, as pointed out by Colledge *et al.*, cholera has been an endemic in India for centuries but did not appear in Europe until 1832. Cholera itself is therefore unlikely to have selected for mutant alleles of CFTR. On the other hand, resistance to typhoid fever might be a selective factor explaining the high prevalence of ΔF508 CFTR in CF carriers.

1.2.1.4.1 Infection with *S. aureus* and *B. cepacia*

Infections of CF mouse models can also have different outcomes depending on the methods used. Using single or repetitive intranasal infection with *S. aureus*, Snouwaert *et al.* reported that $CFTR^{tm1UNC}$ mice could clear the bacteria as efficiently as CFTR heterozygous mice (255). On the other hand, intratracheal instillation of *S. aureus* led to an inflammatory reaction, but did not lead to chronic

lung disease (42). Davidson *et al.,* using daily aerosol challenges with *S. aureus* in $CFTR^{tm1HGU}$ mice reported higher bacterial loads and more pronounced disease in the lungs of CF mice compared to their littermate controls although no infectious dose was reported in the paper. CF mice showed a higher incidence of goblet cell hyperplasia, mucus retention and bronchiolitis when compared with control mice (48).

Establishing bacterial infection in rodent lungs is more difficult for *B. cepacia* than for *S. aureus*. Davidson *et al.* infected $CFTR^{tm1HGU}$ mice with aerosolized *B. cepacia* daily for a month. CF mice exhibit a distinct pathology from that of control mice. Lungs of non-CF mice showed milder and more focal histologically pathological changes than CF mice. CF mice had increased pneumonia and mucus retention, destruction of small airways, and extensive edema. Downey and collaborators also studied *B.cepacia* infection, but did so in $CFTR^{tm1UNC}$, using intranasal instillation (234). Nine days after the last instillation, CF knockout mice displayed persistence of viable bacteria with chronic severe bronchopneumonia. Out of the 16 CFTR knockout infected mice, two died. This relatively low mortality rate is comparable to the human mortality rate. The $CFTR^{tm1UNC}$ mice demonstrated an enhanced pulmonary inflammatory response characterized by infiltration of neutrophils and macrophages into the peribroncholear and perivascular space. Neutrophils and macrophages were shown to be defectively activated, which might contribute to bacterial persistence. Furthermore, Downey *et al.* also showed that the predilection for enhanced pulmonary inflammation and injury was dependent in part on bacterial virulence, through infection of CF mice with more or less virulent strains of *B. cepacia.*

1.2.1.4.2 Infection with *P. aeruginosa*

Human CF patients develop chronic *P. aeruginosa* lung infection, whereas spontaneous colonization with the typical CF pathogens, including *P. aeruginosa,* has not been detected in the CF animals. Furthermore, specific techniques have to be used to mimic *P. aeruginosa* chronic infection lasting more than a month in animals. The bacteria must be inoculated intratracheally with immobilizing agents

such as agar, agarose or seaweed alginate. Administration of free *P. aeruginosa* provides a model for acute lung infection, with either rapid clearance of the bacteria or sepsis with subsequent death. Infection induced by aerosol exposure is acute, and bacteria are rapidly cleared from the lungs in about 24-48 hours (283;266). The entrapment of *P. aeruginosa* in agar beads seems to slow down the growth of the bacteria within the beads compared to outside of the beads, resembling the biofilm state. Initial studies examining the effect of exposure to *P. aeruginosa* in $CFTR^{tm1HGU}$, $CFTR^{tmUNC}$ and $CFTR^{tm1KTH}$ mice showed no increase in susceptibility to *P. aeruginosa.* These results might be due to the methods of instillation used and might also depend on the mouse genetic background of the CF mice used in the study (50). Using agar beads laden with *P. aeruginosa* to mimic colonization has proven more successful, as demonstrated by Van Heeckeren with $CFTR^{tm1UNC}$ mice (121). The infected CF mutant mice in this study displayed bacterial proliferation associated with decreased survival rate after infection, increase in the production of pro-inflammatory cytokines, decrease in the production of IL-10 and decrease in pulmonary iNOS. However, Van Heeckeren and colleagues used unilateral infection and the genetic background of the mice was not reported. Our laboratory has used B6-$CFTR^{tm1UNC}$ KO mice, as previously described (99). These mice were infected intratracheally with mucoid *P. aeruginosa* in agar beads, in a bilateral way. A higher mortality and a higher bacterial burden were shown in the lungs of the CF mice. However, both wildtype (WT) mice and *Cftr*-KO developed severe bronchopneumonia and showed the same level of neutrophilic infiltration. Homozygous $CFTR^{tm1G551D}$ mice were also infected with entrapped mucoid strains of *P. aeruginosa.* After 3 days, these CF mice had a defect in bacterial clearance with a higher bacterial load and altered concentrations of pro-inflammatory mediators, showing excessive inflammation (179). Unlike other models, $CFTR^{tm1G551D}$ mice showed a reduced rate of clearance of the bacteria although they do not have a higher mortality rate, suggesting that this model might better mimic chronic lung infection. However, the infected CF mice were harvested three days after infection. A study on a longer term basis should be done to confirm that these CF mice have a lower mortality

rate. Also, a recent model of intratracheal infection, using a *P. aeruginosa* strain that possess a stable mucoid phenotype due to a deletion in *mucA,* allows infection without the need for agar embedding (125). This model has to be further characterized.

Growth impairment (retardation) and chronic malnutrition have been associated with the progression of lung disease in human CF patients. The relationship between those three factors is not well understood. The effect of malnutrition on pulmonary clearance of *P. aeruginosa* was studied in CF mouse models. We did not see a correlation between body weight and bacterial burden in CF mice (99). On the other hand, Van Heeckeren showed that weight loss correlates with the concentration of pro-inflammatory cytokines after agarose embedded *P. aeruginosa* infection in B6 male mice (285) and in $CFTR^{tm1UNC}$ mice (121), suggesting a correlation between pulmonary clearance of the bacteria and body weight. Other studies reported that malnutrition compromised the pulmonary defenses against *P. aeruginosa* colonization in B6 WT mice, exposed to aerosolized bacteria (276;307). As well, Deretic and colleagues showed that malnourished $CFTR^{tm1UNC}$ mice displayed variable pulmonary clearance of aerosolized *P. aeruginosa* (276;307). $CFTR^{tm1UNC}$ FABP-hCFTR mice, with the intestinal defect corrected, did not show this variability in *P. aeruginosa* clearance and cleared the bacteria quite efficiently (276). Based on these findings, McMorran *et al.* suggested a potential relationship between nutrition, intestinal defect and lung disease. Study of $CFTR^{tm1G551D}$ mice also showed a correlation between weight loss and ineffective clearance of *P. aeruginosa* (179). Further studies need to be done to clarify this relationship. Furthermore, gender may also influences weight and pulmonary clearance in B6-$CFTR^{tm1UNC}$ mice as explained above (112;259).

1.2.2 Other animal models for CF disease studies

The mouse model is extensively used for human diseases because of its availability and its usability for genetic manipulations. However, researchers frequently need to use other species that are more closely related to humans by the similarity of their disease phenotype and of their genetic diversity (Table 1.3). The

use of many different animal models is needed since cystic fibrosis is a complex disease affecting multiple organs in different ways and has more than a thousand different mutations in the *Cftr* gene. The following table summarizes research findings using different species such as ferret, cat, pig, rabbit, sheep, and rat.

Table 1.3 Animal models used to study cystic fibrosis

	Usefulness
Ferret	Gene therapy Airway mucus secretion Effect of *P. aeruginosa* on airway ASL
Cat	*P. aeruginosa* airway infection Effect of *P. aeruginosa* on airway Airway secretion content
Pig	CFTR function Airway mucus secretion Gene therapy
Rabbit	Gene therapy ASL CFTR expression CFTR gene
Sheep	CFTR gene Male genital duct epithelium Airway mucus Gene therapy
Rat	Alternative chloride channel Submucosal glands *P. aeruginosa* airway infection Effect of *P. aeruginosa* on airway

Overall, it is hardly realistic to choose a single animal model to study this disease. Some animal models are closer to humans phylogenically in regards to the CFTR gene genomic sequence, while others are similar in regards to the phenotypes observed in a specific organ. In this review, we wanted to explore

some of the CF animal models with their advantages and similarities to the human CF disease. All of these models should be considered useful tools for the understanding of this devastating genetic disease.

1.3 Rational

My research studies were focused on the regulation of the inflammatory response in CF. Here are the premices and technical specifications that I based myself to design the experiments.

1.3.1 Premises

- CF patients infected with *P. aeruginosa* have been shown to have a dysregulated immune response (among others low IL-10 and high TNF levels) compared to unaffected people.
- Fatty acids are involved in the regulation of cell function, membrane fluidity and trafficking, inflammation and mucin secretion. Interestingly, CF patients have been shown to have dysregulated fatty acids profiles
- Female CF patients have a worse prognostic than male patients.
- Existing CF mouse models display most of the CF disease symptoms except for the lung phenotype. Our *Cftr*-KO mice (110;147)represent a unique model of spontaneously occurring CF lung disease.
- Many techniques have been developed in order to establish lung infection in rodents. A model of chronic lung infection, using tracheotomy to inoculate the bacteria, has been extensively used by us and others, in the CF mouse model of lung infection (invasive procedure). Is this procedure the most adequate for CF studies in mice? Could the procedure in itself affect the immune response?
- Fenretinide, a synthetic retinoid (vitamin A analogue) has chemo-protective and anti-tumor activities. It also inhibits IL-8 production induced by TNF in endothelial cells and induces synthesis of ceramide in endothelial cells. Interestingly, ceramide is crucially important for *P. aeruginosa*

internalization and the failure to generate ceramide-enriched membrane platforms in infected cells results in an unabated inflammatory response characterized by the massive release of interleukins and septic shock

1.3.2 Hypothesis

- Male and female mice, in our mouse model, differentially eradicate the lung infections
- IL-10 is an essential anti-inflammatory mediator during the course of the pulmonary infection
- *Cftr*-KO mice developing spontaneous lung disease are in an inflammatory state even before they get lung-infected with *P. aeruginosa* bacteria
- The use of a less invasive lung infection procedure will allow to study the inflammatory response in the lungs of CF animals more efficiently and accurately
- Fatty acids deficiencies of CF patients lead to dysregulated gene expression that causes an imbalanced inflammatory response. This subsequently leads to an inefficient immune responses against lung bacterial invasion
- Fenretinide acts as an anti-inflammatory agent by modulating the immune response during *P. aeruginosa* lung infection by the induction of ceramide

1.3.3 Specific objectives

- Define the influence of sex on susceptibility to *P. aeruginosa* lung infection in mice
- Analyze the development of inflammation in the presence or absence of IL-10 during *P. aeruginosa* lung infection
- Evaluate the histo-pathological status of non-infected male and female *Cftr*-KO mice developing spontaneous lung disease
- Determine the differences in gene expression profiles between the *Cftr*-KO and their WT control mice
- Develop a technique that creates a lung infection that resembles bacterial colonization with *P. aeruginosa* observed in human CF. This new

technique should eliminate the inflammation which can occur due to the tracheotomy and simplify the infection procedure thus improving the survival rate of the CF animals

- Establish the fatty acids levels in our *Cftr*-KO mouse model and verify if DHA supplementation can affects the histopathological status of *Cftr*-KO mice
- Assess the impact of DHA during chronic *P. aeruginosa* lung infection
- Provide fenretinide to the mice as a diet supplement and verify first, if it increases ceramide levels in our *Cftr*-KO mouse model and second, assess the impact of fenretinide during chronic *P. aeruginosa* lung infection

CHAPTER II

Preface

Cystic fibrosis patients infected with *P. aeruginosa* bacteria have been shown to have dysregulated cytokine profiles, shown by higher levels of TNF, IL-8, and lower levels of IL-10 in the bronchoalveolar lavage fluid compared to healthy controls. In order to verify the role of IL-10 during lung infection with *P. aeruginosa*, we compared several inflammation parameters during the course of lung infection using IL-10 KO mice and their WT controls. As mentioned previously, gender plays an important role in the rate of survival of CF patients. Female CF patients have a lower survival age than male CF patients. Our laboratory has also previously observed that a large number of *Cftr*-KO female mice had lower survival rate *in utero* when compared to their *Cftr*-KO male counterparts. Also, the *Cftr*-KO females were more susceptible to *P. aeruginosa* infection than *Cftr*-KO males up to the point that not enough female mice survived to provide results which could be statistically analyzed. The following thesis chapter presents the studies that were aimed at investigating the importance of both gender and IL-10 in the susceptibility of B6 mice to pulmonary infection with *P. aeruginosa*.

CHAPTER II.

INFLUENCE OF GENDER AND IL-10 DEFICIENCY ON THE INFLAMMATORY RESPONSE DURING LUNG INFECTION WITH *PSEUDOMONAS AERUGINOSA* IN MICE

based on published manuscript

Guilbault, C., *Stotland, P., Lachance, C., Tam, M.F., Keller, A., Thompson-Snipes, L., Cowley, E., Hamilton, T.A., Eidelman, D.H., Stevenson, M.M., Radzioch, D.*
Immunology 2002 Nov; 107(3):297-305

2.1 Abstract

Female patients diagnosed with cystic fibrosis have a worse prognosis compared to male CF patients. Furthermore, CF patients infected with *P. aeruginosa* have been shown to have dysregulated cytokine profiles, as higher levels of tumor necrosis factor alpha, interleukin-8, and lower levels of interleukin-10 are found in the bronchoalveolar lavage fluid compared to healthy controls. The present study was aimed at investigating the importance of gender and IL-10 in the susceptibility of C57BL/6 mice to pulmonary infection with *P. aeruginosa*. We found that wildtype females were more susceptible than males to infection, as we observed greater weight loss, higher bacterial load, and inflammatory mediators in their lungs. IL-10 knockout mice, both females and males, had higher levels of TNF in the lungs compared to wildtype mice and maintained higher level of polymorphonuclear cells and lower level of macrophages for a longer period of time. Our results demonstrate that the number of bacteria recovered from the lungs of IL-10 knockout male mice was significantly higher than that observed in their wildtype male counterparts and we show that neutralization of IL-10 in infected

female mice for a prolonged period of time leads to increased susceptibility to infection. Results reported in this study clearly demonstrate that females, both WT and IL-10 KO are more susceptible to *P. aeruginosa* infection than males, and that they mount a stronger inflammatory response in the lungs.

2.2 Introduction

Cystic Fibrosis (CF), a disease characterized by a dysregulated inflammatory response in the lung environment, appears to be due to an imbalance in cytokine production. The dysregulation of the immune response would impair the proper clearance of the bacterial infection in the lungs by *P aeruginosa.* Furthermore, a recent study showed a correlation between cytokine pattern and the clinical course of CF (300). Cytokine profile analyses in BALF, respiratory epithelial cells obtained from CF patients, as well as sputum of CF children, indicated higher levels of TNF, IL-1 and IL-8 and less IL-10 compared to healthy subjects (17;18;69;175;203). These results correlated with the predominance of neutrophils found in the lungs of CF patients infected with *P. aeruginosa* (12;16). Other studies showed no significant differences in the IL-10 levels in BALF of young CF patients compared to healthy controls (195). From these divergent observations, it is not yet clear what the actual importance of IL-10 is in the regulation of the inflammation in CF lung.

Previously reported data suggest that the prognosis of the disease is worse in CF female patients compared to CF male patients (82). It has been shown extensively that sex hormones can affect the immune response (46;183), governing the gender-related differences observed in many diseases and disorders (9;45;44;61;239;316). Unfortunately, human CF studies using both male and female adults and/or children did not analyze or report any differences in IL-10 levels between genders (18;17;16;189;195;203;300). Nevertheless, the influence

of IL-10 has already been shown in gender-related differences of the immune response (2;143;297).

Interleukin 10 (hIL-10) is an 18-kDa protein that was originally identified as a T helper 2 (Th2) mediator of the immune response (159). IL-10 is produced relatively late following activation of T cells or monocytes/macrophages and has miscellaneous functions depending on the cell type, stimulus, and the target cell (184). Among others, IL-10 has previously been shown to inhibit the production of pro-inflammatory cytokines like TNF and chemokines like IL-8 (81). This pleiotropic cytokine has been shown to be involved in many aspects of the immune response; consequently, it is not surprising that it plays a pivotal role in the pathogenesis of several diseases and disorders. Since the proper balance, as well as the adequate temporal and spatial expression of IL-10, is essential for efficient immune response, the dysregulated production of IL-10 can also lead to undesirable effects during the course of infection. In fact, neutralization of IL-10 or administration of anti-IL-10 is shown to enhance clearance of *Mycobacterium avium* (13) as well as augment the survival of mice infected by *Klebsiella* pneumonia (104). In contrast, the lack or insufficient production of IL-10 can also be detrimental to the host (51;260;109;172). A study with IL-10-deficient transgenic mice, repeatedly exposed to mucoid *P. aeruginosa*, showed higher mortality and lung pathology compared to B6 control animals (306). It was also demonstrated that in *P. aeruginosa* pneumonia, systemic administration of IL-10 improved the host condition (238;263). Chmiel and colleagues observed that IL-10 attenuates excessive inflammation in *P. aeruginosa* infected male mice. More severe weight loss and increased area of lung inflammation was observed in IL-10 KO compared to their male WT controls (32). Although the authors found a trend toward lower bacterial count at day 3 post-infection, no statistical significance was found. However, these authors observed substantial improvement in the extent of inflammation when the male CD1 mice were treated with the recombinant human IL-10. We were wondering whether similar or different improvement in handling *P. aeruginosa* lung infection and inflammation could also be observed in female

mice. To test this hypothesis, we first defined the influence of gender on susceptibility using WT B6 mice infected with 10^5 *P. aeruginosa* entrapped in agar beads. Next, we looked at the influence of gender on the susceptibility to *P. aeruginosa* infection and development of inflammation in the presence or absence of IL-10, and finally, we analyzed the effects of IL-10 neutralization on bacteriology, secretory activity and inflammatory cell distribution in the lungs of female mice.

2.3 Material and Methods

2.3.1 Mice. Age- and gender- matched C57BL/6 mice, 8-10 weeks old, purchased from Charles River (St-Constant, Quebec, CA) were used in the IL-10 neutralization experiments. C57BL/6 mice (n = 91; females 11.2 ± 2.2 weeks old and males 14.0 ± 6.0 weeks old) and C57BL/6-IL-10 knockout mice (n = 83; females 13.2 ± 1.4 and males 14.6 ± 5.1 weeks old), were used for the IL-10 knockout study according to the guidelines and regulations of the Canadian Council on Animal Care. IL-10 knockout mice were confirmed by histology to be free of inflammatory bowel disease. Mice were kept in SPF facility; food and water were provided ad libitum.

2.3.2 *P. aeruginosa*. *P. aeruginosa* strain 508 was kindly provided by Dr. Jacqueline Lagacé (University of Montreal, Montreal, QC). This strain has a mucoid appearance when grown on blood agar and was originally isolated from the sputum of a CF patient at Ste-Justine Hospital, Montreal, QC.

2.3.3 Inoculum's preparation and infection of mice. In order to establish a model of prolonged infection, bacteria-impregnated agar beads were prepared as previously described (237) and were used for lung infection. Briefly, log phase bacteria were concentrated and added to warm 1.5% trypticase soy agar (Difco, Detroit, MI). This mixture was added to heavy mineral oil and stirred

rapidly first at 52°C, followed by cooling with continuous stirring. The oil-agar mixture was centrifuged to sediment the beads. The oil was removed and the beads washed. The size of the beads was verified microscopically and only those preparations containing beads predominantly 100-150 μm in diameter were used as inoculum. The number of bacteria was estimated after homogenizing the bacteria-impregnated bead suspension. The inoculum was prepared by diluting the bead suspension in sterile Dulbecco's phosphate-buffered saline (PBS; Invitrogen, Mississauga, ON) to 2-4 x 10^6 colony-forming units (CFU)/ ml. Mice were anaesthetized with a combination of ketamine (15 mg/ml) and xylazine (2 mg/ml) administered intramuscularly at a dose of 0.2 ml. Following a transverse cervical incision, the trachea was exposed and intubated with a sterile, flexible 22-gauge cannula attached to a 1.0 ml syringe. An inoculum of 50 μl was implanted via the cannula into the lung. After inoculation, all incisions were closed by suture. No animal developed wound infection and healing occurred in 2-3 days. Previously published data showed only mild signs of inflammation in lungs of mice injected with sterile agar beads (99;32). Two doses were tested in this model of infection using B6 WT and B6 IL-10 KO mice. When using an infection dose of $2x10^5$ CFU, high mortality rates were observed; about 40% of the WT mice and more than 80% of the IL-10 KO mice did not survive the infection. When the infection dose was lowered to 10^5 CFU, we were able to observe more than 90% survival for all the mice infected. It was therefore possible to study prolonged lung infection in both WT and IL-10 KO mice.

2.3.4 Bronchoalveolar lavage. Mice were sacrificed by CO_2 overdose, exsanguinated by cutting the vena cava, and the circulation was flushed by slow intracardiac infusion of divalent cation-free Hank's balanced salt solution (HBSS; Invitrogen). The trachea was cannulated with a 22-gauge intravenous catheter placement unit (Critikon) connected to two 5 ml syringes via a 3-way stopcock with rotating collar (Namic U.S.A., Glens Falls, NY). The alveoli of infected mice were washed 3 times with a total volume of 1.4 ml of divalent cation-free HBSS. The volume of BALF recovered was approximately 1.2 ml. Alveolar cells were

centrifuged and the supernatant was used for CFU counts determination; it was then stored at -20°C until assayed for cytokine concentrations. Cells were resuspended in 0.5 ml of Dulbecco's Modified Eagle Medium (DMEM; Invitrogen) supplemented with 10% fetal bovine serum (FBS; Hyclone, Logan, UT), diluted in Turk's solution and counted using a hematocytometer. The proportions of macrophages, lymphocytes, and PMN were calculated after counting approximately 300 alveolar cells on cytospin preparations stained with Diff-Quick (American Scientific Products, McGaw Park, IL).

2.3.5 Lung homogenates. Lungs from infected mice were harvested and homogenized for 60 sec at high speed (homogenizer PT10135 Brinkmann Instruments Co., Mississauga, ON) in 4 ml of sterile PBS (Invitrogen). Serial 10-fold dilutions of lung homogenates were plated on petri dishes containing trypticase soy agar (TSA). The number of CFU per lung was counted after overnight incubation at 37°C. For cytokines measurements, lung homogenates were centrifuged at 1500x g at 4°C for 10 min and the supernatants were removed and stored at -20°C until assayed for cytokine concentrations.

2.3.6 Cytokine measurements. The concentration of TNF protein in lung tissue homogenates from infected animals was determined by a double sandwich enzyme-linked immunosorbent assay (ELISA) as previously described (98). Briefly, 96-well polyvinyl chloride microtitre Immulon II plates (Dynatech, Chantilly, VA) were coated at 4°C overnight with hamster anti-murine TNF mAb (R&D Systems, Minneapolis, MN). Plates were then washed, incubated with blocking buffer [PBS, 0.1% Tween 20, and 1% bovine serum albumin (BSA; Sigma, Oakville, ON)], and sequentially incubated at room temperature with various dilutions of lung homogenate samples, polyclonal rabbit anti-murine TNF Ab, peroxidase-conjugated goat anti-rabbit IgG Ab (BioRad, Hercules, CA), and peroxidase substrate (ABTS; Roche, Laval, QC). The intensity of the colorimetric reaction was determined by spectrophotometry at 405 nm. The levels of TNF were calculated with reference to a standard curve established with recombinant murine

TNF (R&D Systems). N51/KC protein concentrations were measured by ELISA kit (R&D Systems) according to manufacturer's instructions.

2.3.7 Anti-Murine IL-10 mAb and Neutralization Protocol. Anti-IL-10 monoclonal antibody (mAb) was raised as ascites in BALB/c mice. Briefly, mice previously primed with pristane intraperitoneally (i.p.) were given $5x10^6$ JES-2A5 hybridoma cells i.p. (American Type Culture Collection, Rockville, MD). Ascites fluid was drained from peritoneal cavity after 10-14 days. The IgG fraction from the ascites fluid was purified by affinity chromatography, using protein G-Sepharose columns. Purified antibody was further dialysed and the concentration was determined by ELISA. For IL-10 neutralization experiments, randomly designated animals were treated with anti-murine IL-10 mAb JES-2A5 or rat IgG (Sigma) as control Ab (134;238). Mice were administered 200 μg of JES-2A5 or rat IgG i.p. on days -2, 0, 2, and 4 during the course of *P. aeruginosa* infection.

2.3.8 Statistical analyses. Data were analyzed using SPSS V10.0.7 software (SPSS Inc, Chicago, IL) for Kaplan-Meier survival analysis followed by a multiple comparison log rank test, and Sigma Stat V2.03 software for all other analyses (SPSS Inc). Statistically significant differences between means and medians of studied groups were evaluated using Student's t-test and nonparametric Mann-Whitney U test, respectively. Kruskal-Wallis ANOVA on ranks combined with pair wise multiple comparison procedures (Dunn's method) were used to evaluate differences between multiple groups. Pearson and Spearman's correlation tests were used to evaluate the relationship between different parameters. Significance was set at a two-tailed p value of ≤ 0.05.

2.4 Results

In order to evaluate the bacterial concentration needed to create a chronic infection in the lungs, we have administered different doses of *P. aeruginosa* bacteria in IL-10 KO mice and their WT controls and observed the survival rate and the cellular inflammatory response of infected mice. As shown in Figure 2.1 (panel A), the mortality was high especially in IL-10 KO mice when $2x10^5$ CFU were used (at day 3 post-infection; less than 20% survival for IL-10 KO, and about 60% survival for WT mice). Although we could see the same trends in the inflammatory response between the WT and IL-10 KO mice with either doses of infection, $2x10^5$ CFU and $1x10^5$ CFU, the survival rate was much higher with the later dose. Therefore, in these studies, we used $1x10^5$ CFU (panel B) where we could observe a substantial inflammatory response, with an appreciable fraction of animals survival to study (more than 90% survival at this dose for both IL-10 KO and WT control animals.

2.4.1 Gender differences in susceptibility to *P. aeruginosa* lung infection in B6 mice.

In order to evaluate the role of gender during lung infection with *P. aeruginosa*, B6 male and female mice were infected intratracheally with $1x10^5$ *P. aeruginosa* entrapped in agar beads. We wanted to verify how early post-infection a difference in susceptibility to infection could be seen between males and females. In fact, striking differences between the males and the females were observed at day 3 to 4 post-infection.

2.4.1.1 Survival of mice infected with *P. aeruginosa*. No significant difference was observed in survival when we compared the males with the females ($p = 0.055$). No mouse died due to surgery or anesthesia, and no bacteria were found in the spleens of infected animals.

Figure 2.1. Survival rate of WT (solid) and IL-10 KO (open) mice after intratracheal infection with different doses of *P. aeruginosa* entrapped in agar beads. (A, upper panel) Animals were infected with $2x10^5$ *P. aeruginosa* (IL-10 KO n = 24, WT n = 14). Less than 20% of IL-10 KO mice survived by 4 days post-infection compared to 61% in WT animals. (B, lower panel) Animals were infected with $1x10^5$ *P. aeruginosa* (IL-10 KO n = 107, WT n = 109). Mice from both groups had a survival higher than 90%.

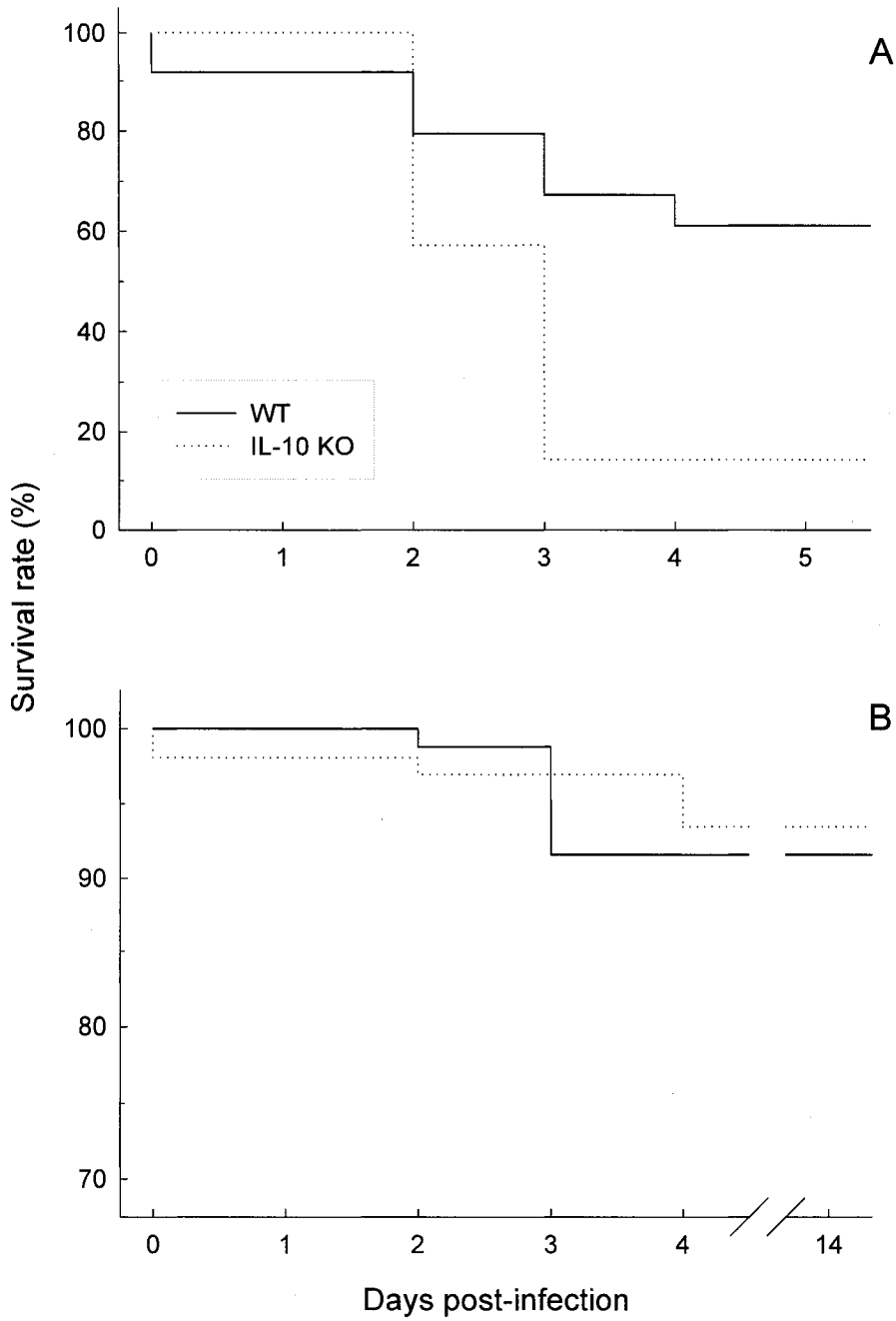
A
B
100
80
60
40
20
0
WT
IL-10 KO
0
1
2
3
4
5
100
90
80
70
0
1
2
3
4
14
Survival rate (%)
Days post-infection

2.4.1.2 Variations in body weight during lung infection.

The progression of the infection was monitored by the weight losses and gains of mice every day over the period of infection. The maximal loss was seen during the first 2-3 days post-infection, when the percentage of weight loss ranged from 10% to 22%. After 3 days post-infection, the animals started to regain weight. We observed that males regained their weight faster than females ($p \leq 0.001$) (Table 2.1). However, 14 days post-infection, the majority of mice recovered their original weight.

Table 2.1 Sex differences in B6 mice during *P. aeruginosa* lung infection

		Female		Male	
CFU counts	BALF ($x10^4$)	210.0 [2]	(79.0-745.0)	2.0	(0.0-10.8)
	Lungs ($x10^6$)	160.0 [2]	(131.0-228.0)	1.4	(0.6-3.3)
Alveolar cells (%)	PMN	88.1	(79.7-89.3)	87.9	(84.0-88.2)
	Macrophages	11.9	(10.7-20.3)	11.9	(11.8-16.0)
	Lymphocytes	0.0	(0.0-0.0)	0.0	(0.0-0.0)
Cytokines (ng/ml)	TNF	1.3 [2]	(0.6-2.0)	0.5	(0.4-0.5)
	N51/KC	0.5 [2]	(0.3-1.9)	0.2	(0.1-0.2)
Weight[1] change (%)		22.2 ± 0.7 [2]		18.0 ± 0.7	

Values are medians of 7 animals with quartiles in brackets and represent 3 independent experiments performed in the same conditions.

[1] Values are means ± SEM

[2] Medians of the females compared to the males are significantly different at day 3 post-infection ($p \leq 0.05$).

2.4.1.3 Recruitment of alveolar cells to the site of infection.

No significant difference was seen between male and female mice in the numbers of alveolar cells recruited to the infected lungs or in the numbers of PMN, macrophages and lymphocytes in the BALF (Table 2.1).

2.4.1.4 Cytokines levels in the lungs of infected B6 mice.

We assessed the concentration of TNF and N51/KC protein secretion in the lung during *P. aeruginosa* infection. Females had significantly higher TNF ($p = 0.029$) and N51/KC ($p = 0.004$) levels (Table 2.1), which coincided with a significantly higher weight loss, and bacterial burden in the lung.

2.4.1.5 Bacterial burden in the BALF and lungs.

Susceptibility to *P. aeruginosa* lung infection in female mice in comparison to their male counterparts was evaluated by the bacterial load found in the BALF samples, as well as in the lung tissue homogenates of infected mice. We observed a 100-1000 fold difference in CFU counts between the BALF and the lung tissue homogenates obtained from infected mice throughout the infection (Table 2.1). We also observed significant lower CFU counts for male compared to female mice at day 3 post-infection in the BALF ($p = 0.003$) and in the lungs ($p = 0.010$). Similar significant differences could also be observed at day 4 post-infection (data not shown).

Overall, our results clearly demonstrate major differences in the inflammatory response to *P. aeruginosa* lung infection between the males and females.

2.4.2 Influence of IL-10 in *P. aeruginosa* lung infection in mice

Next, we wanted to assess the role of IL-10 during lung infection in the context of the mice gender. To evaluate the role of IL-10, we used IL-10 KO male and female mice on the B6 genetic background. Mice were intratracheally infected with $1x10^5$ *P. aeruginosa* entrapped in agar beads. We then assessed their susceptibility and inflammatory parameters during the course of infection. We evaluated the weight loss throughout the infection, the bacterial load found in the BALF samples, as well as in the lung homogenates of infected mice, and the numbers of alveolar cells recruited to the lung (PMN, macrophages, and

lymphocytes). We also looked at different cytokines present at specific time points.

2.4.2.1 Survival of mice infected with *P. aeruginosa*. No mouse died due to surgery or anesthesia, and no bacteria were found in the spleens of infected animals. Survival was monitored 3 times per day. The survival curves of the IL-10 KO and WT mice did not significantly differ from each other for either male (WT = 91.0%, IL-10 KO = 88.5%; $p = 0.970$) or female (WT = 100.0%, IL-10 KO = 72.7%; $p = 0.232$) animals.

2.4.2.2 Variations in body weight during lung infection. Several reports have demonstrated that substantial weight loss occurs in CF patients during acute, exacerbated pulmonary infection (76;192). Therefore, the weight of mice was monitored every day over the course of infection. The maximal weight loss was seen during the first 3-4 days post-infection, when the percentage of weight loss ranged from 19% to 23% (Figure 2.2). Three to four days post-infection, the animals started to regain weight, and after 14 days post-infection, the majority of mice recovered their original weight. We observed significant differences in the kinetics of weight loss variation during infection between the WT (18.0 ± 0.7) and IL-10 KO (23.3 ± 0.6) males at day 3 post-infection ($p \leq 0.001$) (Figure 2.2, panel A). Similar significant differences in the weight loss were observed at day 4 ($p \leq 0.001$) post-infection between the WT (13.3 ± 4.9) and IL-10 KO (23.2 ± 5.3) males. As for the female mice, IL-10 KO (22.4 ± 2.0) mice lost significantly more weight at day 4 post-infection ($p = 0.038$) compared to the WT mice (15.9 ± 2.0) (Figure 2.2, panel B).

Figure 2.2 Mean weight loss of WT (*solid*) and IL-10 KO (*open*) mice during *P. aeruginosa* lung infection. Data are presented as the mean percentage of weight loss of fourteen to ninety one mice since the first day of infection. Significant (*) differences were found between IL-10 KO and WT mice at day 3, day 4, day 5 and day 6 post-infection for males (A). Significant (*) differences were found between IL-10 KO and WT mice at day 4 and day 6 post-infection for females (B). The results are pooled from 4 independent experiments conducted under the same conditions.

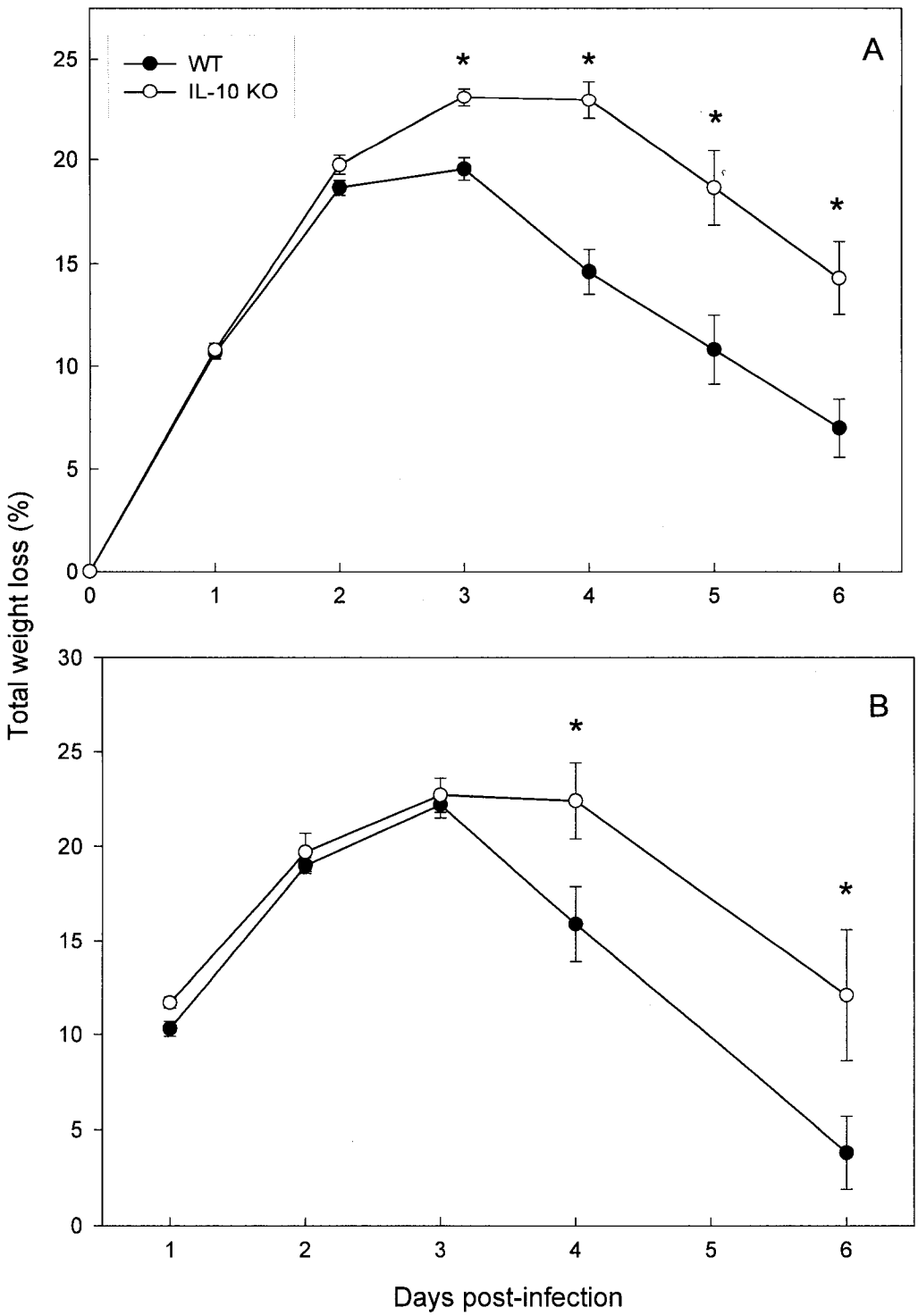
A
WT
IL-10 KO
Total weight loss (%)
25
20
15
10
5
0
0
1
2
3
4
5
6
*
*
*
*
B
30
25
20
15
10
5
0
1
2
3
4
5
6
*
*
Days post-infection

2.4.2.3 Recruitment of alveolar cells to the site of infection. In order to determine if IL-10 is involved in the regulation of the inflammatory cell recruitment to the lungs during the course of *P. aeruginosa* infection, we measured the number of alveolar cells recruited to the lung and the percentages of PMN, macrophages, and lymphocytes found in the lungs throughout the infection. As shown in Figure 2.3 (panel A), there was a significantly higher number of alveolar cells in the lung of IL-10 KO males than the WT controls at day 4 post-infection ($p \leq 0.001$). No difference in the amount of alveolar cells could be seen earlier in the infection. We did not observe any significant difference in the recruitment of alveolar cells between IL-10 KO and WT female mice neither at day 3 or 4 post-infection (Figure 2.3; panel B).

As shown in Table 2.2, there were differences in the subtypes of inflammatory cells found in the lung milieu of IL-10 KO and WT animals. At the early stage of infection (day 1 post-infection), there was no difference between the IL-10 KO and the WT mice either in the absolute number of alveolar cells found in the lungs, nor in the relative abundance of the subtype of alveolar cells (Figures 2.3 and 2.4). However, we observed more PMN and fewer macrophages in the lungs of IL-10 KO mice compared to their WT counterparts at day 4 post-infection, for both males and females (Table 2.2). At day 6 and day 14 post-infection, the percentage of PMN in the lungs decreased as the percentage of macrophages augmented in WT males compared to earlier days post-infection (Figure 2.4). This switch in cell population also occurred, although at a much slower pace in IL-10 KO mice. Altogether, the absolute and relative numbers of PMN and macrophages clearly demonstrate the dysregulation in cellular recruitment due to the lack of IL-10 protein expression in the lung. Overall, the lowest number of inflammatory cells observed in the WT males compared to all other groups (IL-10 KO males, IL-10 KO females and WT females), correlate with the lowest amount of CFU counts found in the lung of these mice compared to the other three groups at day 4 post-infection.

Figure 2.3 Alveolar inflammatory cells in the lungs of *P. aeruginosa* infected mice. The number of alveolar cells from the BALF was evaluated in IL-10 KO (*open*) and WT (*solid*) male (A) and female (B) mice 4 days post-infection. Data are presented as individual values of seven to ten mice and the horizontal line represents the median. Significant (*) difference was found between IL-10 KO and WT males ($p \leq 0.001$). These results illustrate 3 independent experiments performed under the same conditions.

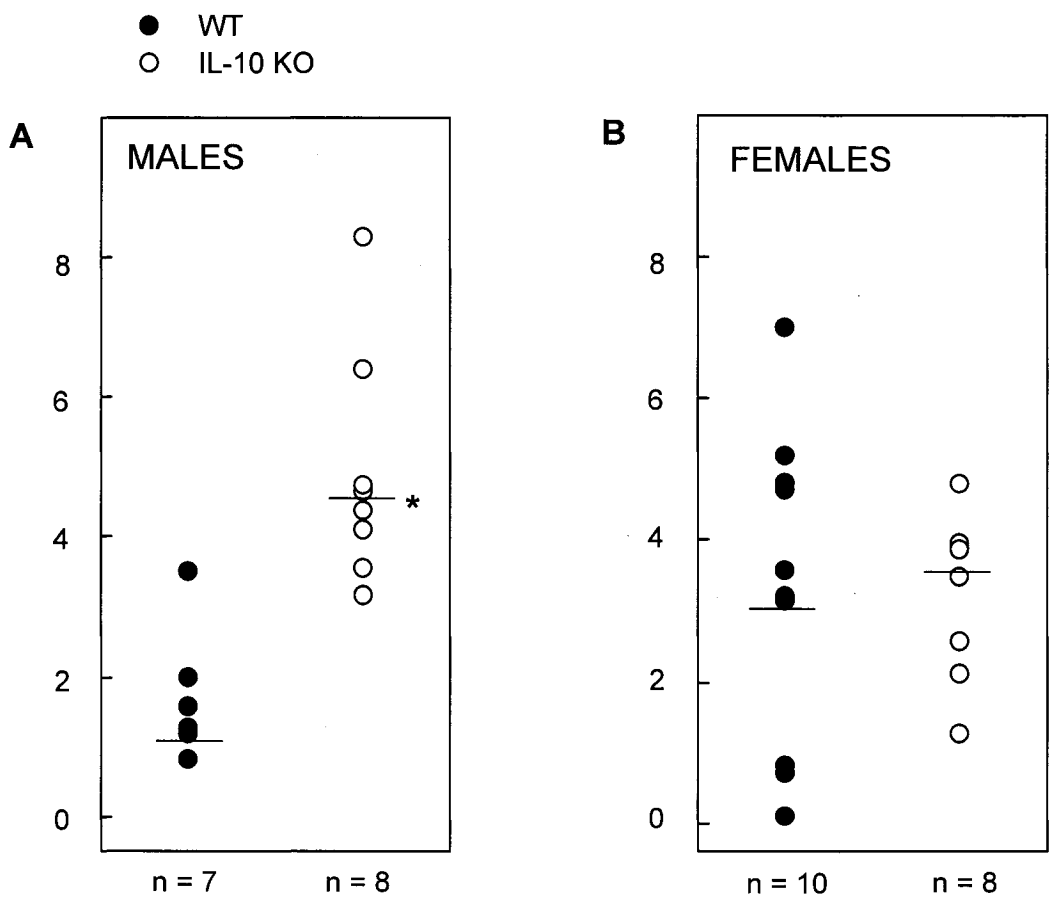
WT
IL-10 KO
A
MALES
B
FEMALES
8
6
4
2
0
*
n = 7
n = 8
n = 10
n = 8
10^6 Alveolar cells/lung

Figure 2.4 Recruitment of inflammatory cells in the lungs of *P. aeruginosa* infected mice. BALF were collected from WT (*solid*) and IL-10 KO (*open*) mice and the numbers of alveolar macrophages, lymphocytes, and PMN were calculated on the basis of the differential cell counts of Diff-Quick cytospin preparations. Data are presented as the relative numbers of specific inflammatory cell types of six to seventeen individual mice and the horizontal line represents the median. Significant (*) differences were found between IL-10 KO mice and their WT counterparts at day 4 post-infection (PMN: $p \leq 0.001$; macrophages: $p \leq 0.001$) and day 6 post-infection (PMN: $p = 0.015$; macrophages: $p = 0.015$). These results are pooled from 4 independent experiments.

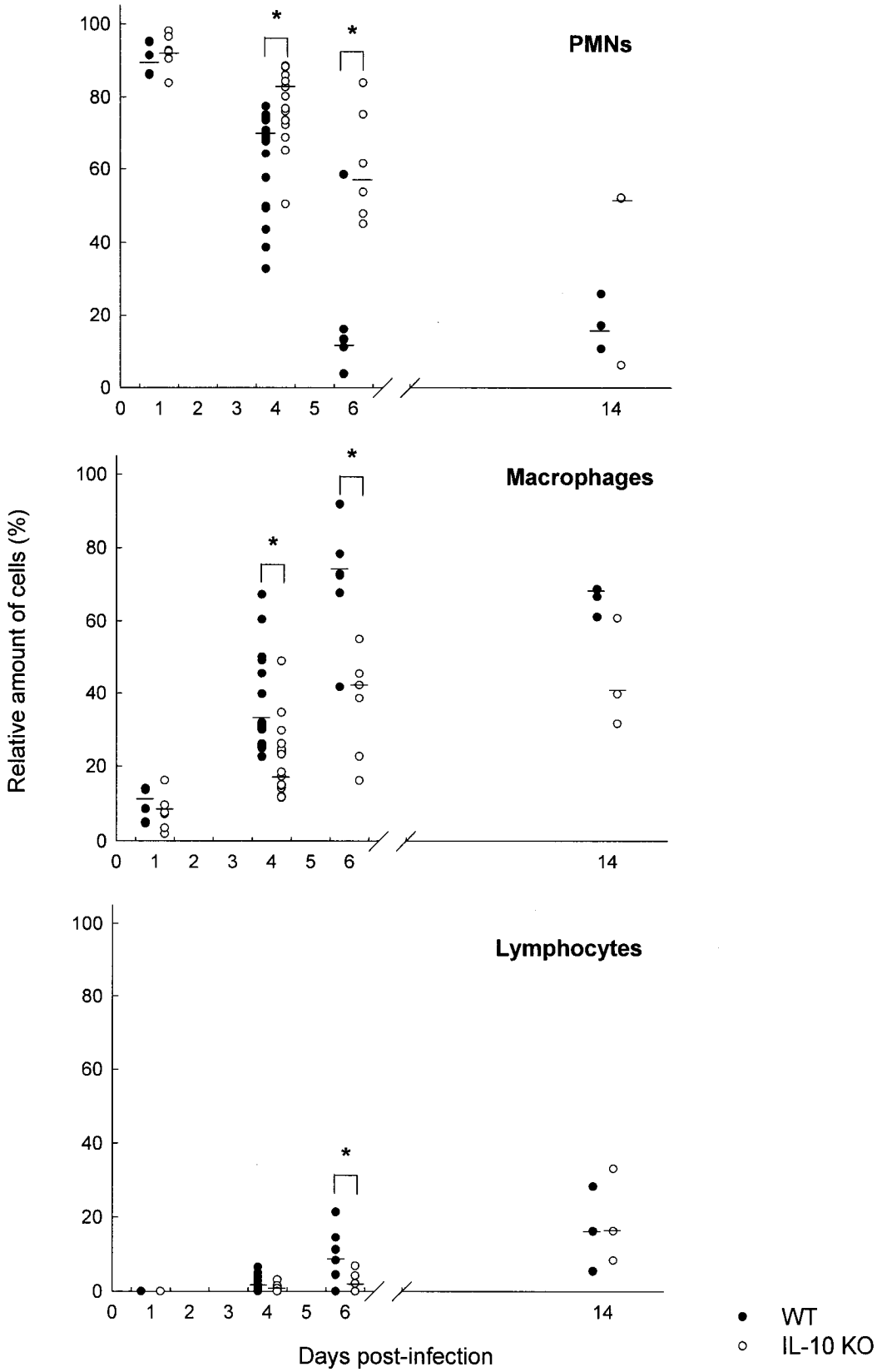
PMNs
Macrophages
Lymphocytes
Relative amount of cells (%)
Days post-infection
WT
IL-10 KO

Table 2.2 Recruitment of inflammatory cells into the lungs of infected mice

Sex	Genotype	N [2]	Alveolar cells (%)		
			PMN	Macrophages	Lymphocytes
Females	WT	10	68.1 [1] (57.5-73.8)	31.7 [1] (25.9-39.7)	0.2 (0.0-1.7)
	IL-10 KO	8	86.2 (75.3-88.4)	13.4 (11.6-24.6)	0.0 (0.0-0.5)
Males	WT	7	68.2 [1] (45.1-70.8)	30.3 [1] (26.4-48.9)	1.5 (0.2-4.6)
	IL-10 KO	8	78.1 (68.9-83.5)	21.4 (16.0-30.0)	0.4 (0.0-1.2)

Values are medians with quartiles in brackets.
[1] Medians of WT mice compared to those of IL-10 KO mice are significantly different at 4 days post-infection ($p \leq 0.05$) for the same sex.
[2] Number of animals; represent 3 different experiments performed under the same conditions.

2.4.2.4 Levels of TNF in the lungs of infected IL-10 KO and WT mice. To establish whether the higher susceptibility to lung infection observed in IL-10 KO mice was associated with TNF protein secretion, the levels of TNF were measured in the lung tissue homogenates following *P. aeruginosa* infection. In IL-10 KO male mice, we found significantly higher levels of TNF ($p = 0.029$) 3 days following *P. aeruginosa* infection, which coincided with a significantly higher weight loss, bacterial burden and cellularity in the lung compared to WT males. In females, IL-10 KO mice had significantly higher TNF levels in the lungs [0.56 ng/ml (0.37 - 0.73)] compared to WT mice [0.25 ng/ml (0.20-0.26)] at day 4 post-infection ($p \leq 0.001$). Since the differences were seen earlier in males than females, the overabundance of TNF in the lung of infected animals seems to correlate with more severe outcome in a time dependent fashion.

2.4.2.5 Levels of N51/KC in the lungs of infected IL-10 KO and WT mice. Since we observed high numbers of PMN in infected IL-10 KO mice compared to WT animals, we assessed the implication of N51/KC chemoattractant in the lung of IL-10 KO infected mice. We found significantly higher N51/KC levels in females IL-10 KO (94.9 pg/ml (30.6-157.6)) compared to females WT (26.7 pg/ml (23.8-33.0)) ($p = 0.026$). We also observed a tendency

towards higher N51/KC levels in IL-10 KO male mice compared to WT animals both at day 3 and 4 post-infection, although these differences were not statistically significant.

2.4.2.6 Bacterial burden in the BALF and lungs. We also observed a significantly higher number of CFU counts in the IL-10 KO compared to WT males in both lungs ($p = 0.022$) and BALF ($p = 0.008$) at day 3 post-infection (data not shown). Similar significant differences between WT and IL-10 KO males were observed at 4 days post-infection again in both lungs ($p = 0.021$; Figure 2.5; panel A) and BALF ($p = 0.021$; Figure 2.5; panel B) suggesting that IL-10 KO males are more susceptible to *P. aeruginosa* lung infection compared to the WT controls. Both WT and IL-10 KO female mice were very sensitive to lung infection, and we did not observe any significant differences in CFUs in the BALF and lungs of these mice (Figure 2.5). Significant differences were observed at day 4 post-infection between males and females WT mice in the CFU counts in BALF ($p = 0.042$) and lung tissue homogenates ($p \leq 0.001$) (data not shown). No difference in the bacterial burden was observed between female and male IL-10 KO mice (data not shown). The difference in the CFU counts observed between the IL-10 KO and the WT animals at day 4 post-infection occurred independently of weight or age since there was no correlation between the CFU counts in the lungs and the weight or the age of the animals in all the experiments (Table 2.3).

Table 2.3 Lack of correlation between the numbers of viable *P. aeruginosa* in the lungs of infected mice and weight or age at day 4 post-infection

CFU vs age		CFU vs weight	
IL-10 KO	WT	IL-10 KO	WT
r = 0.08	r = 0.28	r = -0.34	r = -0.22
p = 0.767	p = 0.286	p = 0.205	p = 0.403

Figure 2.5 Bacterial burden in the lungs of *P. aeruginosa* infected mice. The CFU counts were assessed in the lung tissue homogenates (A) and BALF (B) of IL-10 KO (*open*) and WT (*solid*) mice 4 days post-infection. Data are presented as individual values of seven to ten mice and the horizontal line represents the median. Significant (*) differences were found between IL-10 KO and WT males in the CFU counts in lung tissue homogenates ($p = 0.021$), and BALF ($p = 0.021$). These results illustrate 3 independent experiments performed under the same conditions.

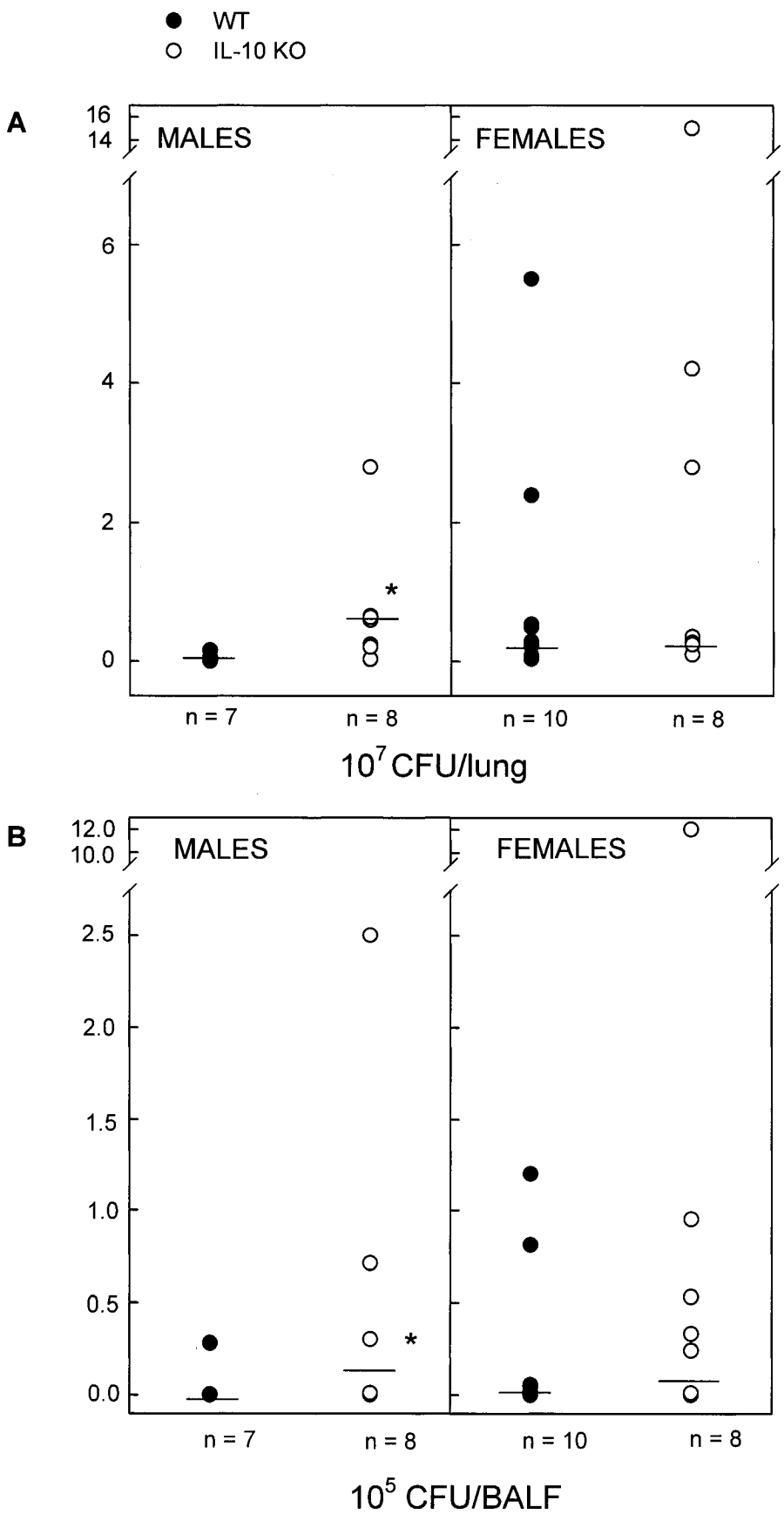
WT
IL-10 KO
A
MALES
FEMALES
16
14
6
4
2
0
*
n = 7
n = 8
n = 10
n = 8
10^7 CFU/lung
B
MALES
FEMALES
12.0
10.0
2.5
2.0
1.5
1.0
0.5
0.0
*
n = 7
n = 8
n = 10
n = 8
10^5 CFU/BALF

2.4.3 Effects of anti-IL-10 neutralization on the course of *P. aeruginosa* infection

Since we found that female mice, both WT and IL-10 KO, were extremely susceptible to infection with *P. aeruginosa*, it was possible that the absence of IL-10 during their development affected the overall maturation of the immune system. Alternatively, it is possible that the kinetics of the infection differ between males and females and to observe any difference in CFU, later time points post-infection would have been more appropriate for the analysis of female mice. To test those two possibilities, we decided to assess the susceptibility of female mice at day 7 and day 14 post-infection, and instead of using IL-10 KO mice, we performed systemic IL-10 neutralization using anti-IL-10 neutralizing antibodies.

Groups of B6 female mice were treated intraperitoneally with 4 doses of neutralizing anti-IL-10 (200 μg/dose) or isotype matched rat IgG (200 μg/dose). As shown in Table 3, treatment of animals with anti-IL-10 resulted in a significantly higher bacterial load in the lung ($p = 0.050$) at day 7 post-infection compared to IgG treated mice. Interestingly, the increased bacterial proliferation following *P. aeruginosa* infection was associated with significantly higher concentrations of TNF in the lungs of mice ($p = 0.012$). In order to determine if IL-10 influenced the composition of the cells at the site of infection, the cell composition of BALF was also analyzed. Neutralization of IL-10 also resulted in a significantly higher influx of PMN ($p = 0.001$) and a significant decrease in the numbers of macrophages recovered from the airways ($p \leq 0.001$) compared to WT control infected animals (Table 2.4). No significant differences in the number of lymphocytes were observed following systemic depletion of IL-10. At day 14 post-infection, both experimental groups almost resolved the infection and inflammation (data not shown). Overall, the WT females used in the above study were very much more susceptible to infection and developed more inflammation when IL-10 protein was neutralized.

Table 2.4 Effects of IL-10 neutralization on *P. aeruginosa* lung infection in B6 mice

	Antibody treatment	N[3]	Quartiles 25%	**50% (Median)**	75%	p value
CFU per lung [1]	IgG	15	1.6×10^4	**4.8×10^4**	9.2×10^4	p = 0.050
	Anti-IL-10	16	3.6×10^4	**24.0×10^4**	190×10^4	
TNF (ng/ml) [1]	IgG	13	12.1	**20.7**	38.4	p = 0.012
	Anti-IL-10	16	29.0	**50.8**	88.7	
PMN (%) [1, 2]	IgG	11	58.2	**66.0**	69.8	p = 0.001
	Anti-IL-10	17	72.8	**76.0**	80.5	
Macrophages (%) [1, 2]	IgG	11	23.2	**26.0**	34.8	$p \leq 0.001$
	Anti-IL-10	17	12.0	**16.0**	20.2	
Lymphocytes (%) [2]	IgG	11	5.0	**7.0**	10.0	p = 0.495
	Anti-IL-10	17	4.0	**6.0**	8.2	

[1] Medians of the two treatment groups are significantly different at 7 days post-infection ($p \leq 0.05$).
[2] Values are calculated based on the cytospin differential staining analysis of BALF harvested from *P. aeruginosa* infected B6 mice.
[3] Number of animals; represent 3 different experiments performed under the same conditions.

The studies illustrated in this manuscript represent, to our knowledge, the first comprehensive analysis of the effects of sex and IL-10 on the inflammatory response and susceptibility to lung infection with *P. aeruginosa.*

2.5 Discussion

In the current study, we assessed the effect of gender on infection and inflammation using a mouse model of lung infection with *P. aeruginosa.* Using B6 male and female mice infected with *P. aeruginosa,* we found differences in the inflammatory response to the bacteria between both sexes. Females had a higher inflammatory response in terms of cytokines secreted, which correlated with a higher bacterial load, and a more severe weight loss compared to males (Table 2.1).

These differences in inflammation influenced by gender prompted us to look at the effect of IL-10 in *P. aeruginosa* lung infection focusing on the gender issue. Therefore, we infected IL-10 KO male and female mice and their respective controls, and extensive analysis of various parameters of susceptibility was performed. We observed that IL-10 KO males were much more susceptible to *P. aeruginosa* lung infection compared to WT males. This was observed in the weight loss, the bacterial load in the lung, and in the cellular inflammatory response (Figures 2.2 - 2.5, Table 2.2). As for the females, WT and IL-10 KO mice were extremely sensitive to the infection, comparable with the CFU levels of males IL-10 KO. Overall, we were able to observe higher weight loss, inflammatory cytokine responses, and dysequilibrated PMN-macrophages ratio in the IL-10 KO females compared to WT females. We have chosen to analyze the parameters of inflammation between day 3 and 4 following *P. aeruginosa* lung infection since we could already see major differences in the inflammatory response between the IL-10 KO and the WT animals and these were the days most frequently used in other similar studies (99).

Chmiel and colleagues also analyzed early time points during the course of *P. aeruginosa* infection and reported a trend towards a lower bacterial burden for WT male mice after bacterial inoculation compared to their IL-10 KO counterparts at 3 days post-infection, although this difference was not significant. In the present study, we showed that IL-10 KO males have significantly more CFU counts in the lungs and BALF both at day 3 and 4 post-infection compared to WT mice. The number of infected animals used in our study most likely contributed to the statistical significance that we were able to achieve. At day 3 to 4 post-infection, both WT and IL-10 KO females were similarly susceptible to infection. However, we could already see a very clear difference in the level of inflammatory cytokines. These differences did not result from the altered maturation of the immunological system in IL-10 KO mice that were devoid of IL-10 during development since we saw similar differences in the inflammatory cytokine levels when we neutralized IL-10 in WT mice during the course of infection.

Several reports demonstrated that substantial weight loss occurred in CF patients during acute exacerbated pulmonary infection. This weight loss might be due to changes in energy expenditure, although the exact cause of these changes is still not well understood (192;249;248;264;292). Previous studies showed a correlation between weight loss or energy expenditure and inflammatory cytokines (76;285). In our mouse model, both IL-10 KO and control animals lost weight during the course of infection, but IL-10 KO showed a more pronounced weight loss. Interestingly, we found that WT mice recovered from the weight loss more quickly than IL-10 KO mice. Overall, similar association between the weight loss and CFU was suggested by Heeckeren and colleagues with a CF mouse model (285). The time points of maximal weight loss presented in this study corresponded with differences observed between the IL-10 KO and the WT mice in the CFU counts, number of inflammatory cells recruited, and levels of TNF observed in the lungs.

Upon *P. aeruginosa* colonization of the lungs, inflammatory cells are recruited into the lung to initiate an immune response cascade, which ultimately leads to clearance of the bacteria. Since IL-10 is principally an anti-inflammatory cytokine that down regulates TNF and MIP-2, we hypothesized that IL-10 KO mice should have greater cell recruitment to the lung than WT, thereby allowing a better environment for the eradication of the infection. We demonstrated a significantly higher number of inflammatory cells present in the infected lungs in the IL-10 KO males ($p \leq 0.001$; Figure 2.3, panel A), that was associated with a higher bacterial burden. Our results showed that although the recruitment of an appropriate number of inflammatory cells is important, the type of cells recruited to the lung is also crucial. It was previously shown, in mouse models of *P. aeruginosa* lung infection, that an exaggerated inflammatory response dominated by PMN correlated with susceptibility to infection, whereas a modest inflammatory response dominated by macrophages correlated with resistance (237). In CF patients infected with *P. aeruginosa,* a persistent inflammation dominated by PMN neutrophils is observed (12). Moreover, BALF studies have suggested that CF

infants, showing no clinically apparent lung disease, developed very early a predominant neutrophilic lung inflammation (157). We also observed in our study that the switch from PMN to macrophages predominance in the BALF was initiated at a later time point for IL-10 KO animals compared to WT controls, emphasizing the importance of IL-10 to initiate this change. Overall, our results suggest that PMN overabundance and/or dysfunction interfer with clearance of the bacteria from the lungs. Considering that PMN exert their antibacterial activity by releasing reactive oxygen species, proteases and diverse cytokines, an excess of PMN at the later phase of infection could provoke more harm than good by damaging lung tissues and thereby affecting the efficient eradication of the bacteria. Therefore, the number of PMN, as well as the time point at which the relative abundance of alveolar cells switches from a predominantly PMN to a predominantly macrophage cell population, seems to be of crucial importance.

Since IL-10 inhibits the production of TNF and IL-8 (81), we also investigated the effect of the lack of IL-10 on TNF and N51/KC protein secretion kinetics in the lung. Our previous results show the beneficial effects of a transiently increased TNF level (during the first 24 hours) in *P. aeruginosa* resistant mice strain compared to susceptible strains in order to efficiently eradicate the bacteria from the lungs (98). Our present data suggest that higher and prolonged expression of TNF in the lung is not always beneficial for the mice in terms of efficiency of the immune response and clearance of the bacteria throughout the time of infection. Furthermore, as demonstrated in adult respiratory distress syndrome, the ratio of IL-10 and TNF production may play a pivotal role in the balance between protection and pathogenesis in *P. aeruginosa* lung infection (5). Altogether, these results suggest that the proper timing and quantity of TNF protein secretion, as well as other inflammatory mediators in the lung environment, are mandatory in order to adequately control other immunological mediators which would lead to an efficient eradication of the bacterial infection.

In BALF as well as respiratory epithelial cells recovered from CF patients, high levels of the chemoattractant IL-8 (human orthologue of murine N51/KC and MIP-2) are observed corresponding to high number of PMN (16;17;175;69). N51/KC is known to be down regulated by IL-10 at the mRNA level (151;153). We found significantly higher N51/KC levels in IL-10 KO *P. aeruginosa* infected females compared to their WT controls. We also observed a trend towards higher N51/KC levels in the IL-10 KO males, although these differences did not reach statistical significance either at day 3 or 4 post-infection. Interestingly, there was a significant difference between WT male and female mice in their ability to produce N51/KC, and higher susceptibility to *P. aeruginosa* infection observed in WT females and correlated with higher levels of N51/KC present in the infected lungs. We also observed a difference between WT male and female animals at day 3 post-infection (Table 2.1) where females had higher levels of N51/KC in the lung. These results suggest that N51/KC might be an important player during the course infection, but other mediators are also of importance.

Overall, differences observed between female and male WT mice, with respect to the weight loss, bacterial load, and cytokines production, are consistent with previously reported data suggesting that the prognosis of the disease is worse in CF female patients compared to CF male patients (82;183;61;44;316;45;239). Unfortunately, most of the CF human studies using both male and female adults and/or children did not analyze or report any differences in IL-10 levels between genders (16;18;17;195;203;300;189). Nevertheless, the importance of IL-10 is clearly demonstrated in the gender-related differences of the immune response (297), associating sex steroids with the secretion of IL-10 (2), and gender-related difference in IL-10 administration therapy (143).

Taken together, the results presented here demonstrate a major difference between the males and the females in the susceptibility to lung infection reinforcing the importance of studying pulmonary diseases taking gender into account. Our data also show the importance of a proper balance in the cytokine

production and type of alveolar inflammatory cells in a timely manner, and reinforce the importance of IL-10 protein secretion during lung infection with *P. aeruginosa*.

CHAPTER III

Preface

The previous chapter clearly showed the significance of the proper regulation of the immune system to create an efficient inflammatory response against *P. aeruginosa* in the lungs. However, many differences that are observed in early-age CF patients compared to normal healthy controls exist prior to any bacterial infection. These differences observed at the basal level remain unexplained. However, because many phenotypic expressions of the disease do not directly correlate with the type of mutation of the *Cftr* gene, this implies the existence of modifier genes also influencing the CF disease. We therefore decided to characterize the lung environment of *Cftr*-KO prior to any bacterial infection. Using a mouse model that develops the CF lung disease phenotype, we extensively analyzed the differential gene expression pattern between the normal lungs of WT mice and the affected lungs of *Cftr*-KO uninfected mice. The following chapter presents the studies aimed at identifying genes involved in the CF mice lung disease model, using microarray analysis, quantification of candidate gene mRNA and protein expression approaches.

CHAPTER III.

DISTINCT PATTERN OF LUNG GENE EXPRESSION IN THE *Cftr*-KO MICE DEVELOPING SPONTANEOUS LUNG DISEASE COMPARED TO THEIR LITTERMATE CONTROLS

based on submitted manuscript

Guilbault, C., *Novak, J., Martin, P., Boghdady, M.L., Saeed, Z., Guiot, M.C., Hudson, T. and D. Radzioch., submitted August 2005 to Physiological Genomics Journal*

3.1 Abstract

Cystic fibrosis is caused by a defect in the CFTR protein that functions as a chloride channel. Dysfunction of the CFTR protein results in salty sweats, pancreatic insufficiency, intestinal obstruction, male infertility and severe pulmonary disease. Most of the morbidity and mortality in CF patients result from pulmonary complications. The differences observed in early-age CF patients, prior to bacterial infection, remain unexplained. Many phenotypic expressions of the disease do not directly correlate with the type of mutation of the *Cftr* gene, consequently implying the existence of modifier genes influencing the severity of the CF disease. Using a mouse model that develops the CF lung disease phenotype at 12 weeks of age, we extensively analyzed the differential gene expression pattern between the normal lungs of WT mice and the affected lungs of *Cftr*-KO uninfected mice. This paper is aimed at identifying genes involved in the CF mice lung disease model, using microarray analysis followed by quantification of candidate gene mRNA and protein expression approaches. The data presented in this manuscript demonstrate several very interesting candidate genes clearly illustrating the differences in the lung environment of WT and *Cftr*-KO mice.

These findings point to distinct mechanisms of gene expression regulation in mice with CF and in control mice.

3.2 Introduction

The CF disease is caused by a defect in the CFTR protein that functions as a chloride channel regulated by cyclic AMP. Most of the morbidity and mortality in CF patients result from pulmonary complications. Chronic infection of the lungs with mucoid strains of *P. aeruginosa*, which tends to persist in most patients, results in an exaggerated neutrophilic inflammatory response and in a dysregulated production of pro-inflammatory cytokines as IL-1, IL-6, IL-8 and TNF, and low levels of the anti-inflammatory IL-10 in BAL fluids (266;186;141;121).

The differences observed in early-age CF patients, prior to bacterial infection, remain unexplained. Many phenotypic features of the disease do not directly correlate with the type of mutation of the *Cftr* gene (314). This would imply the involvement of other factors contributing to the *Cftr* gene genotypes, which may influence the disease phenotypes. Interestingly, the existence of modifier genes influencing the severity of the CF disease was first documented by studies performed by Höpken and colleagues (126). They have shown that the C5a receptor plays a very important role in mediating polymorphonuclear (PMN)-dependent clearance of the mucosal bacterial organisms in the lung. Interestingly, C5a-receptor-deficient mice challenged with sub lethal inocula of *P. aeruginosa* become extremely susceptible to infection by secondary bacterial strains such as *Staphylococcus sp.* and *H. influenza.* These and other studies have clearly shown that modifier genes and potential susceptibility loci are important in modulating CF disease severity associated with the lungs, the intestine and the weight phenotypes in CF (114;115;116;126).

Since the discovery of the *Cftr* gene, no natural animal model was found; however, a number of animal models have been developed (for a review, see

reference Nelson *et al.* (193)). Animal models represent the best surrogate for understanding the complexities of the human system, provided that the results from experimental animal studies are extrapolated wisely. Most CF models developed are murine models, in view of the fact that the mouse genome is similar to that of human; also, because its entire genome sequence has been established, mouse models are now extensively used for the genome-wide examination of gene expression. A number of investigators have generated *Cftr* gene KO mice by targeted gene disruption (38;48;58;86;198;256;281;312). Although the generated mice have most of the symptoms of CF, only a few of them display the CF lung phenotype (193).

C57BL/6$^{H/M}$-*Cftr*.ko mice described by Kent and colleagues (147) represent a unique model of spontaneously occurring CF lung disease. Our laboratory participated in developing and characterizing various backcrosses of *Cftr*-KO mice, including the C57BL/6$^{H/M}$-*Cftr*.ko mice (147;110). Histological evaluation of the lungs was performed on this CF mouse model in order to identify the pathological state of the animals from 3 to 20 weeks of age. We observed that the uninfected *Cftr*-KO mice showed increased hyperplasia of epithelial cells, basement membrane thickening, as well as enhanced inflammatory cell infiltration into the lung tissue compared to the WT uninfected controls. We used this animal model for the studies on gene expression regulation in non-infected and *P. aeruginosa*-lung infected CF mice and their littermate controls (111;110).

To our knowledge, all previous studies on genetic expression differences between normal and *Cftr*-deficient animals used CF mutants that do not spontaneously acquire lung disease (144;213;288;301;303). We therefore used the mouse model of CF that develops spontaneous lung disease to analyze the differential gene expression pattern in the normal lungs of WT mice and the affected lungs of *Cftr*-KO mice. The aim of this paper is to identify candidate genes associated with the lung disease phenotype observed in these mice. The comprehensive analysis of the data presented in this manuscript clearly shows

differences in the lung environments of WT and *Cftr*-KO mice involving gene expression regulation and identifies several novel candidate genes that seem to be associated with CF lung disease.

3.3 Material and Methods

3.3.1 Mice. Age- and gender- matched C57BL/6 WT mice (n = 9 females, n = 13 males) and C57BL/6-*Cftr*$^{-/-}$ (*Cftr*-KO) inbred mice (n = 10 females, n = 12 males) were housed (1 - 4 animals/cage), bred and maintained in a barrier facility unit under specific pathogen-free conditions. WT mice were fed with the NIH-31 modified mouse irradiated diet (Harlan Teklad, Indianapolis, IN) (until 3 weeks prior to experiment when they were transfer on the same diet as *Cftr*-KO), whereas *Cftr*-KO mice were fed the Peptamen liquid diet (Nestle Canada, Brampton, ON), starting at 14 days of age. The liquid diet, freshly made every morning, was provided in 50 ml centrifuge tubes (Sarstedt, Montreal, QC). Mice had *ad libidum* access to sterile acidified water. Experimental procedures with the mice were conducted in accordance with the Canadian Council on Animal Care and with the approval of the Animal Care Committee of the McGill University Health Center, Montreal, QC, Canada.

3.3.2 Lung histopathology. Lungs were removed from the mouse, inflated with 10% buffered formalin acetate (Fisher Scientific, Nepean, ON) and immersed in that buffer for a minimum of 36 hrs. The lungs were then trimmed and embedded in paraffin. Paraffin sections were sliced 3 μm thick using a Reichert-Jung microtome. Lung sections were cut at regular intervals to get sections at different depths of the lung. Three sections were used for each of the following standard staining methods: Haematoxylin and eosin (HE), Periodic-Acid Schiff (PAS) and Masson's Trichrome (MT). Each parameter of lung morphology was observed under these specific stains and scored using scales specific to each parameter, as described in section 4.3.8 (110).

3.3.3 RNA extraction. Total RNA was isolated from the lung tissue using TRIzol (Invitrogen, Burlington, ON). The quality of the RNA was assessed first using electrophoresis in a 2.2 M formaldehyde 2% agarose gel and then using a 2100 Bioanalyzer with the RNA 6000 Nano LabChip kit (Agilent Technologies, Germany). The RNA samples were used for microarray only when they were of a high quality and integrity.

3.3.4 Microarray experiment. Twenty μg of total RNA from each sample was reverse transcribed using a oligo-dT primer containing a T7 RNA polymerase-binding site. An *in vitro* transcription was performed on this cDNA and the resulting cRNA was biotinylated via incorporation of biotinylated dUTP and dCTP. The cRNA samples were then fragmented in 40 mM Tris acetate, 100 mM potassium acetate, and 30 mM $MgCl_2$ (pH 8.1) at 95°C. cRNA was hybridized to an Affymetrix GeneChips MG-U74Av2 for 16 hours at 45°C, washed, stained and scanned with a Hewlett Packard Gene Array scanner. The hybridization assays and data collection were performed at the McGill University and Genome Quebec Innovation Centre (Montreal, QC). Affymetrix Analysis Microarray Suite MAS 5 software was used to estimate the expression level for each probe set from the recorded laser intensity of 11 probe pairs. Prior to the analysis, all arrays were globally pre-normalized to 100% of the array mean. The dispersion patterns were examined for all pair-wise combinations of the same type (WT-WT, *Cftr*-KO- *Cftr*-KO), as well as WT - *Cftr*-KO arrays for both female and male samples. In the case of several samples, we observed small deviations from linearity and introduced appropriate corrections. Generally, the plots exhibited low-dispersion characteristics with few strongly over- and/or under-expressed genes.

3.3.5 Microarray data processing. For microarray analysis, we used lung mRNA from three pairs of male and five pairs of female mice. In the first step of analysis, we characterized the dispersion properties of the samples in pair-wise comparisons, using the consecutive sampling program (197). Briefly, the program's main subroutine ranks the genes according to the mean expression, takes

as statistical "consecutive" samples 12 consecutive genes and calculates the characteristic function that approximates standard deviation of the dispersion plot as a linear function of the mean expression. Complementary subroutines determine boundaries of the probability intervals, as well as calculate the percentage of the consecutive samples that violate the Kolmogorov-Smirnov normality test and other parameters. To determine which genes have significantly different expression levels between the WT and *Cftr*-KO samples, we analyzed the data using both the consecutive sampling and coincidence test (197) and Robust Multi-array Analysis (RMA) (15;133). We limited the comparison range to about 7450 genes that have mean expressions above 10. First, for the males, using the consecutive sampling method, we identified all genes for which the level of expression in WT and *Cftr*-KO was different at the 0.8 probability (80%). Such genes were located above and below the 0.8 probability interval. Furthermore, there were nine possible pair-wise comparisons between WT and *Cftr*-KO samples. We selected as candidates, the genes with expression levels above the 0.8 probability interval in at least 7 out of 9 possible cases. As complementary tests, we employed the Wilcoxon-Mann-Whitney test and the t-test. For the females, we did a similar analysis, selecting the genes with expression above the 0.8 probability interval in at least 15 out of 25 possible cases. Since the amount of mRNA samples from females (n = 5 for each group) was higher than from males (n = 3 for each group), we could further process the female mouse data and confirm the results using RMA.

3.3.6 Subsequent gene expression analyses. The gene expression patterns of arrays were compared by hierarchical clustering (10 arrays for females, 6 arrays for males). Cluster analysis was performed for 81 genes from females and 116 genes from males that met the necessary criteria. This clustering analysis was done using CLUSFAVOR[1] with the centroid method (204). The distance between the arrays was measured as Euclidean distance. The array data of the experimental sets (WT and *Cftr*-KO) common to both sexes were also compared according to gene ontology. Gene ontologies were analyzed using GENMAPP~MAPPFinder[2] V.2.0 (63) in all selected candidate genes.

3.3.7 Real-time polymerase chain reaction. The mRNA expression levels were also quantified using the quantitative real-time reverse transcription (RT)-PCR method. Genes of interest, whose expression levels were changed depending on the *Cftr* genotype in the microarray experiments were selected. Primers were designed for these selected genes. Total RNA was treated with DNase I and reverse-transcribed into cDNA using the DNA-free kit (Ambion Inc., Austin, TX). The cDNA was amplified in the MX4000 system (Stratagene) using the Brillant SYBR Green QPCR kit (Stratagene, Cedar Creek, TX) according to the manufacturer's instruction. The amount of cDNA was calculated based on the threshold cycle (C_T) value and standardized by the amount of the house-keeping gene using the $2^{-\Delta\Delta C}{}_T$ method (168):

$$\Delta\Delta C_T = (C_{T,\text{Target}} - C_{,\text{GADPH}})_{\text{Time } x} - (C_{T,\text{Target}} - C_{,\text{GADPH}})_{\text{Time } 0})$$

where the "target" represents the gene of interest tested. Each gene expression was standardized by the expression of a house-keeping gene, glyceraldehyde-3-phosphate dehydrogenase (GAPDH). The melting curve, as well as agarose gel electrophoresis analyses, were also performed to confirm that a single product of expected length was amplified.

3.3.8 Method of mouse lung infection with *P. aeruginosa* instilled in agarose beads. In order to establish a model of prolonged lung infection, *P. aeruginosa* strain 508 (110) were impregnated in agar beads. The bead suspension was freshly prepared the day before each experiment, as previously described, and stored at 4°C overnight. The number of bacteria was determined after homogenizing the bacteria-impregnated beads' suspension. Inoculum was prepared by diluting the beads suspension to 2 x 10^7 CFU per mL. Mice were anaesthetized with a combination of ketamine (7.5 mg/ml) and xylazine (0.5 mg/ml) administered intraperitoneally at a dose of 20 ml/kg of body weight. Once the mouse was successfully anaesthetized, the animal was installed under binoculars (Microscope M650, Wild Leitz, Willowdale, ON) in the vertical position and was held on a restraining board by holding the animal by its upper

incisor teeth, as previously described (110). The tongue was then gently pulled to the side of the mouth and a 26-G gavage needle was inserted into the mouth and guided through the pharynx to gently touch the vocal cords to see the lumen of the trachea; the needle was then introduced into the trachea to reach the lung for the bilateral injection of the 50 µl inoculum's. After inoculation the animal regained righting reflex within an hour. A final dose of 1 x 10^6 *P. aeruginosa* was used for infection in WT and *Cftr*-KO mice. Mice were monitored 3 times daily; the maximum weight loss allowed was 15%. Mice were sacrificed by CO_2 overdose.

3.3.9 Immunostaining (IHC). The formalin-inflated lung sections were deparaffinized and hydrated to distilled water in the following sequence: xylene wash (5 min), xylene wash (x 2), 100% ethanol wash (x 2), 95% ethanol wash (x 2), 70% ethanol wash, distilled water, 2 minutes each. Slides were then placed in the DAKO Autostainer: Universal Staining System machine (DAKO Corporation, Cartinteria, CA) for the following treatment steps: 3% H_2O_2 (in distilled water) for 10 min.; Tris-buffer for 5 min.; Proteinase K (DAKO) for 5 min.; Protein block (DAKO) for 10 min.; Rabbit polyclonal anti-matrix metalloproteinase (MMP)-9 antibody (Ab) (Chemicon International, Temecula, CA) or SLPI Ab (kindly provided by Dr Aihao Ding from Cornell University) for 60 min.; Tris-buffer for 5 min. (x 2); biotinylated goat anti-rabbit immunoglobulin (Ig)G (DAKO) for 30 min.; Tris-buffer for 5 min. (x 2); streptavidin-horseradish peroxidase complex for 30 min.; Tris-buffer for 5 min. (x 2); AEC Substrate Chromogen solution for 10 min.; distilled water for 5 min. Slides were then removed from the DAKO Autostainer and counterstained in Harris' hematoxylin for 1 min., and they were then mounted using AquaMount Mounting Media. They were left to dry for at least 24 hours before analysis. The expression of the proteins analyzed in the lung was assessed by scoring the intensity of the immunostain. The stain intensity was scored according to the following arbitrary scale ranging from 0 to 5, where 0 refers to no stain, and 5 indicates that all structures in the lung were stained. A score of 1 represented sporadic staining; a score of 2 was given when the lung displayed some staining, mostly in the alveoli. Moderate staining, expressed

mostly in capillaries and larger blood vessels throughout the lung surface, was given a score of 3; and when alveoli and blood vessels were relatively all stained, but not the airways, a score of 4 was given. The averaged score was then calculated to a relative percentage of protein expression to illustrate the comparison between the different groups studied.

3.3.10 IgGs measurements. The levels of IgG were assessed in plasma samples prepared from uninfected animals with the Mouse IgG_1 ELISA Set (Bethyl Laboratories Inc., Montgomery TX) and with the Mouse IgG_{2a} ELISA Set (BD Biosciences, San Diego, CA) according to the manufacturer's instructions. Briefly, 96-well polyvinyl chloride microtitre Immulon II plates (Dynatech, Chantilly, VA) were coated at 4° C overnight with anti-mouse IgG_1 or anti-mouse IgG_{2a} capture Abs. Plates were then washed, incubated with blocking buffer (IgG_1: 50mM Tris, 0.14M NaCl, 1% bovine serum albumin pH 8.0; IgG_2: PBS, 10% FBS, pH 7.0), and sequentially incubated at room temperature with various dilutions of plasma samples, biotinylated anti-mouse IgG_1 Ab or biotinylated anti-mouse IgG_{2a} Ab, avidin-horseradish peroxidase-conjugated Ab and peroxidase substrate. The intensity of the colorimetric reaction was determined by spectrophotometry at 405 nm. The levels of IgG_1 were calculated with reference to a 4 parameter logistic (4PL) standard curve established with recombinant mouse IgG_1 supplied with the ELISA kit. The levels of IgG_{2a} were calculated with reference to a linear standard curve established with recombinant mouse IgG_{2a} supplied with the ELISA kit.

3.3.11 Statistical analyses. Analyses were performed for each gender separately because of the known gender differences in the immune response (112). Data was analyzed using SigmaStat V3.01 software (SPSS Inc, Chicago, IL). Statistically significant differences between means and medians of studied groups were evaluated using Student's t-test and the nonparametric Mann-Whitney U test, respectively. One-way ANOVA and Kruskal-Wallis ANOVA on ranks, combined with pair-wise appropriate multiple comparison procedures, were used to evaluate differences between multiple groups. Significance was set at a two-tailed p value

of ≤ 0.05. Specific statistical methods used for the intensity of the microarray probes analyses were described earlier in the subsection "Microarray data processing".

3.4 Results

3.4.1 Mouse model of CF. Histological evaluation (Table 3.1) of the lungs of our B6 CF mouse model was performed as reported in Guilbault *et al.* (110). As represented in Figure 3.1, the uninfected *Cftr*-KO mice showed enhanced inflammatory cell infiltration (panel A), fibrosis (panel B), as well as increased hyperplasia of epithelial cells (panel C) in the lung tissue compared to the WT uninfected controls.

Table 3.1 Histopathological evaluation of lungs from non-infected *Cftr*-KO and WT mice.

		cell hyper-plasia	cell meta-plasia	basement membrane thickening	Inflamma-tory cell infiltration	mucus accumulation		fibrosis	
						small airways	large airways		
		HE	*HE*	*HE*	*PAS*	*PAS*	*PAS*	*MT*	*HE*
♀	WT	**1.8**[1]	1.9	1.7	**1.8**[2]	1.4	4.7	1.3	1.4
	KO	**2.3**	1.4	1.5	**2.5**	1.3	4.7	1.3	1.3
♂	WT	**1.0**[1]	1.5	1.0	**1.5**[2]	1.5	5.0	N/D	1.5
	KO	**2.8**	1.5	1.7	**2.1**	1.3	4.4	1.5	1.5

[1] Scores of the *Cftr*-KO are significantly different compared to the WT for females ($p = 0.005$) and males ($p = 0.041$).

[2] Scores of the *Cftr*-KO are significantly different compared to the WT for females ($p = 0.015$) and males ($p = 0.035$).

HE, Haematoxylin and eosin; PAS, Periodic-Acid Schiff; MT, Masson's Trichrome

N/D; not detectable

Figure 3.1 Histopathological status of the lungs of uninfected WT and *Cftr*-KO mice. Representative haematoxylin- & eosin- stained (A, C) and Masson's Trichrome (B) stained lung sections that were prepared from uninfected WT and *Cftr*-KO mice. Sections from *Cftr*-KO mice show cell infiltration in the bronchi and alveoli (A), fibrosis (B) and hyperplasia of the epithelium (C), as compared with sections from WT mice that show a normal lung structure.

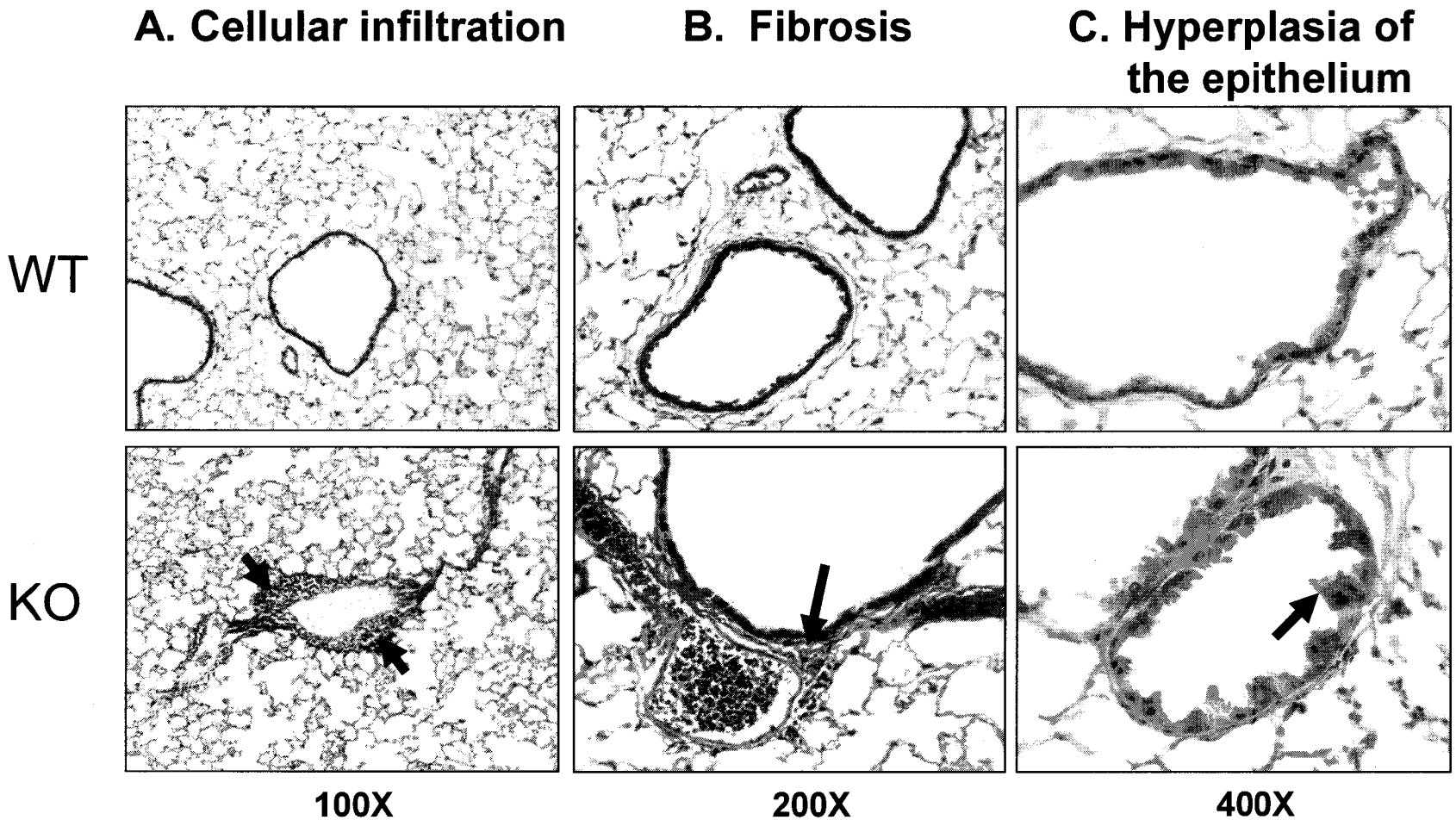
A. Cellular infiltration
B. Fibrosis
C. Hyperplasia of the epithelium
WT
KO
100X
200X
400X

3.4.2 Genes differentially expressed between WT and *Cftr*-KO mice – microarray analyses. As the first step of analysis, we characterized dispersion properties of the samples in pair-wise comparisons using the consecutive sampling program (197). To determine which genes have significantly different expressions between the WT and *Cftr*-KO samples, we analyzed the data using the consecutive sampling and coincidence test (197) for males and females. The Robust Multiarray Analysis (15;133) was also performed, but only for the females, since for males we did not have a sufficient amount of samples (n = 3 for males, n = 5 for female mice).

First, using the consecutive sampling method, we identified all genes, of which the level of expression in the female WT and *Cftr*-KO groups of mice was different at 0.8 probabilities (80%). Such genes are located above and below the 0.8 probability interval. Furthermore, for the selection of candidate genes, we required that a given gene be above (up-regulation of gene expression in *Cftr*-KO versus WT) or below (down-regulation) the probability interval 0.8 in 15 out of 25 possible comparisons (*Cftr*-KO1 vs. WT1, *Cftr*-KO2 vs. WT1, *Cftr*-KO3 vs. WT1, *Cftr*-KO1 vs. WT2, etc.). The red squares and green triangles in Figure 3.2A show the up-regulated and down-regulated averaged values of the candidate genes, respectively. Table 3.2 summarizes the set of the candidate genes for females specifically. We selected a total of 81 probes; 62 probes showed higher expression in *Cftr*-KO compared to WT (55 probe sets passed the Wilcoxon test) and 19 probes had lower expressions (11 probe sets passed the Wilcoxon test) (see also Appendix 2).

Next, we performed a similar analysis using the mRNA samples purified from the lungs of the male *Cftr*-KO and WT mice. In the males, there are nine possible pair-wise comparisons between WT and *Cftr*-KO samples. For the selection of candidate genes, we required that a given gene probe be above or below the probability interval of 0.8 in 7 comparisons. The red squares and green triangles in Figure 3.2B show the up-regulated and down-regulated averaged

values of the candidate genes, respectively. Table 3.3 summarizes the set of candidate genes for males specifically. We selected a total of 116 probes; 102 probes showed higher expression in the *Cftr*-KO compared to the WT (83 probe sets passed the Wilcoxon test) and 14 probes had lower expression (11 probe sets passed the Wilcoxon test and 12 passed the t-test) (see also Appendix 2). Table 3.4 shows the candidate genes common to both females and males.

Table 3.2 Genes differentially expressed between *Cftr*-KO and WT females

Over-expressed Genes in *Cftr*-KO	Fold difference	P value*	Affymetrix probe†
immunoglobulin heavy chain 4 (serum IgG1) (Igh-4)	6.8	0.048	99420_at (4)
immunoglobulin heavy chain (Igh-VJ558)	3.9	0.016	97574_f_at (4)
immunoglobulin kappa chain variable 8 (V8) (Igk-V8)	3.6	0.008	101718_f_at (13)
Immunoglobulin light chain variable region	3.1	0.004	94725_f_at
immunoglobulin joining chain (Igj)	2.8	0.007	102372_at
recombinant antineuraminidase single chain Ig VH and VL domains (LOC56304)	2.7	0.031	100721_f_at
Sh3kbp1 binding protein 1 (Shkbp1)	2.1	0.028	162238_r_at
protein tyrosine phosphatase non-receptor type 8 (Ptpn8)	1.8	0.008	92356_at
histocompatibility 2 class II antigen E beta (H2-Eb1)	1.6	0.004	102848_f_at
schlafen 1 (Slfn1)	1.6	0.016	102264_at
POU domain class 2 associating factor 1 (Pou2af1)	1.5	0.004	93915_at
Under-expressed Genes in *Cftr*-KO			
epithelial membrane protein 2 (Emp2)	1.8	0.048	103243_at
deleted in polyposis 1-like 1 (Dp111)	1.7	0.008	96134_at
tubulin beta 2 (Tubb2)	1.7	0.016	161614_r_at
aldehyde dehydrogenase family 1 subfamily A7 (Aldh1a7)	1.6	0.004	94778_at
scavenger receptor class B member 1 (Scarb1)	1.5	0.048	100095_at
syndecan 1 (Sdc1)	1.5	0.004	96033_at

* Statistically significant at $p < 0.05$

† In parentheses: total number of probes for that gene differentially expressed between *Cftr*-KO and WT; the probe with the highest fold difference is presented in the table

Figure 3.2 Dispersion plots of the average values from microarray analysis. Experimental points and boundary of the 0.8 probability interval for females (A) and males (B) *Cftr*-KO over WT mRNA samples. Candidate genes are shown as red squares (up regulated), green triangles (down regulated) (coincidence test) and diamonds (RMA).

A. Females

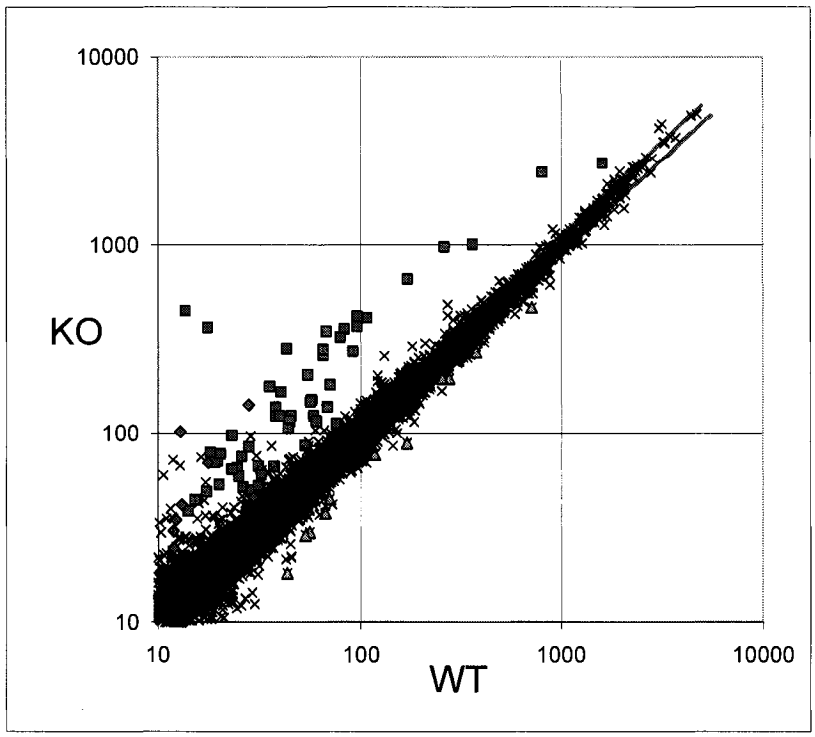

B. Males

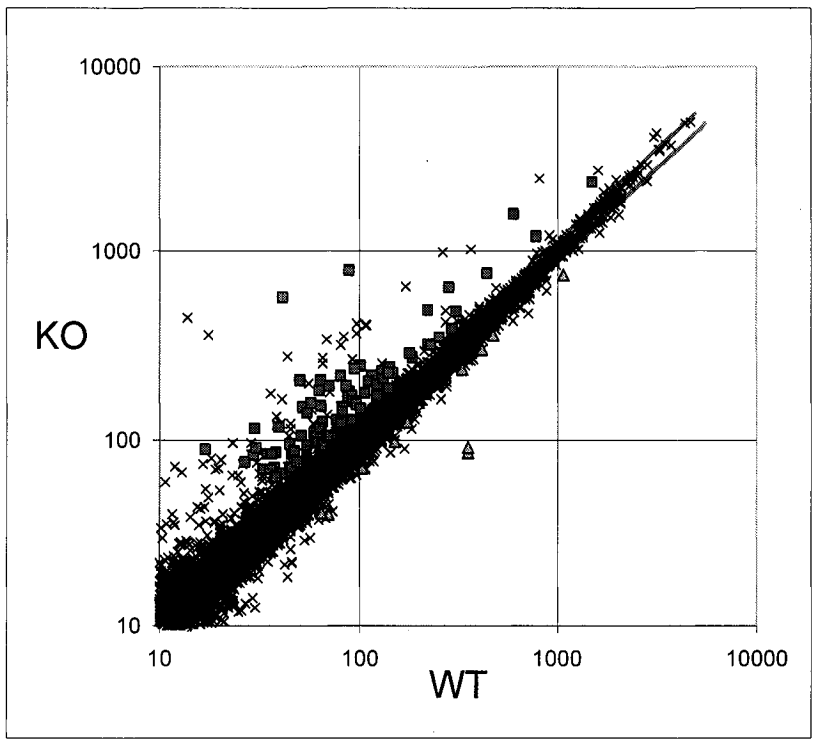

Table 3.3 Genes differentially expressed between *Cftr*-KO and WT males

Over-expressed Genes in *Cftr*-KO	Fold difference	P value*	Affymetrix probe†
immunoglobulin heavy chain 4 (serum IgG1)(Igh-4)	12.1	0.003	99420_at (3)
immunoglobulin heavy chain (Igh-VJ558)	7.6	0.005	100583_at
histocompatibility 2 class II locus DMa (H2-DMa)	4.1	0.015	162346_f_at
chemokine (C-C motif) ligand 5 (Ccl5)	3.8	0.018	98406_at
immunoglobulin kappa chain variable 8 (Igk-V8)	3.3	0.007	101331_f_at (10)
immunoglobulin joining chain (Igj)	3.0	0.007	102372_at
colony stimulating factor 3 receptor (granulocyte) (Csf3r)	2.8	0.007	93198_at
Interferon-inducible GTPase (Iigp-pending)	2.8	0.044	103963_f_at (2)
serine (or cysteine) proteinase inhibitor clade A member 3G (Serpina3g)	2.7	0.041	102860_at
recombinant antineuraminidase single chain Ig VH and VL domains (LOC56304)	2.7	0.031	100721_f_at
placenta-specific 8 (Plac8)	2.5	0.021	98092_at
transporter 1 ATP-binding cassette sub-family B (Tap1)	2.5	0.040	103035_at
S100 calcium binding protein A8 (calgranulin A) (S100a8)	2.4	0.002	103448_at
membrane-spanning 4-domains subfamily A member 6B (Ms4a6b)	2.3	0.007	102104_f_at
interleukin 1 beta (Il1b)	2.3	0.018	103486_at
Interferon-g induced GTPase (Gtpi-pending)	2.3	0.043	98410_at
schlafen 2 (Slfn2)	2.3	0.003	92472_f_at (2)
S100 calcium binding protein A9 (calgranulin B) (S100a9)	2.1	0.003	103887_at
interleukin 7 receptor (Il7r)	2.1	0.002	99030_at
paired-Ig-like receptor B (Pirb)	2.1	0.005	98003_at
protein tyrosine phosphatase receptor type C (Ptprc)	2.1	0.001	101048_at
regenerating islet-derived 3 gamma (Reg3g)	2.1	0.021	96064_at
UDP-N-acetyl-alpha-D-galactosamine:(N-acetyl-neuraminyl)-galactosylglucosylceramide-beta-1 4-N-acetylgalactos- aminyltransferase (Galgt1)	2.0	0.011	103367_at

CD37 antigen (Cd37)	1.9	0.024	98980_at
complement component 1 q subcomponent alpha polypeptide (C1qa)	1.9	0.032	98562_at
T-cell receptor beta variable 13 (Tcrb-V13)	1.9	0.005	93105_s_at
angiopoietin-like 4 (Angptl4)	1.9	0.007	96119_s_at
RAS-related C3 botulinum substrate 2 (Rac2)	1.9	0.024	103579_at
lipocalin 2 (Lcn2)	1.8	0.023	160564_at
Mammary tumor virus locus 43	1.8	0.006	92780_f_at
histocompatibility 2 class II antigen E beta (H2-Eb1)	1.8	0.004	94285_at
complement component 4 (within H-2S) (C4)	1.8	0.002	103033_at
complement component 1 q subcomponent beta polypeptide (C1qb)	1.8	0.008	96020_at
lymphocyte protein tyrosine kinase (Lck)	1.8	0.013	102809_s_at
histocompatibility 2 Q region locus 10 (H2-Q10)	1.7	0.046	101898_s_at
chemokine (C-C motif) ligand 9 (Ccl9)	1.7	0.013	104388_at
CD79B antigen (Cd79b)	1.7	0.014	161012_at
integrin beta 7 (Itgb7)	1.7	0.035	100906_at
lysosomal-associated protein transmembrane 5 (Laptm5)	1.7	0.007	161819_f_at
sema domain immunoglobulin domain (Ig) trans-membrane domain (TM) and short cytoplasmic domain (semaphorin) 4A (Sema4a)	1.7	0.012	94063_at
coronin actin binding protein 1A (Coro1a)	1.6	0.028	96648_at
Fibrinogen-like protein 2 (Fgl2)	1.6	0.030	97949_at
selectin platelet (p-selectin) ligand (Selpl)	1.6	0.004	103488_at
signal transducer and activator of transcription 1 (Stat1)	1.6	0.028	101465_at
immunoglobulin heavy chain 6 (heavy chain of IgM) .....(Igh-6)	1.6	0.024	93584_at
complement component 1 q subcomponent gamma polypeptide (C1qg)	1.6	0.027	92223_at
Ribosomal protein S6 kinase 90kD polypeptide 4 (Rps6ka4)	1.6	0.009	93602_at
protein tyrosine phosphatase non-receptor type 8 (Ptpn8)	1.6	0.014	92356_at
interferon inducible protein 1 (Ifi1)	1.6	0.012	97409_at
interferon activated gene 205 (Ifi205)	1.5	0.046	94224_s_at

B lymphoid kinase (Blk)	1.5	0.022	95893_at
protein kinase C beta (Prkcb)	1.5	0.012	99510_at
T-cell receptor alpha joining region (Tcra-J)	1.5	0.017	97944_f_at
ecotropic viral integration site 2 (Evi2)	1.5	0.004	98026_g_at
Mouse MHC (Qa) Q2-k gene for class I antigen, exons 1-3	1.5	0.027	102161_f_at
pleckstrin homology Sec7 and coiled/coil domains binding protein (Pscdbp)	1.5	0.004	104256_at
proteoglycan secretory granule (Prg)	1.5	0.015	94085_at
regulator of G-protein signaling 19 (Rgs19)	1.5	0.042	103606_r_at
secretory leukocyte protease inhibitor (Slpi)	1.5	0.006	92858_at
spleen tyrosine kinase (Syk)	1.5	0.032	100425_at
TYRO protein tyrosine kinase binding protein (Tyrobp)	1.5	0.016	100397_at
Williams-Beuren syndrome chromosome region 5 homolog (human) (Wbscr5)	1.5	0.016	103690_at
zeta-chain (TCR) associated protein kinase (Zap70)	1.5	0.033	93662_s_at
Under-expressed Genes in *Cftr*-KO			
heat shock protein 1B (Hspa1b)	4.0	0.048	100946_at
heat shock protein 1A (Hspa1a)	3.9	0.041	93875_at
NS1-associated protein 1 (Nsap1-pending)	1.8	0.032	94985_at
presenilin 1 (Psen1)	1.6	0.001	102201_s_at
prion protein (Prnp)	1.5	≤0.001	100606_at
protocadherin alpha 6 (Pcdha6)	1.5	0.011	101650_at
immunoglobulin superfamily member 4 (Igsf4)	1.5	0.005	93605_r_at
alanine and arginine rich domain containing protein (Aard)	1.5	0.001	160968_at
twisted gastrulation protein (Twg-pending)	1.5	0.028	102032_at

* Statistically significant at $p < 0.05$

† In parentheses: total number of probes for that gene differentially expressed between *Cftr*-KO and WT; the probe with the highest fold difference is presented in the table

Table 3.4 Genes differentially expressed between *Cftr*-KO and WT mice common to females and males

immunoglobulin heavy chain 4 (serum IgG1)	(Igh-4)
immunoglobulin heavy chain (J558 family)	(Igh-VJ558)
immunoglobulin joining chain	(Igj)
immunoglobulin kappa chain variable 8 (V8)	(Igk-V8)
recombinant antineuraminidase single chain Ig VH and VL domains (LOC56304)	
S100 calcium binding protein A8 (calgranulin A)	(S100a8)
Immunoglobulin light chain variable region	
protein tyrosine phosphatase non-receptor type 8	(Ptpn8)
histocompatibility 2 class II antigen E beta	(H2-Eb1)
prion protein	(Prnp)

For comparison, Figure 3.3 shows the results of two-way hierarchical clustering for the female (A) and male (B) samples, respectively. In both cases the algorithm appropriately arranges the WT and *Cftr*-KO samples in the same clusters. In summary, we identified a total of 116 genes in males, and 81 genes in females, which are differentially expressed between *Cftr*-KO and their WT control mice.

3.4.3 Other potential candidate genes. This list of genes was generated based on microarray data from lung mRNA of male mice that were analyzed by Affymetrix Analysis Microarray Suite MAS 5 software (Appendix 3). Briefly, the mean expression level for each probe was scaled to 1000, statistical (unpaired) analysis on mean-scale normalized data was performed and the genes which qualified had a P value <0.05 and had at least 2 out of 3 Present or Marginal Calls. The candidate genes that were detected from less restrictive analysis were also very interesting. Since the differences arising in the *Cftr*-KO compared to their WT control mice, in terms of lung histopathology, happen over time, the gene expression associated with this lung disease condition might be small in comparison to their WT controls. By using very restrictive methods of gene selection, it is possible to fail at identifying important candidate genes. This analysis highlighted 445 statistically significant genes, which were differently expressed in the *Cftr*-KO compared to the WT (Appendix 3). Of these 445 genes of interest, we evaluated each gene individually with respect to the specific CF lung disease phenotype. The results of this extensive analysis are presented in Table 3.5, listing the genes which are in close distance to loci associated with lung phenotypes, as described in Haston *et al.* (115), corresponding to interstitial thickening, alveoli count, and fibrosis phenotypes. Appendix 3 also lists the genes or the ones which are in the same family of genes, identified as candidate genes associated with the CF phenotype following whole genome scan.

Figure 3.3 Cluster analysis of microarray experiment in WT and *Cftr*-KO mice. Differentially expressed genes were selected and subjected to cluster analysis; 81 genes are represented for the female (A) mice (n = 5 per group), 116 genes are represented for the male (B) mice (n = 3 per group). Each column represents the genes expression of one mouse. Data in the same row represent that of same gene. All the WT and *Cftr*-KO mice are grouped together.

A. Females

B. Males

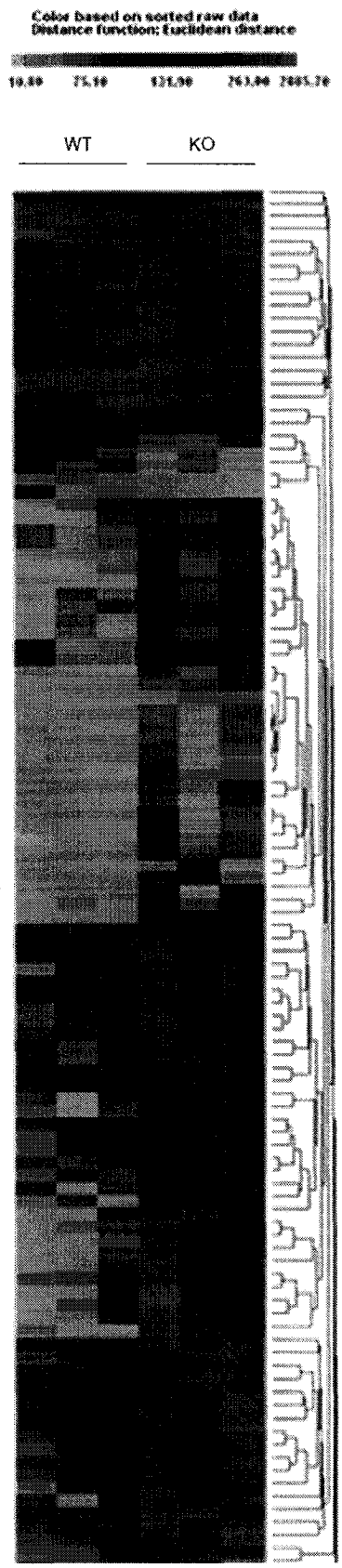

Table 3.5 Candidate genes located within previously identified region associated with lung phenotypes* corresponding to "interstitial thickening", "alveoli count", and "fibrosis"

Phenotype association *	Chromo-some	Peak region ± 20 cM	Gene	Mouse Cytoband (cM)	Fold difference KO/WT
Interstitial thickening	Chr:12	32-72	immunoglobulin heavy chain 4 (serum IgG1)	58	13.5
			immunoglobulin heavy chain (J558 family)	59	8.8
			arginase type II	34	1.7
			G-protein coupled receptor 25	46	1.8
			Ena-vasodilator stimulated phosphoprotein	53	1.7
			RIKEN cDNA 2310061N23 gene	50	1.5
			RIKEN cDNA 2810462M08 gene	32	1.8
	Chr:2	25-65	lipocalin 2	27.0	1.7
Fibrosis	Chr:2	67.5-107.5	interleukin 1 beta	73.0	2.9
	Chr:17	0-27.6	complement component 4 (within H-2S)	18.8	1.7
			histocompatibility 2 class II locus Mb1	18.58	1.7
	Chr:6	41.5-94.1	killer cell lectin-like receptor subfamily G member 1	59.2	2.6
			C-type (calcium dependent carbohydrate recognition domain) lectin superfamily member 8	56.5	1.7
			killer cell lectin-like receptor subfamily D member 1	62.52	1.5
	Chr:10	0-32	glycoprotein 49 A	29	1.5
Alveoli count	Chr:X	0-21.4	Wiskott-Aldrich syndrome homolog (human)	2.0	1.5
	Chr:14	28-68	B lymphoid kinase	28.0	1.5

* as described in Haston *et al.* (115)

3.4.4 Validation of gene expression differences found by microarray data. To validate microarray data, the expression of seven candidate genes was analyzed using quantitative real-time-RT-PCR as described in the Materials and Methods section. Primer sequences for the selected candidate genes are listed in Table 3.6. IL-1β and calgranulin A (S100a8) genes were selected because of their known involvement in CF lung disease. IL-7R gene was chosen because we previously observed an IL-7R protein increase in the lung of *Cftr*-KO mice infected with *P. aeruginosa* (110). MMP-9, Arginase (Arg)-2, Ccl5 and T-cell receptor-a-J (Tcra-J) genes were selected because of their previously reported involvement in inflammation and their potential role in the CF lung priming. Figure 3.4 illustrate the relative differences in the expression of these genes in the lungs of WT and *Cftr*-KO mice (9 to 17 mice per group). Using quantitative real-time-RT-PCR, we were able to confirm the differences in the gene expression between WT and *Cftr*-KO originally found using Affymetrix chips for all selected seven selected genes. Moreover, we were able to confirm for the genes which expression differences were as small as 1.5 to 2.0 fold.

Table 3.6 Primer sequences for the validation of selected candidate genes

Gene name	Sense	Anti-sense
Arg-2	5'-AAGGTATGGGTTTAAGTGCGCTGC-3'	5'-CGACTTGGGATCCAGAAAGTGAAGGA-3'
MMP-9	5'-TTCTTCTCTGGACGTCAAAT-3'	5'-CCTAGACCCAACTTATCCAG-3'
Ccl5	5'-CCAGAGAAGAAGTGGGTTCAAG-3'	5'-GGAAGCGTATACAGGGTCAGAATC-3''
S100a8	5'-CCATGCCCTCTACAAGAATGAC-3'	5'-CTACTCCTTGTGGCTGTCTTTG-3'
Il-1 beta	5'-GTCTTCCTAAAGTATGGGCTGGAC-3'	5'-GAGTCTCCTAGAGATTGAGCTGTC-3'
IL-7R	5'-TCTCTCTCTCTCTCTCTCTCTC-3'	5'-GTCTGCATCTTCTAGGTCTCCATC-3'
Tcra-J	5'-GAACCGATTCTGCTCTGAGATG-3'	5'-CTCCCATTCTCCTTTGTTCCTG-3'

Figure 3.4 Validation of the difference in mRNA expression between WT and *Cftr*-KO mice for selected genes. Lung mRNA abundance from WT (*black*) and *Cftr*-KO (*white*) mice was determined by quantitative real-time-RT-PCR. Values were calculated using the $2^{-\Delta\Delta C}{}_{T}$ method (168) as described in the Experimental procedures section, where mRNA expression of *Cftr*-KO over WT samples were normalized to GADPH. Data are presented as the mean mRNA relative expression levels calculated as $2^{-\Delta\Delta C}{}_{T} \pm$ SEM; the number of mice per group varied from 8 to 15 mice.

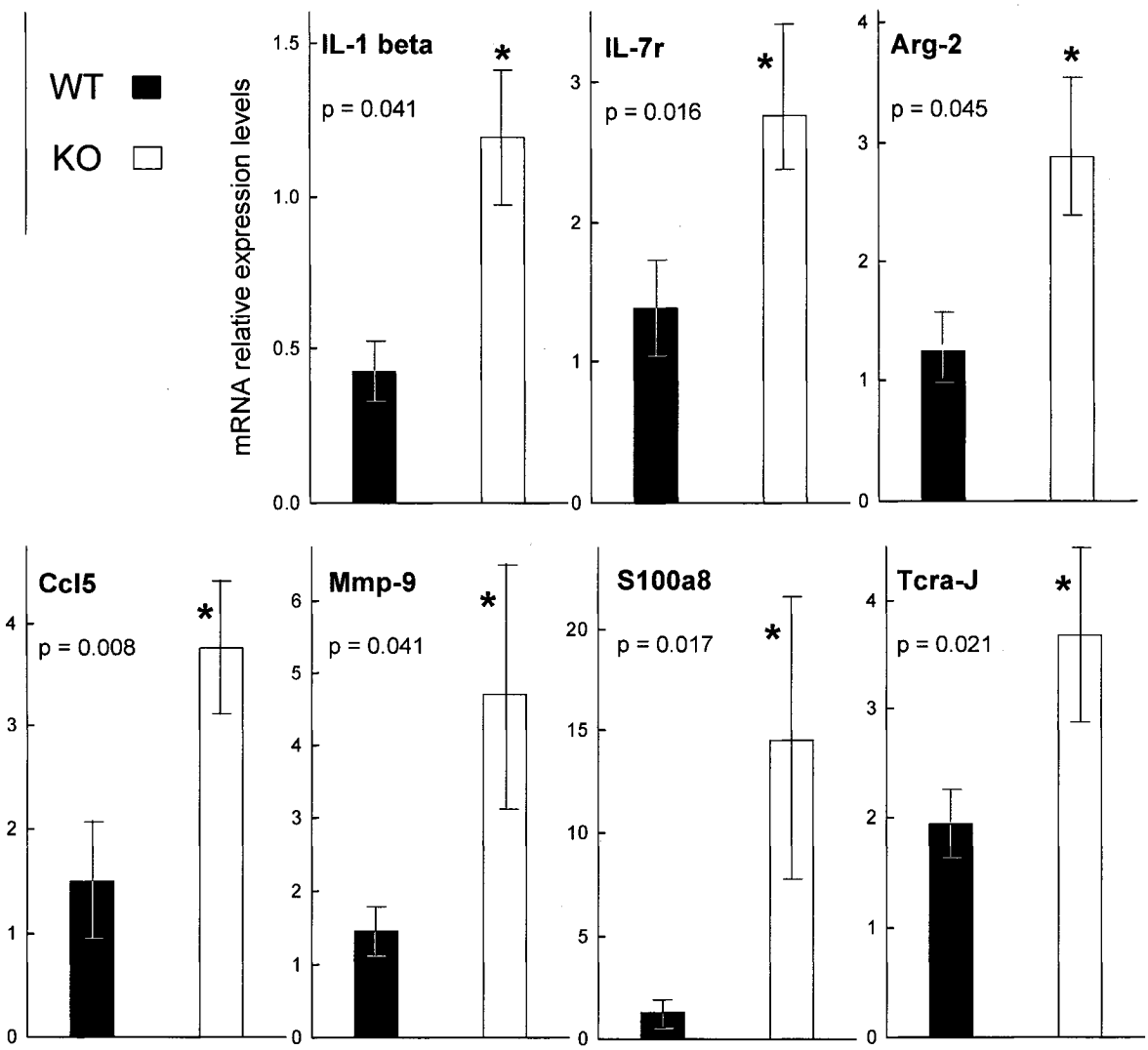
WT
KO
mRNA relative expression levels
IL-1 beta
p = 0.041
IL-7r
p = 0.016
Arg-2
p = 0.045
Ccl5
p = 0.008
Mmp-9
p = 0.041
S100a8
p = 0.017
Tcra-J
p = 0.021

3.4.5 Gene ontology classification. Next, we processed all generated microarray results for both genders using GENMAPP and MAPPFinder softwares[2] to sort the genes into categories depending on their known functions [gene ontology (GO)] to enable us to define specific biological processes involved in the lung disease phenotype. GO-based analysis separates the selected candidate genes into 3 major categories: Biological process, Molecular function, and Cellular component. These 3 categories subdivide further into gene functions. Figure 3.5 illustrates some of these sub-classes in which several genes had their expression affected by the lack of the *Cftr* gene in uninfected mice. It is noteworthy that a given gene product may exhibit one or more functions. This section focuses on the functional categories of the genes differentially expressed in the *Cftr*-KO compared to their WT control lungs.

The biological process category (Figure 3.5, panel A) includes the genes whose products relate to biological phenomenon, mediated by one or more gene products. This category can be sub-divided into 3 main classes, including cell communication, physiological process and cellular process; it also contains the majority of candidate genes we found. In summary, we observed many differences in gene expression in the *Cftr*-KO compared to the WT lungs for genes involved in "cell communication", in particular 1 gene from cell adhesion, 2 genes from signal transduction and 1 gene involved in the intracellular signaling cascade. We also observed genes associated with physiological process, for example 4 genes involved in the regulation of transcription and 3 genes implicated in macromolecule biosynthesis and protein metabolism. Most interestingly in that category, we observed many genes involved in the immune response (3 genes) more specifically in B-cell activation as well as other genes involved in B-cell proliferation and positive regulation of B-cell proliferation. Finally, differentially expressed genes were found to be implicated in cellular process, as in the response to oxidative stress, protein modification, cell death and cell cycle categories.

Figure 3.5 Gene ontology-based analysis; effect of *Cftr* deletion on gene expression in the lungs of mice. Genes differentially expressed between WT and *Cftr*-KO mice lungs are represented by their functional categories: Biological process categorization (A), Molecular function categorization (B) and Cellular component categorization (C).

A. Biological Process

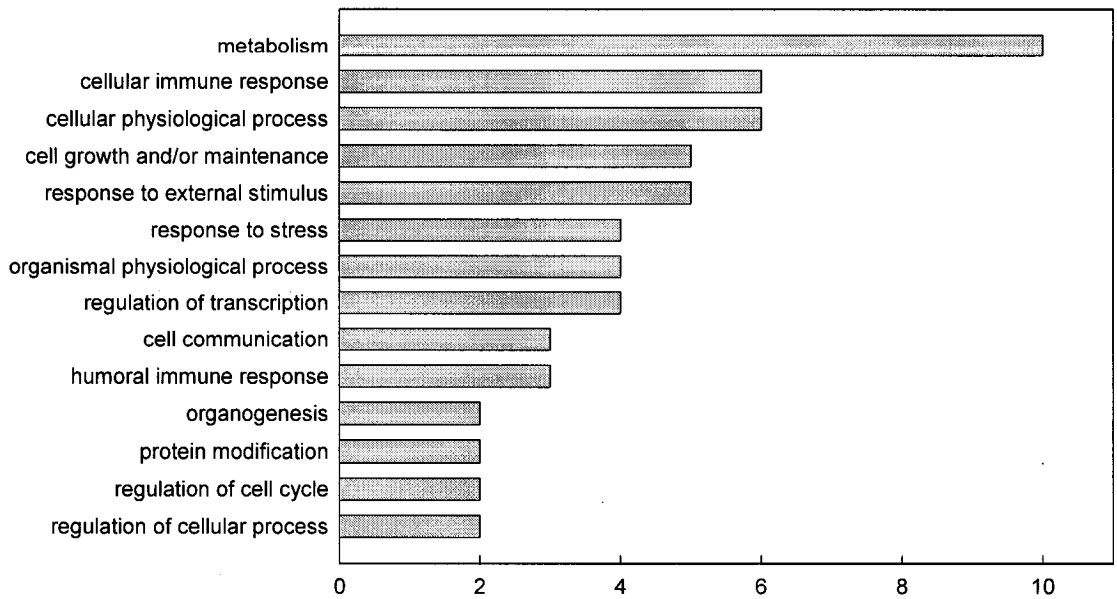

B. Molecular Function

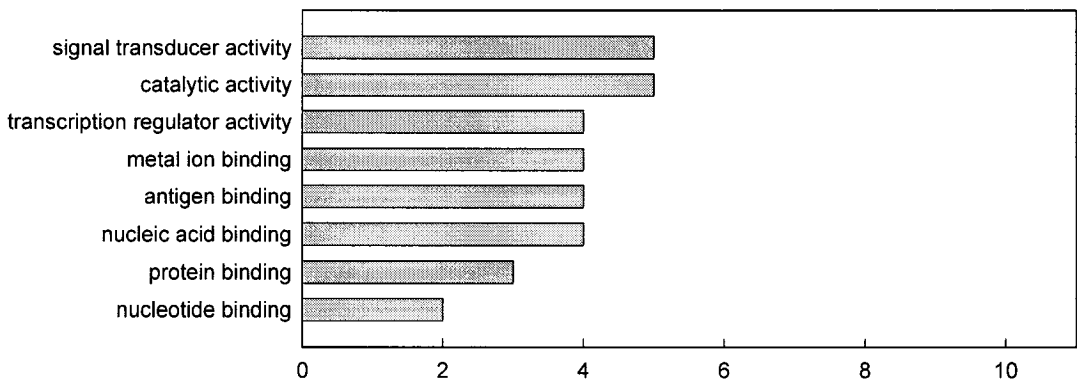

C. Cellular component

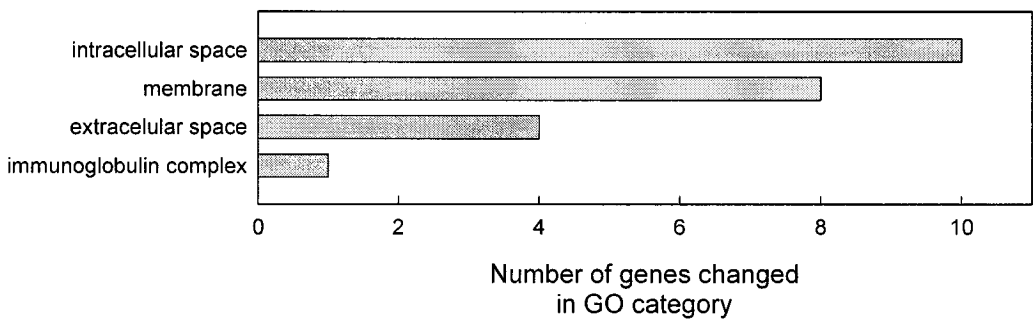

The molecular function category (Figure 3.5, panel B) includes the genes whose products' elemental activities, such as catalysis or binding describe the actions at the molecular level. In summary, we observed different gene expression patterns in the *Cftr*-KO compared to WT lungs for genes involved in binding activity, more specifically in GTP-binding (2 genes), metal ion-binding (4 genes) and nucleic acid binding (4 genes); some were also involved in protein binding, in particular 2 genes involved in the cytoskeletal protein binding and 1 gene involved in actin binding. We also observed genes associated with catalytic activity, for example GTPase and protein-tyrosine-phosphatase activity. Nonetheless, we observed 5 genes related to signal transducer activity, among which 4 genes are specific for receptor activity. Finally, 4 differentially expressed genes were found to be implicated in transcription regulator activity.

The cellular component category (Figure 3.5, panel C) includes the genes whose products are part of cells; these include the extracellular environments, products that may be a component of one or more parts of a cell structure, and products that are parts of macromolecular complexes. In summary, as many as 10 genes differentially expressed between the *Cftr*-KO and WT lungs are categorized as genes encoding proteins present in the intracellular space; 5 genes encoding proteins localized in the nucleus, whereas another 5 genes seem to localize and function in the cytoplasmatic compartment, more precisely with the Golgi apparatus and the endoplasmic reticulum. We also observed many genes encoding structural membrane proteins like integral plasma membrane (5 genes), lipid raft (1 gene) and B-cell receptor complex (1 gene). Also of interest, one gene from the protein complex category was also seen, specifically involved in the regulation of circulating-immunoglobulin-complexes.

Overall, gene ontology based analysis gives us a global picture of the functional systems implicated in the differential gene expression between the lungs of uninfected *Cftr*-KO and WT mice (Figure 3.6).

Figure 3.6 Representation of candidate genes potentially involved in the manifestation of the lung disease phenotype observed in the *Cftr*-KO mice developing spontaneous lung disease. The genes are classified by functional categories; up regulated (*arrow*) genes in the *Cftr*-KO compared to WT mice; down regulated *(arrow*) genes in the *Cftr*-KO compared to WT mice.

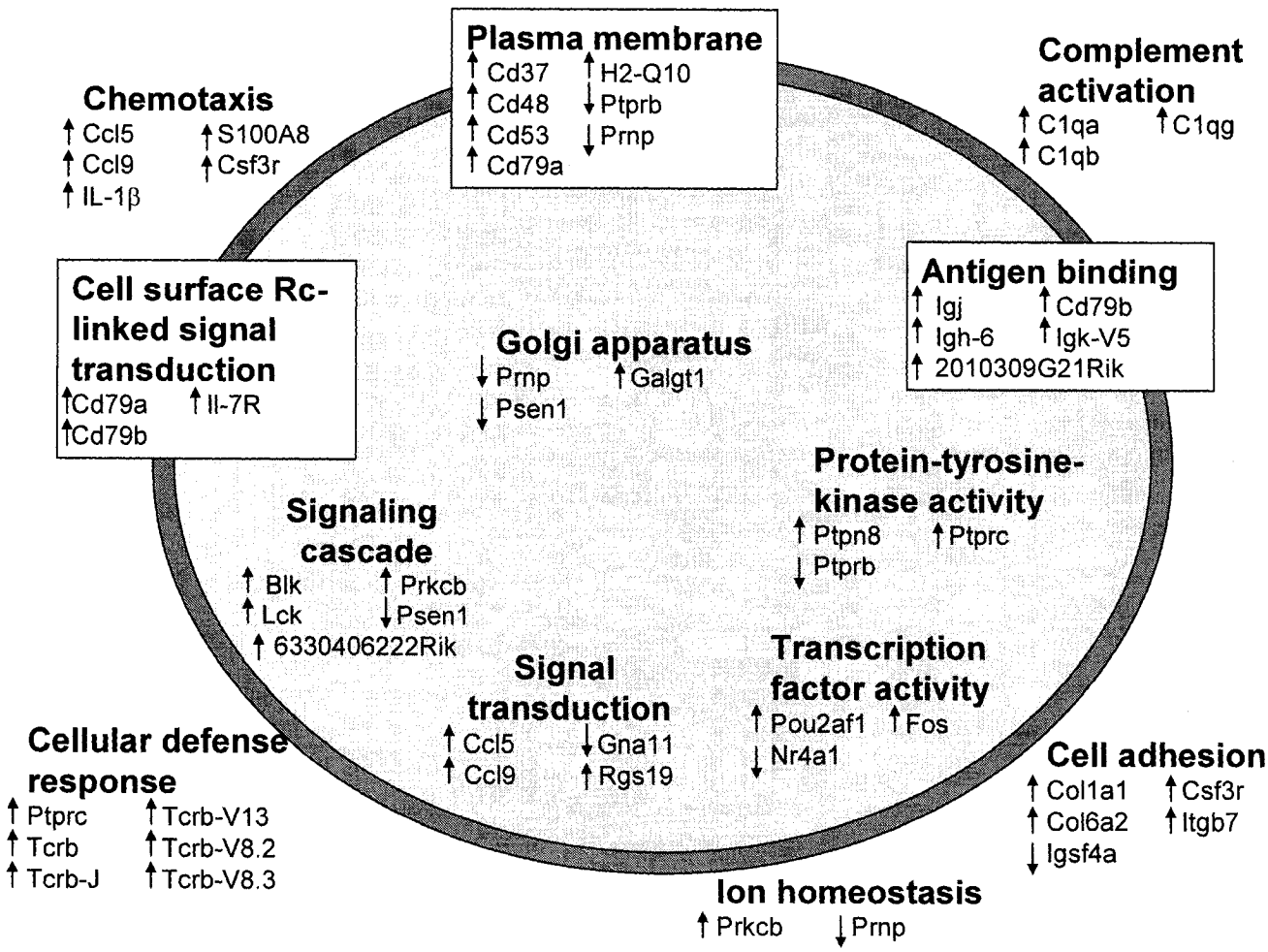
Plasma membrane
↑ Cd37 ↑ H2-Q10
↑ Cd48 ↓ Ptprb
↑ Cd53 ↓ Prnp
↑ Cd79a
Chemotaxis
↑ Ccl5 ↑ S100A8
↑ Ccl9 ↑ Csf3r
↑ IL-1β
Complement activation
↑ C1qa ↑ C1qg
↑ C1qb
Cell surface Rc-linked signal transduction
↑Cd79a ↑ Il-7R
↑Cd79b
Antigen binding
↑ Igj ↑ Cd79b
↑ Igh-6 ↑ Igk-V5
↑ 2010309G21Rik
Golgi apparatus
↓ Prnp ↑ Galgt1
↓ Psen1
Protein-tyrosine-kinase activity
↑ Ptpn8 ↑ Ptprc
↓ Ptprb
Signaling cascade
↑ Blk ↑ Prkcb
↑ Lck ↓ Psen1
↑ 6330406222Rik
Signal transduction
↑ Ccl5 ↓ Gna11
↑ Ccl9 ↑ Rgs19
Transcription factor activity
↑ Pou2af1 ↑ Fos
↓ Nr4a1
Cellular defense response
↑ Ptprc ↑ Tcrb-V13
↑ Tcrb ↑ Tcrb-V8.2
↑ Tcrb-J ↑ Tcrb-V8.3
Cell adhesion
↑ Col1a1 ↑ Csf3r
↑ Col6a2 ↑ Itgb7
↓ Igsf4a
Ion homeostasis
↑ Prkcb ↓ Prnp

3.4.6 Protein expression in the lungs. To further confirm the results obtained from quantitative real-time-RT-PCR, we looked at the MMP-9 protein levels in the lung using lung sections from WT and *Cftr*-KO mice fixed in formaline (WT n = 7; *Cftr*-KO n = 8). We observed an increase in MMP-9 protein expression in the uninfected *Cftr*-KO compared to their WT uninfected control mice (Figure 3.7; panel A) (see Experimental Procedures section for details on scoring analysis). The uninfected *Cftr*-KO mice showed 36.4% higher MMP-9 protein expression compared to the WT uninfected mice, where there was only small or no expression detected in their lungs (mean (±SEM) expression scores for WT mice of 1.3 ± 0.5 compared to a mean score of 1.9 ± 0.4 for *Cftr*-KO mice (p = 0.05). Next, we evaluated the MMP-9 protein expression levels of *P. aeruginosa*-lung-infected WT and *Cftr*-KO mice 3 days post-infection. As expected, we observed an increase in MMP-9 when the mice were infected with *P. aeruginosa* in the lungs; WT infected mice had a 69.4% increase in MMP-9 protein expression compared to small or no expression in the WT uninfected animals (WT uninfected = 1.3 ± 0.5; WT- *P. aeruginosa* = 2.3 ± 0.6; p = 0.013), and similarly, *Cftr*-KO infected mice had 73.3% higher expression of MMP-9 protein compared to *Cftr*-KO uninfected animals (*Cftr*-KO uninfected = 1.9 ± 0.4; *Cftr*-KO- *P. aeruginosa* = 3.3 ± 0.5; p = 0.010) (Figure 3.7, panel B). Interestingly, we observed a very similar mean difference of approximately 40% between the levels of MMP-9 expression in *Cftr*-KO mice and their WT controls, independently of their infectious status (infected with *P. aeruginosa* = 39.5% or uninfected = 36.4%). The comparative analysis of the MMP-9 protein in the lungs of WT and *Cftr*-KO mice clearly demonstrates that the lungs of uninfected *Cftr*-KO already show an elevated expression of MMP-9.

Since many probes of variable chains were shown to be over-expressed in the lungs of *Cftr*-KO mice compared to their controls, we assessed the levels of IgG1 and IgG2a in the plasma of uninfected *Cftr*-KO and WT mice. We observed a statistically significant 1.7-fold increase in the mean concentration of IgG1 in the uninfected *Cftr*-KO mice (7593 ± 1021 ng/ml, n = 6) compared to their WT

Figure 3.7 Immunostaining on the lungs of WT and *Cftr*-KO mice. Representative MMP-9 immunostaining (40X to 400X) from uninfected and *P. aeruginosa* -infected mice at 3 days post-infection, from lung sections that were prepared from WT and *Cftr*-KO mice. Sections from uninfected *Cftr*-KO mice show 36.4% more MMP-9 protein expression compared to WT mice that show small or no expression (uninfected panel). An increase in MMP-9 is observed when the mice were infected with *P. aeruginosa* in the lungs; WT infected mice had a 69.4% increase in MMP-9 protein expression compared to WT uninfected animals. Similarly, *Cftr*-KO infected mice had 73.3% higher expression of MMP-9 protein compared to *Cftr*-KO uninfected animals.

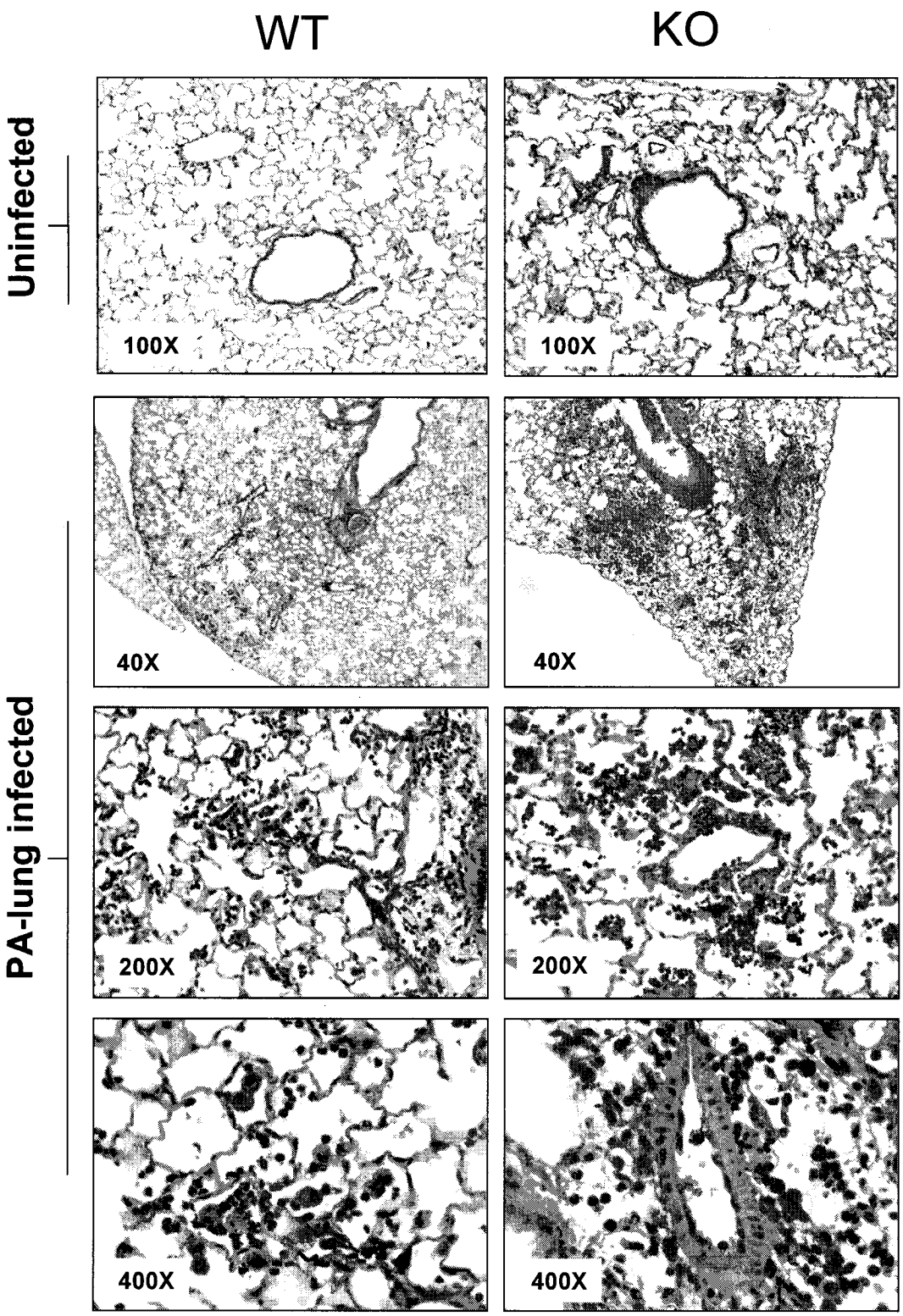
WT
KO
Uninfected
PA-lung infected
100X
100X
40X
40X
200X
200X
400X
400X

uninfected controls (4514 ± 587 ng/ml, n= 8) (p = 0.017). Although a trend towards higher levels of IgG2a was observed in the plasma of uninfected *Cftr*-KO mice (53 ± 8 ng/ml) compared to their uninfected WT controls (38 ± 3 ng/ml), this difference did not reach statistical significance (p = 0.137).

Since we found a significant difference at the level of Slpi mRNA expression between WT and *Cftr*-KO uninfected mice (p = 0.006), we also analyzed the level of SLPI protein expression in the lungs of uninfected WT and *Cftr*-KO mice by IHC staining. Interestingly, we found a striking difference at the level of SLPI protein expression in the lungs of uninfected *Cftr*-KO mice compared to their uninfected WT control mice (p = 0.015). The WT mice had low to no protein expression detected (median score of 0.5; 0.0 (25%) – 0.5 (75%); n = 10) and the *Cftr*-KO mice showed low to moderate SLPI protein expression in the lungs (median score of 1.0; 0.8 (25%) – 1.3 (75%); n = 12).

Overall, these increases in MMP-9, IgG1 and SLPI protein levels seem to be consistent with the hypothesis that the lungs of *Cftr*-KO mice are in a heightened activation state even prior to experimental infection with *P. aeruginosa*.

3.5 Discussion

Cystic fibrosis patients display several disease symptoms, including intestinal obstruction, infertility, pancreatic insufficiency and chronic lung infections. Although it is well documented that this wide spectrum of symptoms results from dysfunction of the CFTR protein, the exact mechanism of disease development has not yet been elucidated.

Chronic lung infections resulting in a gradual loss of function and high mortality are particularly difficult to handle since no universal treatment able to prevent or reverse lung damage has yet to be developed. Since we developed the

cystic fibrosis mouse model which displays the CF lung phenotype without infection, we used this model to perform genome-wide transcriptional analysis of gene expression in the lungs of these CF mice compared to their WT littermate controls. The spontaneous lung disease observed in uninfected *Cftr*-KO mice is characterized by the increased hyperplasia of epithelial cells, basal membrane thickening and inflammatory cell infiltration in the lung tissue compared to control littermates. We have previously reported that lung disease starts to develop between 12 and 16 weeks (147;110) of age and gradually progresses. In this study, we have used 20 weeks old CF mice that display very striking changes in their lungs compared to their littermate controls. We have performed a very meticulous comparison of gene expression patterns between the lungs of CF mice and their controls using multiple animals of both genders. Gene chip expression analysis has subsequently been corroborated using real-time RT-PCR quantification and protein expression analysis for selected genes.

Tables 3.2, 3.3 and 3.4 show lists of the over- and under-expressed candidate genes, obtained for the probability interval 0.8; they contain a total of 116 candidate genes in males and 81 candidate genes in females, which are differentially expressed between *Cftr*-KO and their WT control mice. Due to the fundamental differences in females' and males' inflammatory regulations and *P. aeruginosa* infection susceptibilities, both genders were analyzed together and separately.

When comparing the gene expression patterns between *Cftr*-KO mice (both males and females) and their control littermates, it was evident that many more genes were up regulated rather than down regulated in the lungs of *Cftr*-KO mice than in WT controls. Several of the identified genes belong to the Ig family, more specifically in heavy chains (Igh-VJ558, Igh-4), joining chain (Igj) and kappa chain (Igk-V8) genes (common for females and males). Several other genes (or chip probes of the same gene) of immunoglobulin chains were also identified to be differentially expressed in the *Cftr*-KO males or *Cftr*-KO females compared to

their WT controls (Igh-VJ558, Igh-4, Igk-V8, Igh-6, IgI-V1 and Igk-V28). A total of 24 probes in females and 18 probes in males of immunoglobulin chains were up-regulated in the *Cftr*-KO compared to their WT controls. Anomalies in the production of immunoglobulins (hypo- and hyper-gammaglobulinemia) in CF patients and animal models have been reported in the literature (27;124;176;188;208;217). Regarding immunoglobulin heavy chains, abnormal levels of IgG in patients with CFTR mutations were reported by several investigators. Raman and colleagues found decreased levels of IgG in children with CFTR mutations with chronic rhinosinusitis, but free of the CF symptoms (217). Mathews *et al.* and Hodson *et al.* reported lower levels of the IgG in CF patients with less severe disease and elevated levels in cases of more advanced stages (176;124). Generally, IgG is over-expressed in the lungs compared to other tissues (94). Moreover, most of the murine model studies have not reported any significant changes in the immunoglobulin family of genes (42;75;129;146;210;258;262;277;303;311). Recently, Norkina *et al.* reported a significant increase in the expression of the immunoglobulin kappa variable chains V-5, V-8 and V-28 in the intestine of the CF mouse (196). Our data clearly show an increase in the mRNA expression in the lungs of *Cftr*-KO mice compared to their WT controls for several Ig genes which correlate with higher IgG1 protein expression in the plasma of *Cftr*-KO mice compared to WT.

The up regulation of several genes that belong to the immunoglobulin family was also accompanied by the up regulation of several genes, which suggests an overall enhancement of B-cell functions, antigen presentation and antigen binding. Genes such as MHC class II (H2-Eb1, H2-DMa, H2-Q10, H2-DMb1), cytokines (IL-1 beta, IL-7R), complement components (C1qa, C1qb, C1qg, C3, C4), antigens (CD37, CD79a, CD79b, CD52, CD19, CD48, CD53) and other B-cell related genes such as B-cell translocation gene 3 (Btg3), B-lymphoid kinase (Blk) and paired-Ig-like receptor B (Pirb) were differentially expressed in *Cftr*-KO mice.

Other genes that were up-regulated in the *Cftr*-KO mice includes calgranulins that function as inflammatory cytokines expressed abundantly in infiltrating monocytes and granulocytes under conditions of chronic inflammation. Elevated amounts of calgranulins (A and B) were found in the serum of patients with cystic fibrosis and clinically normal heterozygous carriers (68;67). Interestingly, calgranulin A (S100a8) and calgranulin B (S100a9) genes were up regulated in our mouse model that develops lung disease and also in the lungs of gut-corrected CF mice which lack the lung disease phenotype (303). Other members of the S100 calcium binding protein family of genes were down-regulated in *Cftr*-KO mice, notably S100a6 (calcyclin) and S100a13, one of the most recently identified members of the S100 family, as illustrated in Appendix 3.

T-cell related genes were found to be up-regulated in the lungs of *Cftr*-KO mice compared to their WT counterparts. More specifically, members of the recently identified Schlafen (Slfn) gene family such as Slfn1 (Table 3.2), Slfn 2 (Table 3.3), Slfn 3 and Slfn 4 (Appendix 3), have been implicated in an as yet unidentified, regulatory mechanism involved in T-cell development and growth control. The Schlafen gene family has also been observed in the CF mouse small intestine by Norkina *et al.* (196;244). We observed the up-regulation of the following genes: thymus cell antigen 1 theta (Thy1), lymphocyte protein tyrosine kinase (Lck), T-cell specific GTPase (Tgtp), T-cell receptors (Tcrb-V13, Tcra-J), lymphocyte cytosolic protein 1 (Lcp), granzyme A (Gzma; T cell- and natural killer cell-specific serine protease) and fibrinogen-like protein 2 (Fgl2), which exerts immunosuppressive effects on T-cell proliferation and dendritic cell maturation.

Chemokines regulate the cell trafficking of various types of leukocytes through interactions with a subset of transmembrane, G-protein-coupled receptors. These are involved in macrophage recruitment during inflammation and also play a role in the development, homeostasis and function of the immune system. The mRNA expression of three chemokine genes of the C-C motif subfamily of chemokines and one chemokine receptor gene was found to be elevated in *Cftr*-KO

lungs compared to their WT counterparts: Ccl6, previously known as "macrophage inflammatory protein-related protein (MRP)-1"; Ccl9, also known as "macrophage inflammatory protein (MIP-1)-gamma" or MRP-2; Ccl5, known as RANTES, and its receptor Ccr5 (Appendix 3), which also binds the chemokines MIP-1-alpha and MIP-1-beta with high affinity.

We also found that several other proteins known to be involved in the general inflammatory response had their gene expression affected by the *Cftr* gene ablation. Serum amyloid A3 (Saa3), which is expressed particularly in macrophages and known as an acute phase reactant (also observed recently by Norkina *et al.*), Arg2, which is closely involved in the cellular production of NO, integrin (Itgb7) and lipocalin 2 (Lcn2) were all up-regulated in the *Cftr*-KO lungs.

We previously observed in our *Cftr*-KO mouse model that their lung environment differs from the normal WT lungs (Figure 3.1) (110). A few genes found in the present study are related to the structure of the cell and might explain some of the differences we observe in the *Cftr*-KO lungs, such as tubulin (Tubb2), actinin (Actn1) and epithelial membrane protein (Emp2) (Table 3.4). We also found genes involved in the proteolytic degradation of the extracellular matrix such as matrix metalloproteinases (Mmp-9, Mmp-11, Adam-8; Appendix 3) and cathepsin H, which is involved in the conversion of pro-MMPs into active MMPs. Interestingly, an increase in the expression of cathepsin H was shown to be associated with lung disease in lung cancer patients (245).

Furthermore, in our analyses, constitutive expression of protease inhibitors, especially serine protease inhibitors, was differentially expressed in the lungs when comparing *Cftr*-KO mice with lung disease and their WT health littermate controls. Serine protease inhibitors are multifunctional molecules and are involved in angiogenesis, apoptosis, maintenance of the extracellular matrix and, most interestingly, in inflammation. The production of these inhibitors in the lung tissue should not be ignored since they may play a very important regulation function in

the lungs. It is possible that their over-expression might activate the mechanisms that contribute to a progressive fibrosis development. Proteinase inhibitors, such as secretory leukoproteinase inhibitor (SLPI), synthesized and secreted by pulmonary epithelium and macrophages, are further augmented following lung exposure to endotoxin expressed by *P. aeruginosa* and inflammatory cytokines such as TNF and IL-1 (235), IL-10 and IL-6 (140). SLPI protein has been implicated in wound healing processes (7), pulmonary inflammation (14) and in gram-negative and gram-positive bacterial infections (140) as an anti-inflammatory mediator. SLPI is considered as a major elastase inhibitor in the respiratory tract and more importantly associated with neutrophil elastase inhibition (8;243), but also involved in improving anti-oxidant protection by raising gluthatione levels in the lungs (289). In CF, it was hypothesized that an increase in SLPI could be beneficial to the control of lung functions since it can control the abnormally high levels of elastase found in the lung and characteristic of CF disease (243), associated with the exacerbation of the immune response. Our mRNA data from the microarray experiment has shown a significant difference between WT and *Cftr*-KO in SLPI mRNA expression in male mice. These data are consistent with a clinical observation in male CF patients (288). We observe a clearly increased expression of this important mediator in the lungs of the *Cftr*-KO male mice with spontaneous lung disease compared to their WT littermate controls (Table 3.3). Our findings also show that the lung milieu is primed, showing elevated levels of SLPI protein in the lungs of *Cftr*-KO compared to WT mice, even prior to *P. aeruginosa* lung infection and might increase even further following *P. aeruginosa* infection (data not shown). This difference in SLPI mRNA levels between *Cftr*-KO and WT mice is consistent with previous reports demonstrating that alginate from *P. aeruginosa* can interact with leukocyte elastase, disturbing the overall balance of protease-antiprotease in infected CF lungs (304). Overall, these results support the hypothesis that the CF lung milieu is dysregulated not only in terms of inflammatory responses to bacterial pathogens, but even before the mice are infected, at the gene expression levels, either directly by CFTR-deficiency itself, or secondary to the *Cftr* gene defect, by modifier genes. SLPI is certainly an

important player in the fight against various bacterial species in the lungs, particularly in CF pathogenesis, but its effects have to be studied in a broad context, since it interacts with many components of the host immune response as well as the pathogen itself.

The gene Col6a2, procollagen type VI alpha 2, encodes one of the three alpha chains of type VI collagen, a beaded filament collagen found in most connective tissues. The product of this gene contains several domains that have been shown to bind extracellular matrix proteins, an interaction that explains the importance of this collagen in organizing matrix components. Also, the gene Col1a1, procollagen type I alpha 1, encodes the major component of type I collagen, the fibrillar collagen found in most connective tissues, and the only component of the collagen found in cartilage. Furthermore, we observed a third gene involved in the composition of collagen, Col14a1, procollagen type XIV alpha 1. Interestingly, we found that the expression of these three genes were higher in the *Cftr*-KO lungs compared to normal lungs, which might be an important factor in the lung disease phenotype we observe in these mice.

Prnp gene was also found to be under-expressed in *Cftr*-KO males (1.5 fold) and females (1.8 fold) compared to WT control mice. The protein encoded by this gene is involved in lipid raft formation. These lipids rafts are specialized membrane domains composed mainly of cholesterol and sphingolipids, and are relatively poor in polyunsaturated lipids such as glycerophospholipids (252). The formation of these membrane domains is promoted by the presence of cholesterol in the lipid bilayer. Since the hexagonal rings of cholesterol can pack tightly against the saturated hydrocarbon chains of membrane lipids, it allows these lipids to assemble into cohesive units floating in the mass of loosely packed polyunsaturated plasma membrane components (247). Interestingly, it has been shown that the internalization of *P. aeruginosa* bacteria in nasal and tracheal epithelium involves the formation of lipid rafts (250;251). These large lipid raft platforms may concentrate as yet unknown intracellular signaling molecules and

binding receptors involved in the cellular response to *Pseudomonas* infection in addition to CFTR.

Interestingly, in an attempt to correlate our findings with current knowledge, we correlated the loci of the genes we found with the loci associated with the CF lung disease phenotype, namely interstitial thickening, fibrosis and alveoli count, as previously described by Haston *et al.* (115). The immunoglobulin gene Igh-4 and Igh-VJ558 heavy chains, as well as Ena-vasodilator stimulated phosphoprotein (Evl), lipocalin 2 (Lcn2) and Arg2, were found to be localized in the genetic region associated with the "interstitial thickening" phenotype. Arg2 was also observed to be differentially expressed in the pancreas and duodenum of CF mouse KO (144).

Moreover, seven other genes were associated with the "fibrosis" phenotype, more specifically IL-1 beta, complement component 4 (C4), histocompatibility 2 class II (H2-DMb1), C-type lectin superfamily member 8 (Clecsf8), glycoprotein 49 A (Gp49a), killer cell lectin-like receptor subfamily G member 1 (Klrg1) and subfamily D member 1 (Klrd1). Finally, B lymphoid kinase (Blk) was found to be in the region associated with the "alveoli count" phenotype.

Human studies of CF have performed gene expression analyses on blood samples or on human epithelial cell lines. Moreover, Zielenski's laboratory presented results identifying secondary genes, other than *Cftr*, influencing the clinical severity of CF disease (78;64). A number of genes found by Zielinski *et al.* were also associated with CF lung disease in human (Appendix 3). Among the genes identified in our study which are differentially expressed between WT and *Cftr*-KO mice and which could play an important role in CF lung disease, were genes such as IL-1 beta, IL-8R, and CLCA1, GSTM1, HSP40 and HSP70. We also observed other genes differentially expressed between *Cftr*-KO and WT, including Slc22a and Slc, Aquaporin, and the Clca family of genes, which belong to the same family as some of the identified genes in the human CF study.

Overall, this wide-genome screening lead us to reveal several candidate genes involved in cellular physiological processes, as well as in the immune response, signal transducer and antigen binding activities, and matrix remodeling. These genes might contribute to the development of CF lung disease prior to *P. aeruginosa* lung infection. Our results strongly suggest that the control of the immune system is crucial to prevent the development of the disease.

FOOTNOTES

[1] http://mbcr.bcm.tmc.edu/genepi/

[2] http://www.genmapp.org/

CHAPTER IV

Preface

The data presented in the previous chapter clearly illustrate the differences in the lung environment of WT and *Cftr*-KO mice prior to bacterial infection. We further wanted to characterize the *Cftr*-KO mouse model during *P. aeruginosa* lung infection to better understand the dysregulation of the immune response observed in the CF patients when they're compared to healthy controls. In order to do that, we used our *Cftr*-KO mouse model that develops spontaneous lung disease. However, the *Cftr*-KO mice are smaller than normal mice and are more sensitive to housing and nutritional conditions, and also more susceptible to infection, leading to small amounts of animals being available for experiments. Because of these characteristics, we sought to find an alternative way to study the inflammatory response during lung *P. aeruginosa* infection which would permit to study a larger number of *Cftr*-KO mice. The following chapter present the studies performed to improve the lung infection procedures to ultimately facilitate the use of *Cftr*-KO mice in CF research.

CHAPTER IV.

CYSTIC FIBROSIS LUNG DISEASE FOLLOWING INFECTION WITH *PSEUDOMONAS AERUGINOSA* IN THE CFTR KNOCKOUT MICE USING NOVEL NON-INVASIVE DIRECT PULMONARY INFECTION TECHNIQUE

based on published paper

Guilbault, C., *Martin, P., Houle, D., Boghdady, M.-L., Guiot, M.-C., Marion, D. and Radzioch, D. Laboratory Animals. July 2005 volume 39, pages 336-352.*

4.1 Abstract

To better understand the mechanism of lung infection with *P. aeruginosa*, many techniques have been developed in order to establish lung infection in rodents. A model of chronic lung infection, using tracheotomy to inoculate the bacteria, has been extensively used in the CF mouse model of lung infection. The *Cftr*-KO mice are smaller than normal mice and are more sensitive to housing and nutritional conditions, leading to small amounts of animals being available for experiments. Because of these characteristics, and because of the invasiveness of the infection procedure which we, and others, have been using to mimic the lung infection, we sought to find an alternative way to study the inflammatory response during lung *P. aeruginosa* infection. The technique we describe here consists of the injection of bacterial beads directly into the lungs through the mouth without the need of any tracheal incisions. This technique of direct pulmonary delivery enables much faster infection of the animals compared to the intratracheal technique previously used. The use of this less invasive technique allows the exclusion of the surgery-related inflammation. Our results show that, using the

direct pulmonary delivery technique, the *Cftr*-KO mice were more susceptible to *P. aeruginosa* lung infection compared to their WT controls, as shown by their increased weight loss, higher bacterial burden and more elevated PMN alveolar cell recruitment into the lungs. These differences are consistent with the pathological profiles observed in CF patients infected with *P. aeruginosa*. Overall, this method simplifies the infection procedure in terms of its duration and invasiveness, and improves the survival rate of the *Cftr*-KO mice when compared to the previously used intratracheal procedure.

4.2 Introduction

The cystic fibrosis (CF) disease is caused by a defect in the CFTR channel. Dysfunction of the CFTR protein results in salty sweat, pancreatic insufficiency, intestinal obstruction, male infertility and severe pulmonary disease. Most of the morbidity and mortality in CF patients result from pulmonary complications. Chronic infection of the lungs with mucoid strains of *P. aeruginosa*, which tend to persist in most patients, results in an exaggerated neutrophilic inflammatory response and in a dysregulated production of cytokines: high levels of proinflammatory cytokines (IL-1, IL-6, IL-8, TNF) and low levels of anti-inflammatory IL-10 in bronchoalveolar lavage fluid (BALF) (266;186;141;121).

Since the discovery of the *Cftr* gene and because no natural animal model is known, a number of animal models have been developed (for a review, see reference Nelson *et al.* (193)). Animal models represent the best surrogate for the complexities of the human system, providing that the results from experimental animal studies are extrapolated carefully. Most models developed have been murine models; a number of investigators have generated *Cftr* gene knockout mice by targeted gene disruption (38;48;58;86;198;256;281;312). Although the generated mice have most of the symptoms of CF, only very few of them display the CF lung phenotype (193). However, the analysis of susceptibility to infection with *P. aeruginosa* of various strains of mice was useful in the identification of

genes other than CFTR that influence the severity of the CF disease. When the first *Cftr*-KO mice were generated, their analysis clearly showed that mice are much more resistant to *P. aeruginosa* infection than human CF patients. Unlike human CF patients, spontaneous colonization in the animals with the typical CF pathogens, including *P. aeruginosa,* has not been detected, perhaps due to the maintenance of the *Cftr*-KO mice in pathogen-free conditions. In the ensueing few years, it became very apparent that the genetic background of the *Cftr*-KO mice is very important since many of the strains of mice express alternative calcium-regulated chloride channels (91). Since the discovery of the *Cftr* gene, C57BL/$6^{H/M}$-*Cftr*.ko mice described by Kent and colleagues (147) represent a unique model of spontaneously occurring CF lung disease. Our laboratory participated in developing various backcrosses of *Cftr*-KO mice including the C57BL/$6^{H/M}$-*Cftr*.ko mice, and the studies presented in this manuscript were performed using this unique spontaneous lung disease model.

To better understand the mechanism of lung infection with *P. aeruginosa*, many techniques have been developed in order to establish both acute and chronic lung infection. Delivery of free *P. aeruginosa* (207;185;218;182) directly into the nose or by aerosol techniques (191;87;180) produced an acute infection model. In order to create a model of chronic lung infection, Cash *et al.* (29) developed a rat model of lung infection using *P. aeruginosa* embedded in agarose beads, which later was modified by Starke *et al.* (261) for mouse models. The bacteria are inoculated intratracheally with immobilizing agents such as agar, agarose or seaweed alginate. The entrapment of *P. aeruginosa* in agar beads seems to slow the growth of the bacteria within the beads compared to outside, resembling the biofilm state (283), and this method has consequently been extensively used in most of the CF mouse models of lung infection.

Adding to the complexity of mimicking *P. aeruginosa* lung infection in mouse models of CF, the *Cftr*-KO mice themselves are challenging to work with. These mice are smaller than normal mice and are more sensitive to housing and

nutritional conditions, leading to a small amount of animals being available for experiments. Because of these characteristics specific to *Cftr*-KO mice, and also because of the invasiveness of the infection procedure which we, and others, have been using to improve persistence of the lung infection, we sought to find an alternative way to study the lung inflammatory response during *P. aeruginosa* infection. We have previously demonstrated a very clear difference in susceptibility to lung infection between *Cftr*-KO and WT animals using a method of intratracheal instillation; however, we were wondering if the surgery performed during this procedure and the consequently enhanced inflammation associated with the healing process contributed to susceptibility of mice to infection with *P. aeruginosa*.

The original technique detailed in this paper consists of the injection of bacterial beads directly into the lungs through the mouth without the need for any tracheal incisions. Moreover, this technique of direct pulmonary delivery infects the animals much faster compared to the intratracheal technique previously used. Since *Cftr*-KO mice are smaller, more sensitive and more fragile than WT control mice, these ameliorations of the technique benefit them greatly and allow us to study a larger number of animals. We also observed much lower mortality rates, especially in *Cftr*-KO mice. Finally, the use of a less invasive technique compared to the tracheal surgery also permits the exclusion of the surgery-related inflammation while trying to study the inflammatory response to bacterial infection.

Overall, we developed an infection technique that allows the animals to recuperate faster from the infection procedure, creating a lung infection that resembles bacterial colonization with *P. aeruginosa* observed in humans. The purpose of this paper is to describe the details of this technique that, in our opinion, is far more superior compared to any other previously available techniques. We also present a detailed comparison of the inflammatory responses induced by infection with *P. aeruginosa* using this method between *Cftr*-KO and their

littermate controls that is helpful in understanding the basis of CF lung disease. Taken as a whole, the data presented in this manuscript clearly shows the usefulness of the described new method of lung infection to study the mechanisms involved in the regulation of inflammation induced by *P. aeruginosa* infection in our CF mouse model.

4.3 Material and Methods

4.3.1 Mice. Age- and gender- matched C57BL/6 mice (n = 88 females, and n = 49 males) and C57BL/6-*Cftr*$^{-/-}$ (*Cftr*-KO) inbred mice (n = 9 females, and n = 10 males) were kept murine pathogen-, helicobacter- and parasite- free. They were housed (1 - 4 animals/cage), bred and maintained in a barrier facility unit under specific pathogen-free conditions with a 12-hr light/dark cycle, at 22°C ± 2 and a relative humidity of 50% ± 5. The animals were kept in polycarbonate micro-isolator cages (Lab Products, Maywood NJ) with sterile corn bedding (Anderson, Bestmonro, LA) and maintained in ventilated rack (Lab Products) with a cycle of 50 changes of fresh hepa filter air per hour in each cage. WT mice were fed with the NIH-31 modified mouse irradiated diet (Harlan Teklad, Indianapolis, IN) (until 3 weeks prior to experiment; they were then fed liquid diet as *Cftr*-KO mice) whereas *Cftr*-KO mice were fed the Peptamen liquid diet (Nestle Canada, Brampton, ON), starting at 14 days of age. The liquid diet, freshly made every morning, was provided in 50 ml centrifuge tubes (Sarstedt, Montreal, QC). One week prior to infection, the WT controls were switched from the solid diet to the Peptamen liquid diet. All mice had *ad libidum* access to sterile acidified water. Experimental procedures with the mice were conducted in accordance with the Canadian Council on Animal Care and with the approval of the Animal Care Committee of the McGill University Health Center, Montreal, Quebec, Canada.

4.3.2 *P. aeruginosa.* *P. aeruginosa* strain 508 was kindly provided by Dr. Jacqueline Lagacé (University of Montreal, Montreal, QC). This strain has a mucoid appearance when grown on blood agar and was originally isolated from the

sputum of a CF patient at Ste-Justine Hospital, Montreal, QC. Bacteria stocks are stored at -80°C until used.

4.3.3 Inoculum preparation. In order to establish a model of prolonged lung infection, bacteria-impregnated agar beads were freshly prepared the day before each experiment and stored at 4°C overnight. A 1 ml aliquot of inoculum from the frozen stock was used to inoculate 250 ml of 4% proteose peptone broth. The bacterial suspension was then placed in a shaking incubator overnight at 37°C. A 100 microliter aliquot from this suspension was used to inoculate 100 ml of broth that was aliquoted in 15 ml tubes (Sarstedt, Montreal, QC); 6 ml per tube. Bacteria were grown for approximately 3 hours in a shaking incubator at 37°C, until they reached a mid-log phase. Either 8 or all of the 16 tubes containing log phase bacteria were pooled together, depending on the desired bacterial concentration of the beads. The bacteria were concentrated and resuspended in 5 ml of Dulbecco's phosphate-buffered saline (PBS; Invitrogen, Mississauga, ON). A 1 ml or 5 ml aliquot of the concentrated bacterial broth was added to warm (52°C) 1.5% trypticase soy agar (Difco, Detroit, MI) (agarose beads free of bacteria were prepared using PBS instead of a bacterial suspension). This mixture was quickly added to warm (52°C) heavy mineral oil and stirred rapidly, first at room temperature for 6 minutes, followed by ice cooling with continuous stirring for 10 minutes. The speed of the stirring was predetermined and remained consistent for every agarose-bacterial suspension production. The oil-agar mixture was centrifuged to sediment the beads. The oil was removed and the beads were washed 4 times with PBS. The size of the beads was verified microscopically and only those preparations containing beads predominantly 100-250 micrometers in diameter were used as inoculum. The number of bacteria was determined after homogenizing the bacteria-impregnated bead suspension. Inoculum was prepared by diluting the beads suspension to 0.5 - 20 x 10^6 CFU/ ml.

4.3.4 Description of the method of mouse lung infection with *P. aeruginosa* instilled in agarose beads. Mice were anaesthetized with a combination of ketamine (7.5 mg/ml) and xylazine (0.5 mg/ml) administered intraperitoneally at a dose of 20 ml/kg of body weight. We initially tried a shorter acting anaesthetic, 2,2,2 Tribromoethanol (Avertin; SIGMA-Aldrich, Oakville, ON), but this anesthesia was not consistent. Once the mouse was successfully anaesthetized (with no pedal or ocular reflex), the animal was installed under binoculars (Microscope M650, Wild Leitz, Willowdale, ON) in the vertical position and was held on a restraining board by holding the animal by its upper incisor teeth, as shown in Figure 4.1, panel A. The tongue was then gently pulled to the side of the mouth (to depress the tongue in order to see the vocal cords, Figure 4.1, panel B). A curved 26-G gavage needle was then inserted into the mouth and guided through the pharynx to gently touch the vocal cords to see the lumen of the trachea; the needle was then introduced into the trachea to reach the lung for the bilateral injection of the inoculum (see Appendix I for additional illustrations). Inoculums ranging from 30 to 100 microliters were used, but the 50 microliter volume was the preferred volume with regards to the consistency of CFU injected. The injected 50 microliter volume did not lead to any distress in the mice. After inoculation the animal usually regained righting reflex within an hour. Many doses were tested using this technique, ranging from 0.5 to 20 x 10^6 *P. aeruginosa*. A final dose of 1 x 10^6 *P. aeruginosa* was used for infection using WT and *Cftr*-KO mice. The weight of each mouse was recorded prior to and during the course of infection.

4.3.5 Mice evaluation. After infection, the food was placed at the bottom of the cage, fecal and urine secretions were checked and removed everyday. Mice were monitored 3 times daily; the maximum weight loss allowed was 15%. Mice were sacrificed by CO_2 overdose.

Figure 4.1 Direct pulmonary method of infection. Microscope and mouse holding system for lung infection (A). View from the microscope of the vocal cords open and close positions (B).

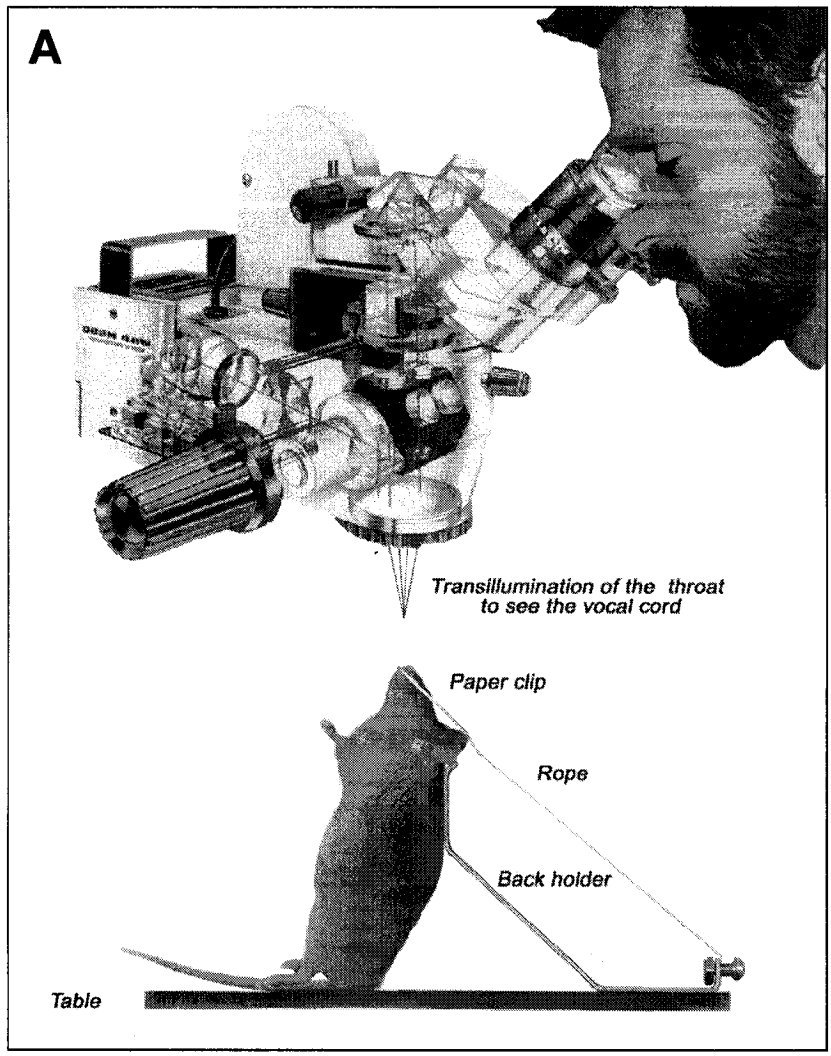
A
Transillumination of the throat
to see the vocal cord
Paper clip
Rope
Back holder
Table

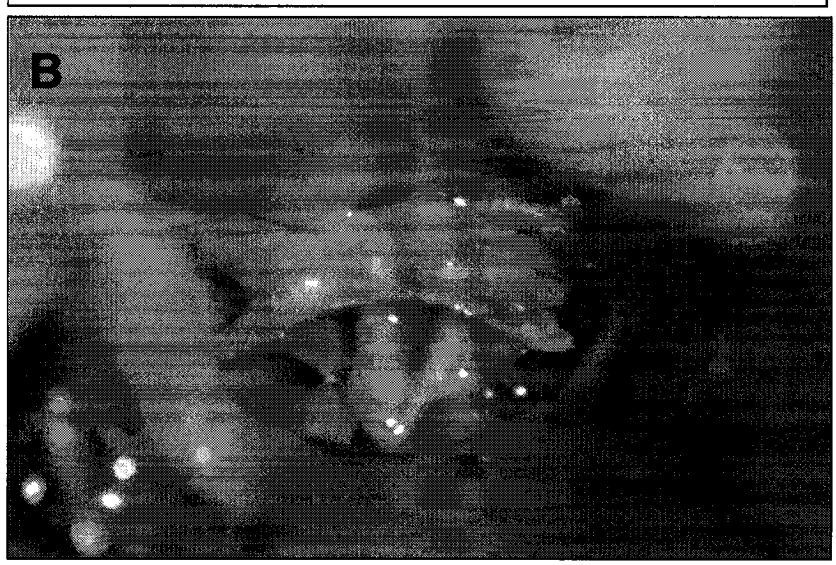
B

4.3.6 Bronchoalveolar lavage. Circulation was flushed by slow intracardiac infusion of divalent cation-free Hank's balanced salt solution (HBSS; Invitrogen, Mississauga, ON). The trachea was cannulated with a 22-gauge intravenous catheter placement unit (Critikon, GE Medical Systems, Tampa, FL) connected to two 5 ml syringes via a 3-way stopcock with a rotating collar (Namic U.S.A., Glens Falls, NY). The alveoli of infected mice were washed 3 times (total of 1.4 ml) with divalent cation-free HBSS. The volume of BALF recovered was approximately 1.2 ml. Alveolar cells were centrifuged and the supernatant was used for CFU count determination before being stored at -20°C, until assayed for cytokine concentrations. Cells were resuspended in 0.5 ml of Dulbecco's Modified Eagle Medium (DMEM; Invitrogen) supplemented with 10% fetal bovine serum (FBS; Hyclone, Logan, UT), diluted in Turk's solution and counted using a hematocytometer. The proportions of macrophages, lymphocytes and PMN were calculated after counting approximately 300 alveolar cells on cytospin preparations stained with Diff-Quick (American Scientific Products, McGaw Park, IL).

4.3.7 Lung homogenates. Lungs from infected mice were harvested and homogenized for 60 sec at high speed (homogenizer PT10135 Brinkmann Instruments Co., Mississauga, ON) in 4 ml of sterile PBS (Invitrogen). Serial 10-fold dilutions of lung homogenates were plated on Petri dishes containing TSA. The number of CFU per lung was counted after overnight incubation at 37°C. For cytokine measurements, lung homogenates were centrifuged at 1500 x g at 4°C for 10 min; the supernatants were then removed, aliquoted in new tubes and stored at -20°C until assayed for cytokine concentrations.

4.3.8 Lung histopathology. Lungs were removed from the mouse, inflated with 10% buffered formalin acetate (Fisher Scientific, Nepean, ON) and immersed in that buffer for a minimum of 36 hrs. The lungs were then trimmed and embedded in paraffin. Paraffin sections were sliced 3 μm thick using a Reichert-Jung microtome. Lung sections were cut at regular intervals to get sections at different depths of the lung. Three cuts were made for each of the

following standard staining methods: Haematoxylin and eosin (HE), Periodic-Acid Schiff (PAS) and Masson's Trichrome (MT). Each parameter of lung morphology was observed under these specific stains and analyzed using scales specific to each parameter. For hyperplasia of the epithelium and cell metaplasia, a score of 1 indicated no change; a score of 2 represented 0-25% of the airway surface was affected; a score of 3 represented 26-50% of the airway surface was affected; a score of 4 meant that 51-75% of all airway surface was affected; and finally a score of 5 indicated that 76-100% of the airway surface was covered by these pathologies. For inflammatory cell infiltration, basement membrane thickening and fibrosis, the scale was composed of scores 1, 2 and 3. A score of 1 represented the absence of any of these pathologies; a score of 2 indicated the presence of either a few inflammatory cells, some basement membrane thickening or some fibrosis (these last 2 seen thinly accumulated around the airways, showing the airway wall about 2 to 5 times thicker than a control airway); a score of 3 was given when the specimens showed the presence of many inflammatory cells in the blood vessels around the airways or a significant amount of fibrosis and basement membrane thickening around the airways (seen in thick dense layers around the airways, making the airway wall more than 5x thicker than a normal airway). Mucus accumulation was analyzed separately for large airways (bronchi) and for smaller airways (bronchioles), because this phenomenon have occurred generally more often in large airways than in smaller airways. No mucus accumulation was expressed by a score of 1 for small airways and a score of 4 for large airways; some mucus accumulation (covering less than 50% of airway surface) was expressed by a score of 2 for small airways and 5 for large airways; mucus accumulation covering the airway surface almost completely was expressed by a score of 3 for small airways and 6 for large airways.

4.3.9 Cytokine measurements. The levels of 22 cytokines/chemokines (IL-1α, IL-1β, IL-2, IL-4, IL-5, IL-6, IL-7, IL-9, IL-10, IL-12 (p70), IL-13, IL-15, IL-17, IFN (interferon)-γ, TNF, GMCSF (granulocyte-macrophage colony-stimulating factor), MIP-1α (macrophage inflammatory protein 1 alpha, MCP-1

(monocyte chemotactic protein-1), N51/KC (cytokine-induced neutrophil chemmoattractant), RANTES (Regulated on activation, normal T expressed and secreted), IP-10 (interferon-γ-inducible protein 10), G-CSF were assessed in lung homogenates prepared from infected animals with the Mouse Cytokine/Chemokine LINCO*plex* kit (Linco Research, Inc, St-Charles, MO) using Luminex™ technology and assayed with the Luminex^{100}IS™ system by Linco Research, Inc. The cytokine detection limit for this assay was 3.2 pg/ml.

4.3.10 Statistical analyses. Data was analyzed using Sigma Stat V3.01 software (SPSS Inc, Chicago, IL). Statistically significant differences between means and medians of studied groups were evaluated using Student's t-test and the nonparametric Mann-Whitney U test, respectively. One-way ANOVA and Kruskal-Wallis ANOVA on ranks, combined with pair-wise multiple comparison procedures (Dunn's method), were used to evaluate differences between multiple groups. Significance was set at a two-tailed p value of ≤ 0.05.

4.4 Results

4.4.1 Method of infection.

Mice are small animals compared to other CF animal models like ferrets, cats, pigs, rabbits, sheep and rats. Therefore, we used a microscope to properly inject the bacterial inoculums directly into the lung (Figure 4.1). In order to make sure that the injection was into the lungs exclusively, preliminary experiments were performed using a blue dye to localize the site of inoculation. As shown in Figure 4.2, inoculation was nicely spread throughout the lungs. The injection procedure was performed numerous times until fluidity in the mouse handling and perfect replicates were obtained.

4.4.2 *P. aeruginosa* dose determination for the establishment of lung infection. Since this direct pulmonary method of infection is less invasive than the intratracheal method, and because there is a susceptibility difference between

Figure 4.2 Site of injection into the lungs. A blue dye was injected into the lungs (volume between 30 to 50 ul) using the transpulmonary injection technique. Different views of the lungs are shown: Inside the mouse (A), frontal position (B), dorsal position (C) of the lungs. After complete necropsy, no dye was found in the stomach of mice.

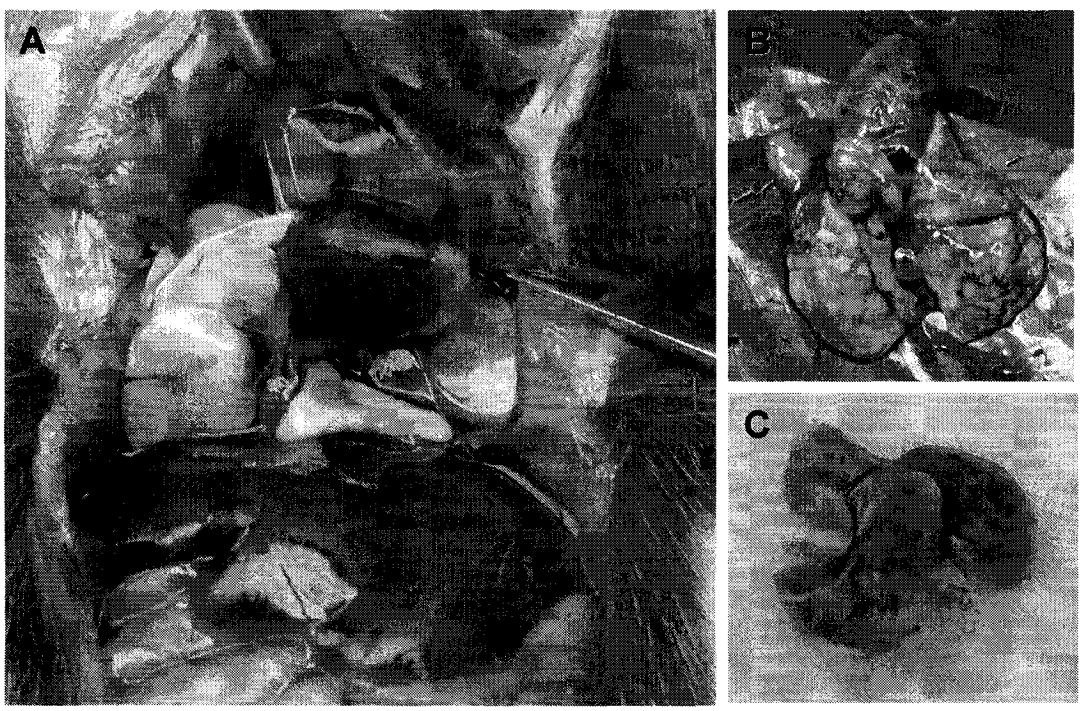
A
B
C

female and male mice to *P. aeruginosa* lung infection (112), it was necessary to re-assess the appropriate dose of *P. aeruginosa* needed to create the pulmonary infection. Therefore, we evaluated numerous different doses, ranging from 0.5 to $80x10^5$ *P. aeruginosa* embedded in agarose beads, by comparing the weight loss during infection, the bacterial burden and also the recruitment of alveolar cells into the lungs (Figure 4.3) of female and male WT mice (Table 4.1).

Table 4.1 Characteristics of mice used in direct pulmonary infection procedures

	Females	Males
Age (weeks)	21.6 ± 0.88	18.6 ± 0.58
Body weight; before infection (g)	27.5 ± 0.46	22.2 ± 0.61

Values are means ± SEM and represent the pool of animals from 9 independent experiments.

4.4.2.1 Bacterial burden in the lungs and survival: The dose of *P. aeruginosa* we previously utilized in our CF mouse model is $1\text{-}2x10^5$ *P. aeruginosa* per mouse. Using this dose, almost no bacteria could be found in the lungs 3 days post-infection in males (Figure 4.3, panel B). Using our new method of infection, we observed almost complete clearance of bacteria from the lungs when doses ranging from $2x10^5$ to $8x10^5$ *P. aeruginosa* were used, for both females (figure 4.3, panel A; $p = 0.181$) and males (figure 4.3, panel B; $p = 0.293$). At the $8x10^5$ *P. aeruginosa* dose and at all lower doses, all mice (100%) survived the infection procedure and recuperated from the intervention. Given that the initial doses tried were not affecting the survival rate of the mice and that no major difference could be seen in the bacterial burden of the lungs, we considerably increased the dose of bacteria injected into the lung and applied doses ranging from $0.8x10^6$ to $8x10^6$ *P. aeruginosa* per mouse. With the highest dose of *P. aeruginosa* tried, all mice died within few hours following infection. Only 25% of the animals survived when the dose of $5x10^6$ *P. aeruginosa* was used. When we infected the mice with $2.5x10^6$ *P. aeruginosa*, 66% of the mice survived, but the majority of the surviving animals lost more than 15% of their body weight and had to be

sacrificed. When the mice were infected with $1x10^6$ *P. aeruginosa*, we observed a survival rate of 95.8%, therefore this dose of bacteria seemed to be the most appropriate for the analysis of the inflammatory responses in the lungs of the mice.

4.4.2.2 Alveolar cells in BALF samples: The recruited inflammatory alveolar cells followed the same trend seen in the CFU, as no statistical difference was observed between the doses ranging from $2x10^5$ to $8x10^5$ *P. aeruginosa* for females (Figure 4.3, panel C; $p = 0.223$) and males (Figure 4.3, panel D; $p = 0.927$). However, the number of inflammatory cells in BALF samples from females increased with the dose of *P. aeruginosa* injected into the lungs (Figure 4.3, panel C), with a statistically significant increase ($p = 0.010$) found between the $8x10^5$ *P. aeruginosa* dose (1.49 ± 0.29 cells) and the uninfected samples (0.16 ± 0.04 cells; data not shown).

4.4.2.3 Weight monitoring during *P. aeruginosa* lung infection: Mice, both female and male, infected with *P. aeruginosa* lost between 7 to 12% of their body weight by day 2 post-infection and slowly started regaining weight by day 3 post-infection, independent of the dose injected, which ranged from 2 to $8x10^5$ *P. aeruginosa* per mouse (Figure 4.3, panels E and F). Also, no statistical difference was observed in the total mean weight loss of the mice between these three *P. aeruginosa* doses for all days post-infection analyzed (day 1 post-infection; females $p = 0.414$ & males $p = 0.182$, day 2 post-infection; females $p = 0.097$ & males $p = 0.390$, and day 3 post-infection; females $p = 0.171$ & males $p = 0.390$). Mice injected with empty beads lost approximately 5% of their body weight the first day of infection, started gaining weight the second day after infection and regained it completely by day 3 (data not shown).

In light of these results, the optimal dose chosen for the infection in our CF mouse model was $1x10^6$ *P. aeruginosa*, as it created a significant inflammatory response in the lungs of the mice without impairing the overall well-being of the animal during the infection and with the obtainment of a reasonable survival rate.

Figure 4.3 Determination of the *P. aeruginosa* dose with transpulmonary infection technique. Female and male WT mice were infected with different doses of *P. aeruginosa* embedded in agarose beads and were examined at 3 days post-infection for bacterial burden in the lung (A, B), recruitment of inflammatory cells into the lung (C-D), and for weight loss during the course of infection (E-F). Increasing amounts of CFU and alveolar inflammatory cells were observed in the lungs correlating with *P. aeruginosa* lung infection. Mice infected with *P. aeruginosa* lost weight during the first 2 days of infection then restarted gaining weight at day 3 post-infection, independently of the *P. aeruginosa* infection dose. Data is presented as the mean ± SEM and pooled from 2 different experiments done under the same conditions (females: 3 to 7 mice per group; males: 3 to 6 mice per groups).

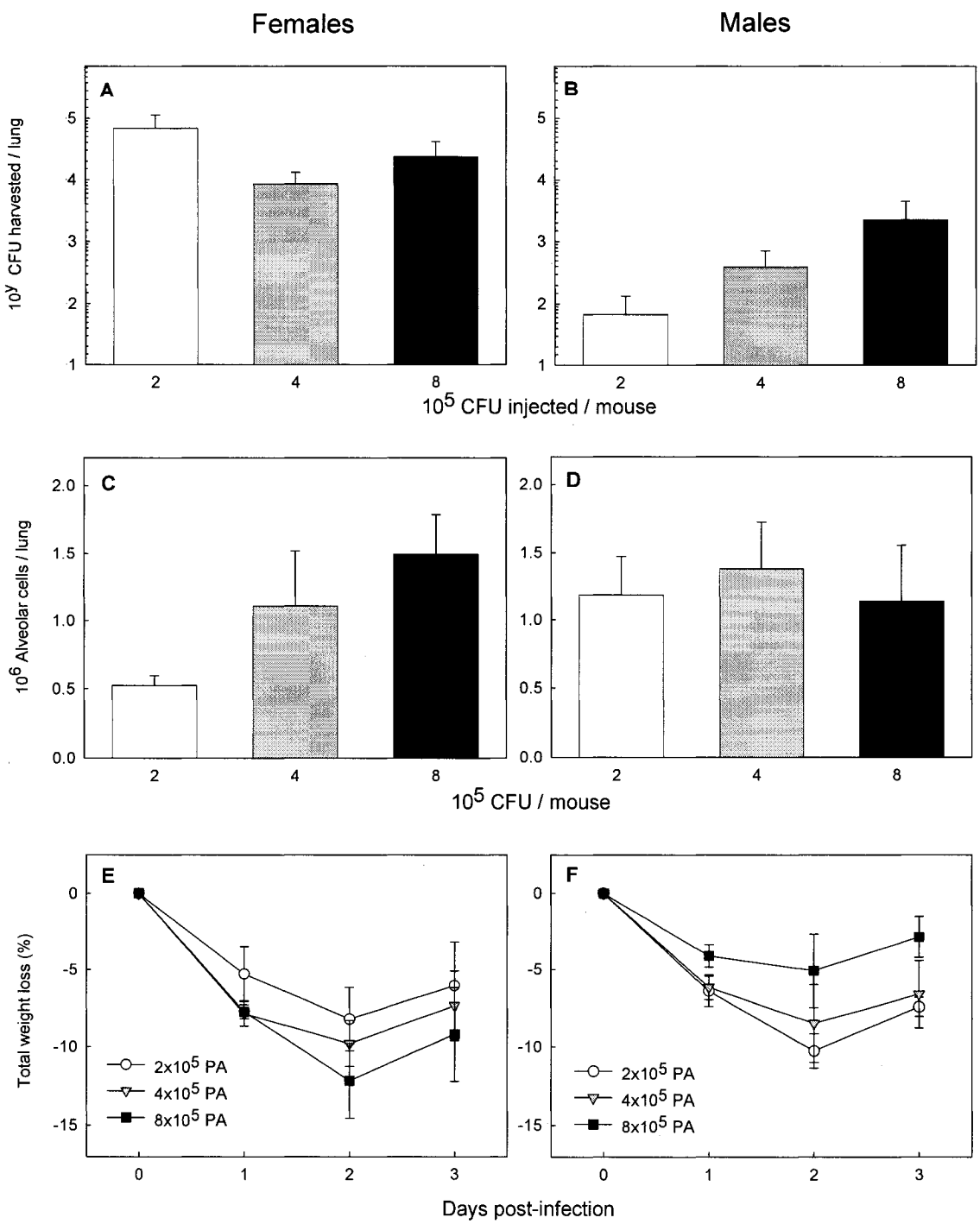
Females
Males
A
B
10^Y CFU harvested / lung
10^5 CFU injected / mouse
C
D
10^6 Alveolar cells / lung
10^5 CFU / mouse
E
F
Total weight loss (%)
$2x10^5$ PA
$4x10^5$ PA
$8x10^5$ PA
Days post-infection

4.4.3 *P. aeruginosa* direct pulmonary infection in KO and WT mice

Histological evaluation of the lungs was previously performed on our CF mouse model in order to identify the pathological state of the animals before lung infection (Table 3.1). In brief, as seen in Figure 4.4, the uninfected *Cftr*-KO mice showed increased hyperplasia of epithelial cells, basement membrane thickening (panels D and F), as well as enhanced inflammatory cell infiltration in the lung tissues (panel E) compared to the WT uninfected controls (panels A-C). Subsequently, using this newly developed and perfected technique, we infected *Cftr*-KO mice showing signs of lung pathology and their WT controls with $1x10^6$ *P. aeruginosa* and evaluated their inflammatory response.

Females displayed much higher susceptibility to *P. aeruginosa* lung infection than males in our mouse models [(112), and unpublished observations]. Although we have used both genders to determine the optimal and tolerable dose with the direct pulmonary technique, when studying the CF lung disease in our CF mouse model, we predominantly used males due to a very high mortality rate observed in females. Consequently, the figures included in this section illustrate only results generated using male *Cftr*-KO and littermate controls and the results from the females are only described.

4.4.3.1 Weight monitoring during *P. aeruginosa* lung infection: The mean weight loss of *Cftr*-KO mice was shown to be higher than those seen in WT mice at 2 days ($p \leq 0.001$) and 3 days ($p = 0.001$) post-infection for both males (Figure 4.5, panel A) and females (data not shown). A significant difference was also seen between the female and the male mice, for both WT and *Cftr*-KO animals, as females lost more weight than males (data not shown, day 2 post-infection $p \leq 0.001$ and day 3 post-infection $p = 0.001$). No difference was observed between any of the *Cftr*-KO and WT groups for both genders at day 1 post-infection ($p = 0.070$).

Figure 4.4 Histological examination of the lungs of uninfected WT and *Cftr*-KO mice. Representative haematoxylin- & eosin- stained lung sections that were prepared from uninfected WT (A-C) and *Cftr*-KO (D-F) mice. Sections from WT mice show a normal lung structure. Sections from *Cftr*-KO mice show cell infiltration in the bronchi and alveoli, and hyperplasia of the epithelium. Panels C and F illustrate a higher magnification of the airways of uninfected WT and *Cftr*-KO mice showing normal and hyperplasia of the epithelium, respectively.

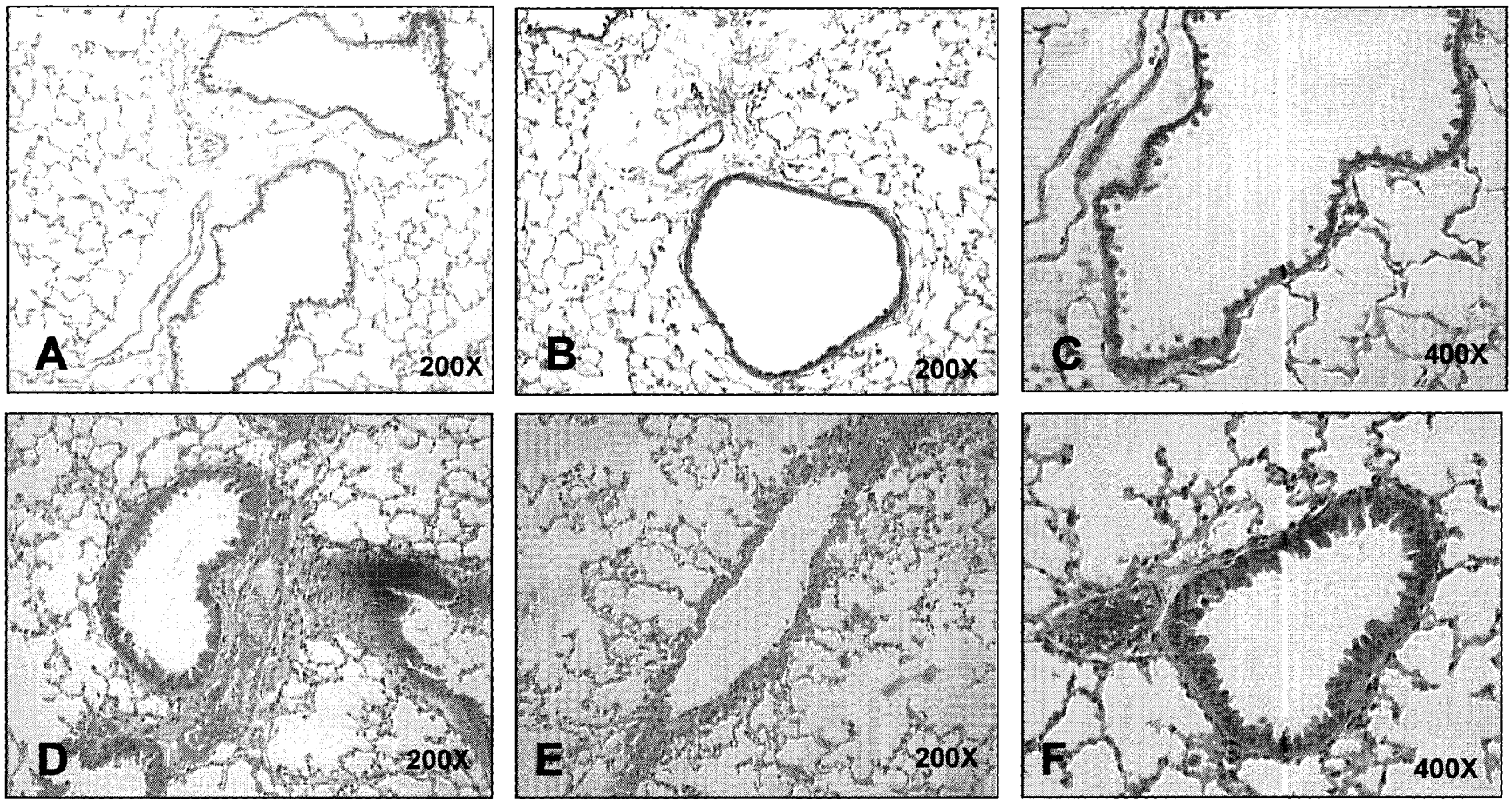
A
200X
B
200X
C
400X
D
200X
E
200X
F
400X

4.4.3.2 Bacterial burden in the lungs and survival: The CFU counts were assessed in the lung tissue homogenates of *Cftr*-KO and WT males 3 days after infection. A significantly higher number of bacteria was found in the *Cftr*-KO compared to the WT males in the lung tissue homogenates (Figure 4.5, panel B, $p = 0.039$). A difference was also observed between females and males, where females had between 30- to 300- fold higher numbers of bacteria in the lungs compared to the male mice. Yet, because of the high variability seen in the females in terms of CFU, no statistical significance could be reached (data not shown, $p= 0.086$).

4.4.3.3 Alveolar inflammatory cells in BALF samples: The number of alveolar cells from the BALF was evaluated in *Cftr*-KO and WT mice 3 days after infection with $1x10^6$ *P. aeruginosa* embedded in agar beads. No difference was found between the *Cftr*-KO and WT for both male (Figure 4.5, panel C, $p = 0.155$) and female animals (data not shown, $p= 0.700$). Moreover, no difference was observed between the genders for both genotypes in term of recruitment of cells into the lungs (data not shown, WT $p = 0.683$ and *Cftr*-KO $p = 0.946$). However, when we compared the different types of inflammatory cells found in the lungs, we observed significant differences between the WT and the *Cftr*-KO mice in the mean percentages of the different groups of cells (Figure 4.5, panel D). *Cftr*-KO mice had higher PMN counts ($p = 0.044$), lower lymphocyte counts ($p = 0.033$) and a clear trend towards lower macrophage counts as well, even though that last difference was not statistically significant ($p = 0.107$). In addition, WT female mice recruited more PMN and less lymphocytes in the lungs compared to the WT male mice, comparable to the levels observed in the *Cftr*-KO males (data not shown).

4.4.3.4 Cytokine expression in the lungs of *P. aeruginosa* infected WT and *Cftr*-KO mice: Lung homogenates from male mice were tested for 22 different cytokines. Statistically higher levels were observed in *Cftr*-KO mice compared to their WT controls for N51/KC ($p = 0.041$), IL-9 ($p \leq 0.001$),

Figure 4.5 Inflammatory response in WT and *Cftr*-KO mice during lung infection with 1x10^6 *P. aeruginosa* embedded in agar beads. Using the transpulmonary infection technique, WT (*grey*) and *Cftr*-KO (*white*) male mice were evaluated during *P. aeruginosa* lung infection. Mean weight loss is represented as the percentage of weight loss since the first day of infection (A). The CFU counts were assessed in the lung tissue homogenates 3 days after infection and data is presented as mean ± SEM (B). The number of alveolar cells from the BALF was evaluated 3 days after infection and data is presented as mean ± SEM (C). The recruitment of inflammatory cells in the lungs of WT and *Cftr*-KO mice was evaluated 3 days after infection: the numbers of alveolar macrophages, lymphocytes, and PMN were calculated on the basis of the differential cell counts of Diff-Quick cytospin preparations (D). These results illustrate 2 independent experiments (n = 3 per group for each experiment) performed under the same conditions.

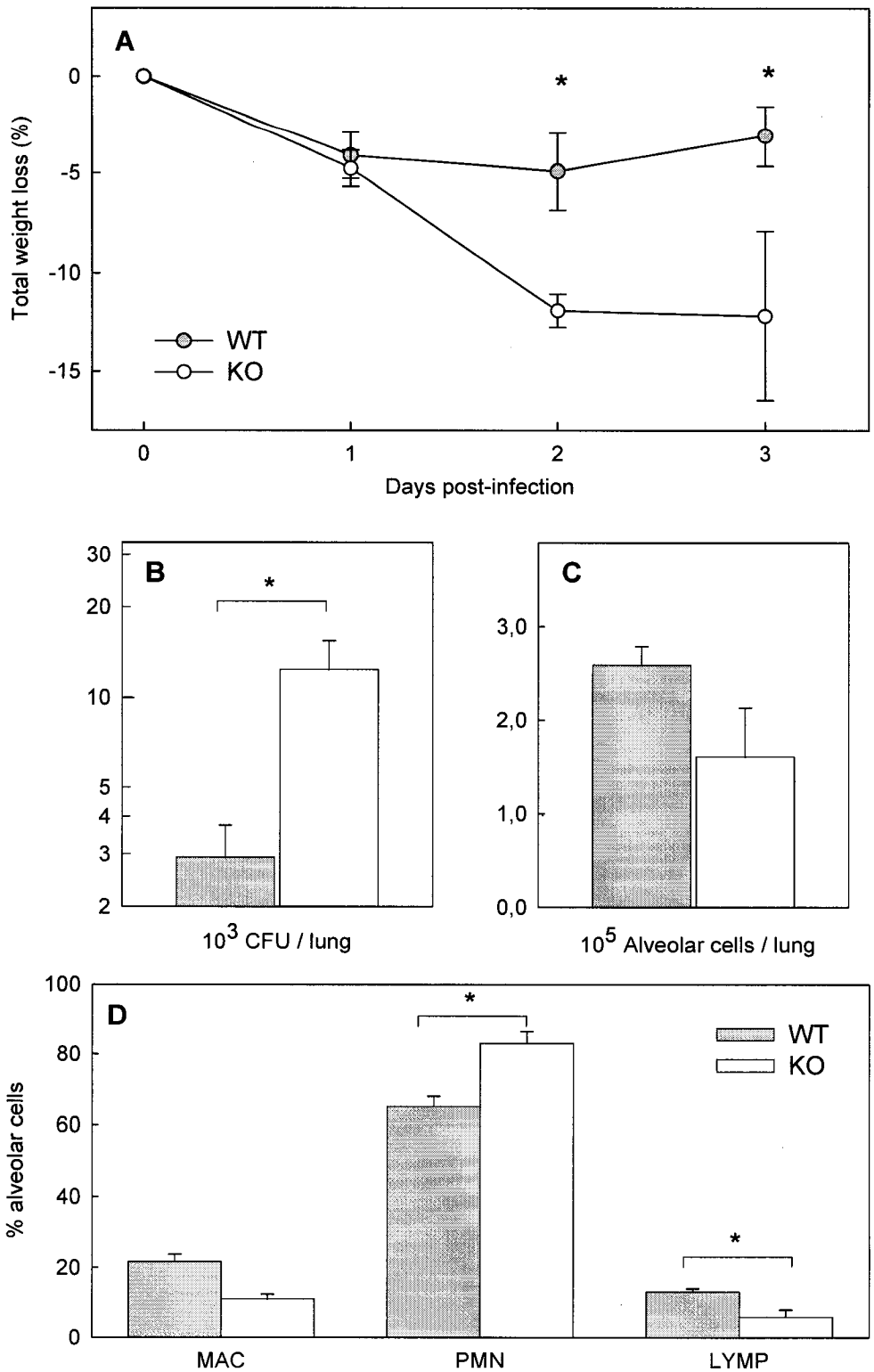
A
Total weight loss (%)
0
-5
-10
-15
*
*
WT
KO
0
1
2
3
Days post-infection
B
30
20
10
5
4
3
2
*
10^3 CFU / lung
C
3,0
2,0
1,0
0,0
10^5 Alveolar cells / lung
D
% alveolar cells
100
80
60
40
20
0
*
*
WT
KO
MAC
PMN
LYMP

Figure 4.6 Cytokines expression into the lungs of WT and *Cftr*-KO infected mice. Lung homogenates from male WT (*solid*) and *Cftr*-KO (*open*) mice infected with $1x10^6$ *P. aeruginosa* were tested for 22 different cytokines. Statistically significant differences (*) were observed in the levels of protein expression between the *Cftr*-KO mice compared to their WT controls for N51/KC ($p = 0.041$), IL-9 ($p \leq 0.001$), GM-CSF ($p \leq 0.001$), IL-15 ($p = 0.008$), and IL-7 ($p \leq 0.001$). Data is presented as individual values and the horizontal line represents the median. These results illustrate 2 independent experiments performed under the same conditions.

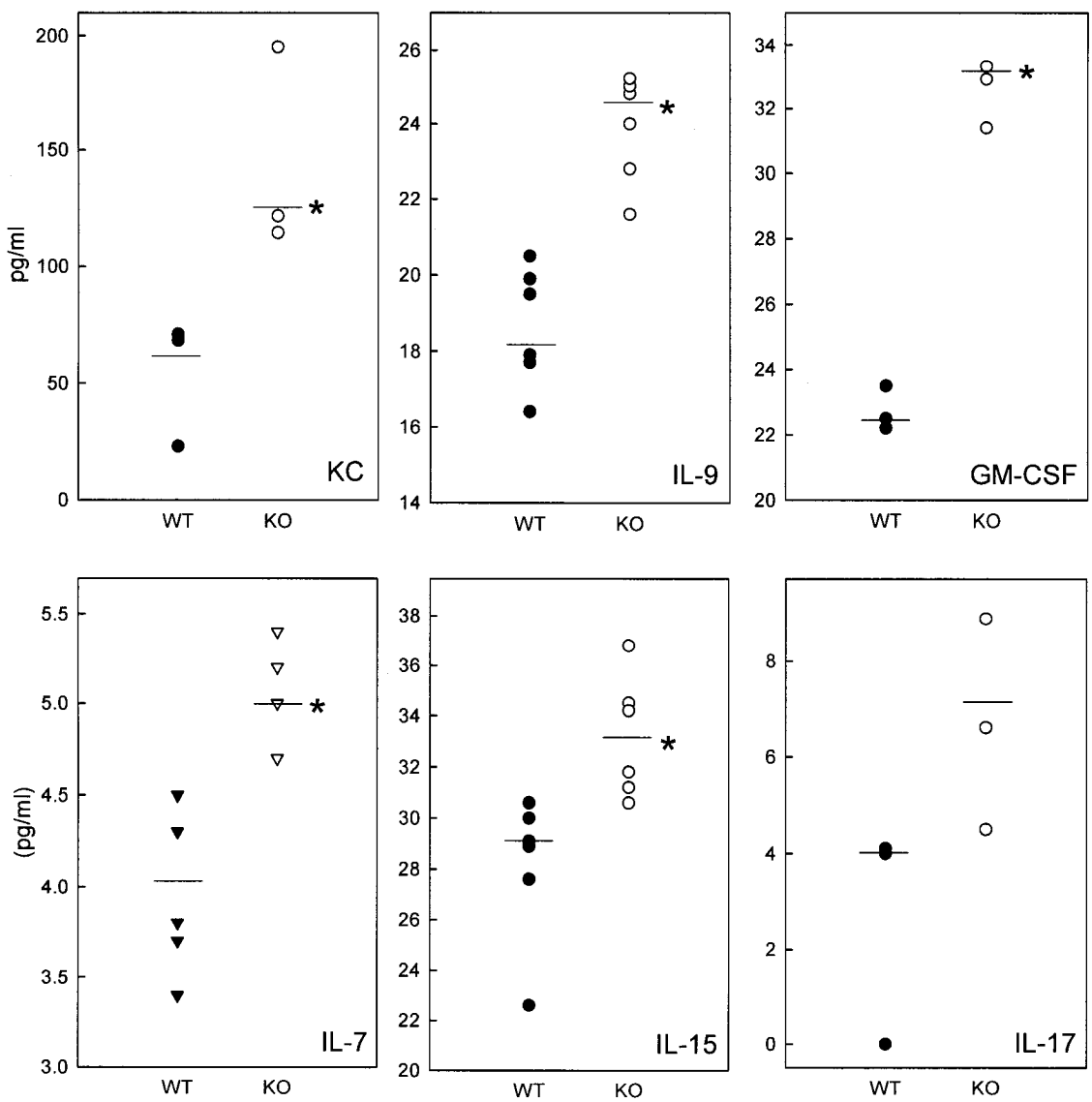
pg/ml
200
150
100
50
0
KC
WT
KO
*
26
24
22
20
18
16
14
IL-9
34
32
30
28
26
24
22
20
GM-CSF
(pg/ml)
5.5
5.0
4.5
4.0
3.5
3.0
IL-7
38
36
34
32
30
28
26
24
22
20
IL-15
8
6
4
2
0
IL-17

GMCSF ($p \leq 0.001$), IL-15 ($p = 0.008$), and IL-7 ($p \leq 0.001$) (Figure 4.6). All other cytokines measured were either not detectable or not significantly different between WT and *Cftr*-KO mice at the timepoint tested (Table 4.2).

Table 4.2 Cytokine levels in lung homogenates of *P. aeruginosa* infected *Cftr*-KO and WT mice 3 days post-infection.

Cytokines	WT			KO		
	(pg/ml)	Quartiles 25%	75%	(pg/ml)	Quartiles 25%	75%
MIP-1α [1]	191.7	88.7	216.1	255.7	88.2	393.9
MCP [1]	108.9	64.2	125.6	137.4	61.3	187.4
Rantes [1]	19.2	12.6	21.5	10.6	9.3	14.6
IFNγ [1]	9.1	6.3	10.7	10.1	2.5	10.4
IL-1β [1]	29.9	15.9	42.8	24.4	9.7	45.9
G-CSF [1]	155.1	70.2	184.1	270.0	117.8	433.2
IP-10 [1]	189.7	112.9	216.4	159.5	81.7	190.5
IL-1α [1]	975.5	397.9	1403.5	1194.4	375.5	1945.8
IL-6 [1]	60.6	27.5	138.9	123.9	47.9	188.5
IL-10 [1]	0.0	0.0	0.0	19.3	4.8	21.2
TNF [1]	7.4	1.9	8.9	6.2	1.5	8.7
IL-2	ND			ND		
IL-4	ND			ND		
IL-5	ND			ND		
IL-12	ND			ND		
IL-13	ND			ND		

Values are medians of 3 to 6 animals with quartiles
ND; levels of cytokine is below the level of detection of the assay (< 3.2 pg/ml)
[1] Medians are not significantly different at day 3 post-infection (p values between 0.200 and 1.000) in the *Cftr*-KO compared to the WT mice

4.5 Discussion

With many possible mutations in the *Cftr* gene, cystic fibrosis is a complex disease, affecting many organs with varying intensities, frequently leading to death. What makes this disease difficult to study is the fact that no known natural animal model exists. Although many animal models have been used to study CF disease, the *Cftr* gene knockout mouse model seems to be the most frequently used when researching the different aspects of the disease and trying to better understand the CF lung disease. Various original techniques (acute and chronic models) using *P. aeruginosa* and *B. cepacia* (280) were developed for mice to mimic the infection of the lungs of CF patients. However, even though rodents are easier to work with compared to other animal models, they are much more resistant to all kinds of microbes and microorganisms when compared to humans. It is, therefore, quite challenging to establish conditions allowing the lung bacterial colonization of mice. Nevertheless, many techniques were developed and are routinely used to study the progress of CF lung disease. Two of these techniques involve the inhalation by mice of the bacteria following the aerosolization or the inoculation of bacteria through the nose (257). These models of infection are primarily used to study the acute inflammatory response in the lungs, since the animals clear the bacteria very rapidly. Several investigators, including us, have used a technique of intratracheal infection of the lungs with *P. aeruginosa* bacteria embedded in agar beads (98;99;112;121;147;285). This method of infection involves the inoculation of the bacteria into the lungs via a tracheotomy (described in section 2.3.3, illustrated in Figure 4.7). It also requires that the bacteria are enmeshed into agarose or agar, allowing the bacteria to stay longer in the lung environment, mimicking, at least to some extent, the chronicity of the lung infection observed in CF afflicted patients. This method has proven to be useful in the study of bronchopulmonary chronic infection. However, a more "natural" colonization technique was used in a rat model of CF and other lung studies, involving direct inoculation of the microorganism into the lungs via the mouth without a temporary tracheotomy (294). This method of delivering the bacteria directly into the lungs

Figure 4.7 Intratracheal method of infection. Once the mouse is anasthesized, a transverse cervical incision is made allowing the trachea to be exposed. Then a small incision is performed between two rings of the trachea and it can therefore be intubated for inoculation. After inoculation, all incisions are closed by suture.

Photograph by Daniel Houle

without surgical incision of trachea was very appealing to us since it lead to much less physical and inflammatory stress in the animals

The difficulty lies in the fact that it is much more challenging to adapt this procedure for a mouse model due to the difference in size between a mouse trachea and the rat trachea. Another study, working with a model of immunocompromised host, has used a similar methodology using *Klebsiella pneumoniae* in B6D2F/J mice (145). The CF mouse model proves to be even more challenging since the *Cftr*-KO mice are much smaller than normal mice and consequently they have smaller tracheas than WT mice. *Cftr*-KO mice are also more sensitive to manipulations than WT mice. Therefore, lesser amount of manipulations of the animals might potentially lead to a smaller mortality rate, and consequently a greater number of *Cftr*-KO mice available for analysis. We then decided to adapt this method so it could be used in our CF mouse model of lung infection with *P. aeruginosa*.

As described in this paper, the anaesthetized mouse was installed comfortably in an upright position with its back leaning against a solid metal holder. The mouse was maintained in that position by a modified paper clip attached with a rope to the back holder. The paper clip also insured that the mouth was kept open during the procedure with a clear view of the vocal cords. The use of the microscope allowed for faster intervention since it gave precision to the operator. The overall time of the procedure was less than 2 minutes per animal, from the moment of installation of the mouse on the holder to the post-infection recovery station. The mouse's breathing rhythm was uninterrupted. Interestingly, this technique allowed the use of a higher dose of bacteria before significant mortality was observed compared to the surgical instillation method previously used in our mouse colony. At 1 to $2x10^5$ dose of *P. aeruginosa* (using the direct pulmonary technique), all animals survived and had cleared the bacteria by the 3rd to the 5th day post-infection. At that dose of $1x10^6$ *P. aeruginosa* per mouse, we were able to establish a long lasting infection in the lungs mimicking the

inflammatory response in CF lung disease. Doses higher than $1x10^6$ *P. aeruginosa* per mouse lead to either excessive weight loss, respiratory distress or drastic mortality rates.

Once the *P. aeruginosa* infection dose was established, we were able to evaluate the differences in lung pathology between *Cftr*-KO mice and their WT controls. The primary goal was to establish a long lasting lung infection that would reproduce, at least in some aspects, CF lung disease. While the infection method does not involve any surgical procedure, it still induces between 3 and 14 % weight loss during the first 3 days post-infection. WT animals lost significantly less weight during infection compared to *Cftr*-KO mice (Figure 4.5). When using direct pulmonary technique of infection, we also found significantly higher bacterial burden in *Cftr*-KO mice compared to WT mice. Although the amount of alveolar cells recruited to the lungs was not different between WT and *Cftr*-KO mice, we observed a clear imbalance in the types of inflammatory cells recruited, with relatively more PMN and a trend towards less macrophage counts in the lungs of the *Cftr*-KO mice compared to their WT controls. Using direct pulmonary method of lung infection, we were able to establish a similar immune response to *P. aeruginosa* as we observed in CF patients infected with *P. aeruginosa*. The CF patients also display imbalanced influx of PMNs compared to macrophages in the lung, compared to non-CF patients.

Our mouse model of CF is one of few models known to develop lung disease even prior to their infection with bacteria. Therefore, it was very interesting to evaluate the differences in the cytokine profile between the *Cftr*-KO and their WT controls during infection using the direct pulmonary technique. Cytokines, including N51/KC, a murine homologue of IL-8 (18;69;179;285), IL-9, a mediator of airway hyper-responsiveness and mucus overproduction (118;119), as well as GM-CSF (232), known to be differently expressed in the lungs of CF patients, were also found to be expressed at a higher level in our *Cftr*-KO mice. We have only analyzed the levels of cytokines secreted at one time point (day 3

post-infection) due to the limited amount of *Cftr*-KO mice available. It is possible and very likely, based on our previous published observations (99), that 3 days post-infection timepoint might not be also appropriate for monitoring the levels of IL-1β and IL-10, which were either not detectable or not significantly different between WT and *Cftr*-KO mice at the timepoint tested (Table 4.2). Interestingly, we found a few cytokines less studied in the context of CF, to be significantly different between *Cftr*-KO and WT infected mice. One of them was IL-7, a cytokine known to play an essential function in T cell development. Another was IL-15, shown to stimulate the growth of natural killer cells, activated peripheral blood T lymphocytes (96;97;101), tumor infiltrating lymphocytes (TILs) (163), and B cells (4), was also differently expressed in the lungs of infected *Cftr*-KO as compared to controls.

Overall, we describe in this paper a method allowing us to establish long lasting lung infection, creating a different inflammatory response in WT and *Cftr*-KO mice infected with *P. aeruginosa*. The *Cftr*-KO mice were more susceptible to *P. aeruginosa* lung infection compared to their WT controls, as shown by their increased weight loss, higher bacterial burden and more elevated PMN alveolar cell recruitment into the lungs. These differences are consistent with the pathological profiles observed in the CF patient infected with *P. aeruginosa*. This method simplifies the infection procedure in terms of its duration, invasiveness, and improvement in the survival rate of the CF animals when compared to the previously used intratracheal procedure. We hope that the use of this method will stimulate even more research using mice as a model of lung infection, to better understand the molecular basis of CF lung disease and eventually help to develop successful therapies applicable to CF patients infected with *P. aeruginosa*.

CHAPTER V

Preface

The direct method of lung infection described in the previous chapter simplifies the infection procedure in terms of its duration and invasiveness, improving the survival rate of the *Cftr*-KO mice when compared to the previously used intratracheal procedure. We therefore pursued our studies using this perfected infection method.

Cystic fibrosis disease is not only characterized by excessive lung inflammation but also by lipid imbalance in the CF-affected organs. Interestingly, docosahexanoic acid (DHA), an essential fatty acid, has been shown to have anti-inflammatory properties and to reverse intestinal and pancreatic pathologies in a CF mouse model. We were therefore interested in observing of the impact of the administration of DHA on the histopathological status seen in our spontaneous lung disease *Cftr*-KO mice. We also were wondering if DHA would have an impact on the course of infection in *Cftr*-KO mice compared to their untreated *Cftr*-KO counterparts. The first part of this chapter presents the nutritional studies associated with the treatment of DHA in CF mice with CF disease.

It has also been demonstrated that other lipids and lipid mediators, such as sphingolipids and ceramides, are crucially important for internalization and efficient clearance of *P. aeruginosa*. Fenretinide, a drug already approved for clinical-trial cancer patients, induces an increase in the cellular level of ceramide. We therefore whypothesized that the administration of fenretinide would diminish the bacterial burden in the lungs of *P. aeruginosa* infected *Cftr*-KO mice compared to their untreated *Cftr*-KO mice controls. The second part of this chapter presents the studies showing the effects of fenretinide treatment during the course of lung infection with *P. aeruginosa* in *Cftr*-KO mice.

CHAPTER V.

PROTECTIVE EFFECT TREATMENTS WITH DHA AND FENRETINIDE IN CFTR KNOCKOUT MICE WITH CF LUNG DISEASE

based on published paper

Guilbault, C., *Nelson, A., Martin, P., Stotland, P., Guiot, M.C., DeSanctis, J.B., and D. Radzioch. Immunology 2004, July 2004; 79-88.*

and

work in progress

Protective effect of fenretinide on lipid metabolism and susceptibility to P. aeruginosa in mice with cystic fibrosis lung disease

5.1 Protective effect of DHA treatment in non-infected *Cftr*-knockout mice with CF lung disease

5.1.1 Abstract

CF disease is characterized by excessive lung inflammation, recurrent bacterial infections and lipid imbalance in the CF-affected organs. The study of mice models has established that the excessive inflammation is due to higher levels of pro-inflammatory mediators and to lower levels of anti-inflammatory mediators. Interestingly, DHA, an essential fatty acid, has been shown to have anti-

inflammatory properties and to reverse intestinal and pancreatic pathologies in a CF mouse model. The treatment with DHA has not been systematically evaluated in CF mice with CF lung disease. We hypothesized that the treatment with this fatty acid might decrease the lung inflammation observed in our *Cftr*-KO mouse model which develops spontaneous lung disease. Our results demonstrated that the survival of CF mice was dramatically improved when mice were fed with a high caloric liquid diet. We observed no significant change in the weight gains of *Cftr*-KO mice between the different diets. Supplementation of a liquid diet with DHA significantly improved the amount of phospholipid-bound DHA in the ileum, pancreas and plasma in our CF mouse model. Lastly, our results also showed that DHA supplementation reduced spontaneous lung inflammation in our *Cftr*-KO mice.

5.1.2 Introduction

Cystic fibrosis is the most common recessive autosomal disorder, affecting 1 in 2 500 Caucasian newborns (55). The pathology of CF is explained by a defect in the CFTR channel that functions as a chloride channel regulated by cyclic AMP (267). Dysfunction of the CFTR protein results in salty sweat, pancreatic insufficiency, intestinal obstruction, male infertility and severe pulmonary disease. CF is associated with chronic pulmonary infections of bacteria such as *P. aeruginosa, Staphyloccocus aureus* and *Burholderia cepacia*, ultimately leading to pulmonary failure and death. Since the discovery of the CFTR gene, a number of investigators have generated *Cftr* gene knockout mice by targeted gene disruption (193). Although the generated mice have most of the symptoms of CF, only very few of them display the CF lung phenotype. The C57BL/6$^{H/M}$-*Cftr*.ko described by Kent and colleagues (147) represents an unique model of spontaneously occurring CF lung disease which we are using in the present study.

CF patients are known to be hypermetabolic, showing much higher energy expenditure and higher levels of substrate oxidation (23). Therefore, CF patients

need a high caloric diet to fulfill the daily energy requirements. Moreover, a deficiency in essential fatty acid metabolism has been well documented in CF patients (79;95;127;224;225). Freedman and colleagues have shown that oral administration of DHA to *Cftr*-KO mice (which did not develop spontaneous lung disease) corrected the lipid imbalance and normalized the histology in the ileum and pancreas (84). Interestingly, neutrophil infiltration into the lungs of the *Cftr*-KO mouse model they used in response to endotoxins was also reduced by DHA. Membrane-bound DHA competitively inhibits the oxygenation of AA (arachidonic acid) by cyclooxygenase (152) and causes a decrease in the amount of AA available for eicosanoids. This leads to further effects, since eicosanoids modulate TNF and nitric oxide (NO) production (290).

The goal of this study was to evaluate the impact of a high caloric diet and DHA supplementation on the general health and on the CF-affected organs in our mouse model of CF. We compared the weight gain of the mice which were fed with different types of diet, and evaluated if oral supplementation of fatty acids could improve deficiencies observed previously in other CF mouse models. Moreover, we assessed the effect of DHA on the inflammatory state of the lungs of the *Cftr*-KO mice.

5.1.3. Material and Methods

5.1.3.1 Mice. Inbred mice used in our study were bred in our animal facility (from C57BL/6J heterozygous breeding pairs). Age- and gender- matched C57BL/6-*Cftr*$^{+/+}$ (WT) mice, (♀; n = 45, ♂; n = 41), C57BL/6-*Cftr*$^{+/-}$ (HZ) mice (♀; n = 34, ♂; n = 50) and C57BL/6-*Cftr*$^{-/-}$ (*Cftr*-KO) mice (♀; n = 21, ♂; n = 11) were murine pathogen-, helicobacter- and parasite- free. They were housed (1 - 4 animals/cage), bred and maintained in a barrier facility unit under specific pathogen-free conditions with a 12-hrs light/dark cycle, at 22°C ± 2 and at 50% ± 5 humidity. The animals were kept in polycarbonate (Lab Products, Maywood NJ) micro-isolator cages with sterile maple hardwood bedding (PWI, St-Hyacinthe,

QC) or corn bedding (Anderson, Bestmonro, LA) and maintained in ventilated racks (Lab Products), with a cycle of 50 changes of fresh hepa filter air per hour in each cage. Mice were fed with either the NIH-31-modified irradiated mouse diet (Harlan Teklad, Indianapolis, IN) or a liquid diet starting at 14 days of age [Peptamen liquid diet (Nestle Canada, Brampton, ON] or Bioserv liquid diet (BioServ Inc., Frenchtown, NJ). The liquid diets were provided in 50-ml centrifuge tubes (Fisher Scientific Ltd, Nepean, ON); these diets were freshly prepared every morning. All mice had *ad libidum* access to sterile acidified water. Experimental procedures with the mice were conducted in accordance with the Canadian Council on Animal Care and with the approval of the Animal Care Committee of the McGill University Health Center, Montreal, Quebec, Canada.

5.1.3.2 Fatty acid diet supplementation. DHA (Sigma-Aldrich, Oakville, ON), protected from light, was incorporated into the Peptamen liquid diet with specific monitoring of quantity assimilated. The administration was scheduled every 2nd day for the first 2 weeks, then every day for the last week. Each dose contained 40 mg/mouse/day and was prepared fresh daily.

5.1.3.3 Fatty acid analysis. Minced tissues and blood plasma were immersed in 1 mM butylated hydroxyanisole (BHA) in chloroform and methanol (2:1 vol) until the analysis was performed. Lipids were extracted from tissue homogenates and blood plasma with chloroform/methanol (2:1), as previously described (83). Identification of phospholipids was done by thin-layer chromatography extraction (282). Also, fractionated lipids were dried and resuspended in heptane: methanol: sulfuric acid (5:1:1) for free fatty acid extraction. Diazomethane was used to esterify the fatty acids released (240) and the esters were identified by GC/MS (Hewlett Packard5880A, WCOT capillary column (Supelco-10, 35 m x 0.5 mm, 1 μm thick)) using commercial standards (Sigma-Aldrich).

5.1.3.4 Lung histopathology. Lungs were removed from each mouse, inflated with 10% buffered formalin acetate (Fisher, Ottawa, ON) and immersed in the buffer for a minimum of 36 hrs. The lungs were then cut and embedded in paraffin. Paraffin sections were sliced 3 μm thick using a Reichert-Jung microtome. Three cuts were made for each of the following standard staining methods: HE, PAS and MT. These slides were scored for inflammatory cell infiltration, cell hyperplasia-metaplasia, basement membrane thickening, mucus accumulation, collagen deposition and fibrosis. Each parameter of lung morphology was observed under specific stains and analyzed using scales specific to each parameter. For cell hyperplasia and cell metaplasia, a score of 1 indicated none; a score of 2 represented 0-25% of airway surface affected by these; a score of 3 represented 26-50% of airway surface affected by these; a score of 4 meant that 51-75% of all airway surface was affected by these; and finally a score of 5 indicated 75-100% of the airway surface covered by these pathologies. For inflammatory cell infiltration, basement membrane thickening and fibrosis, the scale was composed of scores 1, 2 and 3. A score of 1 represented the absence of any of these pathologies; a score of 2 indicated the presence of either a few inflammatory cells, some basement membrane thickening or some fibrosis (these last 2 seen thinly accumulated around the airways, showing the airway wall about 2x-5x thicker than in a control airway); a score of 3 showed the presence of many inflammatory cells in the blood vessels around the airways or pronounced fibrosis and basement membrane thickening around the airways (seen in thick dense layers around the airways, making the airway wall more than 5x thicker than in a normal airway). Mucus accumulation was analyzed separately for large airways (bronchi) and for smaller airways (bronchioles). No mucus accumulation was expressed by a score of 1 for small airways and a score of 4 for large airways; some mucus accumulation (covering less than 50% of airway surface) was expressed by a score of 2 for small airways and 5 for large airways; mucus accumulation covering airway surface almost completely was expressed by a score of 3 for small airways and 6 for large airways.

5.1.3.5 Statistical analyses. Data were analyzed using Sigma Stat V3.01 software (SPSS Inc, Chicago, IL). Statistically significant differences between means and medians of studied groups were evaluated using Student's t-test and nonparametric Mann-Whitney U test, respectively. One way ANOVA and Kruskal-Wallis ANOVA on ranks combined with pair wise multiple comparison procedures (Holm-Sidak method and Dunn's method respectively) were used to evaluate differences between multiple groups. Significance was set at a two-tailed p value of ≤ 0.05.

5.1.4 Results

5.1.4.1 Monitoring of weight. Since we observed that *Cftr*-KO mice in our mouse model are smaller than their WT controls, we followed their weight gain every week after providing them with different diets, hoping to find a diet which could improve their weight gain profile. Over a period of 18 weeks, statistically significant differences were seen between the mean weight of WT and *Cftr*-KO mice for females ($p \leq 0.001$; figure 5.1 panel A) and males ($p = 0.07$, figure 5.1 panel B) for Peptamen and Bioserv diets. WT animals had a much higher mean weight compared to *Cftr*-KO mice. In the meantime, when we compared the mean weight of the *Cftr*-KO mice between the two liquid diets, we did not observe any significant difference between the groups, and this was true for both genders. No statistical analysis could be performed on the solid diet groups since only one female *Cftr*-KO mouse, and none of the male *Cftr*-KO mouse survived until the 20^{th} week on the solid diet. Overall, the *Cftr*-KO mice did not gain more weight on any of the tested diets. However, we observed a much better survival rate on the liquid diets than on the solid one (Table 5.1). The Peptamen diet allowed for much better survival of *Cftr*-KO mice (80%) than the Bioserv diet (46%). Since food was changed daily, some normal intestinal bacteria were found in the diet before its replacement the following morning; however a much smaller amount of bacteria were found in the Peptamen compared to the Bioserv diets (data not shown).

Figure 5.1 Mean weight gain of WT (*solid*) and *Cftr*-KO (*open*) female (A) and male (B) mice fed with liquid (Bioserv (*circle*), Peptamen (*triangle*)) or standard solid diet (*square*). Weight was taken every 7 days starting from 2 weeks of age and for a total period of 20 weeks. The overall mean weight gain of *Cftr*-KO mice was shown to be significantly (*) lower than those seen in WT mice on Peptamen and on Bioserv diets for both females ($p \leq 0.001$) and males ($p = 0.007$). No statistical analysis was performed for the solid diet-fed mice because of the small number of *Cftr*-KO animals which survived. Peptamen (♀; WT n = 34, *Cftr*-KO n = 6 / ♂; WT n = 47, *Cftr*-KO n = 6), Bioserv (♀; WT n = 20, *Cftr*-KO n = 11/ ♂; WT n = 17, *Cftr*-KO n = 5), Solid (♀; WT n = 19, *Cftr*-KO n = 1 / ♂; WT n = 14, *Cftr*-KO n = 0).

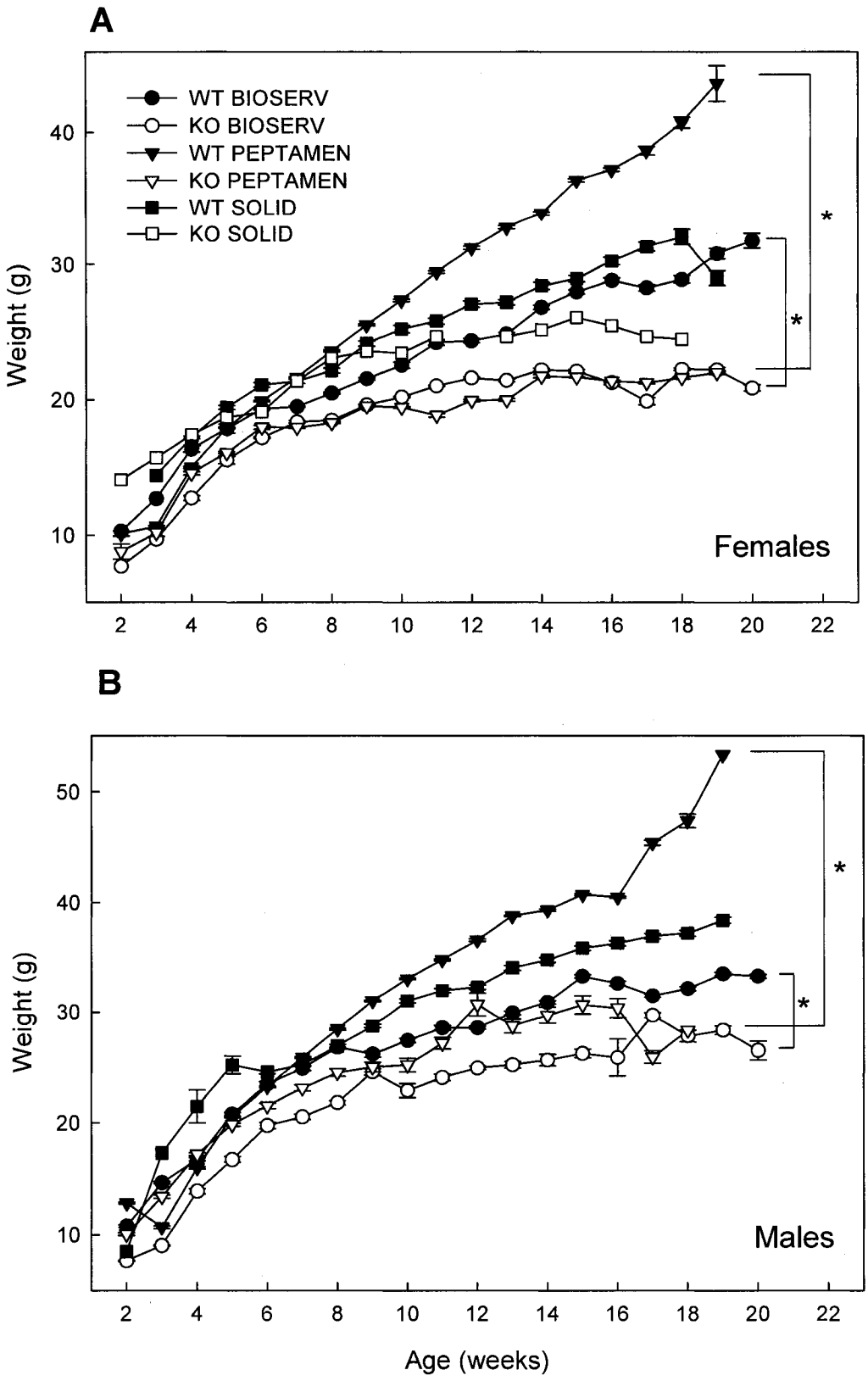
A
WT BIOSERV
KO BIOSERV
WT PEPTAMEN
KO PEPTAMEN
WT SOLID
KO SOLID
Weight (g)
Females
B
Males
Age (weeks)

Table 5.1 Survival of *Cftr*-KO mice and their WT controls fed with different diets

Diet	Survival Rate	
	Cftr-KO	WT
Regular (Solid)	2 %	100 %
Bioserv *	46 %	100 %
Peptamen *	80 %	100 %

* Liquid diets

5.1.4.2 Free and phospholipid-bound DHA profiles in organs. DHA incorporated in phospholipids in uninfected WT and *Cftr*-KO mice was analyzed. Analysis of fatty acid composition was performed on lungs, plasma, pancreas, ileum, and liver samples from WT and *Cftr*-KO mice supplemented with DHA and those that were not (figure 5.2). We observed significantly higher levels of DHA in WT compared to *Cftr*-KO mice in the lungs, plasma, pancreas, and ileum, where there was almost no DHA at all ($p \leq 0.001$). Supplementation of DHA to *Cftr*-KO mice significantly increased the DHA levels found in the plasma and ileum of these mice compared to *Cftr*-KO untreated animals, but did not reach the level of the WT, as a difference still exists between the WT and *Cftr*-KO DHA-treated mice (panels A, B, and C). Levels of DHA in the liver were not different between the four groups analyzed (panel D).

5.1.4.3 Lung histology analysis. Qualitative analysis of the lungs from uninfected *Cftr*-KO mice and WT controls, whose diets were supplemented or not with DHA, was performed. *Cftr*-KO mice showed the following signs of lung pathology; cell hyperplasia in the epithelium, thickening of the basal membrane and areas of interstitial thickening (Figure 5.3 panel C). However, *Cftr*-KO mice supplemented with DHA (panel D) still showed thick basal membranes, but showed less hyperplasia and inflammatory cell infiltrations than the untreated *Cftr*-KO mice, comparable to what is seen in WT mice (panels A & B).

Figure 5.2 DHA incorporated in phospholipids in uninfected WT and *Cftr*-KO mice. Analysis of fatty acid composition was performed on the plasma (panel A), pancreas (panel B), ileum (panel C), and liver (panel D) of WT (*fill boxes*) and *Cftr*-KO (*open box*) mice supplemented (*crossed lines*) or not (*no line*) with DHA. For the ileum and plasma, statistically (*) higher DHA was found in the WT mice compared to the *Cftr*-KO mice in both DHA-treated and non-treated groups ($p \leq 0.001$). Also, *Cftr*-KO mice treated with DHA had higher levels of DHA bound in phospholipids compared to levels in untreated *Cftr*-KO animals (panels A and C). Statistical difference is also observed between the WT mice and the *Cftr*-KO DHA-treated mice in plasma, pancreas and ileum. No difference was observed in the liver between the four groups analyzed.

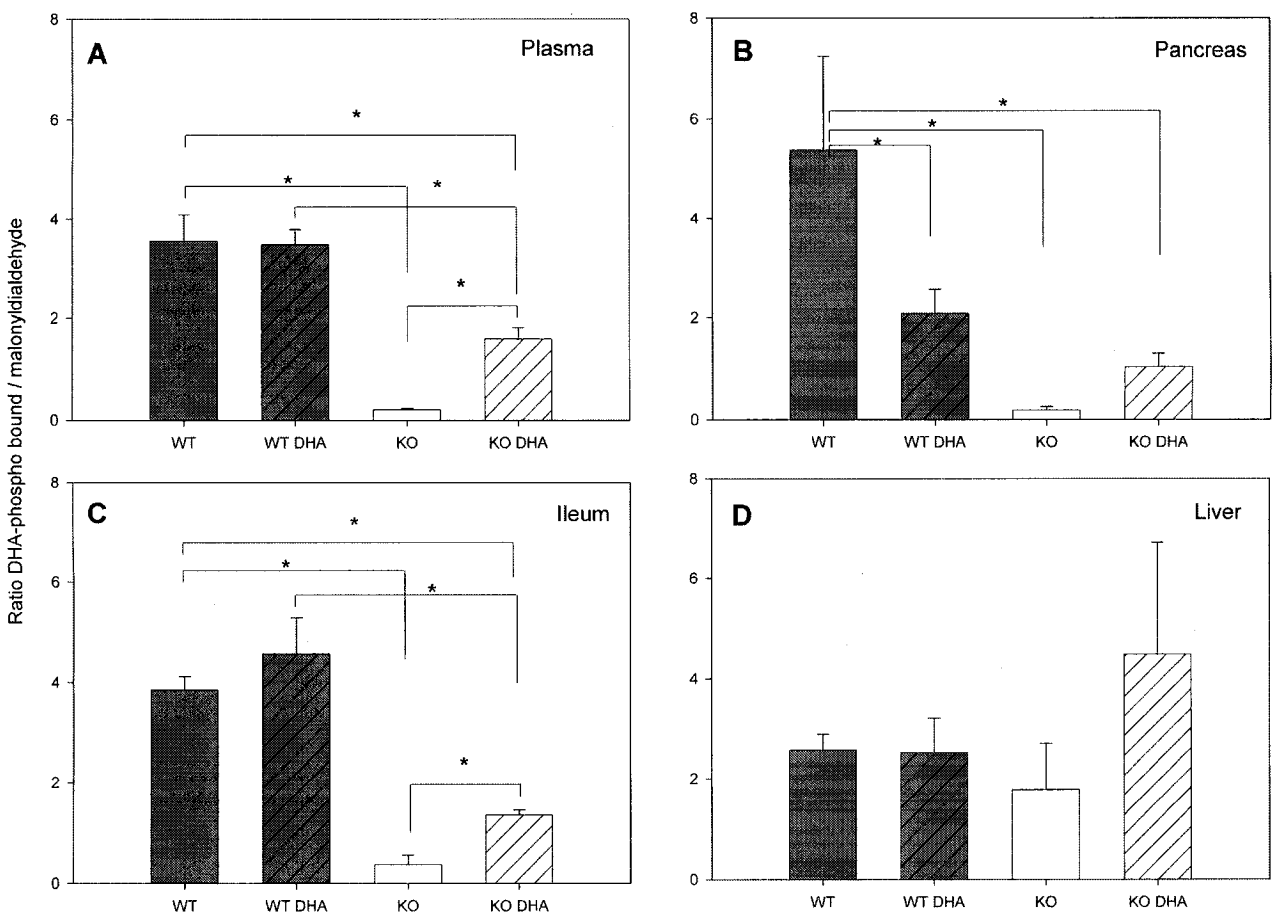
A
Plasma
B
Pancreas
C
Ileum
D
Liver
Ratio DHA-phospho bound / malonyldialdehyde
0
2
4
6
8
WT
WT DHA
KO
KO DHA
*

Figure 5.3 Histological examination of the lungs of *Cftr*-KO mice and their WT controls. Representative hematoxylin- & eosin- (panels A, C, D) and Masson's trichrome- (panel B) stained lung sections prepared from uninfected WT (A, B) and *Cftr*-KO (C, D) mice (×200). Panels A and B, from sections of uninfected WT mice, show a normal lung structure. Panel C from untreated mice shows evidence of cell infiltration in the bronchi and alveoli and epithelial cell hyperplasia. Panels D from sections of uninfected *Cftr*-KO mice treated with DHA show decrease cell infiltration and less hyperplasia compared to untreated *Cftr*-KO mice.

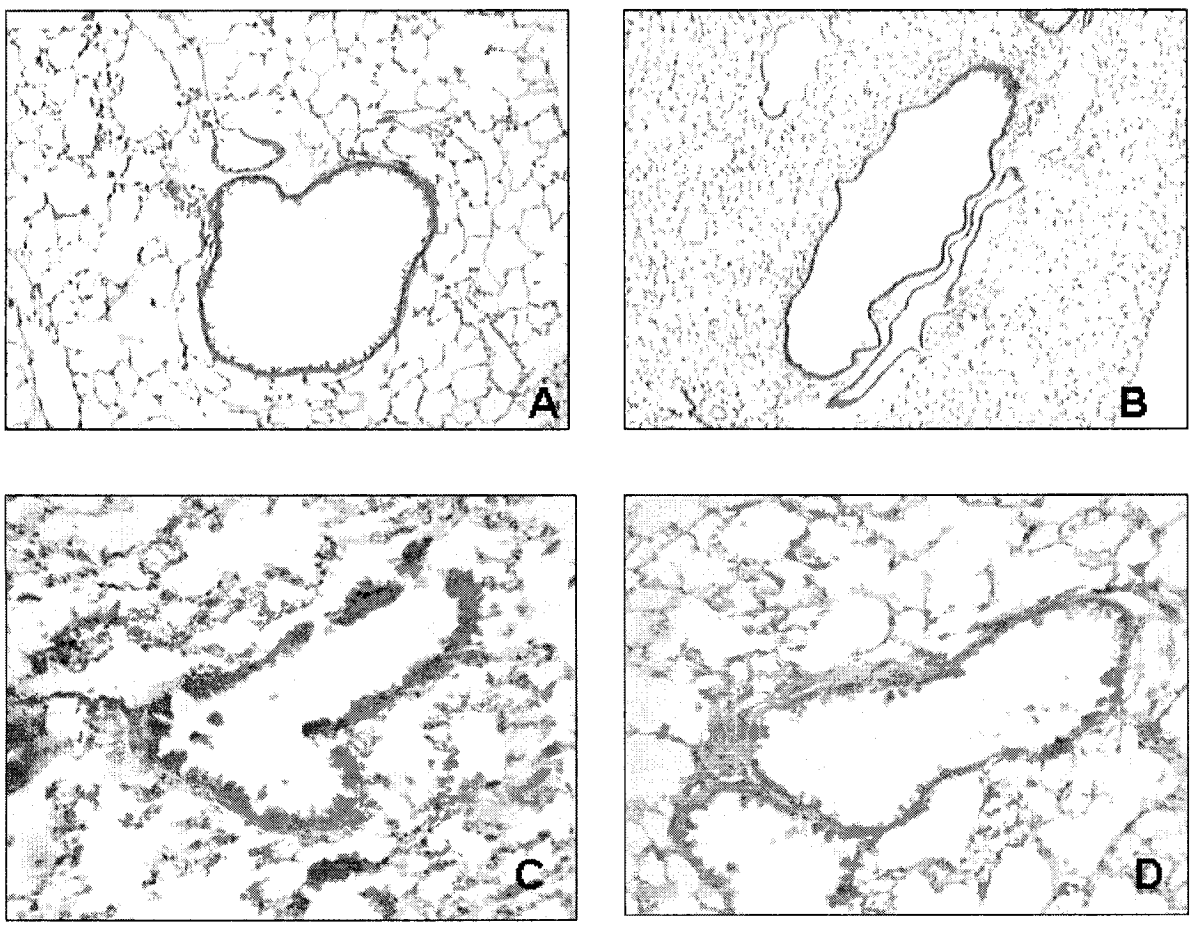
A
B
C
D

5.1.5 Discussion

It has been well-established that the mean resting energy expenditure in patients with cystic fibrosis is greater than in controls (23). Since the intestinal transport of nutrients seems to be disturbed as a result of both a defective Cl-secretion and impairment in absorption, nutritional intake by CF patients has to be carefully monitored. Moreover, CF patients were shown to suffer from fatty acid deficiencies (14-18), and the average weight of CF patients is significantly lower than age-matched controls. Since we observed a similar tendency in our *Cftr*-KO mouse model (significantly higher mean weight for WT compared to HZ and *Cftr*-KO mice, and significantly higher mean weight for HZ compared to *Cftr*-KO mice, $p \leq 0.001$, Figure 5.1 and data not shown), we decided to investigate if different mouse diets could influence their growth and weight gain. We observed, over a period of 18 weeks, the weight gain between male and female, *Cftr*-KO, HZ, and WT mice, on three different diets; the solid chow diet and two different liquid diets: Bioserv and Peptamen. The two later ones have the advantage of increasing survival of the *Cftr*-KO mice (Table 5.1), most certainly by preventing intestinal obstruction, which is frequently seen in CF due to an increase in mucus secretion. However, none of these liquid diets showed an increase in mean weight gain in the *Cftr*-KO.

Several animal models of CF generated by targeted gene disruption show most of the CF symptoms; however, only a few of these display the CF lung phenotype. *Cftr*-KO mice developed in collaboration with Drs. Tsui and Kent show spontaneous lung disease. These mice, which were not exposed to any lung pathogens, showed an infiltration of inflammatory cells and mucus accumulation leading to progressive lung impairment, and therefore represent a unique model of spontaneously occurring lung disease. Using this animal model, we supplemented the diet of the *Cftr*-KO mice and their controls with esterified-DHA for three weeks and then analyzed the fatty acid composition of CF-affected organs, the lung morphologies and the expression of inflammatory markers. As expected, we found

no DHA incorporated in cell membrane phospholipids in the lungs of *Cftr*-KO mice (Figure 5.2), whereas levels detected in control mice ranged from 5 to 10%. Supplementation of the diet with DHA was able to significantly increase the amount of membrane-bound DHA in all tested organs in *Cftr*-KO mice, including the lungs.

We have also evaluated the effect of treatment with esterified DHA on the CF lung pathology. Preliminary data of DHA-treated *Cftr*-KO mice compared to untreated *Cftr*-KO and WT mice were very promising, showing much less hyperplasia in the lung although a thick basal membrane could still be observed. We are now thoroughly investigating lung pathology improvements in more detail and performing gene expression analysis of the lungs of *Cftr*-KO treated with DHA compared to untreated *Cftr*-KO, to establish the extent of improvements at the biochemical level of inflammation parameters.

Taken together, these results corroborate the importance of a high caloric diet in CF patients and suggest that DHA could be used as a potential therapy to improve lung disease in CF patients.

5.2 Protective effect of fenretinide on lipid metabolism and susceptibility to *P. aeruginosa* in mice with cystic fibrosis lung disease

5.2.1 Abstract

It has recently been demonstrated that ceramide is crucially important for *P. aeruginosa* internalization and its use as a treatment leads to very efficient clearance of *P. aeruginosa* from infected lungs. We therefore assessed the effect of fenretinide, a drug inducing ceramide, using our *Cftr*-KO mouse model of *P. aeruginosa* lung infection. The results presented in this study clearly show that the *Cftr*-KO mice have impaired basal ceramide levels in both uninfected and *P. aeruginosa*-infected animals. We also observed that fenretinide efficiently induced ceramide levels in the lungs and plasma of our CF mouse model. Most importantly, the ceramide levels induced by the fenretinide treatment incredibly improved the bacterial clearance in the lungs of the *Cftr*-KO mice. Moreover, the DHA/AA index ratio was significantly increased in the *Cftr*-KO mice treated with fenretinide compared to their untreated controls and this is due mostly to the decrease of phospholipid-incorporated AA levels. These results may prove to be highly important for CF disease.

5.2.2 Introduction

CF is characterized by excessive lung inflammation followed by recurrent bacterial infections. CF patients suffer from a lipid imbalance in the CF-affected organs (233). Ceramide is a sphingolipid that serves as a secondary messenger. It is generated by the conversion of sphingomyelin by sphingomyelinase enzyme and is produced during cellular responses to extracellular signaling, such as TNF, LPS, IFNγ, and interleukins (30). Some studies suggest that an increase in cellular ceramide levels, induced by a vitamin A analogue, mediates signaling in the cells, ultimately leading to apoptosis (199;77;291). Nieuwenhuis and colleagues (194)

clearly demonstrated that galactosyl ceramide treatment leads to very efficient clearance of *P. aeruginosa* from infected lungs. These findings were based on a previous research by Oda and Wu (200) and were further corroborated by very interesting studies published by Grassme and colleagues (102). These studies demonstrated that ceramide is crucially important for *P. aeruginosa* internalization and that failure to generate ceramide-enriched membrane platforms in infected cells results in an unabated inflammatory response, massive release of interleukins and septic shock (102). However, an excessive ceramide production has also been shown to lead to pulmonary cell apoptosis and emphysema-like disease in mice (205). From these studies, the regulation of ceramide levels seems to be crucial in the maintenance of a proper homeostasis of cells and inflammatory response.

Interestingly, sphingomyelinase (sMase), the enzyme responsible for the conversion of sphingomyelin to ceramide, was shown to be inhibited by glutathione (GSH) (160). Therefore, it is possible, that higher levels of GSH observed in cystic fibrosis cells (164) might negatively affect the generation of intracellular ceramide.

Recently, several studies highlighted the connection between the sphingolipids and the CFTR protein. Ito and colleagues showed that ceramide reduced the airway anion secretion via CFTR in the sphingomyelin pathway through sphingomyelinase (135). This study suggests that the ceramide originating from basolateral sphingomyelin acts on activated CFTR from the cytosolic side, hindering anion secretion. Another study by Boujaoude and colleagues demonstrated that murine epithelial cells (C127/CFTR), expressing wild type CFTR, exhibited higher uptake of sphingosine 1-phosphate (SPP) than the cells expressing a mutant CFTR protein (C127/CFTRΔF508) (22). SPP has emerged as an important lipid messenger for the endothelial differentiation gene receptor family of proteins through which it mediates its biologic effects. These studies supported the hypothesized importance of sphingolipids in cystic fibrosis.

Retinoids are vitamin A analogues that are involved in the regulation of cellular growth, differentiation and death in a broad variety of normal and malignant cell types (165). Fenretinide [*N*-(4-hydroxyphenyl) retinamide, 4-HPR], a semi-synthetic retinoid, has been extensively studied because of its chemo-protective and anti-tumor activities described when used on a variety of malignant cells, including non-small lung cancer, neuroblastoma, Kaposi's sarcoma, breast cancer and glioma (31;80;92;166;211;215;219;287). Treatment with fenretinide leads to generation of reactive oxygen species, the activation of different pathways mediated by retinoid receptors and non-receptors and most interestingly the generation of ceramide, a lipid secondary messenger (268;269;177). Fenretinide has already been approved for clinical trials of cancer patients and is currently being evaluated in clinical chemoprevention trials in lung, breast, and bladder cancer (40). Although the mechanism of action of fenretinide remains unclear, we hypothesized that this drug may have anti-inflammatory effects mediated through ceramide production that could be beneficial to *Cftr* deficient mice infected in the lungs with *P. aeruginosa.*

Therefore, the goal of this study was to evaluate the impact of ceramide levels, induced by supplementation of the Peptamen liquid diet with fenretinide prior to infection, on the course of lung infection with *P. aeruginosa* and lipid metabolism in the *Cftr* gene deficient mouse model.

5.2.3 Materials and Methods

5.2.3.1 Mice. Inbred C57BL/6-*Cftr* mice breeding pairs, heterozygous (HZ) at the *Cftr* locus, were used in our study, maintained and bred at the Animal facility of the Research Institute of the McGill University Health Centre. All babies were genotyped between days 12 and 14 of their life. The animals were kept in cages with sterile corn bedding (Anderson, Bestmonro, LA) and maintained in ventilated racks (Lab Products). Mice were fed with either the NIH-31-modified irradiated mouse diet (Harlan Teklad, Indianapolis, IN) or a

liquid diet starting at 14 days of age (Peptamen liquid diet (Nestle Canada, Brampton, ON)). The liquid diet was provided in 50-ml centrifuge tubes (Fisher Scientific Ltd, Nepean, ON); these diets were freshly prepared every morning. Age- and gender- matched C57BL/6-*Cftr*$^{+/+}$ (WT) mice, (♀; n = 10, ♂; n = 31) and C57BL/6-*Cftr*$^{-/-}$ (*Cftr*-KO) mice (♀; n = 8, ♂; n = 18) were murine pathogen-, helicobacter- and parasite- free. They were housed (1 - 4 animals/cage), bred and maintained in a barrier facility unit under specific pathogen-free conditions. Experimental procedures with the mice were conducted in accordance with the Canadian Council on Animal Care and with the approval of the Animal Care Committee of the McGill University Health Center, Montreal, Quebec, Canada.

5.2.3.2 Fenretinide diet supplementation. Fenretinide (Sigma-Aldrich, Oakville, ON) powder was resuspended into 95% ethanol and was subsequently incorporated in the Peptamen liquid diet; it was protected from light and kept at 4° Celcius before being given to the mice (5 mg/kg per day per mouse). Mock-treated diets were prepared similarly by adding ethanol to the Peptamen diet but omitting the fenretinide supplementation. The diet was given every morning for 28 consecutive days with specific monitoring of the quantity consumed by the mice in each cage.

5.2.3.3 *P. aeruginosa* inoculum preparation. In order to establish a model of prolonged lung infection, bacteria-impregnated agar beads were freshly prepared the day before each experiment, as previously described (110), and stored at 4°C overnight. Briefly, the bacteria (PA strain 508) from an overnight culture were grown for approximately 3 hours in a shaking incubator at 37°C, until it reached a mid-log phase. The log phase bacteria were concentrated and resuspended in 5 ml of Dulbecco's phosphate-buffered saline (PBS; Invitrogen, Mississauga, ON). A 5 ml aliquot of the concentrated bacterial broth was added to 52°C 1.5% trypticase soy agar (Difco, Detroit, MI) (agarose beads free of bacteria were prepared using PBS instead of a bacterial suspension). This mixture was quickly added to 52°C heavy mineral oil and stirred rapidly, first at room

temperature for 6 minutes, followed by ice cooling with continuous stirring for 10 minutes. The oil-agar mixture was centrifuged to sediment the beads. The beads were washed with PBS and their size was verified microscopically and only those preparations containing beads predominantly 100-250 micrometers in diameter were used as inoculum. Inoculum was prepared by diluting the beads suspension to 1 x 10^6 CFUs per 50 microliters (injection volume).

5.2.3.4 Description of the method of mouse lung infection with PA instilled in agarose beads. Mice were anaesthetized with a combination of ketamine (7.5 mg/ml) and xylazine (0.5 mg/ml) administered intraperitoneally at a dose of 20 ml/kg of body weight. Once the mouse was successfully anaesthetized, the animal was installed under binoculars (Microscope M650, Wild Leitz, Willowdale, ON) in the vertical position and was held on a restraining board by holding the animal by its upper incisor teeth, as previously described (110). The tongue was then gently pulled to the side of the mouth and a 26-G gavage needle was inserted into the mouth and guided through the pharynx gently touching the vocal cords to see the lumen of the trachea; the needle was then introduced into the trachea to reach the lung for the bilateral injection of the 50 microliter inoculum. After inoculation the animal regained righting reflex within an hour. A final dose of 1 x 10^6 *P. aeruginosa* was used for infection using WT and *Cftr*-KO mice. Mice were monitored 3 times daily; the maximum weight loss allowed was 15%. Mice were sacrificed by CO_2 overdose.

5.2.3.5 Bronchoalveolar lavage. Circulation was flushed by slow intracardiac infusion of divalent cation-free Hank's balanced salt solution (HBSS; Invitrogen, Mississauga, ON). The trachea was cannulated with a 22-gauge intravenous catheter placement unit (Critikon, GE Medical Systems, Tampa, FL) connected to two 5 ml syringes via a 3-way stopcock with a rotating collar (Namic U.S.A., Glens Falls, NY). The alveoli of infected mice were washed 3 times with 1.4 ml of divalent cation-free HBSS. The volume of BALF recovered was approximately 1.2 ml. Alveolar cells were centrifuged and the supernatant was

used for CFU count determination before being stored at -20°C, until assayed for cytokine concentrations. Cells were resuspended in 0.5 ml of Dulbecco's Modified Eagle Medium (DMEM; Invitrogen) supplemented with 10% fetal bovine serum (FBS; Hyclone, Logan, UT), diluted in Turk's solution and counted using a hematocytometer. The proportions of macrophages, lymphocytes and PMN were calculated after counting approximately 300 alveolar cells on cytospin preparations stained with Diff-Quick (American Scientific Products, McGaw Park, IL).

5.2.3.6 Lung homogenates. Lungs from infected mice were harvested and homogenized for 60 sec at high speed (homogenizer PT10135 Brinkmann Instruments Co., Mississauga, ON) in 4 ml of sterile PBS (Invitrogen). Serial 10-fold dilutions of lung homogenates were plated on petri dishes containing TSA. The number of CFU per lung was counted after overnight incubation at 37°C. For cytokine measurements, lung homogenates were centrifuged at 1500 x g at 4°C for 10 min; the supernatants were then removed, aliquoted in new tubes and stored at -20°C until assayed for cytokine concentrations.

5.2.3.7 Fatty acid analysis. FA analysis was performed as described in the section 5.1.3.3. Briefly, minced tissues were immersed in 1 mM BHA in chloroform and methanol (2:1 vol). Lipids were then extracted from tissue as previously described (83). Identification of phospholipids was done by thin-layer chromatography extraction (282). Also, fractionated lipids were dried and resuspended in heptane: methanol: sulfuric acid (5:1:1) for free fatty acid extraction. Diazomethane was used to esterify the fatty acids released (240) and the esters were identified by GC/MS.

5.2.3.8 Ceramide/Sphingolipids analysis. The concentrations of ceramide in the lung tissue from infected animals were determined by an ELISA. Nunc plate specific for lipid analysis was coated with various dilutions of murine samples. Plates were then washed, incubated with blocking buffer (PBS, 0.1% Tween 20, and 1% bovine serum albumin (BSA; Sigma, Oakville, ON)), and

sequentially incubated with murine anti-ceramide antibody (Ab), peroxidase-conjugated anti-mouse IgG Ab, and peroxidase substrate (ABTS; Roche, Laval, QC). The intensity of the colorimetric reaction was determined by spectrophotometry at 405 nm. The levels of ceramide were calculated with reference to a standard curve.

5.2.3.9 Statistical analyses. Data were analyzed using Sigma Stat V3.1 software (SPSS Inc, Chicago, IL). Statistically significant differences between means and medians of studied groups were evaluated using Student's t-test and nonparametric Mann-Whitney U test, respectively. One way ANOVA and Kruskal-Wallis ANOVA on ranks, combined with the appropriate pair wise multiple comparison procedures were used to evaluate the differences between multiple groups. Significance was set at a two-tailed p value of ≤ 0.05.

5.2.4 Results

5.2.4.1 Ceramide-sphingolipids levels observed in the lungs. Fenretinide is known to induce cellular ceramide, as explained previously. We therefore assessed the ceramide levels in different organs of the mice that were either not treated, mock-treated (EtOH) or treated with fenretinide to assess the basal levels in our CF mouse model. Interestingly, in the lungs and in the plasma of untreated mice, we observed a trend towards lower (3 to 5 folds) median levels of ceramides/sphingolipids in the *Cftr*-KO mice when comparing them to their WT controls (Figure 5.4, CTRL panel, white symbols). However, this difference did not reach statistical significance because of small number of animal tested ($p = 0.234$). Nevertheless, when we infected the mice with *P. aeruginosa* in the lungs (Figure 5.4, CTRL panels, black symbols), we observed significantly (*) lower levels of ceramides/sphingolipids in the lungs of *Cftr*-KO mice compared to WT infected controls in both the lungs (panel A, $p \leq 0.001$) and plasma (panel B, $p \leq 0.001$). Moreover, when we treated the mice with fenretinide, we observed an

increase (†) in the levels of ceramide in the lungs (panel A, $p \leq 0.001$) and plasma (panel B, $p \leq 0.001$) of infected *Cftr*-KO mice compared to the control group of mice (Figure 5.4). We observed a more than 4-fold increase in ceramide levels in the fenretinide-treated *Cftr*-KO mice compared to their mock-treated *Cftr*-KO controls. As for the WT mice, the fenretinide-treated mice had increased median ceramide levels in their lungs and plasma (#, $p \leq 0.001$) compared to their untreated WT control mice. However, this difference reached statistical significance only in the plasma because the lungs showed a very high intragroup variability. Overall, these results suggest that *Cftr*-KO mice have lower basal levels of ceramide in the lungs compared to their WT controls prior and during *P. aeruginosa* infection. Most interestingly, the treatment with fenretinide was able to increase considerably the levels of ceramide in the lungs and plasma tissues in the *Cftr*-KO mice.

5.2.4.2 Weight monitoring during *P. aeruginosa* lung infection.

Consistent with our previously published findings regarding the weight difference between the *Cftr*-KO and WT mice (section 5.1.4.1), we also observed in this study a statistically significant weight difference between the WT (n = 17) and the *Cftr*-KO (n = 14) in their mean weight loss percentage at day 2 and day 3 post-infection, as shown in Table 5.2. We have also carefully monitored if the supplementation of the diet with fenretinide might affect the mean weight loss and found no significant difference the percentage between the fenretinide-treated and the mock-treated control groups at any of the days post-infection (day 1 to day 3 post-infection).

Table 5.2 Mean weight loss of WT and *Cftr*-KO mice during chronic lung infection with *P. aeruginosa*

Days post-infection	Mean weight loss (% of initial weight) WT	± SEM	*Cftr*-KO	± SEM	P value
1	-4.5	0.4	-4.7	0.9	0.799
2	-10.1	0.6	-13.5	1.5	0.030 *
3	-11.2	0.9	-16.2	1.9	0.016 *

SEM; standard error of the mean

* Statistically significant differences between the WT and the *Cftr*-KO mice ($P \leq 0.05$)

Figure 5.4 Ceramide levels observed in the lungs and plasma. Ceramide levels in the lungs (A) and in the plasma (B) were assessed in WT (*triangles*) and *Cftr*-KO (*circles*) mice which were not-infected (*white*) or *P. aeruginosa*-infected at 3 days post-infection (*black*) and that were either not treated or mock-treated (CTRL) or treated with fenretinide (FEN). The ceramide levels in the lungs ($p \leq 0.001$) and in the plasma ($p \leq 0.001$) samples were statistically different between the groups of mice tested. We observed a clear trend towards lower median levels of ceramide in the uninfected *Cftr*-KO mice compared to their uninfected WT controls in both tissues. However, this difference did not reach statistical significance because of the small number of animals tested. Nonetheless, when the mice are infected with *P. aeruginosa*, we observed significantly (*) lower levels of ceramide in the *Cftr*-KO mice compared to WT infected controls in both the lungs (A) and plasma (B). Moreover, the mice treated with fenretinide showed an increase (†) in the levels of ceramide in both the lungs and plasma of infected *Cftr*-KO mice compared to the mock-treated control group of mice (CTRL). The WT mice treated with fenretinide also showed increased median ceramide levels but were only statistically different in the plasma tissue (#) because the lung WT groups showed high intragroup variability.

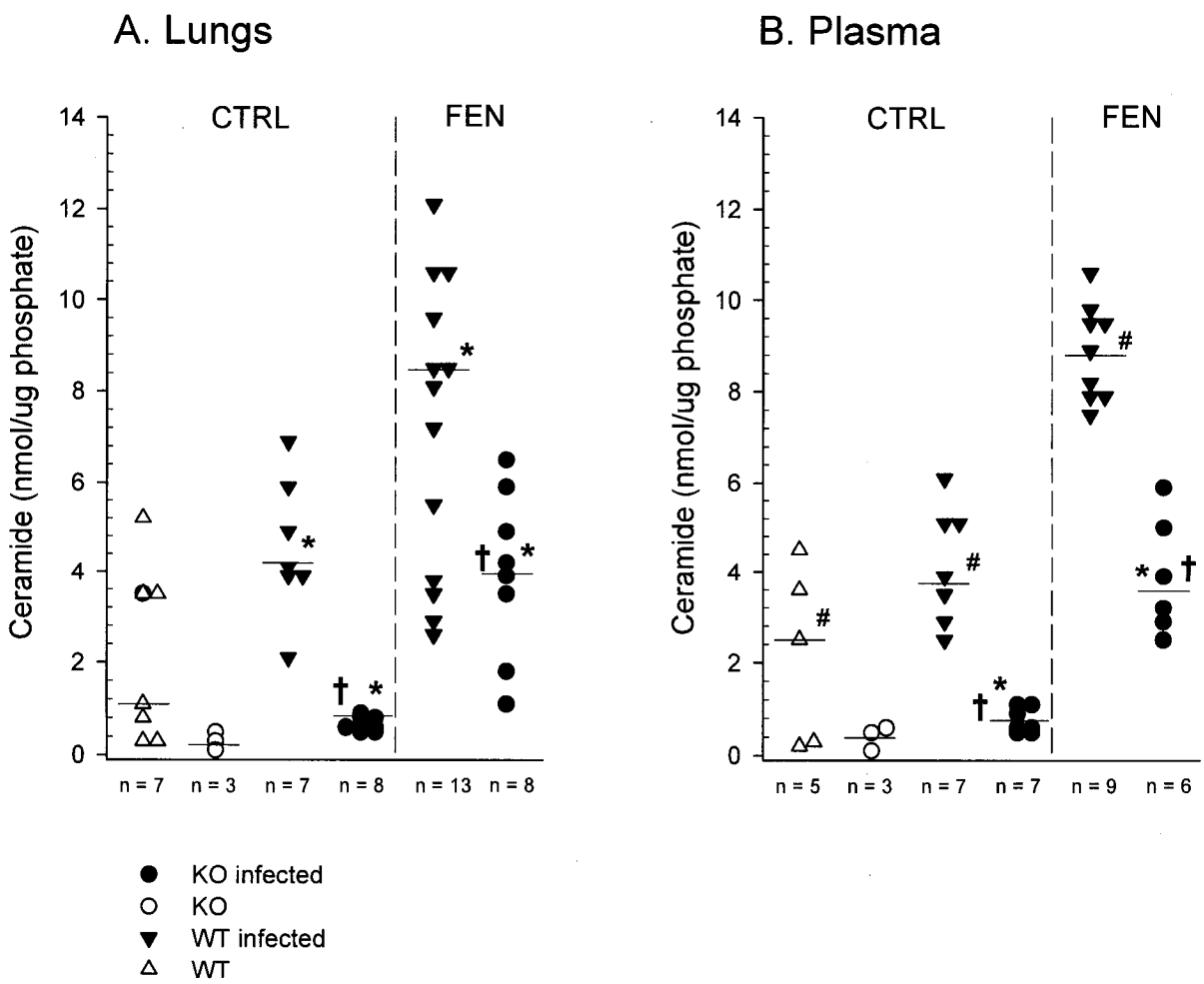
A. Lungs
B. Plasma
CTRL
FEN
Ceramide (nmol/ug phosphate)
0
2
4
6
8
10
12
14
n = 7
n = 3
n = 7
n = 8
n = 13
n = 8
n = 5
n = 3
n = 7
n = 7
n = 9
n = 6
KO infected
KO
WT infected
WT

Table 5.3 Effect of fenretinide treatment on the mean weight loss of WT and *Cftr*-KO mice during chronic lung infection with *P. aeruginosa*

	Mean weight loss (% of initial weight)			
Days post-infection (P value)	WT		*Cftr*-KO	
	CTRL n = 6	FEN n = 11	CTRL n = 6	FEN n = 8
1 (0.598)	-3.9 ± 0.8	-4.8 ± 0.4	-5.7 ± 1.7	-4.0 ± 1.1
2 (0.179)	-10.6 ± 1.3	-9.9 ± 0.5	-14.2 ± 3.2	-12.9 ± 0.9
3 (0.114)	-11.2 ± 1.3	-11.1 ± 1.2	-17.2 ± 3.7	-15.3 ± 1.8

Data are presented as the mean weight loss ± SEM
CTRL: untreated or mock-treated ; FEN: fenretinide-treated
No statistically significant differences was observed between the CTRL and the FEN groups ($P \leq 0.05$) for day 1 to day 3 post-infection

5.2.4.3 Alveolar inflammatory cells in BALF samples. The number of alveolar cells from the BALF were evaluated in both *Cftr*-KO (n = 20) and WT (n = 25) mice 3 days after infection with $1x10^6$ *P. aeruginosa* embedded in agar beads. The treatment with fenretinide had no effect on the cells recruited into the lungs of infected mice compared to the mock-treated mice at day 3 post-infection. Specifically, no significant difference in the mean total number of alveolar cells in the lungs was found between the mock-treated *Cftr*-KO mice ($1.2 x10^6 \pm 1.6 x10^6$) and the fenretinide-treated *Cftr*-KO mice ($1.1 x10^6 \pm 1.3 x10^6$) ($p = 0.530$). Similarly, no significant difference in the mean total number of alveolar cells in the lungs was observed between the mock-treated WT mice ($1.0 x10^6 \pm 1.6 x10^6$) and the fenretinide-treated WT mice ($1.2 x10^6 \pm 1.0 x10^6$) ($p = 0.280$). When the amount of different types of inflammatory cells found in the lungs of fenretinide-treated and mock-treated infected mice were quantified and compared, we found no significant differences between the groups. This applied to all different types of inflammatory cells studied and for both WT and *Cftr*-KO mice (neutrophils: $p = 0.143$; monocytes: $p = 0.223$; lymphocytes: $p = 0.400$). In summary, fenretinide treatment does not influence the amounts of different types of

inflammatory cells in our mouse model of *P. aeruginosa*-lung infection on day 3 post-infection.

5.2.4.4 Bacterial burden in the lungs. Next we assessed if the treatment with fenretinide affects the bacterial load in the lungs of the *Cftr*-KO and WT mice at day 3 post-infection with *P. aeruginosa*. As previously observed, the untreated *Cftr*-KO mice had significantly higher median CFU counts in the lungs compared to their WT counterparts (Figure 5.5, controls panel, $p = 0.004$). As illustrated in the Figure 2 there was approximately a 30-fold difference in the bacterial load in the lungs between *Cftr*-KO and WT mice. Amazingly, the treatment regiment with fenretinide dramatically decreased (10 fold) the median number of bacteria that was found in the treated *Cftr*-KO compared to the untreated *Cftr*-KO mice (untreated *Cftr*-KO = 4.0×10^5 CFU/lung compared to fenretinide treated *Cftr*-KO = 3.8×10^4 CFU/lung, Figure 5.5, $p = 0.004$). Not only could we observe a decrease in the bacterial burden of the *Cftr*-KO, but the CFU counts dropped down to the levels of the WT (no statistically significant difference found between fenretinide-treated *Cftr*-KO and WT groups of mice, $p= 0.086$). Fenretinide had no significant effect on the median number of bacteria found in the lungs of the WT mice compared to their WT untreated *P.aeruginosa* infected controls ($p = 0.240$).

5.2.4.5 Lipid profiles. PUFAs, especially DHA and AA, are known to play a key role in regulating cell function, membrane fluidity, trafficking, inflammation and mucin secretion. We therefore assessed the DHA and AA levels in different organs of the mice that were either untreated, mock-treated or treated with fenretinide which were uninfected or lung-infected with *P. aeruginosa.*

DHA/AA index ratio. Interestingly, in the lungs and in the plasma of untreated mice, we observed a lower median (*; $p \leq 0.001$) index ratio of DHA/AA in the *Cftr*-KO mice compared to their WT controls (Figure 5.6, CTRL panel, white symbols). Also, when we infected the mice with *P. aeruginosa* in the

Figure 5.5 Bacterial burden in the lungs. CFUs were assessed at 3 days post-infection from the lungs of *P. aeruginosa*-infected WT (*black*) and *Cftr*-KO (*white*) mice that were either untreated or mock-treated (CTRL) or treated with fenretinide (FEN). The untreated group of *Cftr*-KO mice had significantly higher median CFU counts in the lungs compared to their WT counterparts (30-fold difference, CTRL panel, $p = 0.004$). The *Cftr*-KO group of mice treated with fenretinide showed a decrease median number of bacteria (10 fold) compared to the untreated *Cftr*-KO mice (CTRL). No difference could therefore be observed between the WT and the *Cftr*-KO group of mice treated with fenretinide (FEN panel, $p= 0.086$). Fenretinide had no significant effect on the median number of bacteria found in the lungs of the WT mice compared to their WT untreated *P.aeruginosa*-infected controls ($p = 0.240$).

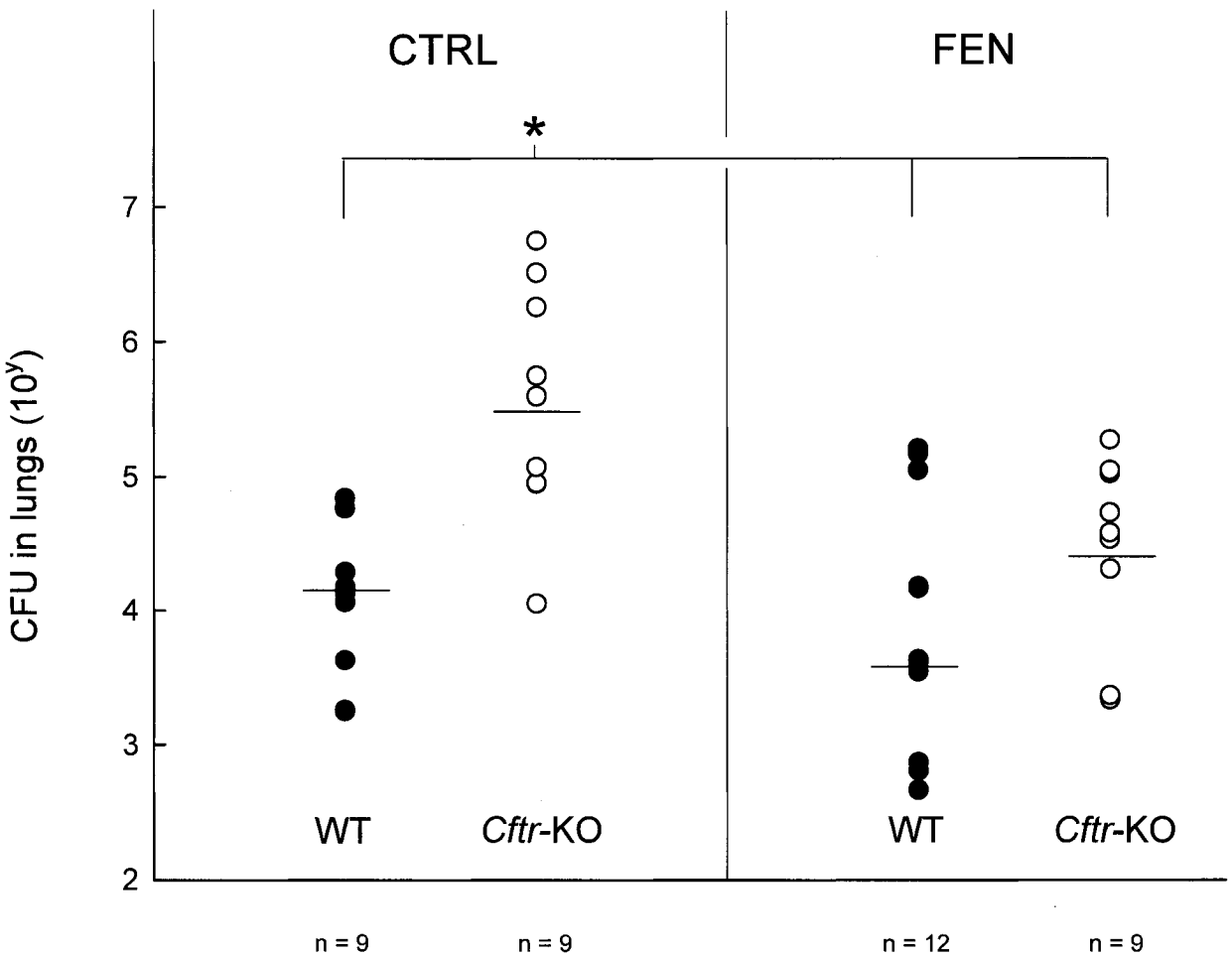
CTRL
FEN
*
CFU in lungs (10^y)
7
6
5
4
3
2
WT
Cftr-KO
WT
Cftr-KO
n = 9
n = 9
n = 12
n = 9

lungs (Figure 5.6, CTRL panels, black symbols), we observed significantly lower (*) median DHA/AA index ratio in the lungs of *Cftr*-KO mice compared to WT infected controls in both the lungs (panel A, $p \leq 0.001$) and plasma (panel B, $p \leq 0.001$). Interestingly, when we treated the mice with fenretinide, we observed an increase in the DHA/AA median index ratio in the lungs and plasma of infected *Cftr*-KO mice compared to the *Cftr*-KO untreated control mice (Figure 5.6). However, this difference reached statistical significance only in the lungs (†) because the plasma samples showed a very high intragroup variability. As for the WT mice, the fenretinide treatment had no effect on the DHA/AA median index ratio in both lungs and plasma compared to their untreated WT control mice. Since fenretinide treatment had an effect on the DHA/AA ratio in the *Cftr*-KO mice but not in the WT mice, the increase observed in the treated *Cftr*-KO mice reached the level at which we could no longer observe a difference between the infected WT and *Cftr*-KO fenretinide-treated mice (panel A, FEN panel) compared to the untreated WT and *Cftr*-KO mice (panel A, CTRL panel). The fenretinide treatment lowered the difference in the median index ratio between the WT and *Cftr*-KO by approximately 10-fold (untreated WT/*Cftr*-KO = 67 fold versus FEN-treated WT/*Cftr*-KO = 7-fold). These results have clearly demonstrated that fenretinide treatment has a very profound impact on the DHA/AA ratio. We have been very excited to find that this treatment protocol was able to normalize the abnormal DHA/AA ratio observed in both uninfected and infected *Cftr*-KO mice to ratios similar as observed in uninfected and infected WT mice.

DHA incorporated in phospholipids. DHA levels in the lungs and in the plasma were assessed in WT and *Cftr*-KO mice which were not-infected or *P. aeruginosa*-infected at 3 days post-infection. The mice were either not treated or mock-treated (CTRL) or treated with fenretinide (FEN). We have evaluated the levels of DHA incorporated in phospholipids and the data are expressed as percentile of total fatty acids (Figure 5.7). The lungs ($p \leq 0.001$) and the plasma ($p \leq 0.001$) samples were statistically different between the groups of mice tested. The *Cftr*-KO *P. aeruginosa* infected mice showed lower median (*)

Figure 5.6 DHA/AA index ratio observed in the lungs and plasma. DHA/AA index ratio in the lungs (A) and in the plasma (B) were assessed in WT (*triangles*) and *Cftr*-KO (*circles*) mice which were not-infected (*white*) or *P. aeruginosa*-infected at 3 days post-infection (*black*) and that were either not treated or mock-treated (CTRL) or treated with fenretinide (FEN). The median index ratios in the lungs ($p \leq 0.001$) and in the plasma ($p \leq 0.001$) samples showed statistical difference between the groups of mice tested. The lungs and the plasma of uninfected mice showed a lower median (*) index ratio of DHA/AA in the *Cftr*-KO mice compared to their WT controls. *P. aeruginosa* infected mice also showed a significantly lower (*) median DHA/AA index ratio in *Cftr*-KO mice compared to WT infected controls in both the lungs and plasma. The fenretinide-treated mice showed an increase in the DHA/AA median index ratio in the lungs and plasma of infected *Cftr*-KO mice compared to the *Cftr*-KO untreated control mice. This difference reached statistical significance only in the lungs (†) because the plasma samples showed a very high intragroup variability. We observed in the WT mice that fenretinide treatment had no effect on the DHA/AA median index ratio in both lungs and plasma compared to their untreated WT control mice.

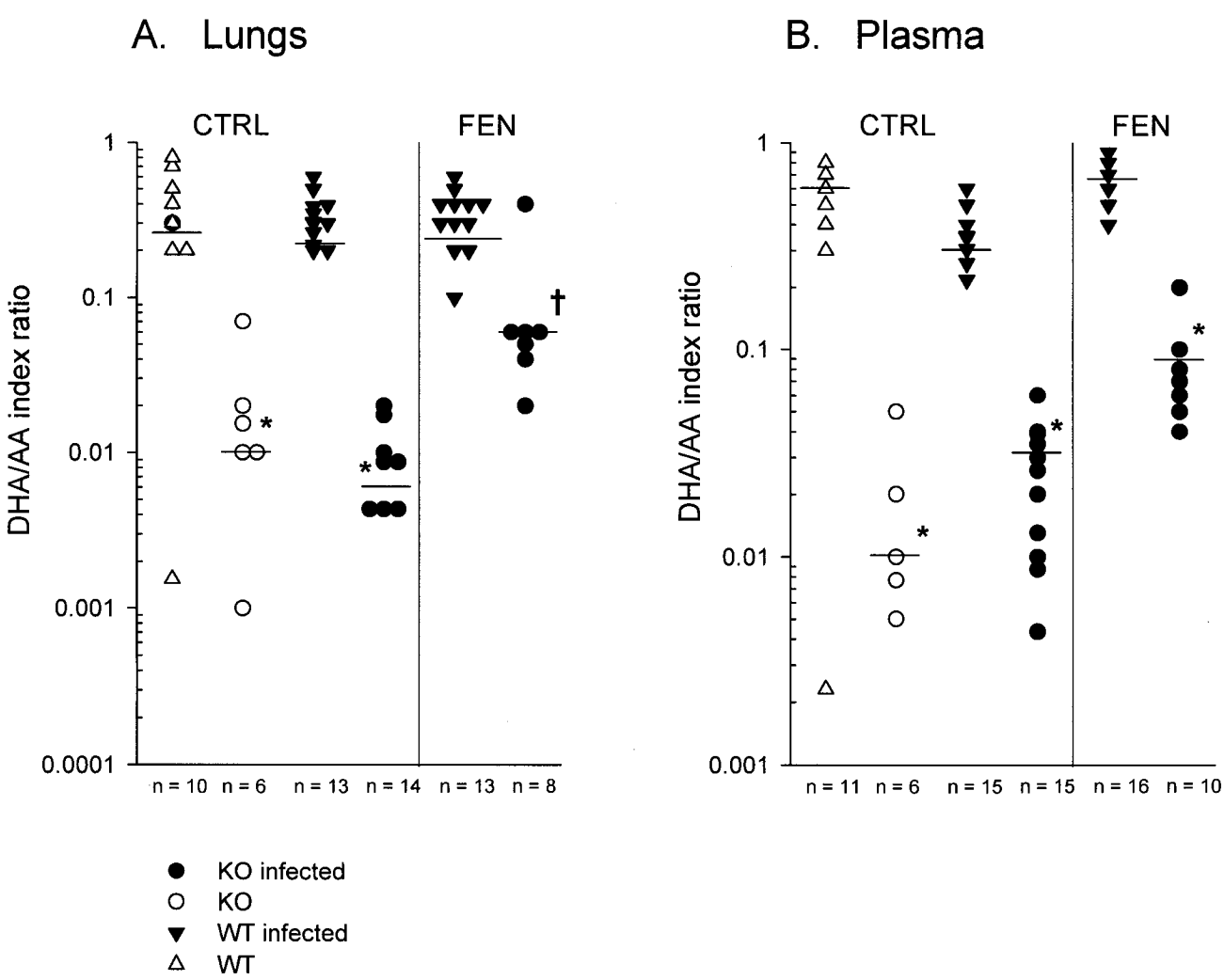
A. Lungs
B. Plasma
CTRL
FEN
DHA/AA index ratio
1
0.1
0.01
0.001
0.0001
n = 10
n = 6
n = 13
n = 14
n = 13
n = 8
n = 11
n = 6
n = 15
n = 15
n = 16
n = 10
*
†
KO infected
KO
WT infected
WT

DHA levels compared to their WT infected controls in both the lungs and the plasma (CTRL panels). The fenretinide-treated mice showed no difference in the median DHA levels in the lungs and plasma of infected *Cftr*-KO mice compared to the *Cftr*-KO untreated control mice. Similarly, the WT treated with fenretinide showed no difference in the median DHA level in both lungs and plasma compared to their untreated WT control mice.

We also evaluated the specific concentration of DHA incorporated in phospholipids expressed in nmol/mg of protein. The *Cftr*-KO uninfected mice showed lower median (*) DHA concentration levels compared to their WT uninfected controls in both the lungs and the plasma (CTRL panels). Similarly, the *Cftr*-KO *P. aeruginosa* infected mice showed lower median (*) DHA levels compared to their WT infected controls in both the lungs and the plasma (CTRL panels). The fenretinide-treated *Cftr*-KO infected mice showed lower median (*) DHA levels compared to their WT infected controls in both the lungs and the plasma (CTRL panels).

These results suggest that the fenretinide-mediated increase observed in the DHA/AA ratio is not due to the levels of DHA incorporated in phospholipids.

Free DHA levels. The median DHA percentile levels in the lungs ($p \leq 0.001$) and in the plasma ($p \leq 0.001$) samples were statistically different between the groups of mice tested. The *Cftr*-KO *P. aeruginosa* infected mice showed lower median (*) DHA levels compared to their WT infected controls in both the lungs and the plasma (CTRL panels). The fenretinide-treated infected WT mice showed a significant difference (#) in the median DHA levels in the lungs and plasma compared to the WT untreated uninfected control mice.

Also, the median DHA concentration levels in the plasma samples were statistically different between the groups of mice tested ($p \leq 0.001$). The *Cftr*-KO infected mice showed lower median (*) DHA levels compared to their WT infected controls in the plasma (CTRL panel). The fenretinide-treated *Cftr*-KO infected mice showed higher median (*) DHA levels in the plasma compared to their WT infected controls.

Figure 5.7 DHA incorporated in phospholipids expressed as percentage of total fatty acids in the lungs and plasma. DHA levels in the lungs (A) and in the plasma (B) were assessed in WT (*triangles*) and *Cftr*-KO (*circles*) mice which were not-infected (*white*) or *P. aeruginosa*-infected at 3 days post-infection (*black*) and that were either not treated or mock-treated (CTRL) or treated with fenretinide (FEN). The median DHA levels in the lungs ($p \leq 0.001$) and in the plasma ($p \leq 0.001$) samples were statistically different between the groups of mice tested. The *Cftr*-KO *P. aeruginosa* infected mice showed lower median (*) DHA levels compared to their WT infected controls in both the lungs and the plasma (CTRL panels). The fenretinide-treated mice showed no difference in the median DHA levels in the lungs and plasma of infected *Cftr*-KO mice compared to the *Cftr*-KO untreated control mice. Similarly, the WT treated with fenretinide showed no difference in the median DHA levels in both lungs and plasma compared to their untreated WT control mice.

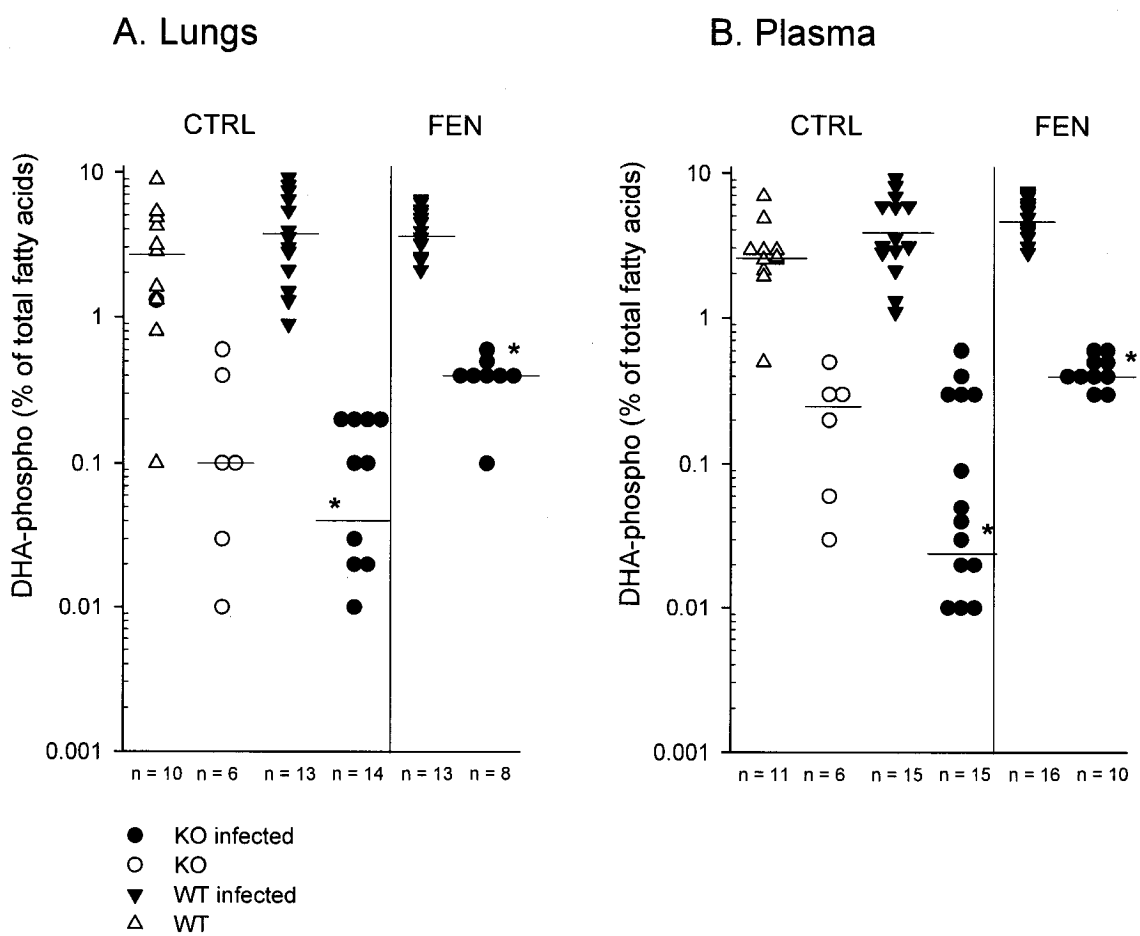
A. Lungs
B. Plasma
CTRL
FEN
DHA-phospho (% of total fatty acids)
10
1
0.1
0.01
0.001
n = 10
n = 6
n = 13
n = 14
n = 13
n = 8
n = 11
n = 6
n = 15
n = 15
n = 16
n = 10
*
KO infected
KO
WT infected
WT

Figure 5.8 Concentration of DHA incorporated in phospholipids in the lungs and plasma. DHA levels in the lungs (A) and in the plasma (B) were assessed in WT (*triangles*) and *Cftr*-KO (*circles*) mice which were not-infected (*white*) or *P. aeruginosa*-infected at 3 days post-infection (*black*) and that were either not treated or mock-treated (CTRL) or treated with fenretinide (FEN). The median DHA levels in the lungs ($p \leq 0.001$) and in the plasma ($p \leq 0.001$) samples were statistically different between the groups of mice tested. The *Cftr*-KO uninfected mice showed lower median (*) DHA levels compared to their WT uninfected controls in both the lungs and the plasma (CTRL panels). Similarly, the *Cftr*-KO *P. aeruginosa* infected mice showed lower median (*) DHA levels compared to their WT infected controls in both the lungs and the plasma (CTRL panels). The fenretinide-treated *Cftr*-KO infected mice showed lower median (*) DHA levels compared to their WT infected controls in both the lungs and the plasma (CTRL panels).

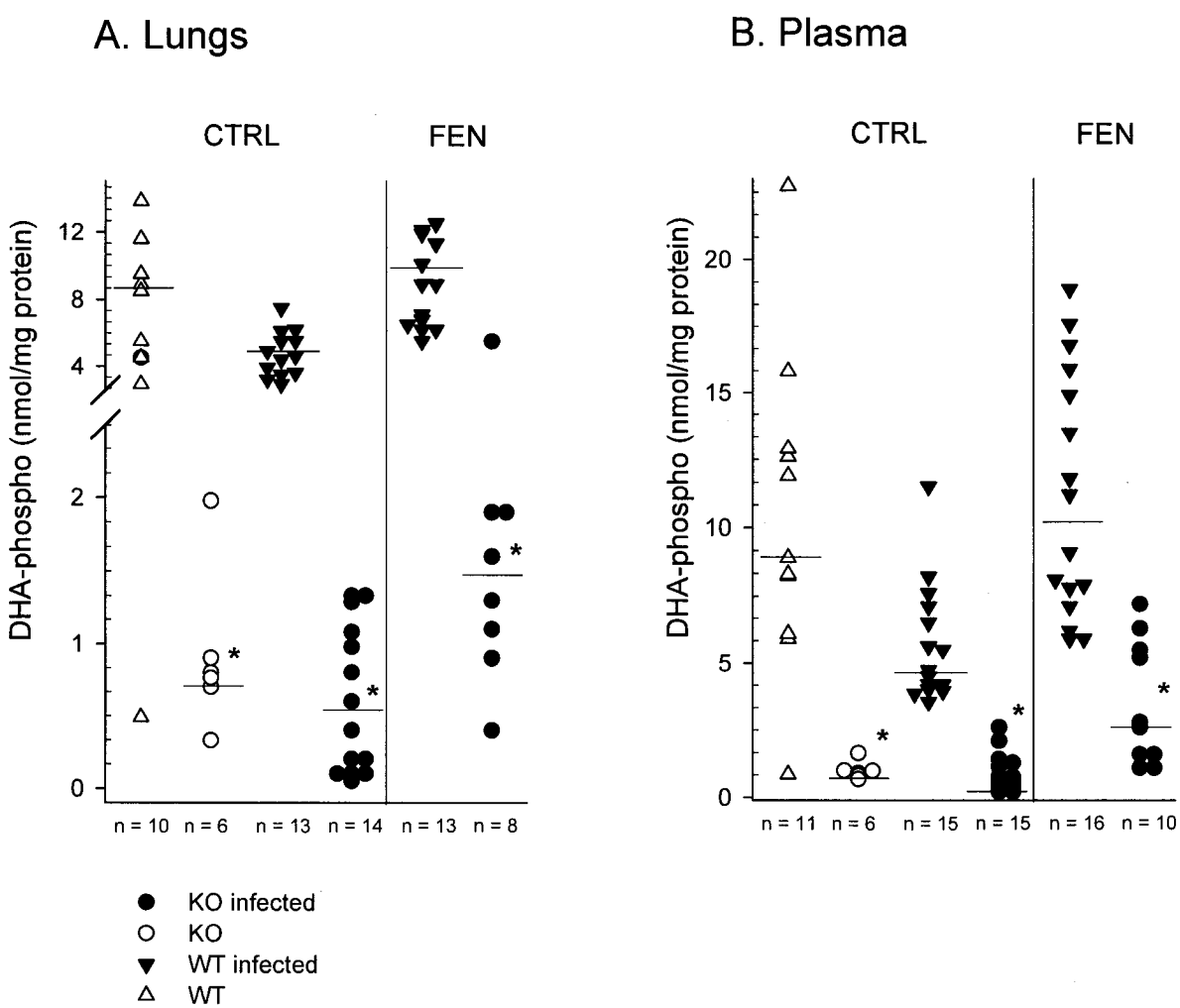
A. Lungs
B. Plasma
CTRL
FEN
DHA-phospho (nmol/mg protein)
12
8
4
2
1
0
20
15
10
5
n = 10
n = 6
n = 13
n = 14
n = 13
n = 8
n = 11
n = 6
n = 15
n = 15
n = 16
n = 10
KO infected
KO
WT infected
WT

Figure 5.9 Free DHA expressed as percentage of total fatty acids in the lungs and plasma. DHA levels in the lungs (A) and in the plasma (B) were assessed in WT (*triangles*) and *Cftr*-KO (*circles*) mice which were not-infected (*white*) or *P. aeruginosa*-infected at 3 days post-infection (*black*) and that were either not treated or mock-treated (CTRL) or treated with fenretinide (FEN). The median DHA levels in the lungs ($p \leq 0.001$) and in the plasma ($p \leq 0.001$) samples were statistically different between the groups of mice tested. The *Cftr*-KO *P. aeruginosa* infected mice showed lower median (*) DHA levels compared to their WT infected controls in both the lungs and the plasma (CTRL panels). The fenretinide-treated infected WT mice showed a significant difference (#) in the median DHA levels in the lungs and plasma compared to the WT untreated uninfected control mice.

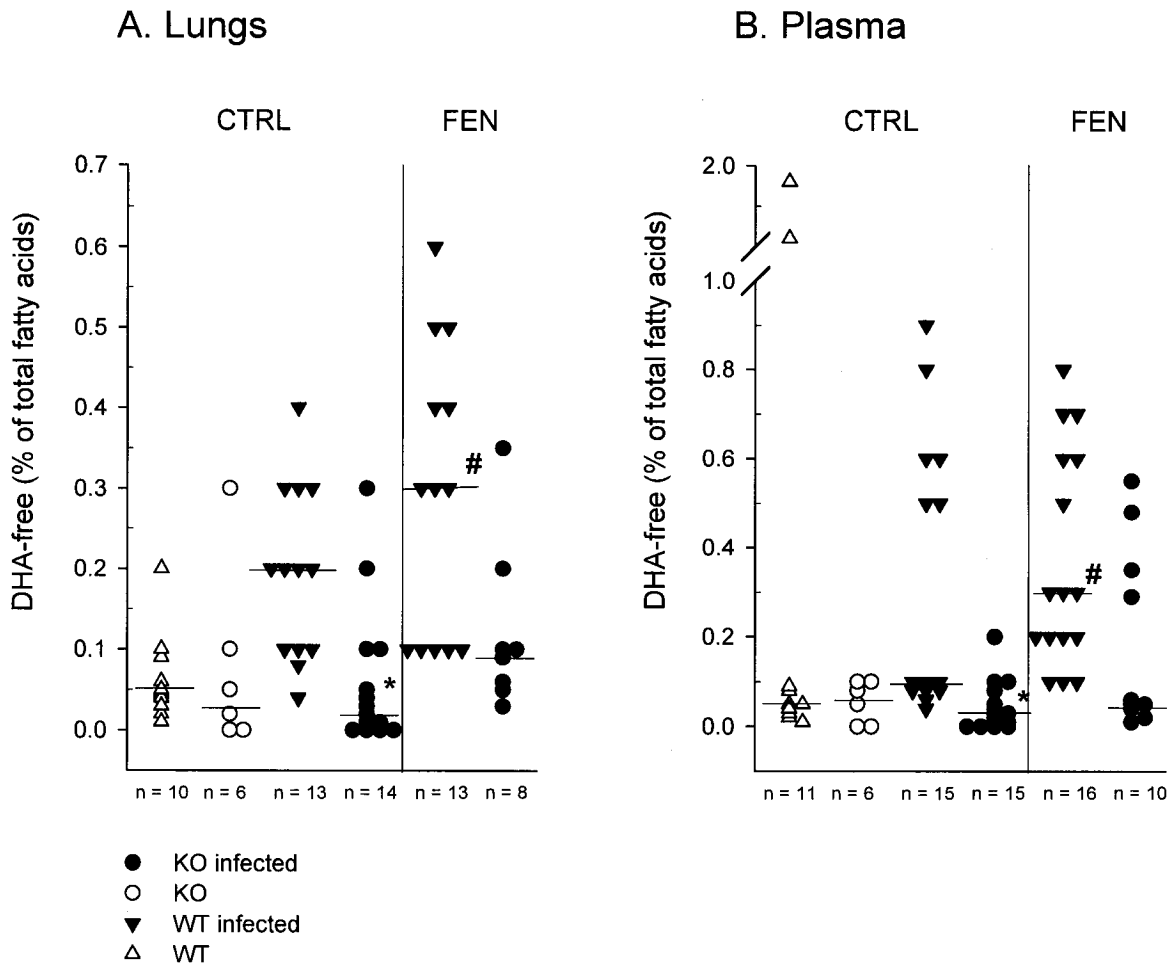
A. Lungs
B. Plasma
CTRL
FEN
DHA-free (% of total fatty acids)
0.7
0.6
0.5
0.4
0.3
0.2
0.1
0.0
2.0
1.0
0.8
0.6
0.4
0.2
0.0
#
*
n = 10 n = 6 n = 13 n = 14 n = 13 n = 8
n = 11 n = 6 n = 15 n = 15 n = 16 n = 10
KO infected
KO
WT infected
WT

Figure 5.10 Concentration of free DHA in the lungs and plasma. DHA levels in the lungs (A) and in the plasma (B) were assessed in WT (*triangles*) and *Cftr*-KO (*circles*) mice which were not-infected (*white*) or *P. aeruginosa*-infected at 3 days post-infection (*black*) and that were either not treated and mock-treated (CTRL) or treated with fenretinide (FEN). The median DHA levels in the plasma ($p \leq 0.001$) samples were statistically different between the groups of mice tested. The *Cftr*-KO infected mice showed lower median (*) DHA levels compared to their WT infected controls in the plasma (CTRL panel). The fenretinide-treated *Cftr*-KO infected mice showed higher median (*) DHA levels compared to their WT infected controls in the plasma.

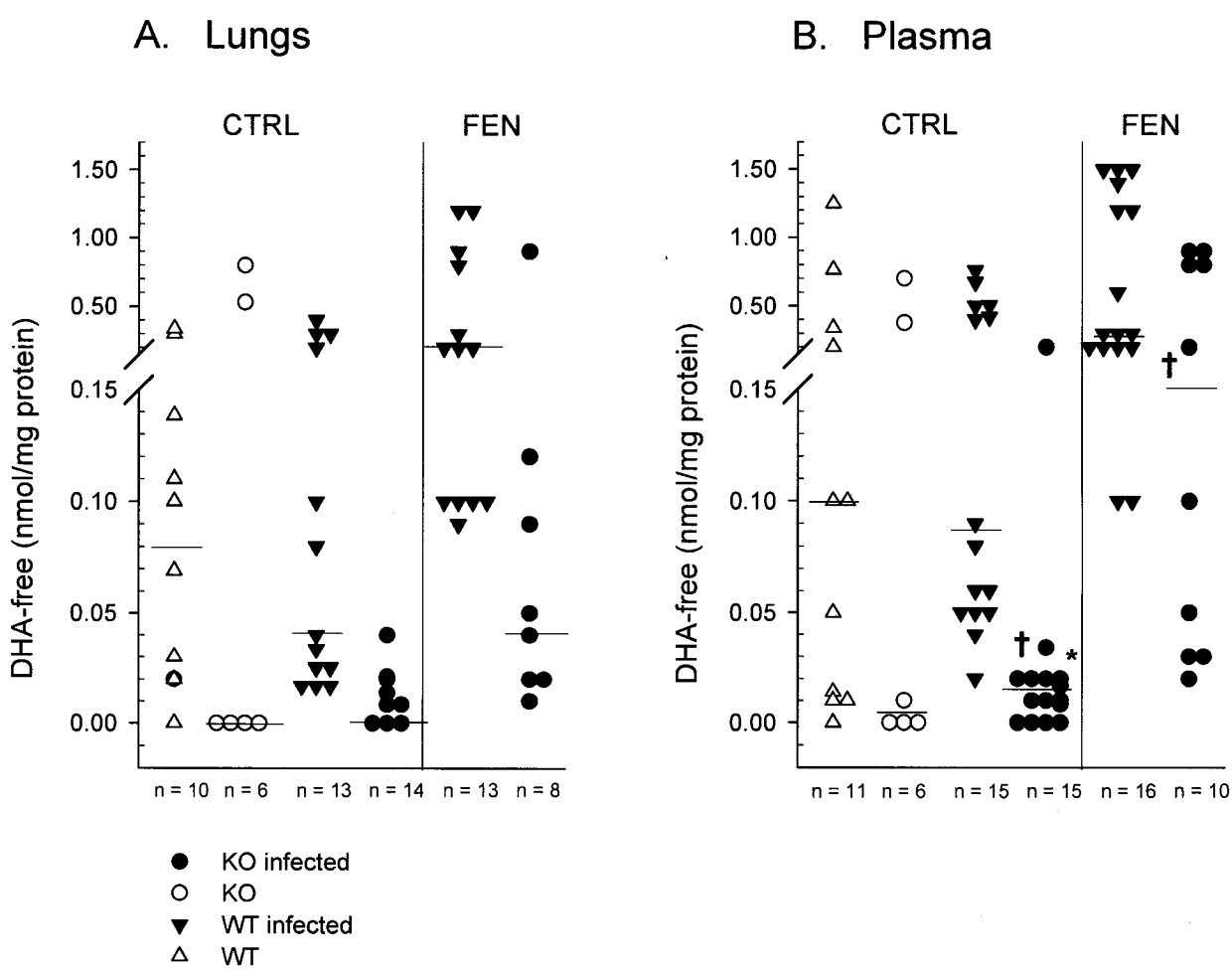
A. Lungs
B. Plasma
CTRL
FEN
DHA-free (nmol/mg protein)
1.50
1.00
0.50
0.15
0.10
0.05
0.00
n = 10
n = 6
n = 13
n = 14
n = 13
n = 8
n = 11
n = 6
n = 15
n = 15
n = 16
n = 10
†
*
KO infected
KO
WT infected
WT

Concentration of AA incorporated in phospholipids. The median DHA levels in the lungs ($p \leq 0.001$) and in the plasma ($p \leq 0.001$) samples were statistically different between the groups of mice tested. The *Cftr*-KO uninfected mice showed higher median (*) AA levels compared to their WT uninfected controls in the plasma samples only. The *Cftr*-KO infected mice showed higher median (*) AA levels compared to their WT infected controls in both the lungs and the plasma (CTRL panels). The fenretinide-treated *Cftr*-KO infected mice showed lower median (*) AA levels compared to their infected *Cftr*-KO untreated controls both in the lungs and the plasma.

5.2.5 Discussion

Recent investigations have demonstrated that treatment with galactosyl ceramide can lead to spectacular improvement in clearance of *P. aeruginosa* from infected lungs (194). Ceramide production can be induced in cells by a vitamin A analogue, fenretinide, which has already been approved for clinical trials on tumor suppression. We therefore studied the effect of this compound on the progression of CF lung disease during the course of *P. aeruginosa* lung infection using the *Cftr* gene deficient mouse model.

We initially assessed the ceramide basal levels in our CF mouse model. As shown in Figure 5.4, we observed a clear trend towards lower ceramide levels in the uninfected *Cftr*-KO mice compared to their WT controls in both the lungs and the plasma samples. Interestingly, sphingomyelinase (sMase), an enzyme responsible for the conversion of sphingomyelin to ceramide, was shown to be inhibited by glutathione (160). Therefore, it is possible, that higher levels of GSH observed in cystic fibrosis cells (164) might negatively affect the generation of intracellular ceramide.

Figure 5.11 Concentration of AA incorporated in phospholipids. AA levels in the lungs (A) and in the plasma (B) were assessed in WT (*triangles*) and *Cftr*-KO (*circles*) mice which were not-infected (*white*) or *P. aeruginosa*-infected at 3 days post-infection (*black*) and that were either not treated or mock-treated (CTRL) or treated with fenretinide (FEN). The median AA levels in the lungs ($p \leq 0.001$) and in the plasma ($p \leq 0.001$) samples were statistically different between the groups of mice tested. The *Cftr*-KO unifected mice showed higher median (*) AA levels compared to their WT unifected controls in the plasma samples only. The *Cftr*-KO infected mice showed higher median (*) AA levels compared to their WT infected controls in both the lungs and the plasma (CTRL panels). The fenretinide-treated *Cftr*-KO infected mice showed lower median (*) AA levels compared to their infected *Cftr*-KO untreated controls for both the lungs and the plasma.

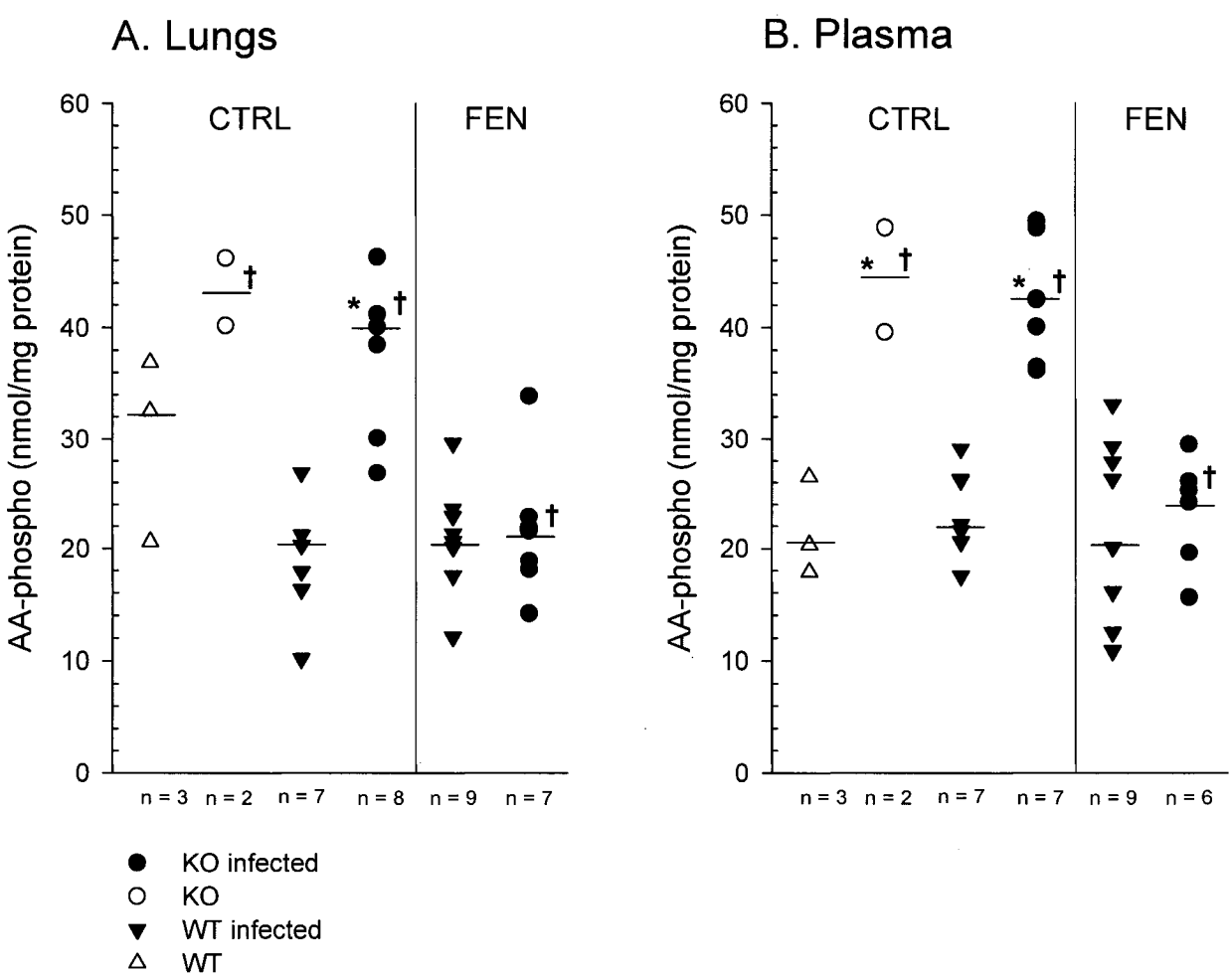
A. Lungs
B. Plasma
CTRL
FEN
AA-phospho (nmol/mg protein)
0
10
20
30
40
50
60
n = 3
n = 2
n = 7
n = 8
n = 9
n = 7
n = 3
n = 2
n = 7
n = 7
n = 9
n = 6
KO infected
KO
WT infected
WT

When mice are infected in the lungs with *P. aeruginosa,* we observe significantly lower levels of ceramide in the lungs and plasma samples of the *Cftr*-KO mice compared to their WT controls. Interestingly, the difference observed in the ceramide levels (Figure 5.4, panel A, CTRL panels) of WT and *Cftr*-KO mice inversely correlated with the bacterial burden found in their lungs (Figure 5.5, CTRL panel).

We then established the effect of fenretinide-induced stimulation of ceramide synthesis on the regulation of lung inflammation and *P. aeruginosa* clearance in mice with CF. As expected, the treatment with fenretinide significantly increased the levels of ceramide observed in the lungs and plasma of *Cftr*-KO mice (Figure 5.4, FEN panels). We could however still observe significantly lower levels of ceramide in fenretinide-treated *Cftr*-KO mice compared to the treated WT mice. The interesting question arising from the observed differences is how much ceramide is sufficient to help fight *Pseudomonas* bacteria. As shown in Figure 5.5, the levels induced by fenretinide in the *Cftr*-KO mice are sufficient to decrease their bacterial burden in the lungs down to the levels of the WT mice.

We further studied the effect of fenretinide treatment by looking at the fatty acid profiles of the different CF-affected organs. We were amazed to observe major increases in the lungs and plasma of *Cftr*-KO mice in DHA and AA ratio levels compared to the untreated *Cftr*-KO control mice (Figure 5.6). However, fenretinide did not affect the DHA/AA ratio index in the WT mice. These results suggest that there is a threshold and that, once attained, no more direct or indirect effect on the fatty acids levels can be seen. These unexpected results lead us to further characterize the fatty acid profiles. Based on our preliminary analyses, we can conclude that fenretinide treatment does not improve the levels of DHA incorporated in the phospholipids (Figures 5.7 and 5.8) in both the lungs and plasma of the *Cftr*-KO mice. These mice still have shown dramatically lower levels of DHA compared to their WT controls. Because the levels of DHA

incorporated in the phospholipids are not affected by fenretinide, the logical explanation for the DHA/AA ratio index increase in the fenretinide-treated *Cftr*-KO mice can only be that fenretinide treatment affects the AA levels. As shown in Figure 5.11, fenretinide treatment indeed brings the levels of AA incorporated in phospholipids down to the levels of WT mice. The untreated *Cftr*-KO mice always show statistically significantly lower levels of AA compared to their WT controls.

Fenretinide, through induction of ceramide levels in the lungs and plasma, lowers the AA levels and improves the DHA/AA ratio in our *Cftr*-KO infected mice. These overall changes in fatty acid levels lead to major improvements in the bacterial clearance in the lungs of *Cftr* deficient mice at 3 days post-infection. In fact, the marked difference in the bacterial burden between the WT and the *Cftr*-KO mice completely vanished.

These impressive improvements in fighting infection in the *Cftr*-KO mice could be explained in different ways. One possibility is that the decreased levels of AA incorporated in phospholipids leads to a better controlled inflammatory response of the host against the bacteria leading to their more efficient clearance from the lungs. It is also possible that excessive AA levels, such as those observed in the *Cftr*-KO mice compared to their WT controls, are related to increased mucus secretion which has deleterious effects in CF lung environment and therefore once this feature improved, the overall efficiency of the host to clear infection is improved as well.

The experiments in progress are exploring further the molecular mechanisms of the anti-inflammatory effects of fenretinide on inflammatory gene expression in CF lungs. Overall, we are hoping that by using our mouse model and by applying our expertise in the analysis of inflammatory gene regulation we will be able to better delineate the important host defenses of *Cftr*-deficient mice during the course of infection with *P. aeruginosa* and to identify pharmacological targets which may be therapeutically modulated to the benefit of CF patients.

The studies described in this chapter are of great importance for understanding the mechanism of CF lung dysfunction and for designing new treatments for patients, such as immunotherapy against pulmonary infection. The ultimate significance of these studies using DHA and fenretinide as diet supplements lies in the usefulness of the results in providing a better rationale for therapeutic management of pulmonary infection in cystic fibrosis patients.

CHAPTER VI

CHAPTER VI.

GENERAL DISCUSSION

6.1 Summary of the results

With many possible mutations in the CFTR gene, cystic fibrosis is a complex disease, affecting many organs with varying intensities, frequently leading to death. It is well established that the prognosis of cystic fibrosis disease is worse in female patients compared to male patients. The progression of inflammation during lung infection, mostly caused by *P. aeruginosa*, is characterized by a dysregulated production of cytokines. This excessive inflammation results in progressive destruction of the airway walls and bronchiectasis. Chronic lung infections resulting in a gradual loss of function and high mortality are particularly difficult to handle since no universal treatment capable of preventing or reversing lung damage has yet been developed.

What makes this disease difficult to study is the fact that no known natural animal model exists. Although many animal models have been used to study CF disease, the *Cftr* gene knockout mouse model seems to be the most frequently used in the studies addressing different aspects of the disease and attempting to better understand the molecular mechanisms leading to CF lung disease. In order to study the inflammatory response evoked by chronic *P. aeruginosa* infection and develop immunomodulatory approaches, a model of chronic pulmonary infection using *P. aeruginosa*-impregnated agar beads introduced surgically into the airways of mice was developed.

In the present study, we have extended our characterization of this model of chronic bronchopulmonary *P. aeruginosa* infection by initially evaluating the impact of gender. This was followed by the determination of the production of

important pro- and anti-inflammatory cytokines from the total lung homogenate and inflammatory cells after intratracheal instillation with *P. aeruginosa*-impregnated agar beads in C57BL/6 normal mice and C57BL/6-IL-10 KO mice (Chapter II). We then performed extensive characterization of our CF mouse model that develops spontaneous lung disease. Using uninfected C57BL/6 *Cftr*-KO mice and their WT littermate controls, we have established the gene expression profile in the lungs as well as the lipid profiles of these mice in the CF-affected organs (Chapter III). Subsequently, since the *Cftr*-KO mice are smaller, more sensitive and display an increased mortality rate compared to their WT controls, we performed series of meticulous experiments in order to perfect the infection methodology and to develop a less invasive and more natural way to infect the *Cftr*-KO mice in the lower parts of the lungs (Chapter IV). Using this improved method of infection, we assessed the effects of different diet supplements, such as DHA and fenretinide, on these mice's ability to handle infection with *P. aeruginosa.* The analysis was done in parallel with a comparative detail analysis of lipid profiles in organs of *Cftr*-KO and WT mice. We also characterized the inflammatory response observed in the infected and uninfected *Cftr*-KO mice compared to their littermate controls (Chapter V). These studies assessed the potential of the tested treatments as preventive agents or as an immunoregulatory treatment, and might now be extended to the preclinical and clinical phase of the studies.

In the first part of this study, we assessed the effects of gender on infection and inflammation by induction of chronic lung infection with *P. aeruginosa.* Using B6 male and female mice infected with *P. aeruginosa*, we found profound differences in the inflammatory response to the bacteria between both sexes. Our results indicated that females had a higher inflammatory response associated with higher levels of cytokines secreted compared to males, which also correlated with a higher bacterial load, and a more severe weight loss compared to males. These gender-related differences in inflammation, as well as the known effects of sex steroids on immunomodulatory functions (6;279), prompted us to look at the effect

of IL-10 in *P. aeruginosa* lung infection focusing on the gender issue. IL-10 may play an important role in controlling over-zealous inflammation frequently observed within the CF lung, as indicated in previous studies (Konstan and Berger, 1993; Konstan et al., 1994; Bonfield et al., 1995a; Bonfield et al., 1995b; Konstan and Berger, 1997). These studies suggest a beneficial role for IL-10 during chronic *P. aeruginosa* infection in maintaining homeostasis by modulating the inflammatory response to environmental irritants. Therefore, we infected IL-10 KO male and female mice and their respective controls, and extensive analysis of various parameters of susceptibility was performed. In our studies, we observed that IL-10 KO males were much more susceptible to *P. aeruginosa* lung infection compared to WT males. This was observed in the weight loss, the bacterial load of the lung, and in the cellular inflammatory response (Figures 2.2 - 2.5, Table 2.2). As for the females, WT and IL-10 KO mice were extremely sensitive to the infection, comparable with the CFU levels of male IL-10 KO mice. Overall, we found higher weight losses, significantly higher inflammatory cytokine responses, and a dysequilibrated PMN/macrophage ratio in the IL-10 KO females compared to WT females.

Upon *P. aeruginosa* colonization of the lungs, inflammatory cells are quickly recruited into the lung to initiate an immune response cascade, which ultimately leads to clearance of the bacteria. Our results showed that although the recruitment of an appropriate number of inflammatory cells is important, the type of cells recruited to the lung is also crucial. Using mouse models of *P. aeruginosa* lung infection it was previously shown, that an exaggerated inflammatory response dominated by PMN correlated with susceptibility to infection, whereas a modest inflammatory response dominated by macrophages correlated with resistance (237). In CF patients infected with *P. aeruginosa,* a persistent inflammation dominated by PMN neutrophils is frequently observed (12). Moreover, BALF studies have suggested that CF infants, showing no clinically apparent lung disease, developed very early a predominant neutrophilic lung inflammation (157). We also observed in our study that the switch from PMN to macrophage

predominance in the BALF was initiated at a later time point for IL-10 KO animals compared to WT controls, emphasizing the importance of IL-10 to initiate this change.

The importance of IL-10 during infection may be due to the ability of this cytokine to maintain an appropriate balance between pro- and anti-inflammatory cytokines (Standiford et al., 1996a; Standiford et al., 1996b; Walley et al., 1996). Thus, given the higher capacity of the WT mice to produce IL-10 in the lungs compared to the IL-10 KO mice, IL-10 may be important in controlling *P. aeruginosa* lung infection and limiting inflammation-induced lung injury in these mice.

Taken together, the results obtained from the studies presented in the Chapter II demonstrate a major difference between the males and the females in the susceptibility to lung infection reinforcing the importance of studying pulmonary diseases while taking gender into account. Other recently published studies confirmed that gender specific gonadal hormones are indeed involved in the differential production of cytokine levels such as IL-4, IL-10 and TNF (231;253;57). Our data show the importance of a proper balance in the cytokine production in a timely manner; they also indicate that it is not only important to evoke inflammatory cells to the sites of infection, but also that the right cell types are present in the appropriate number and ratio. These results reinforce the importance of IL-10 protein secretion during lung infection with *P. aeruginosa.*

It is widely known that in response to chronic bronchopulmonary *P. aeruginosa* infection, the airways react by a pronounced recruitment of inflammatory cells associated with a release of pro- and anti-inflammatory cytokines from both the inflammatory and resident cells (Bonfield et al., 1995; Davis et al., 1996). However, to appropriately characterize the susceptibility to lung infection with *P. aeruginosa* in CF, it is necessary to investigate first the status of the CF lung prior to infection. Is the CF lung milieu different from that of

normal lung? If so, what are the fundamental differences observed in the CF non infected lungs which are likely to influence the outcome of the inflammatory response to *P. aeruginosa*? An interesting study showed that uninfected mature CF small airway grafts, but unmatched non-CF controls, undergo time-dependent neutrophil-mediated inflammation, leading to progressive lung tissue destruction (primary inflammation in human cystic fibrosis small airways). Therefore, in CF, inflammation may arise, at least in part, from a primary defect in the regulation of inflammation, independently of infection. We were therefore interested in exploring further this likely intrinsic difference in inflammatory status of the lung that might exist prior to experimental infection with *P. aeruginosa* using our unique mouse model of CF lung disease (193).

Our laboratory participated in developing and characterizing various backcrosses of *Cftr*-KO mice, including the C57BL/$6^{H/M}$-*Cftr*.ko mice (147;110). Histological evaluation of the lungs was performed on this CF mouse model in order to identify the pathological state of the animals from 3 to 20 weeks of age. We observed that, at a few months old, the uninfected *Cftr*-KO mice showed increased hyperplasia of epithelial cells, basement membrane thickening, as well as enhanced inflammatory cell infiltration into the lung tissue compared to the WT uninfected controls. We used this animal model for the studies presented in this thesis. Initially, we monitored, over a period of 18 weeks, the weight gain between male and female, *Cftr*-KO, HZ, and WT mice, on three different diets; the solid chow diet and two different liquid diets: Bioserv and Peptamen. The two later ones have the advantage of increasing survival of the *Cftr*-KO mice (Table 1), most certainly by preventing intestinal obstruction, which is frequently seen in CF due to an increase in mucus secretion. However, none of these liquid diet feedings resulted in an increase in mean weight gain in the *Cftr*-KO mice.

We then further characterized this model by performing genome-wide transcriptional analysis of gene expression in the lungs of the *Cftr*-KO mice compared to their WT littermate controls. Using 20 weeks old CF mice that

display very striking changes in their lungs compared to their littermate controls, we have performed very meticulous comparisons of gene expression patterns between the lungs of *Cftr*-KO mice and their controls using multiple animals of both genders.

We have generated lists of the over- and under-expressed candidate genes, obtained for the probability interval 0.8; they contain a total of 116 candidate genes in males and 81 candidate genes in females, which are differentially expressed between *Cftr*-KO and their WT control mice. Table 3.4 shows the candidate genes common to both females and males. When comparing the gene expression patterns between *Cftr*-KO mice (both males and females) and their control littermates, it was evident that there was more up regulated genes than down regulated genes in the lungs of *Cftr*-KO mice than in WT controls.

Anomalies in the production of immunoglobulins (hypo- and hyper-gammaglobulinemia) in CF patients and animal models have been reported in the literature (217;208;188;176;124;27). Interestingly, our study demonstrated that several of the identified genes belonging to the Ig family correlated with higher IgG1 protein expression in the plasma of *Cftr*-KO mice compared to WT. The up regulation of several genes that belong to the immunoglobulin family was also accompanied by the up regulation of several genes, which suggests an overall enhancement of B-cell functions, antigen presentation and antigen binding. Other genes that were up-regulated in the *Cftr*-KO mice include calgranulins. Elevated amounts of calgranulins (A and B) were found in the serum of patients with cystic fibrosis and clinically normal heterozygous carriers (68;67). Interestingly, calgranulin A (S100a8) and calgranulin B (S100a9) genes were up regulated in our mouse model. Also, T-cell related genes were found to be up-regulated in the lungs of *Cftr*-KO mice compared to their WT counterparts.

The mRNA expression of chemokine genes and chemokine receptor genes were found to be elevated in *Cftr*-KO lungs compared to their WT counterparts.

We also found that several other proteins known to be involved in the general inflammatory response had their gene expression affected by the deleted *Cftr* gene ablation. Serum amyloid A3, which is expressed particularly in macrophages and known as an acute phase reactant, Arginase 2, which is closely involved in the cellular production of NO, integrin and lipocalin 2, were all up-regulated in the *Cftr*-KO lungs.

We also found genes involved in the proteolytic degradation of the extracellular matrix such as matrix metalloproteinases and cathepsin H, which is involved in the conversion of pro-MMPs into active MMPs. Furthermore, in our analyses, constitutive expressions of protease inhibitors, especially serine protease inhibitors, proved to be differentially expressed in the lungs when comparing *Cftr*-KO mice with lung disease to their WT healthy littermate controls. Interestingly, we found that the expression of three procollagen genes were higher in the *Cftr*-KO lungs compared to normal lungs.

We found a total of seventeen genes that were associated with the lung disease phenotype. Also, human studies of CF have performed gene expression analyses on blood samples or on human epithelial cell lines, identifying secondary genes other than *Cftr*, influencing the clinical severity of CF disease (78;64). Among the genes identified in our study which are differentially expressed between WT and *Cftr*-KO mice and which could play an important role in CF lung disease, were genes such as IL-1 beta, IL-8R, and CLCA1, GSTM1, HSP40 and HSP70.

Overall, these studies highlighted many basic differences between the uninfected *Cftr*-KO mice and their WT controls in terms of gene expression (Chapter III). Studies are currently underway to elucidate the specific roles of these proteins and their gene regulation within the uninfected and *P. aeruginosa* infected murine CF lung.

These previous studies clearly show that *Cftr*-KO mice are in an inflammatory state even prior to *P. aeruginosa* lung infection, compared to normal WT mice. Taking this into account, we were interested to study the susceptibility differences in lungs infected with *P. aeruginosa* betwen the responses of *Cftr*-KO mice and their WT controls. We were therefore very concerned about the *Cftr*-KO mice innate fragility and how this could affect the results of our studies. Various original techniques (acute and chronic models) using *P. aeruginosa* and *B. cepacia* (280) are utilized in mice to mimic the infection of the lungs of CF patients. Several investigators, including us, have used a technique of intratracheal infection of the lungs with *P. aeruginosa* bacteria embedded in agar beads. This method of infection involves the inoculation of the bacteria into the lungs via the incised trachea and also requires that the bacteria are enmeshed into agarose or agar mimicking, at least to some extent, the chronicity of the lung infection observed in CF afflicted patients. This method has proven to be useful in the study of bronchopulmonary chronic infection, as we used in the IL-10 KO mouse model. However, a more "natural" colonization technique was used in a rat model of CF and other lung studies, involving direct inoculation of the microorganism into the lungs via the mouth without a temporary tracheotomy (294). This method of delivering the bacteria directly into the lungs without surgical incision of the trachea was very appealing to us since it lead to much less physical and inflammatory stress for the animals. Considering the *Cftr*-KO mice fragility and inflammatory status prior to infection, we decided to adapt and perfect this direct method of lung delivery originally described for rats so that it would be possible to use it in an animal approximately 5-10 times smaller, such as a mouse.

As described in this thesis (Chapter IV), the use of a special microscope allowed for a faster intervention since it gave precision to the operator and also allowed us the use of a higher dose of bacteria before significant mortality was observed compared to the surgical instillation method previously used in our mouse colony. While the infection method does not involve any surgical procedure, the infection with *P. aeruginosa* still has induced major weight losses

during the first 3 days post-infection. We also found a significantly higher bacterial burden in *Cftr*-KO mice compared to WT mice. Although the amount of alveolar cells recruited to the lungs was not significantly different between WT and *Cftr*-KO mice, we observed a clear imbalance in the types of inflammatory cells recruited, with relatively more PMN and a trend towards less macrophage counts in the lungs of the *Cftr*-KO mice compared to their WT controls.

Overall, using this direct pulmonary method of lung infection, we were able to establish a similar immune response to *P. aeruginosa* as that observed in CF patients infected with these bacteria and with less manipulation and surgical-related stress caused to the mice.

A deficiency in essential fatty acid metabolism has been well-documented in CF patients. Freedman and colleagues have shown that oral administration of DHA to *Cftr*-KO mice corrected the lipid imbalance in the ileum and pancreas. We explored in the first part of Chapter V if treatment with DHA was able to inhibit spontaneous CF lung disease in *Cftr*-KO mice and we found a very impressive effect. By supplementing the diet with DHA, the chronic occurrence of hyperplasia in lung epithelium and inflammatory cell infiltration of uninfected *Cftr*-KO mice was greatly reduced. We are presently exploring these encouraging results further by testing if the protective effect of DHA could be even greater if females with newborn mice are fed DHA enriched diets during the entire period prior to the weaning of their litter. Also, our laboratory is now thoroughly investigating the lung pathology improvements in more detail and performing gene expression analysis of the lungs of *Cftr*-KO treated with DHA compared to untreated *Cftr*-KO, to establish the extent of improvements at the level of biochemical parameters of inflammation.

In the second part of Chapter V, we assessed the effect of fenretinide, a drug inducing ceramide, in *P. aeruginosa* clearance using our *Cftr*-KO mouse model. The results presented in this study clearly show that fenretinide, through induction

of ceramide levels in the lungs and plasma, lowers the AA levels and improves the DHA/AA levels in our *Cftr*-KO infected mice. These overall changes in fatty acid levels lead to major improvements in the bacterial clearance in the lungs of *Cftr* deficient mice at 3 days post-infection. In fact, the marked difference in the bacterial burden between the WT and the *Cftr*-KO mice completely vanished.

Overall, we describe in this thesis several candidate genes involved in cellular physiological processes, as well as in the immune response, signal transducer and antigen binding activities, and matrix remodeling. These genes might contribute to the development of CF lung disease prior to *P. aeruginosa* lung infection. This strongly suggests that the control of the immune system is crucial to prevent the development of the disease.

We also describe a method allowing us to establish long lasting lung infection, creating different inflammatory responses in WT and *Cftr*-KO mice infected with *P. aeruginosa*. This method simplifies the infection procedure in terms of its duration, invasiveness, and improves the survival rate of the CF animals when compared to the previously used intratracheal procedure.

Taken together, the diet supplementation studies using DHA and fenretinide corroborate the importance of a high caloric diet and a balance in the lipid profiles in CF patients and suggest that one or both of these molecules could potentially be used as a therapy to improve lung disease in CF patients.

6.2 Future directions

In the case of the use of mouse model in the research on CF, the major challenge remains the exploration of all the *Cftr* gene functions, but also investigations on the other genes which influence the *Cftr* gene or that are influenced by the *Cftr* mRNA and protein expressions. These other genes will undoubtedly help define the correlation between phenotype and genotype in CF

affected patients. More specifically, we need to confirm the role of the genes identified by gene expression profiling studies using our uninfected *Cftr*-KO mouse model, but we also need to confirm their protein levels. It is also imperative to examine their expression during infection.

Also, further studies need to be performed to supplement the current knowledge on the fatty acid deficiencies observed in CF patients compared to healthy controls. The influence of the fatty acid and lipid profiles before and during infection in CF needs to be determined to better understand their role in fighting the infections. Moreover, we need to understand the mechanism by which fenretinide leads to such dramatic improvements in the clearance of *Pseudomonas* in the lungs of our *Cftr*-KO mice. Also, it would be interesting to verify if the increase of ceramide levels in *Cftr*-KO mice observed following the fenretinide treatment, could improve the histopathological status of the *Cftr*-KO mice that we have consistently observed in the lungs of 20-weeks old *Cftr*-KO mice.

Studies are presently under way to investigate, among other things, the levels of ceramide in the blood of CF patients with mild, moderate or severe lung disease, which are or are not carriers of *P. aeruginosa* in their lungs. The results from this study will definitely lead to a better understanding of the potential of DHA and/or fenretinide as a treatment for lung inflammation of CF patients.

6.3 Importance of the other fields of research

An immense network of research teams all around the world is studying many other very important physiological and biochemical pathways crucial for a better understanding of CF disease. There are also several fields of research that are directly relevant to the understanding of lung inflammatory responses to infection with *P. aeruginosa*, but are not discussed in this thesis.

Because CF is a complex disease, it is a day-to-day challenge for CF-affected children at school, as well as for adults in the workplace. The biggest challenge for CF disease is, in my opinion, to support the continuous team work done by researchers, physicians and caregivers: nurses, social workers, nutritionists, psychologists, psychiatrists, pharmacists and family members. The environment support and the maintenance of a psychologically positive attitude are primordial in order to sustain enthusiasm for the care of CF patients, since their daily routine is composed of several medications, nutritional supplements, various physical treatments, various pain management techniques and everyday psychological challenges.

CHAPTER VII

CHAPTER VII.

CLAIMS TO ORIGINALITY

From the studies on cystic fibrosis described in this thesis, major findings are exposed:

1) Gender differences exist in the inflammatory response to *P. aeruginosa* lung infection, as females are more susceptible than males to lung infection with *P. aeruginosa;*
2) IL-10 is crucial for the proper eradication of *P. aeruginosa* from the lungs;
3) The CF mouse model used in our laboratory represents a unique model of CF disease by its:
   - Spontaneous lung disease development, prior to *P. aeruginosa* infection, that is consistent with the pathological profiles observed in CF patients
   - Gene expression differences observed between the lungs of *Cftr*-KO and WT non- *P. aeruginosa* infected mice,
4) The use of direct pulmonary technique of lung delivery:
   - Allows the exclusion of the surgery-related inflammation,
   - Is a method that simplifies the infection procedure in terms of its duration and invasiveness, and improves the survival rate of the CF animals compared to the intratracheal technique previously used,
   - Allows adequate monitoring and studying of the increased susceptibility to lung infection with *P. aeruginosa* in the *Cftr*-KO mice compared to their WT that are consistent with the pathological profiles observed in CF patients infected with *P. aeruginosa*;

5) DHA diet supplementation corrects the imbalance observed between DHA/AA in CF-related organs and seems to improve the pathophysiological status of the lungs of *Cftr*-KO mice

6) Fenretinide supplementation in the Peptamen diet:
   - Leads to an increase in ceramide levels of *Cftr*-KO and WT mice,
   - Influences the ratio of DHA / AA,
   - Dramatically decreases bacterial load in the *Cftr*-KO mice to the levels of lung infection with *P. aeruginosa* in *Cftr*-KO mice.

APPENDIX I

Supplementary illustrations of the direct non-invasive method of lung infection

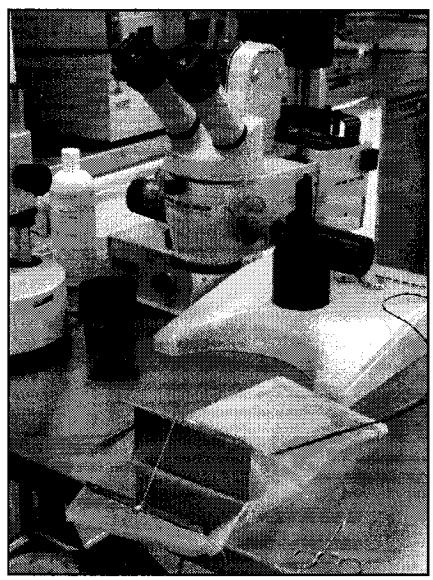

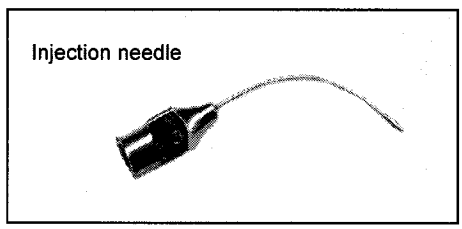

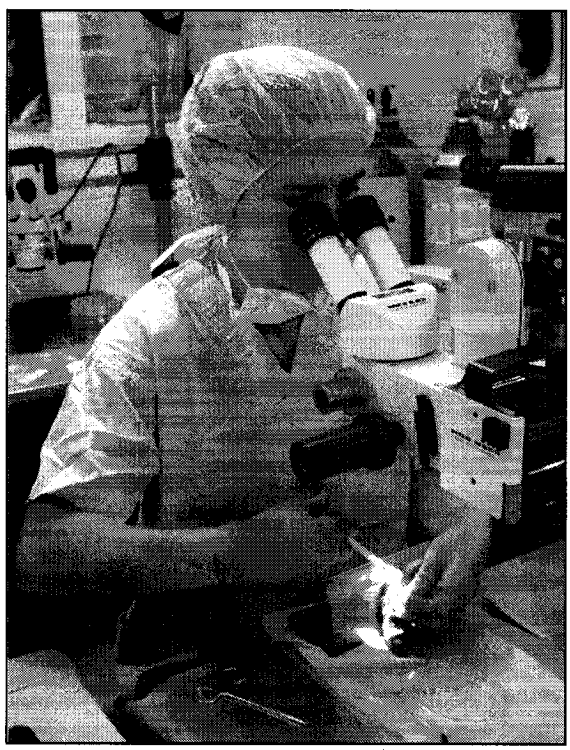

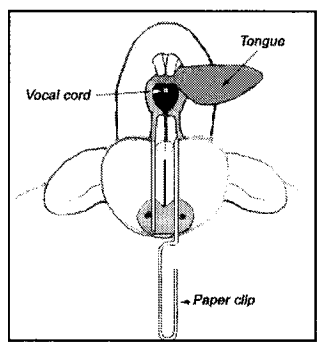

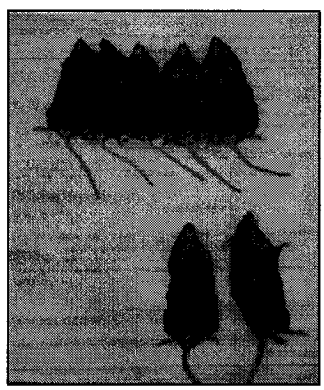

APPENDIX II

Over-expressed Genes in *Cftr*-KO compared to WT mice; genes with either unknown function or with a fold difference lower than 1.5

Females Over expressed in KO	Affymetrix probe
FBJ osteosarcoma oncogene (Fos)	160901_at
proline rich protein 2 (Prp2)	93650_i_at
S100 calcium binding protein A8 (calgranulin A) (S100a8)	103448_at
thymus cell antigen 1 theta (Thy1)	99057_at
expressed sequence AF044077	97564_f_at
expressed sequence M80423	102156_f_at
expressed sequence X00652	96971_f_at
expressed sequence AJ235940	102076_at
expressed sequence X16678	101633_at
RIKEN cDNA 2010309G21 gene	92316_f_at
expressed sequence AU044919	102823_at
expressed sequence AU044919	102824_g_at
expressed sequence AF042798	97563_f_at
expressed sequence AI848479	98524_f_at
expressed sequence V00817	93583_s_at
expressed sequence AF025445	100376_f_at
expressed sequence Y12713	98577_f_at
expressed sequence X02463	100362_f_at
expressed sequence L43568	101751_f_at
expressed sequence L14553	96963_s_at
expressed sequence L33952	100377_f_at
expressed sequence L28059	101320_f_at
expressed sequence X05546	160934_s_at
expressed sequence L28060	101319_f_at
expressed sequence X82691	96975_at
expressed sequence K03461	102155_f_at
expressed sequence AA419684	95184_f_at
expressed sequence AI314034	97178_at
13 days embryo spinal cord cDNA RIKEN	94027_at
clone IMAGE:4216466 mRNA	96839_at

ESTs similar to promyelocyte leukemia Zn finger protein	92202_g_at
adult male aorta and vein cDNA RIKEN	100914_at
expressed sequence M16724	102152_f_at

Females Under expressed in KO	
nuclear protein 1 (Nupr1)	160108_at
glutathione S-transferase omega 1 (Gsto1)	97819_at
adrenomedullin receptor (Admr)	104271_at
actinin alpha 1 (Actn1)	92280_at
B-cell translocation gene 3 (Btg3)	96146_at
nuclear receptor subfamily 4 group A member 1 (Nr4a1)	102371_at
prion protein (Prnp)	100606_at
hnRNP-associated with lethal yellow (Raly)	98511_at
huntingtin-associated protein 1 (Hap1)	102323_at
2 days neonate thymus thymic cells cDNA RIKEN E430025L19 product	103411_at
RIKEN cDNA 5730469M10 gene	161735_r_at
RIKEN cDNA 4832416K17 gene	96269_at
RIKEN cDNA 1200003E16 gene	95595_at

Males Over-expressed in KO	**Affymetrix probe**
expressed sequence AF044077	97564_f_at
expressed sequence M80423	102156_f_at
expressed sequence X00652	96971_f_at
expressed sequence AJ235940	102076_at
expressed sequence X16678	101633_at
RIKEN cDNA 2010309G21 gene	92316_f_at
interferon gamma induced GTPase (Igtp)	160933_at
T-cell specific GTPase (Tgtp)	102906_at
histocompatibility 2 class II locus Mb1 (H2-DMb1)	98035_g_at
CD52 antigen (Cd52)	104606_at
CD19 antigen (Cd19)	99945_at
CD79A antigen (immunoglobulin-	102778_at

associated alpha) (Cd79a)	
procollagen type VI alpha 2 (Col6a2)	93517_at
amyloid beta (A4) precursor protein-binding family B member 1 interacting protein (Apbb1ip-pending)	102710_at
G7e protein (G7e-pending)	104333_at
glutathione reductase 1 (Gsr)	160646_at
glycoprotein 49 A (Gp49a)	100325_at
selenoprotein R (Sepr)	160275_at
serine/threonine kinase 10 (Stk10)	93680_at
tryptophanyl-tRNA synthetase (Wars)	98605_at
C78850 Mouse 3.5-dpc blastocyst cDNA Mus musculus mRNA sequence.	97197_r_at
RIKEN cDNA 6330406L22 gene (6330406L22Rik)	100511_at
CD48 antigen (Cd48)	103089_at
CD53 antigen (Cd53)	94939_at
procollagen type I alpha 1 (Col1a1)	94305_at
lymphocyte cytosolic protein 1 (Lcp1)	94278_at

Males Under expressed in KO	**Affymetrix probe**
expressed sequence AI987814	93512_f_at
protein tyrosine phosphatase receptor type B (Ptprb)	92289_at
RIKEN cDNA 1190002N15 gene (1190002N15Rik)	98594_at
insulin-like growth factor binding protein 3 (Igfbp3)	95082_at
DnaJ (Hsp40) homolog subfamily A member 1 (Dnaja1)	97261_at

APPENDIX III

Genes differentially expressed between CF KO and WT mice (as described in the Results section under *Other potential candidate genes)*

	Gene name	Accession	KO / WT
1	Igh-4	X94418	13.5
2	IgA VDJ heavy chain	X94419	10.8
3	Igh-VJ558	J00475	8.8
4	Ig kappa light chain V	AF044077	5.2
5	Igk-V8	M15520	4.8
6	Ig heavy chain CDR3	AF042798	4.5
7	Ig kappa light chain Vk10c	AF029261	4.5
8	Igj	M90766	4.0
9	Ig rearranged kappa-chain	K03461	3.9
10	Igk-V8	U55641	3.8
11	gcsf receptor	U05894	3.5
12	Igh-4	L33954	3.4
13	Saa3	X03505	3.2
14	Igh-VJ558	AV080003	3.1
15	Il1b	M15131	2.9
16	Igk-V8	U62386	2.9
17	Igh-VJ558	AF036736	2.9
18	Slfn4	AF099977	2.9
19	Ccl5	AF065947	2.9
20	Csf3r	M58288	2.8
21	Igk-V8	U19315	2.8
22	Igk-V8	U60442	2.8
23	Fmnl	AF006466	2.7
24	Ig heavy chain V	AF025445	2.7
25	Klrg1	AF097357	2.6
26	Ig heavy chain V	L33943	2.6
27	Igk-V28	U55576	2.6
28	Ig B cell antigen receptor	L28060	2.6
29	Cd3g	M18228	2.6
30	IgK chain gene C-region	M80423	2.6
31	Gzma	M13226	2.6
32	Igl-V1	J00579	2.6
33	C78850	C78850	2.5
34	Igk-V8	U30629	2.5
35	Ms4a6b	AI504305	2.5
36	S100a9	M83219	2.5
37	Ms4a6b	AI835093	2.4
38	Igk-V8	U30241	2.4
39	Slfn3	AF099974	2.4
40	Cd6	U37543	2.4
41	Cd8b	AV316162	2.3
42	Plac8	AA790307	2.2
43	Ccr7	L31580	2.2

44	Slfn1	AF099972	2.2
45	Ig light chain V	L14554	2.2
46	S100a8	M83218	2.2
47	Il8rb	L13239	2.1
48	Tcrb-J	M20878	2.1
49	Slfn2	AF099973	2.1
50	Il7r	M29697	2.1
51	Cd72	J04170	2.0
52	Cd3d	X02339	2.0
53	Tcrg-V4	M18858	2.0
54	membrane glycoprotein	Z22552	2.0
55	Adam8	X13335	2.0
56	Ccr5	AV370035	2.0
57	Ptprc	M14343	2.0
58	Blr1	X71788	2.0
59	Igh-4	X02466	1.9
60	Mmp9	X72795	1.9
61	Lrmp	U10484	1.9
62	Reg3g	D63362	1.9
63	Slfn2	AF099973	1.9
64	Ncf4	U59488	1.9
65	Pla2g7	U34277	1.9
66	Tcrb-V13	M26056	1.9
67	Pirb	AF038149	1.8
68	Pik3cd	AW124359	1.8
69	Mtv-7 sag	M90535	1.8
70	Ptpn8	M90388	1.8
71	Gpcr25	U39827	1.8
72	VK gene for kappa light chain V	X16678	1.8
73	Galgt1	U18975	1.8
74	Pstpip1	U87814	1.8
75	Rac2	X53247	1.8
76	Angptl4	AA797604	1.8
77	C1qb	M22531	1.8
78	Zap70	U04379	1.8
79	2810462M08Rik	AI842128	1.8
80	Clca1	AF047838	1.8
81	Lcn2	X81627	1.7
82	Casp1	L28095	1.7
83	Arg2	AF032466	1.7
84	Blnk	AF068182	1.7
85	Vig1-pending	AA204579	1.7
86	Sprr2a	AJ005559	1.7
87	C4	X06454	1.7
88	C430015F12Rik	L31532	1.7
89	Clecsf8	AF061272	1.7
90	Ccl9	U49513	1.7
91	Kcnab2	U65592	1.7
92	Evl	AV371846	1.7
93	H2-DMb1	U35330	1.7

94	3300002C04Rik	AA874490	1.7
95	2010309G21Rik	J00592	1.7
96	Selpl	X91144	1.7
97	Tcra-J	AF099808	1.7
98	C76770	C76770	1.6
99	Nfe2	L09600	1.6
100	Evi2	M34896	1.6
101	Acp5	M99054	1.6
102	Ly86	AB007599	1.6
103	Gatm	AI844626	1.6
104*	**Clca3***	**AV373378**	**1.6**
105	Ig Vkappa-PCG-4	X82691	1.6
106	Lck	M12056	1.6
107	Cd79b	J03857	1.6
108	Sema4a	X85991	1.6
109	Apbb1ip-pending	AF020313	1.6
110	Ptprc	M23158	1.6
111	Vav1	D83266	1.6
112	C3	K02782	1.6
113	Wbscr5	AW125574	1.6
114	Cd22	L02844	1.6
115	Ifi1	U19119	1.5
116	Laptm5	AV356071	1.5
117	Klrd1	AF030311	1.5
118	Cd37	U18372	1.5
119	Mest	AF017994	1.5
120	Gp49a	M65027	1.5
121	Blk	M30903	1.5
122	Was	U42471	1.5
123	Blk	AA204265	1.5
124	AW123773	AW123773	1.5
125	Slpi	AF002719	1.5
126	2310061N23Rik	AI158810	1.5
127	Asb3	AV347947	1.5
128	Gdi2	U07951	1.5
129	Ada	M14167	1.5
130	Prkcb	X59274	1.5
131	Usp18	AW047653	1.5
132	Igh-6	X94420	1.5
133*	**Slc22a5***	**AB015800**	**1.5**
134	Ncf2	AB002664	1.5
135	2310035M22Rik	AI851230	1.5
136	Sp100	AF040242	1.5
137	Prg	M34603	1.5
138	6430511D02Rik	AI835274	1.5
139	Rps6ka4	AF074714	1.5
140	Ifi204	M31419	1.4
141	Ebna1bp2	AI845934	1.4
142	Igh-6	V00821	1.4
143	C79764	C79764	1.4

144	Tyrobp	AF024637	1.4
145	Ccl6	AV373027	1.4
146	Dp1l1	AA755260	1.4
147	Prss25	AW047978	1.4
148	AF027865	AF027865	1.4
149	1500034J01Rik	AW046728	1.4
150	Angptl4	AI326963	1.4
151	Cyp7b1	U36993	1.4
152	Gfra1	AF014117	1.4
153	Col14a1	AJ131395	1.4
154	Sp100	AF040242	1.4
155	Tk2	AI843384	1.4
156	Unc93b	AW215456	1.4
157	MGC37568	AI117236	1.4
158	Mrvi1	AI157017	1.4
159	beta-actin	M12481_5_st	1.4
160	Sepr	AI840996	1.4
161	Ptpn18	U49853	1.4
162	Hcph	M68902	1.4
163	Mtf2	S78454	1.4
164	Itk	D14042	1.4
165	Stk10	D89728	1.4
166	Apobec1	U22262	1.4
167	2010005I16Rik	AW122355	1.4
168	0910001A06Rik	AA981015	1.4
169	Col1a1	U03419	1.4
170	Gjb2	M81445	1.4
171	Rbm10	AI842108	1.4
172	Kcnj8	D88159	1.4
173	Lsp1	AV122642	1.4
174	Pscdbp	AI120844	1.4
175	Mmp11	Z12604	1.4
176	Facl2	U15977	1.4
177	Mas1	X67735	1.4
178	2810470K21Rik	AI427631	1.4
179	Casp3	U54803	1.3
180	membrane glycoprotein	Z22552	1.3
181	Cp	U49430	1.3
182	Rgs10	AI847399	1.3
183	2900057C09Rik	AI152789	1.3
184	Pde7a	U68171	1.3
185	Ifit3	U43086	1.3
186	C79673	AA709534	1.3
187	Gprk6	Y15798	1.3
188	1200009F10Rik	AA177621	1.3
189	Evl	U72519	1.3
190	Slpi	AV090497	1.3
191	Gsr	AI851983	1.3
192	Ccnb2	X66032	1.3
193	Rfc2	AA597246	1.3

194	Lcp1	D37837	1.3
195	Tuba7	M13443	1.3
196	Trp53	AB021961	1.3
197	AW457192	AI842675	1.3
198	Rpo1-4	AF000938	1.3
199	Inpp5d	U51742	1.3
200	1300002F13Rik	AW212475	1.3
201	AA675320	AI835624	1.3
202	Slc7a5	AB017189	1.3
203	5430401D19Rik	AI426400	1.3
204	Hpn	AF030065	1.3
205	Bid	U75506	1.3
206	Ddx6	AF038995	1.3
207	Narg1	AW260482	1.3
208	2810417H13Rik	AI122538	1.3
209	Tccr	AF053005	1.3
210	H2A.1	M33988	1.3
211	Rb1	M26391	1.3
212	Pou2af1	Z54283	1.3
213	D10Ertd214e	AI848453	1.3
214	Scn1b	L48687	1.3
215	Mrps15	AI836029	1.3
216	D11Bwg0280e	AW125462	1.3
217	Cpt1a	AF017175	1.3
218	Mknk2	AI845732	1.3
219	Siat1	AI117157	1.3
220	1110057K04Rik	AI851901	1.3
221	1300013B24Rik	AI049144	1.3
222	Sfxn1	AI846308	1.3
223	Il6ra	X51975	1.3
224	Nfatc3	D85612	1.2
225	E330027G05Rik	C77335	1.2
226	Gpr97	AI504074	1.2
227	Glud	X57024	1.2
228	Il16	AF017111	1.2
229	Ian1	AA795946	1.2
230	AI225904	AA711773	1.2
231	Cirbp	D78135	1.2
232	Gltscr2	AI844754	1.2
233	H2ls	AF010452	1.2
234	Etv1	L10426	1.2
235	T11 class I MHC	X16217	1.2
236	BC034204	AW121931	1.2
237	Itgax	AI035495	1.2
238	2400006P09Rik	AW049122	1.2
239	Pscdbp	AI120844	1.2
240	Zfp118	AB024004	1.2
241	Hk2	Y11666	1.2
242	Emu2-pending	AA260139	1.2
243	Lat	AF036907	1.2

244	Tnfrsf1b	X87128	1.2
245	Il15ra	U22339	1.2
246	Tmsb10	AI852553	1.2
247	Hn1	U90123	1.2
248	C85523	C85523	1.2
249	D2Ertd120e	AW121972	1.2
250	Smap1-pending	AI843662	1.2
251	D19Wsu55e	AW122465	1.2
252	Rpl26	X80699	1.2
253	Bet1l	AF003999	1.2
254	Sema4b	AA266467	1.2
255	Bcl2a1b	U23778	1.2
256	2900055D03Rik	AI839395	1.2
257	Ctsh	U06119	1.2
258	Mcmd7	D26091	1.2
259	LOC270138	AI882555	1.2
260	2810405F18Rik	AI646411	1.2
261	Ubce7ip3-pending	AW049735	1.2
262	Rga	X96618	1.2
263	Tpm2	M81086	1.2
264	1300004C11Rik	AW050133	1.2
265	Crlf3	AF046060	1.2
266	Grn	D16195	1.2
267	1200010B10Rik	AI838398	1.2
268	C330008I15Rik	AI844780	1.2
269	D10Wsu52e	AI842208	1.2
270	zinc finger protein	D10627	1.2
271	H2-Ke6	AF100956	1.2
272	Jak1	AI837528	1.2
273	Akt2	U22445	1.1
274	Utx	AJ002730	1.1
275	Mic2l1	AW050035	1.1
276	1110002G11Rik	AI843106	1.1
277	Stxbp2	U19520	1.1
278	D9Bwg1455e	AW045278	1.1
279	Mrpl54	AW060257	1.1
280	Mrpl13	AA666635	1.1
281	2510042P03Rik	AI839518	1.1
282	Ptgs1	M34141	1.1
283	E030024M05Rik	AI553536	1.1
284	D7Ertd784e	AI850288	1.1
285	Tsc1	AI837319	1.1
286	Crip	M13018	1.1
287	C1r	AI132585	1.1
288	Capg	X54511	1.1
289	Mel	AI842492	1.1
290	BC006874	AW046452	1.1
291	Chrac1	AA967263	1.1
292	Cltc	AI840975	1.0
293	Clptm1	D67067	0.9

294	Pafah1b2	AI846932	0.9
295	AA589632	AI840149	0.9
296	Smarcb1	AJ011740	0.9
297	dodecenoyl-CoA delta-isomerase	Z14050	0.9
298	Chp-pending	AW124902	0.9
299	Ndufa7	AF110520	0.9
300	4921505F14Rik	AW123936	0.9
301	Gsn	J04953	0.9
302	Maged1	AB029448	0.9
303	2010321M09Rik	AW050142	0.9
304	B930007L02Rik	AA117417	0.9
305	Nfe2l1	X78709	0.9
306	5230400G24Rik	AI842068	0.9
307	Prkrir	AA879937	0.9
308	0610011B04Rik	AI848871	0.9
309	2310075E07Rik	AI845915	0.9
310	1810011O01Rik	AI852592	0.9
311	Cyb5	AI854779	0.9
312	1500010B24Rik	AI849718	0.9
313	Tpm1	M22479	0.9
314	Gtr2	AB017616	0.9
315	Ercc2	AI843631	0.9
316	Tmod3	AI846797	0.9
317	Gng5	AI843937	0.9
318	Ear2	AF017258	0.9
319	Clic4	AI849533	0.9
320	1110033L15Rik	AW047074	0.9
321	2810405J04Rik	AA855382	0.9
322	Ptprs	X82288	0.9
323	Sox10	AF047389	0.9
324	0610033L03Rik	AI853855	0.9
325	CDC10	AJ223782	0.9
326	LOC225028	AW121182	0.9
327	2410112D09Rik	AW124983	0.9
328	Catns	AW122407	0.9
329	Pvrl2	M80206	0.9
330	1810011O01Rik	AI852592	0.9
331	LOC229543	AW124061	0.9
332	Igfbp4	X76066	0.9
333	1110002H15Rik	AI851810	0.9
334	1110005L13Rik	AW047746	0.9
335	Hop-pending	AW123564	0.9
336	MGC27648	AW123477	0.9
337	1110014L17Rik	AW122685	0.9
338	Fasn	X13135	0.9
339	Atf4	M94087	0.9
340	Ict1	AI844357	0.9
341	AW123016	AW123016	0.9
342	S100a6	X66449	0.9
343	Ugalt2	D87990	0.9

344	Cav3	AV023068	0.9
345	AA407930	AI841579	0.9
346	Tuba1	M28729	0.9
347	2010100O12Rik	AI853864	0.9
348	D2Bwg0891e	AW121364	0.9
349	Fkbp9	AF090334	0.8
350	AI849416	AI849416	0.8
351	B230114J08Rik	AW124185	0.8
352	KIAA0678	AI842938	0.8
353	5330419I01Rik	AA840409	0.8
354	Zfp101	U07861	0.8
355	Ube2i	U82627	0.8
356	Mrpl27	AI844807	0.8
357	Zfp144	AI503821	0.8
358	Igsf4	AF061260	0.8
359	Mylc2a	AA839903	0.8
360	Hoxb5	M26283	0.8
361	AI430822	AI853294	0.8
362	S100a13	X99921	0.8
363	2500002L14Rik	AW061255	0.8
364	Tm4sf2	D26483	0.8
365	H5	X61452	0.8
366	Atp7a	U03434	0.8
367	Ager	L33412	0.8
368	Dnclc1	AF020185	0.8
369	Zfp288	AI987985	0.8
370	3110065C23Rik	AI159572	0.8
371	2510005D08Rik	AW045965	0.8
372	Cds2	AW121668	0.8
373	Vcl	AI462105	0.8
374	Flt1	D88689	0.8
375	2610200G18Rik	AV334573	0.8
376	9030616F16	AI851119	0.8
377*	**Cyp4b1***	**D50834**	**0.8**
378	B4galt1	M27923	0.8
379	1200017E04Rik	AI852087	0.8
380	Actc1	M15501	0.8
381	Polr2g	AI836182	0.8
382	Cry1	AB000777	0.8
383	Myo1b	L00923	0.8
384	Car4	U37091	0.8
385	Gcnt2	AI844853	0.8
386	Cdc5l	AI848968	0.8
387*	**Aqp4***	**U88623**	**0.8**
388	X83328	AW211667	0.8
389	1190002F15Rik	AV367141	0.8
390	Rex3	AA790008	0.8
391	Atp5l	Y17223	0.8
392	Slc15a2	AI846682	0.8
393	Thra	AI841022	0.8

394	Dnaja3	AW060270	0.8
395	1810045K17Rik	AI851104	0.8
396	AI851258	AI851258	0.8
397	Gstm1	AI841270	0.8
398	Ube2a	AF089812	0.8
399	Ogn	AA647799	0.8
400	Itgb1bp1	AJ001373	0.8
401	Osf2-pending	D13664	0.8
402	Stx6	AW124355	0.8
403	Eppb9	AB030483	0.8
404	D12Ertd7e	AI156978	0.8
405	Fnta	D49744	0.8
406	D130005A03	AV360914	0.8
407	Oazin	AF032128	0.8
408	Hes1	D16464	0.8
409	Sgcb	AB024921	0.8
410	1200003F12Rik	AW124271	0.8
411	AA648027	AA648027	0.8
412	1190002N15Rik	AW125453	0.8
413	Crlf1	AA270365	0.8
414	1110033C18Rik	AI839522	0.8
415	Idb3	M60523	0.8
416	Gja1	M63801	0.8
417	G0s2	X95280	0.8
418	Tuft1	AF047704	0.7
419	Mtcp1	Z35294	0.7
420	8430426K15Rik	AI451008	0.7
421	Cct3	AV268209	0.7
422	Slc30a1	U17132	0.7
423	stanniocalcin	U47815	0.7
424	Tstap35b	AV171573	0.7
425	2400004O09Rik	AI846893	0.7
426	EIG180	AB023957	0.7
427	AI987814	AW121801	0.7
428	Elovl1	AI842813	0.7
429	Efna1	U90662	0.7
430	Ldlr	Z19521	0.7
431	Gadd45b	AV138783	0.7
432	Ptprb	X58289	0.7
433	Prnp	M18070	0.7
434	Ywhaq	U56243	0.7
435	Cmkor1	AF000236	0.7
436	2600017P15Rik	AI846542	0.7
437	Aard	AI390412	0.7
438	Ephb3	Z49086	0.7
439	Psen1	L42177	0.7
440	Orc2l	AV094683	0.6
441	Igsf4	AF061260	0.6
442	Epha8	U72207	0.6
443	Cntn1	X14943	0.6

444	Bysl	AI132491	0.6
445	Pcdha6	D86917	0.6

* References (64;78)

APPENDIX IV

List of other published manuscripts

1. Dagenais A, Gosselin D, **Guilbault C**, Radzioch D, Berthiaume Y. Modulation of epithelial sodium channel (ENaC) expression in mouse lung infected with Pseudomonas aeruginosa. Respiratory Research. Respiratory Research. 2005 Jan 6; 6(1):2.

2. Moisan, J., Wojciechowski, W., **Guilbault, C.**, Lachance, C., Di Marco, S., Skamene, E., Matlashewski, G., Radzioch, D. Clearance of infection with Mycobacterium bovis BCG in mice is enhanced by treatment with S28463 (R-848), and its efficiency depends on expression of wild-type Nramp1 (resistance allele). Antimicrobial agents and chemotherapy. 2001 Nov; 45 (11): 3059-3064

3. Cowley, EA., Govindaraju, K., **Guilbault, C.**, Radzioch, D., Eidelman, D. Airway surface liquid composition in mice. American Journal of Physiology Lung Cellular and Molecular Physiology. 2000 Jun; 278 (6):L1213-L1220.

APPENDIX V

List of abstracts and published Conference Proceedings

Conference Proceedings:

1. **Guilbault, C**.; Martin, P.; Boghdady, M-L.; Novak, J. P.; Guiot, M-C.; Radzioch, D. Gene expression analysis of the lungs using a cystic fibrosis mouse model developing spontaneous lung disease. Pediatric Pulmonology, 2000 Oct; 38 (S27): 220.

2. **Guilbault, C**., Nelson, A., Martin, P., Guiot, M-C., DeSanctis, J.B., Radzioch, D. Reduction of lung inflammation by DHA in CFTR knockout mice developing spontaneous lung disease. 12th International Congress of Immunology and 4th Annual Conference of FOCIS, Montreal, Quebec, July 18-23, 2004 (published as an extended abstract in Immunology 2004: 79-88)

3. **Guilbault, C**; Lachance, C; Tam, M. F; Keller, A; Thompson-Snipes, LA; Cowley, E; Eidelman, D; Stevenson, M; Radzioch, D. Inflammatory Response in C57BL/6-IL-10 Knockout Mice During Chronic Lung Infection with *Pseudomonas aeruginosa*. Pediatric Pulmonology, 1999 Oct; 28 (S19): 312.

4. **Guilbault, C**., Stotland, P., Thanassoulis, G., Shiff, D., Cowley, E., Matouk, K., Eidelman, D., Stevenson, M.M., Radzioch, D. Role of inflammatory cytokines in modulation of chronic lung infection with *Pseudomonas aeruginosa* in *Cftr*-knockout mice and other mouse models. Clinical Microbiology and Infection; 1999 5: 5S38-5S39.

5. Radzioch, D., Downey, G., Stotland, P., **Guilbault, C**., Cherepanov, V., Shiff, D., Thanaussoulis, G., Matouk, K., Cowley, L., Eidelman, D., Stevenson, M. Role of inflammatory cytokines in modulating susceptibility to chronic pulmonary infection with *P. aeruginosa* in Cftr-knockout mice and different inbred strains of mice. Pediatric Pulmonology, 1998 Oct; 26 (S17): 102-103.

6. Moltyaner, Y., Thanassoulis, G., Kent, G., Radzioch, D., **Guilbault, C**., Cherapanov, V., Downey, G.P. Influence of genetic background on inflammation and immune dysregulation in cystic fibrosis murine model. The Twelfth Annual North American CF Conference. Pediatric Pulmonology, 1998 Oct; 26 (S17).

Other abstracts:

7. Divangahi, M., **Guilbault, C.**, Radzioch, D., Bao, W., Comtois, A.S., Petrof, B.J. Increased susceptibility of Cftr knockout mice to diaphragm dysfunction after *Pseudomonas* lung infection. The ATS 2003 - Seattle, 99th International Conference. Seattle, Washington, May 16-21, 2003.

8. Moisan, J., Wojciechowski, W., **Guilbault, C.**, Lachance, C., DiMarco, S., Matlashewski, G., Radzioch. Clearance of infection with *M.bovis* BCG in mice is enhanced by the treatment with imidazoquinolines and requires the expression of a wild type (resistant allele) of the *Nrampl* gene. Fiftheenth Spring Meetings of Canadian Society for Immunology, Lake Louise, 2001.

9. Moisan, J., Wojciechowski, W., **Guilbault, C.**, Lachance, C., DiMarco, S., Matlashewski, G., Radzioch. Efficacité des imidazoquinolines contre une infection avec *M. bovis BCG* requiert l'activite de Nrampl. La 43ieme réunion annuelle de CRCQ, Mont St-Anne, Québec, Septembre, 2001.

10. Radzioch, D., Shiff, D., Eidelman, D., Stevenson, M.M., **Guilbault, C.** Regulation of inflammatory responses in a murine model of CF lung disease. Canadian Cystic Fibrosis Foundation - Eleventh Broken Arrow Conference, Antimicrobial therapies in cystic fibrosis. Toronto, Ontario. September 2001.

11. **Guilbault, C.**, Lachance, C., Tam, M.F., Keller, A., Thompson-Snipes, L., Cowley, E., Eidelman, D.H., Stevenson, M.M., Radzioch, D. Influence of gender and IL-10 deficiency on the inflammatory response during chronic lung infection with *Pseudomonas aeruginosa.* The First Annual McGill University Health Center Respiratory Axis Research Day. October 2000.

12. Thanassoulis, G., Matouk, K., DiMarco, S., **Guilbault, C.**, Radzioch, D. IL-10 regulates the expression of TNF-alpha post-transcriptionally in mouse macrophages. Thirteenth Spring Meetings of Canadian Society for Immunology, Lake Louise, March 1999.

13. **Guilbault, C.**, Stotland, P., Thanassoulis, G., Shiff, D., Cowley, E., Matouk, K., Eidelman, D., Stevenson, M., D. Radzioch, D. Role of inflammatory cytokines in modulation of chronic lung infection in *Cftr*-knockout mice and other mouse models. Basic and Clinical Research of Chronic *Pseudomonas aeruginosa* Lung Infection in Cystic Fibrosis and Diffuse Panbronchiolitis, Copenhagen, March 1999.

14. Di Marco, S., Hel, Z., **Guilbault, C.**, Radzioch, D. The effects of LPS, PMA, and IFNgamma on the regulation of TNFalpha production at the posttranscriptional level. The Experimental Medecine Graduate Society of McGill University 3rd Annual Poster Day, Montreal, Quebec, June 1998.

15. **Guilbault, C.**, Stotland, P., Gosselin, D., Cowley, E., Eidelman, D., Kent, G., Tsui, L-C, Stevenson, M., Radzioch, D. Susceptibility to *Pseudomonas* infection of C57BL6-Cftr-knockout mice. Conference on Animal Models. Paris, May 1998.

16. Radzioch, D., **Guilbault, C.**, Stotland, P., Gosselin, D., Dagenais, A., Cowley, L., Ding, A., Berthiaume, Y., Tsui, L-C., Eidelman, D., Stevenson, M. Regulation of gene expression in *Cftr*-knockout mice infected with *P. aeruginosa.* Canadian Cystic Fibrosis Foundation - Tenth Broken Arrow Conference. Mississauga, Ontario. March 1998.

17. Di Marco, S., Hel, Z., **Guilbault, C.**, Radzioch, D. Regulation of TNF production at the posttranscriptional level by LPS, PMA, and IFN-gamma Do TNFalpha 3'UTR mRNA binding proteins play a role? Twelve Spring Meeting of the Canadian Society for Immunology. Saint-Adele. March 1998

APPENDIX VI

Certificates of compliance

Animal use protocol

Radioactivity certificate

Reference List

1. Akabas MH (2000). Cystic fibrosis transmembrane conductance regulator. Structure and function of an epithelial chloride channel. *J Biol Chem* **275**, 3729-3732.

2. Angele MK, Knoferl MW, Schwacha MG, Ayala A, Cioffi WG, Bland KI, & Chaudry IH (1999). Sex steroids regulate pro- and anti-inflammatory cytokine release by macrophages after trauma-hemorrhage. *Am J Physiol* **277**, C35-C42.

3. Arkwright PD, Laurie S, Super M, Pravica V, Schwarz MJ, Webb AK, & Hutchinson IV (2000). TGF-beta(1) genotype and accelerated decline in lung function of patients with cystic fibrosis. *Thorax* **55**, 459-462.

4. Armitage RJ, Macduff BM, Eisenman J, Paxton R, & Grabstein KH (1995). IL-15 has stimulatory activity for the induction of B cell proliferation and differentiation. *J Immunol* **154**, 483-490.

5. Armstrong L & Millar AB (1997). Relative production of tumour necrosis factor alpha and interleukin 10 in adult respiratory distress syndrome. *Thorax* **52**, 442-446.

6. Asai K, Hiki N, Mimura Y, Ogawa T, Unou K, & Kaminishi M (2001). Gender differences in cytokine secretion by human peripheral blood mononuclear cells: role of estrogen in modulating LPS-induced cytokine secretion in an ex vivo septic model. *Shock* **16**, 340-343.

7. Ashcroft GS, Lei K, Jin W, Longenecker G, Kulkarni AB, Greenwell-Wild T, Hale-Donze H, McGrady G, Song XY, & Wahl SM (2000). Secretory leukocyte protease inhibitor mediates non-redundant functions necessary for normal wound healing. *Nat Med* **6**, 1147-1153.

8. bbinante-Nissen JM, Simpson LG, & Leikauf GD (1993). Neutrophil elastase increases secretory leukocyte protease inhibitor transcript levels in airway epithelial cells. *Am J Physiol* **265**, L286-L292.

9. Bebo BF, Jr., Schuster JC, Vandenbark AA, & Offner H (1999). Androgens alter the cytokine profile and reduce encephalitogenicity of myelin-reactive T cells. *J Immunol* **162**, 35-40.

10. Bedrossian CW, Greenberg SD, Singer DB, Hansen JJ, & Rosenberg HS (1976). The lung in cystic fibrosis. A quantitative study including prevalence of pathologic findings among different age groups. *Hum Pathol* **7**, 195-204.

11. Bedwell DM, Kaenjak A, Benos DJ, Bebok Z, Bubien JK, Hong J, Tousson A, Clancy JP, & Sorscher EJ (1997). Suppression of a CFTR premature stop mutation in a bronchial epithelial cell line. *Nat Med* **3**, 1280-1284.

12. Berger M (1991). Inflammation in the lung in cystic fibrosis. A vicious cycle that does more harm than good? *Clin Rev Allergy* **9**, 119-142.

13. Bermudez LE & Champsi J (1993). Infection with Mycobacterium avium induces production of interleukin-10 (IL-10), and administration of anti-IL-10 antibody is associated with enhanced resistance to infection in mice. *Infect Immun* **61**, 3093-3097.

14. Bingle L & Tetley TD (1996). Secretory leukoprotease inhibitor: partnering alpha 1-proteinase inhibitor to combat pulmonary inflammation. *Thorax* **51**, 1273-1274.

15. Bolstad BM, Irizarry RA, Astrand M, & Speed TP (2003). A comparison of normalization methods for high density oligonucleotide array data based on variance and bias. *Bioinformatics* **19**, 185-193.

16. Bonfield TL, Konstan MW, & Berger M (1999). Altered respiratory epithelial cell cytokine production in cystic fibrosis. *J Allergy Clin Immunol* **104**, 72-78.

17. Bonfield TL, Konstan MW, Burfeind P, Panuska JR, Hilliard JB, & Berger M (1995). Normal bronchial epithelial cells constitutively produce the anti-inflammatory cytokine interleukin-10, which is downregulated in cystic fibrosis. *Am J Respir Cell Mol Biol* **13**, 257-261.

18. Bonfield TL, Panuska JR, Konstan MW, Hilliard KA, Hilliard JB, Ghnaim H, & Berger M (1995). Inflammatory cytokines in cystic fibrosis lungs [published erratum appears in Am J Respir Crit Care Med 1996 Oct;154(4 Pt 1):following 1217]. *Am J Respir Crit Care Med* **152**, 2111-2118.

19. Borthwick DW, West JD, Keighren MA, Flockhart JH, Innes BA, & Dorin JR (1999). Murine submucosal glands are clonally derived and show a cystic fibrosis gene-dependent distribution pattern. *Am J Respir Cell Mol Biol* **20**, 1181-1189.

20. Boucher RC (1999). Status of gene therapy for cystic fibrosis lung disease. *J Clin Invest* **103**, 441-445.

21. Boucher RC, Cheng EH, Paradiso AM, Stutts MJ, Knowles MR, & Earp HS (1989). Chloride secretory response of cystic fibrosis human airway epithelia. Preservation of calcium but not protein kinase C- and A-dependent mechanisms. *J Clin Invest* **84**, 1424-1431.

22. Boujaoude LC, Bradshaw-Wilder C, Mao C, Cohn J, Ogretmen B, Hannun YA, & Obeid LM (2001). Cystic fibrosis transmembrane regulator regulates uptake of sphingoid base phosphates and lysophosphatidic acid: modulation of cellular activity of sphingosine 1-phosphate. *J Biol Chem* **276**, 35258-35264.

23. Bowler IM, Green JH, Wolfe SP, & Littlewood JM (1993). Resting energy expenditure and substrate oxidation rates in cystic fibrosis. *Arch Dis Child* **68**, 754-759.

24. Bragonzi A & Conese M (2002). Non-viral approach toward gene therapy of cystic fibrosis lung disease. *Curr Gene Ther* **2**, 295-305.

25. Brennan AL & Geddes DM (2002). Cystic fibrosis. *Curr Opin Infect Dis* **15**, 175-182.

26. Bronsveld I, Mekus F, Bijman J, Ballmann M, de Jonge HR, Laabs U, Halley DJ, Ellemunter H, Mastella G, Thomas S, Veeze HJ, & Tummler B (2001). Chloride conductance and genetic background modulate the cystic fibrosis phenotype of Delta F508 homozygous twins and siblings. *J Clin Invest* **108**, 1705-1715.

27. Bubien JK (2001). CFTR may play a role in regulated secretion by lymphocytes: a new hypothesis for the pathophysiology of cystic fibrosis. *Pflugers Arch* **443 Suppl 1:S36-9. Epub;%2001 Jul 7.**, S36-S39.

28. Burns JL, Gibson RL, McNamara S, Yim D, Emerson J, Rosenfeld M, Hiatt P, McCoy K, Castile R, Smith AL, & Ramsey BW (2001). Longitudinal assessment of Pseudomonas aeruginosa in young children with cystic fibrosis. *J Infect Dis* **183**, 444-452.

29. Cash HA, Woods DE, McCullough B, Johanson WG, Jr., & Bass JA (1979). A rat model of chronic respiratory infection with Pseudomonas aeruginosa. *Am Rev Respir Dis* **119**, 453-459.

30. Chan C & Goldkorn T (2000). Ceramide path in human lung cell death. *Am J Respir Cell Mol Biol* **22**, 460-468.

31. Charles AG, Han TY, Liu YY, Hansen N, Giuliano AE, & Cabot MC (2001). Taxol-induced ceramide generation and apoptosis in human breast cancer cells. *Cancer Chemother Pharmacol* **47**, 444-450.

32. Chmiel JF, Konstan MW, Knesebeck JE, Hilliard JB, Bonfield TL, Dawson DV, & Berger M (1999). IL-10 attenuates excessive inflammation in chronic pseudomonas infection in mice [In Process Citation]. *Am J Respir Crit Care Med* **160**, 2040-2047.

33. Chroneos ZC, Wert SE, Livingston JL, Hassett DJ, & Whitsett JA (2000). Role of cystic fibrosis transmembrane conductance regulator in pulmonary clearance of Pseudomonas aeruginosa in vivo. *J Immunol* **165**, 3941-3950.

34. Clarke LL, Grubb BR, Gabriel SE, Smithies O, Koller BH, & Boucher RC (1992). Defective epithelial chloride transport in a gene-targeted mouse model of cystic fibrosis. *Science* **257**, 1125-1128.

35. Clarke LL, Grubb BR, Yankaskas JR, Cotton CU, McKenzie A, & Boucher RC (1994). Relationship of a non-cystic fibrosis transmembrane conductance regulator-mediated chloride conductance to organ-level disease in Cftr(-/-) mice. *Proc Natl Acad Sci U S A* **91**, 479-483.

36. Clarke LL & Harline MC (1996). CFTR is required for cAMP inhibition of intestinal Na+ absorption in a cystic fibrosis mouse model. *Am J Physiol* **270**, G259-G267.

37. Coakley RD & Boucher RC (2001). Regulation and functional significance of airway surface liquid pH. *JOP* **2**, 294-300.

38. Colledge WH, Abella BS, Southern KW, Ratcliff R, Jiang C, Cheng SH, MacVinish LJ, Anderson JR, Cuthbert AW, & Evans MJ (1995). Generation and characterization of a delta F508 cystic fibrosis mouse model. *Nat Genet* **10**, 445-452.

39. Collins FS (1992). Cystic fibrosis: molecular biology and therapeutic implications. *Science* **256**, 774-779.

40. Costa A, De PG, Decensi A, Formelli F, Chiesa F, Nava M, Camerini T, Marubini E, & Veronesi U (1995). Retinoids in cancer chemoprevention. Clinical trials with the synthetic analogue fenretinide. *Ann N Y Acad Sci* **768:148-62.**, 148-162.

41. Cowley EA, Govindaraju K, Guilbault C, Radzioch D, & Eidelman DH (2000). Airway surface liquid composition in mice. *Am J Physiol Lung Cell Mol Physiol* **278**, L1213-L1220.

42. Cressman VL, Hicks EM, Funkhouser WK, Backlund DC, & Koller BH (1998). The relationship of chronic mucin secretion to airway disease in normal and CFTR-deficient mice. *Am J Respir Cell Mol Biol* **19**, 853-866.

43. Cuthbert AW, Halstead J, Ratcliff R, Colledge WH, & Evans MJ (1995). The genetic advantage hypothesis in cystic fibrosis heterozygotes: a murine study. *J Physiol* **482**, 449-454.

44. Cutolo M, Accardo S, Villaggio B, Barone A, Sulli A, Coviello DA, Carabbio C, Felli L, Miceli D, Farruggio R, Carruba G, & Castagnetta L (1996). Androgen and estrogen receptors are present in primary cultures of human synovial macrophages. *J Clin Endocrinol Metab* **81**, 820-827.

45. Cutolo M, Sulli A, Seriolo B, Accardo S, & Masi AT (1995). Estrogens, the immune response and autoimmunity. *Clin Exp Rheumatol* **13**, 217-226.

46. D'Agostino P, Milano S, Barbera C, Di Bella G, La Rosa M, Ferlazzo V, Farruggio R, Miceli DM, Miele M, Castagnetta L, & Cillari E (1999). Sex hormones modulate inflammatory mediators produced by macrophages. *Ann N Y Acad Sci* **876**, 426-429.

47. Dalemans W, Barbry P, Champigny G, Jallat S, Dott K, Dreyer D, Crystal RG, Pavirani A, Lecocq JP, & Lazdunski M (1991). Altered chloride ion channel kinetics associated with the delta F508 cystic fibrosis mutation. *Nature* **354**, 526-528.

48. Davidson DJ, Dorin JR, McLachlan G, Ranaldi V, Lamb D, Doherty C, Govan J, & Porteous DJ (1995). Lung disease in the cystic fibrosis mouse exposed to bacterial pathogens. *Nat Genet* **9**, 351-357.

49. Davidson DJ & Porteous DJ (1998). Genetics and pulmonary medicine. 1. The genetics of cystic fibrosis lung disease. *Thorax* **53**, 389-397.

50. Davidson DJ & Rolfe M (2001). Mouse models of cystic fibrosis. *Trends Genet* **17**, S29-S37.

51. Davidson NJ, Leach MW, Fort MM, Thompson-Snipes L, Kuhn R, Muller W, Berg DJ, & Rennick DM (1996). T helper cell 1-type CD4+ T cells, but not B cells, mediate colitis in interleukin 10-deficient mice. *J Exp Med* **184**, 241-251.

52. Davies JC (2002). New therapeutic approaches for cystic fibrosis lung disease. *J R Soc Med* **95 Suppl 41**, 58-67.

53. Davies JC (2002). Pseudomonas aeruginosa in cystic fibrosis: pathogenesis and persistence. *Paediatr Respir Rev* **3**, 128-134.

54. Davis PB (1999). The gender gap in cystic fibrosis survival. *J Gend Specif Med* **2**, 47-51.

55. Davis PB, Drumm M, & Konstan MW (1996). Cystic fibrosis. *Am J Respir Crit Care Med* **154**, 1229-1256.

56. de Braekeleer M, Mari G, Verlingue C, Allard C, Leblanc JP, Simard F, Aubin G, & Ferec C (1997). Clinical features of cystic fibrosis patients with rare genotypes in Saguenay Lac-Saint-Jean (Quebec, Canada). *Ann Genet* **40**, 205-208.

57. de GJ, Kruijt L, Scholten JW, Boersma WJ, Buist WG, Engel B, & van Reenen CG (2005). Age, gender and litter-related variation in T-lymphocyte cytokine production in young pigs. *Immunology* **115**, 495-505.

58. Delaney SJ, Alton EW, Smith SN, Lunn DP, Farley R, Lovelock PK, Thomson SA, Hume DA, Lamb D, Porteous DJ, Dorin JR, & Wainwright BJ (1996). Cystic fibrosis mice carrying the missense mutation G551D replicate human genotype-phenotype correlations. *EMBO J* **15**, 955-963.

59. Demko CA, Byard PJ, & Davis PB (1995). Gender differences in cystic fibrosis: Pseudomonas aeruginosa infection. *J Clin Epidemiol* **48**, 1041-1049.

60. Dickinson P, Smith SN, Webb S, Kilanowski FM, Campbell IJ, Taylor MS, Porteous DJ, Willemsen R, de Jonge HR, Farley R, Alton EW, & Dorin JR (2002). The severe G480C cystic fibrosis mutation, when replicated in the mouse, demonstrates mistrafficking, normal survival and organ-specific bioelectrics. *Hum Mol Genet* **11**, 243-251.

61. Djouadi F, Weinheimer CJ, Saffitz JE, Pitchford C, Bastin J, Gonzalez FJ, & Kelly DP (1998). A gender-related defect in lipid metabolism and glucose homeostasis in peroxisome proliferator- activated receptor alpha- deficient mice. *J Clin Invest* **102**, 1083-1091.

62. Dobbin CJ, Soni R, Jelihovsky T, & Bye PT (2000). Cepacia syndrome occurring following prolonged colonisation with Burkholderia cepacia. *Aust N Z J Med* **30**, 288-289.

63. Doniger SW, Salomonis N, Dahlquist KD, Vranizan K, Lawlor SC, & Conklin BR (2003). MAPPFinder: using Gene Ontology and GenMAPP to create a global gene-expression profile from microarray data. *Genome Biol* **4**, R7.

64. Dorfman R, Sandford A, Markiewicz D, Master A, Deng G, Patel M, Corey M, Yuan X, Tan M, Li F, Frangolias DD, Sun L, Pare P, Durie P, Tsui LC, & Zielenski J. Analysis of candidate genes as modifiers of cystic fibrosis. Pediatr.Pulmonol. supplement 27, 220-221. 2004.
Ref Type: Abstract

65. Dorin JR, Dickinson P, Alton EW, Smith SN, Geddes DM, Stevenson BJ, Kimber WL, Fleming S, Clarke AR, Hooper ML, & . (1992). Cystic fibrosis in the mouse by targeted insertional mutagenesis. *Nature* **359**, 211-215.

66. Dorin JR, Dickinson P, Emslie E, Clarke AR, Dobbie L, Hooper ML, Halford S, Wainwright BJ, & Porteous DJ (1992). Successful targeting of the mouse cystic fibrosis transmembrane conductance regulator gene in embryonal stem cells. *Transgenic Res* **1**, 101-105.

67. Dorin JR, Emslie E, & van H, V (1990). Related calcium-binding proteins map to the same subregion of chromosome 1q and to an extended region of synteny on mouse chromosome 3. *Genomics* **8**, 420-426.

68. Dorin JR, Novak M, Hill RE, Brock DJ, Secher DS, & van H, V (1987). A clue to the basic defect in cystic fibrosis from cloning the CF antigen gene. *Nature* **326**, 614-617.

69. Dosanjh AK, Elashoff D, & Robbins RC (1998). The bronchoalveolar lavage fluid of cystic fibrosis lung transplant recipients demonstrates increased interleukin-8 and elastase and decreased IL-10. *J Interferon Cytokine Res* **18**, 851-854.

70. Du M, Jones JR, Lanier J, Keeling KM, Lindsey JR, Tousson A, Bebok Z, Whitsett JA, Dey CR, Colledge WH, Evans MJ, Sorscher EJ, & Bedwell DM (2002). Aminoglycoside suppression of a premature stop mutation in a Cftr-/- mouse carrying a human CFTR-G542X transgene. *J Mol Med* **80**, 595-604.

71. Durie PR, Kent G, Phillips MJ, & Ackerley CA (2004). Characteristic multiorgan pathology of cystic fibrosis in a long-living cystic fibrosis transmembrane regulator knockout murine model. *Am J Pathol* **164**, 1481-1493.

72. Eckman EA, Cotton CU, Kube DM, & Davis PB (1995). Dietary changes improve survival of CFTR S489X homozygous mutant mouse. *Am J Physiol* **269**, L625-L630.

73. Egan M, Flotte T, Afione S, Solow R, Zeitlin PL, Carter BJ, & Guggino WB (1992). Defective regulation of outwardly rectifying Cl- channels by protein kinase A corrected by insertion of CFTR. *Nature* **358**, 581-584.

74. Eggermont E & de Boeck K (1991). Small-intestinal abnormalities in cystic fibrosis patients. *Eur J Pediatr* **150**, 824-828.

75. Eidelman O, Srivastava M, Zhang J, Leighton X, Murtie J, Jozwik C, Jacobson K, Weinstein DL, Metcalf EL, & Pollard HB (2001). Control of the proinflammatory state in cystic fibrosis lung epithelial cells by genes from the TNF-alphaR/NFkappaB pathway. *Mol Med* **7**, 523-534.

76. Elborn JS, Cordon SM, Western PJ, Macdonald IA, & Shale DJ (1993). Tumour necrosis factor-alpha, resting energy expenditure and cachexia in cystic fibrosis. *Clin Sci (Colch)* **85**, 563-568.

77. Erdreich-Epstein A, Tran LB, Bowman NN, Wang H, Cabot MC, Durden DL, Vlckova J, Reynolds CP, Stins MF, Groshen S, & Millard M (2002). Ceramide signaling in fenretinide-induced endothelial cell apoptosis. *J Biol Chem* **277**, 49531-49537.

78. Evtoushenko I, Markiewicz D, Deng G, Patel M, Dorfman R, Corey M, Tan M, Li F, Sun L, Sandford A, Pare P, Durie P, Tsui LC, & Zielenski J. Analysis of human chromosome 6q27 region as a potential modifier locus for pulmonary disease in cystic fibrosis. Pediatr.Pulmonol. supplement 27, 221. 2004.
Ref Type: Abstract

79. Farrell PM, Mischler EH, Engle MJ, Brown DJ, & Lau SM (1985). Fatty acid abnormalities in cystic fibrosis. *Pediatr Res* **19**, 104-109.

80. Ferrari N, Morini M, Pfeffer U, Minghelli S, Noonan DM, & Albini A (2003). Inhibition of Kaposi's sarcoma in vivo by fenretinide. *Clin Cancer Res* **9**, 6020-6029.

81. Fiorentino DF, Zlotnik A, Mosmann TR, Howard M, & O'Garra A (1991). IL-10 inhibits cytokine production by activated macrophages. *J Immunol* **147**, 3815-3822.

82. FitzSimmons SC (1993). The changing epidemiology of cystic fibrosis [see comments]. *J Pediatr* **122**, 1-9.

83. FOLCH J, LEES M, & SLOANE STANLEY GH (1957). A simple method for the isolation and purification of total lipides from animal tissues. *J Biol Chem* **226**, 497-509.

84. Freedman SD, Katz MH, Parker EM, Laposata M, Urman MY, & Alvarez JG (1999). A membrane lipid imbalance plays a role in the phenotypic expression of cystic fibrosis in cftr(-/-) mice. *Proc Natl Acad Sci U S A* **96**, 13995-14000.

85. Freedman SD, Shea JC, Blanco PG, & Alvarez JG (2000). Fatty acids in cystic fibrosis. *Curr Opin Pulm Med* **6**, 530-532.

86. French PJ, van Doorninck JH, Peters RH, Verbeek E, Ameen NA, Marino CR, de Jonge HR, Bijman J, & Scholte BJ (1996). A delta F508 mutation in mouse cystic fibrosis transmembrane conductance regulator results in a temperature-sensitive processing defect in vivo. *J Clin Invest* **98**, 1304-1312.

87. Fritsche KL, Anderson M, & Feng C Consumption of eicosapentaenoic acid and docosahexaenoic acid impair murine interleukin-12 and interferon-gamma production In vivo [In Process Citation]. *J Infect Dis 2000 Sep ;182 (## Suppl 1):S54 -61* **182**, S54-S61.

88. Gabolde M, Guilloud-Bataille M, Feingold J, & Besmond C (1999). Association of variant alleles of mannose binding lectin with severity of pulmonary disease in cystic fibrosis: cohort study. *BMJ* **319**, 1166-1167.

89. Gabriel SE, Brigman KN, Koller BH, Boucher RC, & Stutts MJ (1994). Cystic fibrosis heterozygote resistance to cholera toxin in the cystic fibrosis mouse model. *Science* **266**, 107-109.

90. Gabriel SE, Clarke LL, Boucher RC, & Stutts MJ (1993). CFTR and outward rectifying chloride channels are distinct proteins with a regulatory relationship. *Nature* **363**, 263-268.

91. Gandhi R, Elble RC, Gruber AD, Schreur KD, Ji HL, Fuller CM, & Pauli BU (1998). Molecular and functional characterization of a calcium-sensitive chloride channel from mouse lung. *J Biol Chem* **273**, 32096-32101.

92. Garaventa A, Luksch R, Lo Piccolo MS, Cavadini E, Montaldo PG, Pizzitola MR, Boni L, Ponzoni M, Decensi A, De BB, Bellani FF, & Formelli F (2003). Phase I trial and pharmacokinetics of fenretinide in children with neuroblastoma. *Clin Cancer Res* **9**, 2032-2039.

93. Garred P, Voss A, Madsen HO, & Junker P (2001). Association of mannose-binding lectin gene variation with disease severity and infections in a population-based cohort of systemic lupus erythematosus patients. *Genes Immun* **2**, 442-450.

94. Genter MB, Van Veldhoven PP, Jegga AG, Sakthivel B, Kong S, Stanley K, Witte DP, Ebert CL, & Aronow BJ (2003). Microarray-based discovery of highly expressed olfactory mucosal genes: potential roles in the various functions of the olfactory system. *Physiol Genomics* **16**, 67-81.

95. Gilljam H, Strandvik B, Ellin A, & Wiman LG (1986). Increased mole fraction of arachidonic acid in bronchial phospholipids in patients with cystic fibrosis. *Scand J Clin Lab Invest* **46**, 511-518.

96. Giri JG, Ahdieh M, Eisenman J, Shanebeck K, Grabstein K, Kumaki S, Namen A, Park LS, Cosman D, & Anderson D (1994). Utilization of the beta and gamma chains of the IL-2 receptor by the novel cytokine IL-15. *EMBO J* **13**, 2822-2830.

97. Giri JG, Kumaki S, Ahdieh M, Friend DJ, Loomis A, Shanebeck K, DuBose R, Cosman D, Park LS, & Anderson DM (1995). Identification and cloning of a novel IL-15 binding protein that is structurally related to the alpha chain of the IL-2 receptor. *EMBO J* **14**, 3654-3663.

98. Gosselin D, DeSanctis J, Boule M, Skamene E, Matouk C, & Radzioch D (1995). Role of tumor necrosis factor alpha in innate resistance to mouse pulmonary infection with Pseudomonas aeruginosa. *Infect Immun* **63**, 3272-3278.

99. Gosselin D, Stevenson MM, Cowley EA, Griesenbach U, Eidelman DH, Boule M, Tam MF, Kent G, Skamene E, Tsui LC, & Radzioch D (1998). Impaired ability of Cftr knockout mice to control lung infection with Pseudomonas aeruginosa. *Am J Respir Crit Care Med* **157**, 1253-1262.

100. Govan JR, Brown PH, Maddison J, Doherty CJ, Nelson JW, Dodd M, Greening AP, & Webb AK (1993). Evidence for transmission of Pseudomonas cepacia by social contact in cystic fibrosis. *Lancet* **342**, 15-19.

101. Grabstein KH, Eisenman J, Shanebeck K, Rauch C, Srinivasan S, Fung V, Beers C, Richardson J, Schoenborn MA, Ahdieh M, & . (1994). Cloning of a T cell growth factor that interacts with the beta chain of the interleukin-2 receptor. *Science* **264**, 965-968.

102. Grassme H, Jendrossek V, Riehle A, von Kurthy G, Berger J, Schwarz H, Weller M, Kolesnick R, & Gulbins E (2003). Host defense against Pseudomonas aeruginosa requires ceramide-rich membrane rafts. *Nat Med* **9**, 322-330.

103. Gray MA, Winpenny JP, Porteous DJ, Dorin JR, & Argent BE (1994). CFTR and calcium-activated chloride currents in pancreatic duct cells of a transgenic CF mouse. *Am J Physiol* **266**, C213-C221.

104. Greenberger MJ, Strieter RM, Kunkel SL, Danforth JM, Goodman RE, & Standiford TJ (1995). Neutralization of IL-10 increases survival in a murine model of Klebsiella pneumonia. *J Immunol* **155**, 722-729.

105. Grubb BR (1995). Ion transport across the jejunum in normal and cystic fibrosis mice. *Am J Physiol* **268**, G505-G513.

106. Grubb BR & Boucher RC (1999). Pathophysiology of gene-targeted mouse models for cystic fibrosis. *Physiol Rev* **79**, S193-S214.

107. Grubb BR, Paradiso AM, & Boucher RC (1994). Anomalies in ion transport in CF mouse tracheal epithelium. *Am J Physiol* **267**, C293-C300.

108. Grubb BR, Vick RN, & Boucher RC (1994). Hyperabsorption of Na+ and raised Ca(2+)-mediated Cl- secretion in nasal epithelia of CF mice. *Am J Physiol* **266**, C1478-C1483.

109. Gudmundsson G, Bosch A, Davidson BL, Berg DJ, & Hunninghake GW (1998). Interleukin-10 modulates the severity of hypersensitivity pneumonitis in mice. *Am J Respir Cell Mol Biol* **19**, 812-818.

110. Guilbault C, Martin P, Houle D, Boghdady ML, Guiot MC, Marion D, & Radzioch D (2005). Cystic fibrosis lung disease following infection with Pseudomonas aeruginosa in the Cftr knockout mice using novel non-invasive direct pulmonary infection technique. *Laboratory animals* **39**, 336-352.

111. Guilbault C, Nelson A, Martin P, Stotland PK, Boghdady ML, Guiot MC, De Sanctis JB, & Radzioch D (2004). Protective effect of DHA treatment in non-infected CFTR knockout mice with CF lung disease. *International Proceedings Immunology 2004* 79-88.

112. Guilbault C, Stotland P, Lachance C, Tam M, Keller A, Thompson-Snipes L, Cowley E, Hamilton TA, Eidelman DH, Stevenson MM, & Radzioch D (2002). Influence of gender

and interleukin-10 deficiency on the inflammatory response during lung infection with Pseudomonas aeruginosa in mice. *Immunology* **107**, 297-305.

113. Hamosh A, King TM, Rosenstein BJ, Corey M, Levison H, Durie P, Tsui LC, McIntosh I, Keston M, Brock DJ, & . (1992). Cystic fibrosis patients bearing both the common missense mutation Gly----Asp at codon 551 and the delta F508 mutation are clinically indistinguishable from delta F508 homozygotes, except for decreased risk of meconium ileus. *Am J Hum Genet* **51**, 245-250.

114. Haston CK, Corey M, & Tsui LC (2002). Mapping of genetic factors influencing the weight of cystic fibrosis knockout mice. *Mamm Genome* **13**, 614-618.

115. Haston CK, McKerlie C, Newbigging S, Corey M, Rozmahel R, & Tsui LC (2002). Detection of modifier loci influencing the lung phenotype of cystic fibrosis knockout mice. *Mamm Genome* **13**, 605-613.

116. Haston CK & Tsui LC (2003). Loci of intestinal distress in cystic fibrosis knockout mice. *Physiol Genomics* **12**, 79-84.

117. Hasty P, O'Neal WK, Liu KQ, Morris AP, Bebok Z, Shumyatsky GB, Jilling T, Sorscher EJ, Bradley A, & Beaudet AL (1995). Severe phenotype in mice with termination mutation in exon 2 of cystic fibrosis gene. *Somat Cell Mol Genet* **21**, 177-187.

118. Hauber HP, Manoukian JJ, Nguyen LH, Sobol SE, Levitt RC, Holroyd KJ, McElvaney NG, Griffin S, & Hamid Q (2003). Increased expression of interleukin-9, interleukin-9 receptor, and the calcium-activated chloride channel hCLCA1 in the upper airways of patients with cystic fibrosis. *Laryngoscope* **113**, 1037-1042.

119. Hauber HP, Tsicopoulos A, Wallaert B, Griffin S, McElvaney NG, Daigneault P, Mueller Z, Olivenstein R, Holroyd KJ, Levitt RC, & Hamid Q (2004). Expression of HCLCA1 in cystic fibrosis lungs is associated with mucus overproduction. *Eur Respir J* **23**, 846-850.

120. Heaton ND & Pryor JP (1990). Vasa aplasia and cystic fibrosis. *Br J Urol* **66**, 538-540.

121. Heeckeren A, Walenga R, Konstan MW, Bonfield T, Davis PB, & Ferkol T (1997). Excessive inflammatory response of cystic fibrosis mice to bronchopulmonary infection with Pseudomonas aeruginosa. *J Clin Invest* **100**, 2810-2815.

122. Henry MT, Cave S, Rendall J, O'Connor CM, Morgan K, FitzGerald MX, & Kalsheker N (2001). An alpha1-antitrypsin enhancer polymorphism is a genetic modifier of pulmonary outcome in cystic fibrosis. *Eur J Hum Genet* **9**, 273-278.

123. Higgins CF (1992). Cystic fibrosis transmembrane conductance regulator (CFTR). *Br Med Bull* **48**, 754-765.

124. Hodson ME, Morris L, & Batten JC (1988). Serum immunoglobulins and immunoglobulin G subclasses in cystic fibrosis related to the clinical state of the patient. *Eur Respir J* **1**, 701-705.

125. Hoffmann N, Rasmussen TB, Jensen PO, Stub C, Hentzer M, Molin S, Ciofu O, Givskov M, Johansen HK, & Hoiby N (2005). Novel mouse model of chronic Pseudomonas aeruginosa lung infection mimicking cystic fibrosis. *Infect Immun* **73**, 2504-2514.

126. Hopken UE, Lu B, Gerard NP, & Gerard C (1996). The C5a chemoattractant receptor mediates mucosal defence to infection [see comments]. *Nature* **383**, 86-89.

127. Hubbard VS, Dunn GD, & di Sant'Agnese PA (1977). Abnormal fatty-acid composition of plasma-lipids in cystic fibrosis. A primary or a secondary defect? *Lancet* **2**, 1302-1304.

128. Hull J & Thomson AH (1998). Contribution of genetic factors other than CFTR to disease severity in cystic fibrosis. *Thorax* **53**, 1018-1021.

129. Hybiske K, Ichikawa JK, Huang V, Lory SJ, & Machen TE (2004). Cystic fibrosis airway epithelial cell polarity and bacterial flagellin determine host response to Pseudomonas aeruginosa. *Cell Microbiol* **6**, 49-63.

130. Hyde SC, Emsley P, Hartshorn MJ, Mimmack MM, Gileadi U, Pearce SR, Gallagher MP, Gill DR, Hubbard RE, & Higgins CF (1990). Structural model of ATP-binding proteins associated with cystic fibrosis, multidrug resistance and bacterial transport. *Nature* **346**, 362-365.

131. Hyde SC, Gill DR, Higgins CF, Trezise AE, MacVinish LJ, Cuthbert AW, Ratcliff R, Evans MJ, & Colledge WH (1993). Correction of the ion transport defect in cystic fibrosis transgenic mice by gene therapy. *Nature* **362**, 250-255.

132. Ip WF, Bronsveld I, Kent G, Corey M, & Durie PR (1996). Exocrine pancreatic alterations in long-lived surviving cystic fibrosis mice. *Pediatr Res* **40**, 242-249.

133. Irizarry RA, Bolstad BM, Collin F, Cope LM, Hobbs B, & Speed TP (2003). Summaries of Affymetrix GeneChip probe level data. *Nucleic Acids Res* **31**, e15.

134. Ishida H, Hastings R, Thompson-Snipes L, & Howard M (1993). Modified immunological status of anti-IL-10 treated mice. *Cell Immunol* **148**, 371-384.

135. Ito Y, Sato S, Ohashi T, Nakayama S, Shimokata K, & Kume H (2004). Reduction of airway anion secretion via CFTR in sphingomyelin pathway. *Biochem Biophys Res Commun* **324**, 901-908.

136. Jayaraman S, Joo NS, Reitz B, Wine JJ, & Verkman AS (2001). Submucosal gland secretions in airways from cystic fibrosis patients have normal [Na(+)] and pH but elevated viscosity. *Proc Natl Acad Sci U S A* **98**, 8119-8123.

137. Jayaraman S, Song Y, & Verkman AS (2001). Airway surface liquid osmolality measured using fluorophore-encapsulated liposomes. *J Gen Physiol* **117**, 423-430.

138. Jayaraman S, Song Y, Vetrivel L, Shankar L, & Verkman AS (2001). Noninvasive in vivo fluorescence measurement of airway-surface liquid depth, salt concentration, and pH. *J Clin Invest* **107**, 317-324.

139. Jeyarajah DR, Kielar M, Penfield J, & Lu CY (1999). Docosahexaenoic acid, a component of fish oil, inhibits nitric oxide production in vitro. *J Surg Res* **83**, 147-150.

140. Jin F, Nathan CF, Radzioch D, & Ding A (1998). Lipopolysaccharide-related stimuli induce expression of the secretory leukocyte protease inhibitor, a macrophage-derived lipopolysaccharide inhibitor. *Infect Immun* **66**, 2447-2452.

141. Johnson LG, Boyles SE, Wilson J, & Boucher RC (1995). Normalization of raised sodium absorption and raised calcium-mediated chloride secretion by adenovirus-mediated expression of cystic fibrosis transmembrane conductance regulator in primary human cystic fibrosis airway epithelial cells. *J Clin Invest* **95**, 1377-1382.

142. Jonsson B, Li YH, Noack G, Brauner A, & Tullus K (2000). Downregulatory cytokines in tracheobronchial aspirate fluid from infants with chronic lung disease of prematurity. *Acta Paediatr* **89**, 1375-1380.

143. Kahlke V, Dohm C, Brotzmann K, Schreiber S, & Schroder J (2000). Gender-related therapy: early IL-10 administration after hemorrhage restores immune function in males but not in females. *Shock* **14**, 354-359.

144. Kaur S, Norkina O, Ziemer D, Samuelson LC, & De Lisle RC (2004). Acidic duodenal pH alters gene expression in the cystic fibrosis mouse pancreas. *Am J Physiol Gastrointest Liver Physiol* **287**, G480-G490.

145. Keller CE, Elliott TB, Bentzel DE, Mog SR, Shoemaker MO, & Knudson GB (2003). Susceptibility of irradiated B6D2F1/J mice to Klebsiella pneumoniae administered intratracheally: a pulmonary infection model in an immunocompromised host. *Comp Med* **53**, 397-403.

146. Kelley TJ & Drumm ML (1998). Inducible nitric oxide synthase expression is reduced in cystic fibrosis murine and human airway epithelial cells. *J Clin Invest* **102**, 1200-1207.

147. Kent G, Iles R, Bear CE, Huan LJ, Griesenbach U, McKerlie C, Frndova H, Ackerley C, Gosselin D, Radzioch D, O'Brodovich H, Tsui LC, Buchwald M, & Tanswell AK (1997). Lung disease in mice with cystic fibrosis. *J Clin Invest* **100**, 3060-3069.

148. Kent G, Oliver M, Foskett JK, Frndova H, Durie P, Forstner J, Forstner GG, Riordan JR, Percy D, & Buchwald M (1996). Phenotypic abnormalities in long-term surviving cystic fibrosis mice. *Pediatr Res* **40**, 233-241.

149. Khair-el-Din TA, Sicher SC, Vazquez MA, Wright WJ, & Lu CY (1995). Docosahexaenoic acid, a major constituent of fetal serum and fish oil diets, inhibits IFN gamma-induced Ia-expression by murine macrophages in vitro. *J Immunol* **154**, 1296-1306.

150. Khan TZ, Wagener JS, Bost T, Martinez J, Accurso FJ, & Riches DW (1995). Early pulmonary inflammation in infants with cystic fibrosis. *Am J Respir Crit Care Med* **151**, 1075-1082.

151. Kim HS, Armstrong D, Hamilton TA, & Tebo JM (1998). IL-10 suppresses LPS-induced KC mRNA expression via a translation-dependent decrease in mRNA stability. *J Leukoc Biol* **64**, 33-39.

152. Kinsella JE, Lokesh B, Broughton S, & Whelan J (1990). Dietary polyunsaturated fatty acids and eicosanoids: potential effects on the modulation of inflammatory and immune cells: an overview. *Nutrition* **6**, 24-44.

153. Kishore R, Tebo JM, Kolosov M, & Hamilton TA (1999). Cutting edge: clustered AU-rich elements are the target of IL-10- mediated mRNA destabilization in mouse macrophages. *J Immunol* **162**, 2457-2461.

154. Knowles M, Gatzy J, & Boucher R (1981). Increased bioelectric potential difference across respiratory epithelia in cystic fibrosis. *N Engl J Med* **305**, 1489-1495.

155. Knowles MR, Clarke LL, & Boucher RC (1991). Activation by extracellular nucleotides of chloride secretion in the airway epithelia of patients with cystic fibrosis. *N Engl J Med* **325**, 533-538.

156. Knowles MR, Stutts MJ, Spock A, Fischer N, Gatzy JT, & Boucher RC (1983). Abnormal ion permeation through cystic fibrosis respiratory epithelium. *Science* **221**, 1067-1070.

157. Konstan MW & Berger M (1997). Current understanding of the inflammatory process in cystic fibrosis: onset and etiology. *Pediatr Pulmonol* **24**, 137-142.

158. Konstan MW, Hilliard KA, Norvell TM, & Berger M (1994). Bronchoalveolar lavage findings in cystic fibrosis patients with stable, clinically mild lung disease suggest ongoing

infection and inflammation [published erratum appears in Am J Respir Crit Care Med 1995 Jan;151(1):260]. *Am J Respir Crit Care Med* **150**, 448-454.

159. Lalani I, Bhol K, & Ahmed AR (1997). Interleukin-10: biology, role in inflammation and autoimmunity [published erratum appears in Ann Allergy Asthma Immunol 1998 Mar;80(3):A-6]. *Ann Allergy Asthma Immunol* **79**, 469-483.

160. Lavrentiadou SN, Chan C, Kawcak T, Ravid T, Tsaba A, van d, V, Rasooly R, & Goldkorn T (2001). Ceramide-mediated apoptosis in lung epithelial cells is regulated by glutathione. *Am J Respir Cell Mol Biol* **25**, 676-684.

161. Lee MG, Choi JY, Luo X, Strickland E, Thomas PJ, & Muallem S (1999). Cystic fibrosis transmembrane conductance regulator regulates luminal Cl-/HCO3- exchange in mouse submandibular and pancreatic ducts. *J Biol Chem* **274**, 14670-14677.

162. Leung AY, Wong PY, Yankaskas JR, & Boucher RC (1996). cAMP- but not Ca(2+)-regulated Cl- conductance is lacking in cystic fibrosis mice epididymides and seminal vesicles. *Am J Physiol* **271**, C188-C193.

163. Lewko WM, Smith TL, Bowman DJ, Good RW, & Oldham RK (1995). Interleukin-15 and the growth of tumor derived activated T-cells. *Cancer Biother* **10**, 13-20.

164. Linsdell P & Hanrahan JW (1998). Glutathione permeability of CFTR. *Am J Physiol* **275**, C323-C326.

165. Lippman SM, Kessler JF, & Meyskens FL, Jr. (1987). Retinoids as preventive and therapeutic anticancer agents (Part II). *Cancer Treat Rep* **71**, 493-515.

166. Lippman SM, Lee JJ, Karp DD, Vokes EE, Benner SE, Goodman GE, Khuri FR, Marks R, Winn RJ, Fry W, Graziano SL, Gandara DR, Okawara G, Woodhouse CL, Williams B, Perez C, Kim HW, Lotan R, Roth JA, & Hong WK (2001). Randomized phase III intergroup trial of isotretinoin to prevent second primary tumors in stage I non-small-cell lung cancer. *J Natl Cancer Inst* **93**, 605-618.

167. LiPuma JJ (1998). Burkholderia cepacia. Management issues and new insights. *Clin Chest Med* **19**, 473-86, vi.

168. Livak KJ & Schmittgen TD (2001). Analysis of relative gene expression data using real-time quantitative PCR and the 2(-Delta Delta C(T)) Method. *Methods* **25**, 402-408.

169. Lu CY, Penfield JG, Khair-el-Din TA, Sicher SC, Kielar ML, Vazquez MA, & Che L (1998). Docosahexaenoic acid, a constituent of fetal and neonatal serum, inhibits nitric oxide production by murine macrophages stimulated by IFN gamma plus LPS, or by IFN gamma plus Listeria monocytogenes. *J Reprod Immunol* **38**, 31-53.

170. Mahadeva R, Sharples L, Ross-Russell RI, Webb AK, Bilton D, & Lomas DA (2001). Association of alpha(1)-antichymotrypsin deficiency with milder lung disease in patients with cystic fibrosis. *Thorax* **56**, 53-58.

171. Mahadeva R, Stewart S, Bilton D, & Lomas DA (1998). Alpha-1 antitrypsin deficiency alleles and severe cystic fibrosis lung disease. *Thorax* **53**, 1022-1024.

172. Mallat Z, Besnard S, Duriez M, Deleuze V, Emmanuel F, Bureau MF, Soubrier F, Esposito B, Duez H, Fievet C, Staels B, Duverger N, Scherman D, & Tedgui A (1999). Protective role of interleukin-10 in atherosclerosis. *Circ Res* **85**, e17-e24.

173. Manson AL, Trezise AE, MacVinish LJ, Kasschau KD, Birchall N, Episkopou V, Vassaux G, Evans MJ, Colledge WH, Cuthbert AW, & Huxley C (1997). Complementation of null CF mice with a human CFTR YAC transgene. *EMBO J* **16**, 4238-4249.

174. Marks MI (1984). Respiratory viruses in cystic fibrosis. *N Engl J Med* **311**, 1695-1696.

175. Massengale AR, Quinn FJ, Yankaskas J, Weissman D, McClellan WT, Cuff C, & Aronoff SC (1999). Reduced interleukin-8 production by cystic fibrosis airway epithelial cells. *Am J Respir Cell Mol Biol* **20**, 1073-1080.

176. Matthews WJ, Jr., Williams M, Oliphint B, Geha R, & Colten HR (1980). Hypogammaglobulinemia in patients with cystic fibrosis. *N Engl J Med* **302**, 245-249.

177. Maurer BJ, Metelitsa LS, Seeger RC, Cabot MC, & Reynolds CP (1999). Increase of ceramide and induction of mixed apoptosis/necrosis by N-(4-hydroxyphenyl)- retinamide in neuroblastoma cell lines. *J Natl Cancer Inst* **91**, 1138-1146.

178. McCray PB, Jr., Zabner J, Jia HP, Welsh MJ, & Thorne PS (1999). Efficient killing of inhaled bacteria in DeltaF508 mice: role of airway surface liquid composition. *Am J Physiol* **277**, L183-L190.

179. McMorran BJ, Palmer JS, Lunn DP, Oceandy D, Costelloe EO, Thomas GR, Hume DA, & Wainwright BJ (2001). G551D CF mice display an abnormal host response and have impaired clearance of Pseudomonas lung disease. *Am J Physiol Lung Cell Mol Physiol* **281**, L740-L747.

180. McMurray DN, Jolly CA, & Chapkin RS Effects of dietary n-3 fatty acids on T cell activation and T cell receptor-mediated signaling in a murine model [In Process Citation]. *J Infect Dis 2000 Sep ;182 (## Suppl 1):S103 -7* **182**, S103-S107.

181. Meluleni GJ, Grout M, Evans DJ, & Pier GB (1995). Mucoid Pseudomonas aeruginosa growing in a biofilm in vitro are killed by opsonic antibodies to the mucoid

exopolysaccharide capsule but not by antibodies produced during chronic lung infection in cystic fibrosis patients. *J Immunol* **155**, 2029-2038.

182. Menegazzi R, Busetto S, Cramer R, Dri P, & Patriarca P Role of intracellular chloride in the reversible activation of neutrophil beta(2) integrins: A lesson from TNF stimulation [In Process Citation]. *J Immunol 2000 Oct 15 ;165 (8):4606 -14* **165**, 4606-4614.

183. Miller L, Alley EW, Murphy WJ, Russell SW, & Hunt JS (1996). Progesterone inhibits inducible nitric oxide synthase gene expression and nitric oxide production in murine macrophages. *J Leukoc Biol* **59**, 442-450.

184. Moore KW, O'Garra A, de Waal M, Vieira P, & Mosmann TR (1993). Interleukin-10. *Annu Rev Immunol* **11**, 165-190.

185. Morgan WJ, Butler SM, Johnson CA, Colin AA, FitzSimmons SC, Geller DE, Konstan MW, Light MJ, Rabin HR, Regelmann WE, Schidlow DV, Stokes DC, Wohl ME, Kaplowitz H, Wyatt MM, & Stryker S (1999). Epidemiologic study of cystic fibrosis: design and implementation of a prospective, multicenter, observational study of patients with cystic fibrosis in the U.S. and Canada. *Pediatr Pulmonol* **28**, 231-241.

186. Morissette C, Francoeur C, Darmond-Zwaig C, & Gervais F (1996). Lung phagocyte bactericidal function in strains of mice resistant and susceptible to Pseudomonas aeruginosa. *Infect Immun* **64**, 4984-4992.

187. Morissette C, Skamene E, & Gervais F (1995). Endobronchial inflammation following Pseudomonas aeruginosa infection in resistant and susceptible strains of mice. *Infect Immun* **63**, 1718-1724.

188. Moss RB (1987). Hypergammaglobulinemia in cystic fibrosis. Role of Pseudomonas endobronchial infection. *Chest* **91**, 522-526.

189. Moss RB, Hsu YP, & Olds L Cytokine dysregulation in activated cystic fibrosis (CF) peripheral lymphocytes. *Clin Exp Immunol 2000 Jun ;120 (3):518 -25* **120**, 518-525.

190. Muallem S & Loessberg PA (1990). Intracellular pH-regulatory mechanisms in pancreatic acinar cells. II. Regulation of H+ and HCO3- transporters by Ca2(+)-mobilizing agonists. *J Biol Chem* **265**, 12813-12819.

191. Nakamura N, Hamazaki T, Kobayashi M, & Yazawa K (1994). The effect of oral administration of eicosapentaenoic and docosahexaenoic acids on acute inflammation and fatty acid composition in rats. *J Nutr Sci Vitaminol (Tokyo)* **40**, 161-170.

192. Naon H, Hack S, Shelton MT, Gotthoffer RC, & Gozal D (1993). Resting energy expenditure. Evolution during antibiotic treatment for pulmonary exacerbation in cystic fibrosis. *Chest* **103**, 1819-1825.

193. Nelson A, Guilbault C, & Radzioch D (2003). Animal models used for the study of cystic fibrosis. In ***Recent Research Developments in Cell Research***, ed. Research Signpost.

194. Nieuwenhuis EE, Matsumoto T, Exley M, Schleipman RA, Glickman J, Bailey DT, Corazza N, Colgan SP, Onderdonk AB, & Blumberg RS (2002). CD1d-dependent macrophage-mediated clearance of Pseudomonas aeruginosa from lung. *Nat Med* **8**, 588-593.

195. Noah TL, Black HR, Cheng PW, Wood RE, & Leigh MW (1997). Nasal and bronchoalveolar lavage fluid cytokines in early cystic fibrosis. *J Infect Dis* **175**, 638-647.

196. Norkina O, Kaur S, Ziemer D, & De Lisle RC (2004). Inflammation of the cystic fibrosis mouse small intestine. *Am J Physiol Gastrointest Liver Physiol* **286**, G1032-G1041.

197. Novak JP, Sladek R, & Hudson TJ (2002). Characterization of variability in large-scale gene expression data: implications for study design. *Genomics* **79**, 104-113.

198. O'Neal WK, Hasty P, McCray PB, Jr., Casey B, Rivera-Perez J, Welsh MJ, Beaudet AL, & Bradley A (1993). A severe phenotype in mice with a duplication of exon 3 in the cystic fibrosis locus. *Hum Mol Genet* **2**, 1561-1569.

199. Obeid LM, Linardic CM, Karolak LA, & Hannun YA (1993). Programmed cell death induced by ceramide. *Science* **259**, 1769-1771.

200. Oda T & Wu HC (1995). Protective effect of cell-permeable ceramide analogs against modeccin, ricin, Pseudomonas toxin, and diphtheria toxin. *Exp Cell Res* **221**, 1-10.

201. Oppenheimer EH & Esterly JR (1975). Pathology of cystic fibrosis review of the literature and comparison with 146 autopsied cases. *Perspect Pediatr Pathol* **2**, 241-278.

202. Orenstein DM, Winnie GB, & Altman H (2002). Cystic fibrosis: a 2002 update. *J Pediatr* **140**, 156-164.

203. Osika E, Cavaillon JM, Chadelat K, Boule M, Fitting C, Tournier G, & Clement A (1999). Distinct sputum cytokine profiles in cystic fibrosis and other chronic inflammatory airway disease. *Eur Respir J* **14**, 339-346.

204. Peterson LE (2002). CLUSFAVOR 5.0: hierarchical cluster and principal-component analysis of microarray-based transcriptional profiles. *Genome Biol* **3**, SOFTWARE0002.

205. Petrache I, Natarajan V, Zhen L, Medler TR, Richter AT, Cho C, Hubbard WC, Berdyshev EV, & Tuder RM (2005). Ceramide upregulation causes pulmonary cell apoptosis and emphysema-like disease in mice. *Nat Med* **11**, 491-498.

206. Pier GB (2002). CFTR mutations and host susceptibility to Pseudomonas aeruginosa lung infection. *Curr Opin Microbiol* **5**, 81-86.

207. Pier GB Role of the cystic fibrosis transmembrane conductance regulator in innate immunity to Pseudomonas aeruginosa infections. *Proc Natl Acad Sci U S A 2000 Aug 1 ;97 (16):8822 -8* **97**, 8822-8828.

208. Pier GB & Elcock ME (1984). Nonspecific immunoglobulin synthesis and elevated IgG levels in rabbits immunized with mucoid exopolysaccharide from cystic fibrosis isolates of Pseudomonas aeruginosa. *J Immunol* **133**, 734-739.

209. Pier GB, Grout M, Zaidi T, Meluleni G, Mueschenborn SS, Banting G, Ratcliff R, Evans MJ, & Colledge WH (1998). Salmonella typhi uses CFTR to enter intestinal epithelial cells. *Nature* **393**, 79-82.

210. Pier GB, Grout M, & Zaidi TS (1997). Cystic fibrosis transmembrane conductance regulator is an epithelial cell receptor for clearance of Pseudomonas aeruginosa from the lung. *Proc Natl Acad Sci U S A* **94**, 12088-12093.

211. Ponthan F, Lindskog M, Karnehed N, Castro J, & Kogner P (2003). Evaluation of anti-tumour effects of oral fenretinide (4-HPR) in rats with human neuroblastoma xenografts. *Oncol Rep* **10**, 1587-1592.

212. Primosch RE (1980). Tetracycline discoloration, enamel defects, and dental caries in patients with cystic fibrosis. *Oral Surg Oral Med Oral Pathol* **50**, 301-308.

213. Prince LS, Karp PH, Moninger TO, & Welsh MJ (2001). KGF alters gene expression in human airway epithelia: potential regulation of the inflammatory response. *Physiol Genomics* **6**, 81-89.

214. Puchelle E, Bajolet O, & Abely M (2002). Airway mucus in cystic fibrosis. *Paediatr Respir Rev* **3**, 115-119.

215. Puduvalli VK, Saito Y, Xu R, Kouraklis GP, Levin VA, & Kyritsis AP (1999). Fenretinide activates caspases and induces apoptosis in gliomas. *Clin Cancer Res* **5**, 2230-2235.

216. Quinton PM (1983). Chloride impermeability in cystic fibrosis. *Nature* **301**, 421-422.

217. Raman V, Clary R, Siegrist KL, Zehnbauer B, & Chatila TA (2002). Increased prevalence of mutations in the cystic fibrosis transmembrane conductance regulator in children with chronic rhinosinusitis. *Pediatrics* **109**, E13.

218. Ramsey BW, Pepe MS, Quan JM, Otto KL, Montgomery AB, Williams-Warren J, Vasiljev K, Borowitz D, Bowman CM, Marshall BC, Marshall S, & Smith AL (1999). Intermittent administration of inhaled tobramycin in patients with cystic fibrosis. Cystic Fibrosis Inhaled Tobramycin Study Group. *N Engl J Med* **340**, 23-30.

219. Rao GN, Ney E, & Herbert RA (1998). Effect of retinoid analogues on mammary cancer in transgenic mice with c-neu breast cancer oncogene. *Breast Cancer Res Treat* **48**, 265-271.

220. Ratcliff R, Evans MJ, Cuthbert AW, MacVinish LJ, Foster D, Anderson JR, & Colledge WH (1993). Production of a severe cystic fibrosis mutation in mice by gene targeting. *Nat Genet* **4**, 35-41.

221. Riordan JR, Rommens JM, Kerem B, Alon N, Rozmahel R, Grzelczak Z, Zielenski J, Lok S, Plavsic N, Chou JL, & . (1989). Identification of the cystic fibrosis gene: cloning and characterization of complementary DNA. *Science* **245**, 1066-1073.

222. Rioux JD, Larose Y, Brodeur BR, Radzioch D, & Newkirk MM (1994). Structural characteristics of four human hybridoma antibodies specific for the pp65 protein of the human cytomegalovirus and their relationship to human rheumatoid factors. *Mol Immunol* **31**, 585-597.

223. Robinson P (2001). Cystic fibrosis. *Thorax* **56**, 237-241.

224. Rogiers V, Dab I, Crokaert R, & Vis HL (1980). Long chain non-esterified fatty acid pattern in plasma of cystic fibrosis patients and their parents. *Pediatr Res* **14**, 1088-1091.

225. Rogiers V, Dab I, Michotte Y, Vercruysse A, Crokaert R, & Vis HL (1984). Abnormal fatty acid turnover in the phospholipids of the red blood cell membranes of cystic fibrosis patients (in vitro study). *Pediatr Res* **18**, 704-709.

226. Rohlfs EM, Shaheen NJ, & Silverman LM (1998). Is the hemochromatosis gene a modifier locus for cystic fibrosis? *Genet Test* **2**, 85-88.

227. Rommens JM, Iannuzzi MC, Kerem B, Drumm ML, Melmer G, Dean M, Rozmahel R, Cole JL, Kennedy D, & Hidaka N (1989). Identification of the cystic fibrosis gene: chromosome walking and jumping. *Science* **245**, 1059-1065.

228. Rozmahel R, Gyomorey K, Plyte S, Nguyen V, Wilschanski M, Durie P, Bear CE, & Tsui LC (1997). Incomplete rescue of cystic fibrosis transmembrane conductance regulator deficient mice by the human CFTR cDNA. *Hum Mol Genet* **6**, 1153-1162.

229. Rozmahel R, Heng HH, Duncan AM, Shi XM, Rommens JM, & Tsui LC (1997). Amplification of CFTR exon 9 sequences to multiple locations in the human genome. *Genomics* **45**, 554-561.

230. Rozmahel R, Wilschanski M, Matin A, Plyte S, Oliver M, Auerbach W, Moore A, Forstner J, Durie P, Nadeau J, Bear C, & Tsui LC (1996). Modulation of disease severity in cystic fibrosis transmembrane conductance regulator deficient mice by a secondary genetic factor. *Nat Genet* **12**, 280-287.

231. Sadeghi M, Daniel V, Naujokat C, Wiesel M, Hergesell O, & Opelz G (2005). Strong inflammatory cytokine response in male and strong anti-inflammatory response in female kidney transplant recipients with urinary tract infection. *Transpl Int* **18**, 177-185.

232. Sadikot RT, Christman JW, & Blackwell TS (2004). Molecular targets for modulating lung inflammation and injury. *Curr Drug Targets* **5**, 581-588.

233. Sahu S & Lynn WS (1977). Lipid composition of airway secretions from patients with asthma and patients with cystic fibrosis. *Am Rev Respir Dis* **115**, 233-239.

234. Sajjan U, Thanassoulis G, Cherapanov V, Lu A, Sjolin C, Steer B, Wu YJ, Rotstein OD, Kent G, McKerlie C, Forstner J, & Downey GP (2001). Enhanced susceptibility to pulmonary infection with Burkholderia cepacia in Cftr(-/-) mice. *Infect Immun* **69**, 5138-5150.

235. Sallenave JM (2000). The role of secretory leukocyte proteinase inhibitor and elafin (elastase-specific inhibitor/skin-derived antileukoprotease) as alarm antiproteinases in inflammatory lung disease. *Respir Res* **1**, 87-92.

236. Salvatore F, Scudiero O, & Castaldo G (2002). Genotype-phenotype correlation in cystic fibrosis: the role of modifier genes. *Am J Med Genet* **111**, 88-95.

237. Sapru K, Stotland PK, & Stevenson MM (1999). Quantitative and qualitative differences in bronchoalveolar inflammatory cells in Pseudomonas aeruginosa-resistant and -susceptible mice. *Clin Exp Immunol* **115**, 103-109.

238. Sawa T, Corry DB, Gropper MA, Ohara M, Kurahashi K, & Wiener-Kronish JP (1997). IL-10 improves lung injury and survival in Pseudomonas aeruginosa pneumonia. *J Immunol* **159**, 2858-2866.

239. Sawada M, Alkayed NJ, Goto S, Crain BJ, Traystman RJ, Shaivitz A, Nelson RJ, & Hurn PD (2000). Estrogen receptor antagonist ICI182,780 exacerbates ischemic injury in female mouse. *J Cereb Blood Flow Metab* **20**, 112-118.

240. Schlenk H & Gellerman J. Analytical Chemistry 32[11], 1412-1414. 1960.
Ref Type: Generic

241. Scholte BJ, Davidson DJ, Wilke M, & de Jonge HR (2004). Animal models of cystic fibrosis. *J Cyst Fibros* **3 Suppl 2:183-90.**, 183-190.

242. Schroeder TH, Reiniger N, Meluleni G, Grout M, Coleman FT, & Pier GB (2001). Transgenic cystic fibrosis mice exhibit reduced early clearance of Pseudomonas aeruginosa from the respiratory tract. *J Immunol* **166**, 7410-7418.

243. Schuster A, Hansen G, Zubrod-Eichert C, & Wahn V (1996). Effects of native and oxidation-resistant secretory leukoprotease inhibitor on cystic fibrosis sputum: inhibition of neutrophil elastase activity and of sputum-induced secretion from porcine tracheal submucosal glands. *Pediatr Res* **40**, 732-737.

244. Schwarz DA, Katayama CD, & Hedrick SM (1998). Schlafen, a new family of growth regulatory genes that affect thymocyte development. *Immunity* **9**, 657-668.

245. Schweiger A, Staib A, Werle B, Krasovec M, Lah TT, Ebert W, Turk V, & Kos J (2000). Cysteine proteinase cathepsin H in tumours and sera of lung cancer patients: relation to prognosis and cigarette smoking. *Br J Cancer* **82**, 782-788.

246. Schwiebert EM, Benos DJ, Egan ME, Stutts MJ, & Guggino WB (1999). CFTR is a conductance regulator as well as a chloride channel. *Physiol Rev* **79**, S145-S166.

247. Shaked Y, Engelstein R, & Gabizon R (2002). The binding of prion proteins to serum components is affected by detergent extraction conditions. *J Neurochem* **82**, 1-5.

248. Shepherd RW, Holt TL, Cleghorn G, Ward LC, Isles A, & Francis P (1988). Short-term nutritional supplementation during management of pulmonary exacerbations in cystic fibrosis: a controlled study, including effects of protein turnover. *Am J Clin Nutr* **48**, 235-239.

249. Shepherd RW, Holt TL, Vasques-Velasquez L, Coward WA, Prentice A, & Lucas A (1988). Increased energy expenditure in young children with cystic fibrosis. *Lancet* **1**, 1300-1303.

250. Shin JS & Abraham SN (2001). Caveolae as portals of entry for microbes. *Microbes Infect* **3**, 755-761.

251. Shin JS & Abraham SN (2001). Co-option of endocytic functions of cellular caveolae by pathogens. *Immunology* **102**, 2-7.

252. Simons K & Ikonen E (1997). Functional rafts in cell membranes. *Nature* **387**, 569-572.

253. Singh MP, Rai AK, & Singh SM (2005). Gender dimorphism in the progressive in vivo growth of a T cell lymphoma: involvement of cytokines and gonadal hormones. *J Reprod Immunol* **65**, 17-32.

254. Smith SN, Steel DM, Middleton PG, Munkonge FM, Geddes DM, Caplen NJ, Porteous DJ, Dorin JR, & Alton EW (1995). Bioelectric characteristics of exon 10 insertional cystic fibrosis mouse: comparison with humans. *Am J Physiol* **268**, C297-C307.

255. Snouwaert JN, Brigman KK, Latour AM, Iraj E, Schwab U, Gilmour MI, & Koller BH (1995). A murine model of cystic fibrosis. *Am J Respir Crit Care Med* **151**, S59-S64.

256. Snouwaert JN, Brigman KK, Latour AM, Malouf NN, Boucher RC, Smithies O, & Koller BH (1992). An animal model for cystic fibrosis made by gene targeting. *Science* **257**, 1083-1088.

257. Sokol PA, Sajjan U, Visser MB, Gingues S, Forstner J, & Kooi C (2003). The CepIR quorum-sensing system contributes to the virulence of Burkholderia cenocepacia respiratory infections. *Microbiology* **149**, 3649-3658.

258. Srivastava M, Eidelman O, & Pollard HB (1999). Pharmacogenomics of the cystic fibrosis transmembrane conductance regulator (CFTR) and the cystic fibrosis drug CPX using genome microarray analysis. *Mol Med* **5**, 753-767.

259. Stalings VA (2003). Gender, death and cystic fibrosis: Is energy expenditure a component? *J Pediatr* **142**, 4-6.

260. Standiford TJ, Strieter RM, Lukacs NW, & Kunkel SL (1995). Neutralization of IL-10 increases lethality in endotoxemia. Cooperative effects of macrophage inflammatory protein-2 and tumor necrosis factor. *J Immunol* **155**, 2222-2229.

261. Starke JR, Edwards MS, Langston C, & Baker CJ (1987). A mouse model of chronic pulmonary infection with Pseudomonas aeruginosa and Pseudomonas cepacia. *Pediatr Res* **22**, 698-702.

262. Steagall WK, Elmer HL, Brady KG, & Kelley TJ (2000). Cystic fibrosis transmembrane conductance regulator-dependent regulation of epithelial inducible nitric oxide synthase expression. *Am J Respir Cell Mol Biol* **22**, 45-50.

263. Steinhauser ML, Hogaboam CM, Kunkel SL, Lukacs NW, Strieter RM, & Standiford TJ (1999). IL-10 is a major mediator of sepsis-induced impairment in lung antibacterial host defense. *J Immunol* **162**, 392-399.

264. Steinkamp G, Drommer A, & von der HH (1993). Resting energy expenditure before and after treatment for Pseudomonas aeruginosa infection in patients with cystic fibrosis. *Am J Clin Nutr* **57**, 685-689.

265. Stotland P, Radzioch D, & Stevenson MM. Inflammation in the cystic fibrosis lung. University of Toronto Medical Journal 76[1], 6-11. 1998.
Ref Type: Generic

266. Stotland PK, Radzioch D, & Stevenson MM (2000). Mouse models of chronic lung infection with Pseudomonas aeruginosa: models for the study of cystic fibrosis. *Pediatr Pulmonol* **30**, 413-424.

267. Stutts MJ, Canessa CM, Olsen JC, Hamrick M, Cohn JA, Rossier BC, & Boucher RC (1995). CFTR as a cAMP-dependent regulator of sodium channels. *Science* **269**, 847-850.

268. Sun SY, Li W, Yue P, Lippman SM, Hong WK, & Lotan R (1999). Mediation of N-(4-hydoxyphenyl)retinamide-induced apoptosis in human cancer cells by different mechanisms. *Cancer Res* **59**, 2493-2498.

269. Sun SY, Yue P, & Lotan R (1999). Induction of apoptosis by N-(4-hydroxyphenyl)retinamide and its association with reactive oxygen species, nuclear retinoic acid receptors, and apoptosis-related genes in human prostate carcinoma cells. *Mol Pharmacol* **55**, 403-410.

270. Sweezey N, Tchepichev S, Gagnon S, Fertuck K, & O'Brodovich H (1998). Female gender hormones regulate mRNA levels and function of the rat lung epithelial Na channel. *Am J Physiol* **274**, C379-C386.

271. Sweezey NB, Gauthier C, Gagnon S, Ferretti E, & Kopelman H (1996). Progesterone and estradiol inhibit CFTR-mediated ion transport by pancreatic epithelial cells. *Am J Physiol* **271**, G747-G754.

272. Sweezey NB, Ghibu F, & Gagnon S (1997). Sex hormones regulate CFTR in developing fetal rat lung epithelial cells. *Am J Physiol* **272**, L844-L851.

273. Sweezey NB, Ghibu F, Gagnon S, Schotman E, & Hamid Q (1998). Glucocorticoid receptor mRNA and protein in fetal rat lung in vivo: modulation by glucocorticoid and androgen. *Am J Physiol* **275**, L103-L109.

274. Tablan OC, Chorba TL, Schidlow DV, White JW, Hardy KA, Gilligan PH, Morgan WM, Carson LA, Martone WJ, Jason JM, & . (1985). Pseudomonas cepacia colonization in patients with cystic fibrosis: risk factors and clinical outcome. *J Pediatr* **107**, 382-387.

275. Tam M, Snipes GJ, & Stevenson MM (1999). Characterization of chronic bronchopulmonary Pseudomonas aeruginosa infection in resistant and susceptible inbred mouse strains. *Am J Respir Cell Mol Biol* **20**, 710-719.

276. Tatterson LE, Poschet JF, Firoved A, Skidmore J, & Deretic V (2001). CFTR and pseudomonas infections in cystic fibrosis. *Front Biosci* **6**, D890-D897.

277. Thomas GR, Costelloe EA, Lunn DP, Stacey KJ, Delaney SJ, Passey R, McGlinn EC, McMorran BJ, Ahadizadeh A, Geczy CL, Wainwright BJ, & Hume DA (2000). G551D cystic fibrosis mice exhibit abnormal regulation of inflammation in lungs and macrophages. *J Immunol* **164**, 3870-3877.

278. Tirouvanziam R, Khazaal I, & Peault B (2002). Primary inflammation in human cystic fibrosis small airways. *Am J Physiol Lung Cell Mol Physiol* **283**, L445-L451.

279. Trotter A, Muck K, Grill HJ, Schirmer U, Hannekum A, & Lang D (2001). Gender-related plasma levels of progesterone, interleukin-8 and interleukin-10 during and after cardiopulmonary bypass in infants and children. *Crit Care* **5**, 343-348.

280. Urban TA, Griffith A, Torok AM, Smolkin ME, Burns JL, & Goldberg JB (2004). Contribution of Burkholderia cenocepacia flagella to infectivity and inflammation. *Infect Immun* **72**, 5126-5134.

281. van Doorninck JH, French PJ, Verbeek E, Peters RH, Morreau H, Bijman J, & Scholte BJ (1995). A mouse model for the cystic fibrosis delta F508 mutation. *EMBO J* **14**, 4403-4411.

282. VAN HANDEL E & ZILVERSMIT DB (1957). Micromethod for the direct determination of serum triglycerides. *J Lab Clin Med* **50**, 152-157.

283. van Heeckeren AM & Schluchter MD (2002). Murine models of chronic Pseudomonas aeruginosa lung infection. *Lab Anim* **36**, 291-312.

284. van Heeckeren AM, Schluchter MD, Drumm ML, & Davis PB (2004). Role of Cftr Genotype in the Response to Chronic Pseudomonas aeruginosa Lung Infection in Mice. *Am J Physiol Lung Cell Mol Physiol.*

285. van Heeckeren AM, Tscheikuna J, Walenga RW, Konstan MW, Davis PB, Erokwu B, Haxhiu MA, & Ferkol TW (2000). Effect of Pseudomonas infection on weight loss, lung mechanics, and cytokines in mice. *Am J Respir Crit Care Med* **161**, 271-279.

286. Verkman AS, Song Y, & Thiagarajah JR (2003). Role of airway surface liquid and submucosal glands in cystic fibrosis lung disease. *Am J Physiol Cell Physiol* **284**, C2-15.

287. Veronesi U, De PG, Marubini E, Costa A, Formelli F, Mariani L, Decensi A, Camerini T, Del Turco MR, Di Mauro MG, Muraca MG, Del VM, Pinto C, D'Aiuto G, Boni C, Campa T, Magni A, Miceli R, Perloff M, Malone WF, & Sporn MB (1999). Randomized trial of fenretinide to prevent second breast malignancy in women with early breast cancer. *J Natl Cancer Inst* **91**, 1847-1856.

288. Virella-Lowell I, Herlihy JD, Liu B, Lopez C, Cruz P, Muller C, Baker HV, & Flotte TR (2004). Effects of CFTR, interleukin-10, and Pseudomonas aeruginosa on gene expression profiles in a CF bronchial epithelial cell Line. *Mol Ther* **10**, 562-573.

289. Vogelmeier C, Gillissen A, & Buhl R (1996). Use of secretory leukoprotease inhibitor to augment lung antineutrophil elastase activity. *Chest* **110**, 261S-266S.

290. Wallace FA, Neely SJ, Miles EA, & Calder PC (2000). Dietary fats affect macrophage-mediated cytotoxicity towards tumour cells. *Immunol Cell Biol* **78**, 40-48.

291. Wang H, Maurer BJ, Reynolds CP, & Cabot MC (2001). N-(4-hydroxyphenyl)retinamide elevates ceramide in neuroblastoma cell lines by coordinate activation of serine palmitoyltransferase and ceramide synthase. *Cancer Res* **61**, 5102-5105.

292. Ward SA, Tomezsko JL, Holsclaw DS, & Paolone AM (1999). Energy expenditure and substrate utilization in adults with cystic fibrosis and diabetes mellitus. *Am J Clin Nutr* **69**, 913-919.

293. Warner JO (1992). Immunology of cystic fibrosis. *Br Med Bull* **48**, 893-911.

294. Weksler B, Ng B, Lenert J, & Burt M (1994). A simplified method for endotracheal intubation in the rat. *J Appl Physiol* **76**, 1823-1825.

295. Welsh MJ & Smith AE (1993). Molecular mechanisms of CFTR chloride channel dysfunction in cystic fibrosis. *Cell* **73**, 1251-1254.

296. Widdicombe JH (1986). Cystic fibrosis and beta-adrenergic response of airway epithelial cell cultures. *Am J Physiol* **251**, R818-R822.

297. Wilder RL (1998). Hormones, pregnancy, and autoimmune diseases. *Ann N Y Acad Sci* **840:45-50.**, 45-50.

298. Wilfond BS & Fost N (1992). The introduction of cystic fibrosis carrier screening into clinical practice: policy considerations. *Milbank Q* **70**, 629-659.

299. Wine JJ (1999). The genesis of cystic fibrosis lung disease. *J Clin Invest* **103**, 309-312.

300. Wojnarowski C, Frischer T, Hofbauer E, Grabner C, Mosgoeller W, Eichler I, & Ziesche R (1999). Cytokine expression in bronchial biopsies of cystic fibrosis patients with and without acute exacerbation. *Eur Respir J* **14**, 1136-1144.

301. Wright JM, Zeitlin PL, Cebotaru L, Guggino SE, & Guggino WB (2004). Gene expression profile analysis of 4-phenylbutyrate treatment of IB3-1 bronchial epithelial cell line demonstrates a major influence on heat-shock proteins. *Physiol Genomics* **16**, 204-211.

302. Wright JT, Kiefer CL, Hall KI, & Grubb BR (1996). Abnormal enamel development in a cystic fibrosis transgenic mouse model. *J Dent Res* **75**, 966-973.

303. Xu Y, Clark JC, Aronow BJ, Dey CR, Liu C, Wooldridge JL, & Whitsett JA (2003). Transcriptional adaptation to cystic fibrosis transmembrane conductance regulator deficiency. *J Biol Chem* **278**, 7674-7682.

304. Ying QL, Kemme M, & Simon SR (1996). Alginate, the slime exopolysaccharide of Pseudomonas aeruginosa, binds human leukocyte elastase, retards inhibition by alpha 1-proteinase inhibitor, and accelerates inhibition by secretory leukoprotease inhibitor. *Am J Respir Cell Mol Biol* **15**, 283-291.

305. Yonemitsu Y, Kitson C, Ferrari S, Farley R, Griesenbach U, Judd D, Steel R, Scheid P, Zhu J, Jeffery PK, Kato A, Hasan MK, Nagai Y, Masaki I, Fukumura M, Hasegawa M, Geddes DM, & Alton EW (2000). Efficient gene transfer to airway epithelium using recombinant Sendai virus. *Nat Biotechnol* **18**, 970-973.

306. Yu H, Hanes M, Chrisp CE, Boucher JC, & Deretic V (1998). Microbial pathogenesis in cystic fibrosis: pulmonary clearance of mucoid Pseudomonas aeruginosa and inflammation in a mouse model of repeated respiratory challenge. *Infect Immun* **66**, 280-288.

307. Yu H & Head NE (2002). Persistent infections and immunity in cystic fibrosis. *Front Biosci* **7**, d442-d457.

308. Yu H, Nasr SZ, & Deretic V (2000). Innate lung defenses and compromised Pseudomonas aeruginosa clearance in the malnourished mouse model of respiratory infections in cystic fibrosis. *Infect Immun* **68**, 2142-2147.

309. Zach MS (1990). Lung disease in cystic fibrosis--an updated concept. *Pediatr Pulmonol* **8**, 188-202.

310. Zahm JM, Baconnais S, Davidson DJ, Webb S, Dorin J, Bonnet N, Balossier G, & Puchelle E (2001). X-ray microanalysis of airway surface liquid collected in cystic fibrosis mice. *Am J Physiol Lung Cell Mol Physiol* **281**, L309-L313.

311. Zahm JM, Gaillard D, Dupuit F, Hinnrasky J, Porteous D, Dorin JR, & Puchelle E (1997). Early alterations in airway mucociliary clearance and inflammation of the lamina propria in CF mice. *Am J Physiol* **272**, C853-C859.

312. Zeiher BG, Eichwald E, Zabner J, Smith JJ, Puga AP, McCray PB, Jr., Capecchi MR, Welsh MJ, & Thomas KR (1995). A mouse model for the delta F508 allele of cystic fibrosis. *J Clin Invest* **96**, 2051-2064.

313. Zhou L, Dey CR, Wert SE, DuVall MD, Frizzell RA, & Whitsett JA (1994). Correction of lethal intestinal defect in a mouse model of cystic fibrosis by human CFTR. *Science* **266**, 1705-1708.

314. Zielenski J (2000). Genotype and phenotype in cystic fibrosis. *Respiration* **67**, 117-133.

315. Zielenski J, Corey M, Rozmahel R, Markiewicz D, Aznarez I, Casals T, Larriba S, Mercier B, Cutting GR, Krebsova A, Macek MJ, Langfelder-Schwind E, Marshall BC, DeCelie-Germana J, Claustres M, Palacio A, Bal J, Nowakowska A, Ferec C, Estivill X, Durie P, & Tsui LC (1999). Detection of a cystic fibrosis modifier locus for meconium ileus on human chromosome 19q13 [letter]. *Nat Genet* **22**, 128-129.

316. Zuckerman SH, Bryan-Poole N, Evans GF, Short L, & Glasebrook AL (1995). In vivo modulation of murine serum tumour necrosis factor and interleukin-6 levels during endotoxemia by oestrogen agonists and antagonists. *Immunology* **86**, 18-24.